

5-2010

MECHANISM-BASED STRATEGIES TO ENHANCE THE ACTIONS OF A

fabiola c. gomez

Follow this and additional works at: https://digitalcommons.library.tmc.edu/utgsbs_dissertations



Part of the [Cancer Biology Commons](#), and the [Therapeutics Commons](#)

Recommended Citation

gomez, fabiola c., "MECHANISM-BASED STRATEGIES TO ENHANCE THE ACTIONS OF A" (2010). *The University of Texas MD Anderson Cancer Center UTHealth Graduate School of Biomedical Sciences Dissertations and Theses (Open Access)*. 31.

https://digitalcommons.library.tmc.edu/utgsbs_dissertations/31

This Dissertation (PhD) is brought to you for free and open access by the The University of Texas MD Anderson Cancer Center UTHealth Graduate School of Biomedical Sciences at DigitalCommons@TMC. It has been accepted for inclusion in The University of Texas MD Anderson Cancer Center UTHealth Graduate School of Biomedical Sciences Dissertations and Theses (Open Access) by an authorized administrator of DigitalCommons@TMC. For more information, please contact digitalcommons@library.tmc.edu.

MECHANISM-BASED STRATEGIES TO ENHANCE THE ACTIONS OF A
HSP90 INHIBITOR USING MULTIPLE MYELOMA AS A MODEL

by

Fabiola Cervantes Gomez, B.S.

APPROVED:

Varsha Gandhi, Ph.D.
Supervisory Professor

Juan Fueyo-Margareto, M.D.

Peng Huang, M.D. Ph.D.

Reuben Lotan, Ph.D.

Deepa Sampath, Ph.D.

Christine Stellrecht, Ph.D.

APPROVED:

George Stancel, Ph.D.
Dean, The University of Texas Health Science Center at Houston
Graduate School Biomedical Sciences

MECHANISM-BASED STRATEGIES TO ENHANCE THE ACTIONS OF A
HSP90 INHIBITOR USING MULTIPLE MYELOMA AS A MODEL

A
DISSERTATION

Presented to the Faculty of
The University of Texas
Health Science Center at Houston
and
The University of Texas
M.D. Anderson Cancer Center
Graduate School of Biomedical Sciences
in Partial Fulfillment
of the Requirements

for the Degree of
DOCTOR OF PHILOSOPHY

by

Fabiola Cervantes Gomez, B.S.

Houston, Texas

May, 2010

Dedication

To the most important person in my world, my mom

Acknowledgements

I want to extend my deepest gratitude to my advisor Varsha Gandhi. Thank you for your support, mentorship, and for always embracing my mini-meltdowns with a patient smile.

Thank you to my committee members for all their advice and help with this project during the last five years. Each one of you contributed not only to the development of my project but also to my development as a scientist throughout the years, for that I thank you.

Many thanks to ...

My former labmates, Rina, Jennifer and Cornel, for their support and comprehension through the dissertation writing process. The fact that all of you graduated and moved on to other things in the real world gave me my light at the end of the Ph.D. tunnel.

My current labmates, Alma and Lisa, for all their help in the development of my project. Alma thank you for feeding me during those long endless weekends, your pasta was awesome as always. A big thank you to Lisa, it was really handsome of you to stick around throughout the whole process. I really appreciate your help and most importantly your patience, the writing process would have been so much worse if it were not for you putting up with my crankiness in every step of the way.

All the people in the Cellular and Molecular Pharmacology group. During my doctoral training these past five years you were a family to me, I will miss each and every one of you.

My family and friends, for all their support and for being always willing to help in any way possible to make my life easier during stressful moments. And to my mom for all her unconditional and infinite love, and for always believing in me.

MECHANISM-BASED STRATEGIES TO ENHANCE THE ACTIONS OF A
HSP90 INHIBITOR USING MULTIPLE MYELOMA AS A MODEL

Publication No. _____

Fabiola Cervantes Gomez, B.S.

Supervisory Professor: Varsha Gandhi, Ph.D.

Heat shock protein 90 (HSP90) is an abundant molecular chaperone that regulates the functional stability of client oncoproteins, such as STAT3, Raf-1 and Akt, which play a role in the survival of malignant cells. The chaperone function of HSP90 is driven by the binding and hydrolysis of ATP. The geldanamycin analog, 17-AAG, binds to the ATP pocket of HSP90 leading to the degradation of client proteins. However, treatment with 17-AAG results in the elevation of the levels of antiapoptotic proteins HSP70 and HSP27, which may lead to cell death resistance. The increase in HSP70 and HSP27 protein levels is due to the activation of the transcription factor HSF-1 binding to the promoter region of *HSP70* and *HSP27* genes. HSF-1 binding subsequently promotes *HSP70* and *HSP27* gene expression. Based on this, I hypothesized that inhibition of transcription/translation of HSP or client proteins would enhance 17-AAG-mediated cytotoxicity. Multiple myeloma (MM) cell lines MM.1S, RPMI-8226, and U266 were used as a model. To test this hypothesis, two different strategies were used.

For the first approach, a transcription inhibitor was combined with 17-AAG. The established transcription inhibitor Actinomycin D (Act D), used in the clinic, intercalates into DNA and blocks RNA elongation. Stress inducible (HSP90 α , HSP70 and HSP27) and constitutive (HSP90 β and HSC70) mRNA and protein levels were measured using real time RT-PCR and immunoblot assays. Treatment with 0.5 μ M 17-AAG for 8 hours resulted in the induction of all HSP transcript and protein levels in the MM cell lines. This induction of HSP mRNA levels was diminished by 0.05 μ g/mL Act D for 12 hours in the combination

treatment, except for HSP70. At the protein level, Act D abrogated the 17-AAG-mediated induction of all HSP expression levels, including HSP70. Cytotoxic evaluation (Annexin V/7-AAD assay) of Act D in combination with 17-AAG suggested additive or more than additive interactions.

For the second strategy, an agent that affected bioenergy production in addition to targeting transcription and translation was used. Since ATP is necessary for the proper folding and maturation of client proteins by HSP90, ATP depletion should lead to a decrease in client protein levels. The transcription and translation inhibitor 8-Chloro-Adenosine (8-Cl-Ado), currently in clinical trials, is metabolized into its cytotoxic form 8-Cl-ATP causing a parallel decrease of the cellular ATP pool. Treatment with 0.5 μ M 17-AAG for 8 hours resulted in the induction of all HSP transcript and protein levels in the three MM cell lines evaluated. In the combination treatment, 10 μ M 8-Cl-Ado for 20 hours did not abrogate the induction of HSP mRNA or protein levels. Since cellular bioenergy is necessary for the stabilization of oncoproteins by HSP90, immunoblot assays analyzing for expression levels of client proteins such as STAT3, Raf-1, and Akt were performed. Immunoblot assays detecting for the phosphorylation status of the translation repressor 4E-BP1, whose activity is modulated by upstream kinases sensitive to changes in ATP levels, were also performed. The hypophosphorylated state of 4E-BP1 leads to translation repression. Data indicated that treatment with 17-AAG alone resulted in a minor (<10%) change in STAT3, Raf-1, and Akt protein levels, while no change was observed for 4E-BP1. The combination treatment resulted in more than 50% decrease of the client protein levels and hypophosphorylation of 4E-BP1 in all MM cell lines. Treatment with 8-Cl-Ado alone resulted in less than 30% decrease in client protein levels as well as a decrease in 4E-BP1 phosphorylation. Cytotoxic evaluation of 8-Cl-Ado in combination with 17-AAG resulted in more than additive cytotoxicity when drugs were combined in a sequential manner.

In summary, these data suggest that the mechanism-based combination of agents that target transcription, translation, or decrease cellular bioenergy with 17-AAG results in increase cytotoxicity when compared to the single agents. Such combination strategies may be applied in the clinic since these drugs are established chemotherapeutic agents or currently in clinical trials.

Table of Contents

Dedication	iii
Acknowledgements.....	iv
Abstract.....	v
Table of Contents.....	viii
List of Figures	xiv
List of Tables.....	xix
Abbreviations	xx
CHAPTER 1: Introduction	
Molecular chaperones.....	1
Heat shock proteins	2
Heat shock protein subfamilies	
HSP100 family.....	5
HSP70 family.....	5
HSP60 family.....	6
Small heat shock protein family.....	7
HSP90 family.....	7
HSP90 and cancer	8
HSP90 overexpression and non-oncogene addition	9
HSP90 chaperone cycle	10
HSP90 inhibition	13
17-AAG	14
HSF1 and heat shock protein stress-regulated response.....	19
Antiapoptotic heat shock proteins	23
Proapoptotic heat shock proteins.....	28

Heat shock protein expression and cytotoxicity resistance	29
Actinomycin D	30
8-Chloro-Adenosine	33
Multiple myeloma	38
Significance.....	40

CHAPTER 2: Materials and Methods

Cell lines	41
Materials	41
RNA synthesis	41
Isolation of RNA and quantitative real time RT-PCR	42
Protein extraction and immunoblot assays	43
Immunoprecipitation of HSP90 protein bound to [³ H] 17-AAG.....	44
Annexin V cell death assay.....	46
Perchloric acid extraction of intracellular nucleotides	46
Intracellular nucleotide quantitation by HPLC	47
Statistical analysis.....	48

CHAPTER 3: Results

Aim 1: Actinomycin D

17-AAG treatment results in a dose-dependent increase in heat shock proteins in MM.1S and RPMI-8226 cells	49
17-AAG treatment results in a time-dependent increase in heat shock proteins in MM.1S and RPMI-8226 cells	52
Act D treatment results in a dose-dependent decrease in heat shock proteins in MM.1S and RPMI-8226 cells	52
Act D treatment results in a time-dependent decrease in heat shock proteins in MM.1S and RPMI-8226 cells	57

Inhibition of global RNA synthesis by Act D in MM.1S and RPMI-8226 cells	57
Inhibition of global RNA synthesis by Act D in combination with 17-AAG in	
MM.1S and RPMI-8226 cells	62
Effect of Act D and 17-AAG alone and in sequential combination on heat shock	
protein mRNA levels in MM.1S and RPMI-8226 cells	67
Act D diminished constitutive and stress-inducible <i>HSP90</i> mRNA induced by	
17-AAG in MM.1S and RPMI-8226 cells	67
Act D diminished constitutive <i>HSC70</i> but not stress-inducible <i>HSP70</i> mRNA	
induced by 17-AAG in MM.1S and RPMI-8226 cells	70
Act D diminished <i>HSP27</i> mRNA induced by 17-AAG in MM.1S and RPMI-8226 cells ..	73
Act D diminished HSF-1 mRNA in MM.1S and RPMI-8226 cells	73
Act D diminished 17-AAG-mediated induction of heat shock protein and HSF-1	
expression levels in MM.1S and RPMI-8226 cells	78
Act D diminished 17-AAG-mediated induction of HSP90 α/β expression levels in	
MM.1S and RPMI-8226 cells	81
Act D diminished 17-AAG-mediated induction of constitutive HSC70 and	
stress-inducible HSP70 expression levels in MM.1S and RPMI-8226 cells	81
Act D diminished 17-AAG-mediated induction of HSP27 expression levels in	
MM.1S and RPMI-8226 cells	84
Act D in combination with 17-AAG diminished HSF-1 expression levels in	
MM.1S and RPMI-8226 cells	84
Heat shock protein levels are not diminished in the sequential combination of	
17-AAG followed by Act D in MM.1S cells	91
Increased cytotoxicity of Act D in sequential combination with 17-AAG in	
MM.1S and RPMI-8226 cells	94

Aim 2: 8-Chloro-Adenosine

Inhibition of global RNA synthesis by 8-Cl-Ado in MM.1S and RPMI-8226 cells	100
Effect of 8-Cl-Ado and 17-AAG alone and in sequential combination on heat shock protein mRNA levels in MM.1S and RPMI-8226 cells	100
8-Cl-Ado did not diminish constitutive and stress-inducible <i>HSP90</i> mRNA induced by 17-AAG in MM.1S and RPMI-8226 cells	103
8-Cl-Ado did not diminish constitutive <i>HSC70</i> or stress-inducible <i>HSP70</i> mRNA induced by 17-AAG in MM.1S and RPMI-8226 cells	108
8-Cl-Ado did not diminish <i>HSP27</i> mRNA induced by 17-AAG in MM.1S and RPMI-8226 cells	108
Effect of 8-Cl-Ado and 17-AAG alone and in combination on heat shock protein levels in MM.1S, RPMI-8226, and U266 cells	113
8-Cl-Ado and 17-AAG did not affect HSP90 α/β expression levels in MM.1S or RPMI-8226, only in U266 cells	116
8-Cl-Ado did not diminish 17-AAG-mediated induction of constitutive HSC70 and stress-inducible HSP70 expression levels in MM.1S and RPMI-8226 cells, only in U266 cells	116
8-Cl-Ado did not diminish 17-AAG-mediated induction of HSP27 expression levels in MM.1S, RPMI-8226, or U266 cells	121
Effect of other 8-Cl-Ado and 17-AAG combination sequences on heat shock protein levels in U266 cells	121
17-AAG \rightarrow 8-Cl-Ado sequential combination	126
8-Cl-Ado + 17-AAG simultaneous combination	129
Effect of 8-Cl-Ado and 17-AAG alone and in combination on GRP protein levels in MM.1S cells	132

Effect of 8-Cl-Ado and 17-AAG alone and in combination on STAT3, Raf-1, and Akt client protein levels in MM.1S, RPMI-8226, and U266 cells	137
Combination of 8-Cl-Ado followed by 17-AAG decreased STAT3 expression levels in MM.1S, RPMI-8226, and U266 cells	140
Combination of 8-Cl-Ado followed by 17-AAG decreased Raf-1 expression levels in MM.1S, RPMI-8226, and U266 cells	143
Combination of 8-Cl-Ado followed by 17-AAG decreased Akt expression levels in MM.1S, RPMI-8226, and U266 cells	143
Effect of other 8-Cl-Ado and 17-AAG combination sequences on STAT3, Raf-1, and Akt client protein levels in U266 cells	148
<i>17-AAG→8-Cl-Ado sequential combination</i>	151
<i>8-Cl-Ado+17-AAG simultaneous combination</i>	151
Effect of 8-Cl-Ado and 17-AAG alone and in combination on STAT-3, Raf-1, and Akt client protein mRNA levels in MM.1S and RPMI-8226 cells	156
8-Cl-Ado and 17-AAG alone or in combination did not affect STAT3 transcript levels in MM.1S and RPMI-8226 cells	157
8-Cl-Ado and 17-AAG alone or in combination did not affect Raf-1 transcript levels in MM.1S and RPMI-8226 cells	157
8-Cl-Ado and 17-AAG alone or in combination did not affect Akt transcript levels in MM.1S cells, only effect observed in RPMI-8226 cells for the combination treatment	157
Cellular metabolism: accumulation of 8-Cl-Ado cytotoxic triphosphate and concomitant ATP concentration decrease in MM.1S cells	164
Sequential treatment of 8-Cl-Ado followed by 17-AAG reduces 8-Cl-Ado metabolism and ATP accumulation	167

Immunoprecipitation of HSP90 bound to [³ H] 17-AAG in the combination treatment	
with 8-Cl-Ado.....	170
<i>Immunoprecipitation and immuno-detection of HSP90α/β and RNA Pol II</i>	
<i>as a function</i>	171
<i>Effect of 8-Cl-Ado in the binding of [³H]17-AAG to HSP90</i>	176
Effect of 8-Cl-Ado on 4E-BP1 protein levels in MM.1S cells.....	179
Effect of 8-Cl-Ado and 17-AAG on 4E-BP1 protein levels in U266 cells.....	180
Cytotoxicity of 8-Cl-Ado followed by 17-AAG in MM cell lines	183
Cytotoxicity of 8-Cl-Ado followed by 17-AAG combination sequence in MM cell lines .	186
Cytotoxicity of 17-AAG followed by 8-Cl-Ado combination sequence in MM cell lines .	191
Cytotoxicity of 8-Cl-Ado and 17-AAG simultaneous combination in MM cell lines	194
CHAPTER 4: Discussion	
17-AAG	197
HSP90 and stress response modulation.....	198
Heat shock protein stress response.....	199
Act D mechanism of action as a transcription inhibitor	200
Clinical application of Act D	200
Heat shock protein mRNA transcription inhibition.....	202
Heat shock protein expression inhibition	204
8-Cl-Ado and inhibition of RNA synthesis	205
Decline in ATP levels	209
Protein synthesis and ATP depletion	214
References.....	217
Vita.....	217

List of Figures

Figure 1. HSP90 chaperone cycle	12
Figure 2. Structure of 17-(Allylamino)-17-geldanamycin.....	16
Figure 3. Inhibition of HSP90 chaperone function by 17-AAG	18
Figure 4. Heat shock proteins transcription induction by HSF-1 transcription factor	22
Figure 5. Antiapoptotic heat shock proteins.....	25
Figure 6. Structure of Actinomycin D	32
Figure 7. Structure of 8-Chloro-Adenosine	35
Figure 8. Metabolism of 8-Cl-Ado	37
Figure 9. 17-AAG treatment results in a dose-dependent increase in heat shock proteins in MM.1S and RPMI-8226 cells.....	51
Figure 10. 17-AAG treatment results in a time-dependent increase in heat shock proteins in MM.1S and RPMI-8226 cells.....	54
Figure 11. Act D treatment results in a dose-dependent decrease in heat shock proteins in MM.1S and RPMI-8226 cells.....	56
Figure 12. Act D treatment results in a time-dependent decrease in heat shock proteins in MM.1S and RPMI-8226 cells.....	59
Figure 13. Inhibition of global RNA synthesis by Act D.....	61
Figure 14. Drug schedule for Act D and 17-AAG combination treatment	64
Figure 15. Inhibition of global RNA synthesis by Act D.....	66
Figure 16. Act D diminished constitutive and stress-inducible HSP90 mRNA induced by 17-AAG in MM.1S and RPMI-8226 cells.....	69
Figure 17. Act D diminished constitutive HSC70 but not stress-inducible HSP70 mRNA induced by 17-AAG in MM.1S and RPMI-8226 cells.....	72

Figure 18. Act D diminished HSP27 mRNA induced by 17-AAG in MM.1S and RPMI-8226 cells.....	75
Figure 19. Act D diminished HSF-1 mRNA in MM.1S and RPMI-8226 cells	77
Figure 20. Act D diminished 17-AAG-mediated induction of heat shock protein and HSF-1 expression levels in MM.1S and RPMI-8226 cells.....	80
Figure 21. Act D diminished 17-AAG-mediated induction of HSP90 α/β expression levels in MM.1S and RPMI-8226 cells.....	83
Figure 22. Act D diminished 17-AAG-mediated induction of constitutive HSC70 and stress-inducible HSP70 expression levels in MM.1S and RPMI-8226 cells.....	86
Figure 23. Act D diminished 17-AAG-mediated induction of HSP27 expression levels in MM.1S and RPMI-8226 cells.....	88
Figure 24. Act D in combination with 17-AAG diminished HSF-1 expression levels in MM.1S and RPMI-8226 cells	90
Figure 25. Heat shock protein levels are not diminished in the sequential combination of 17-AAG followed by Act D in MM.1S cells	93
Figure 26. Increase cytotoxicity of Act D in sequential combination with 17-AAG in MM.1S and RPMI-8226 cells	96
Figure 27. Inhibition of global RNA synthesis by 8-Cl-Ado	102
Figure 28. Drug schedule for 8-Cl-Ado and 17-AAG combination treatment.....	105
Figure 29. 8-Cl-Ado did not diminish constitutive and stress-inducible <i>HSP90</i> mRNA induced by 17-AAG in MM.1S and RPMI-8226 cells.....	107
Figure 30. 8-Cl-Ado did not diminish constitutive <i>HSC70</i> or stress-inducible <i>HSP70</i> mRNA induced by 17-AAG in MM-1S and RPMI-8226 cells.....	110
Figure 31. 8-Cl-Ado did not diminish <i>HSP27</i> mRNA induced by 17-AAG in MM.1S and RPMI-8226 cells.....	112

Figure 32. Effect of 8-Cl-Ado and 17-AAG alone and in combination on heat shock protein levels in MM.1S, RPMI-8226, and U266 cells.....	115
Figure 33. 8-Cl-Ado did not affect HSP90 α/β expression levels in MM.1S or RPMI-8226, only in U266 cells.....	118
Figure 34. 8-Cl-Ado did not diminish 17-AAG-mediated induction of constitutive HSC70 and stress-inducible HSP70 expression levels in MM.1S or RPMI-8226, only in U266 cells.....	120
Figure 35. 8-Cl-Ado did not diminish 17-AAG-mediated induction of HSP27 expression levels in MM.1S, RPMI-8226, or U266 cells	123
Figure 36. Effect of other 8-Cl-Ado and 17-AAG combination sequences on heat shock protein levels in U266 cells	125
Figure 37. Effect of other 8-Cl-Ado and 17-AAG combination sequences on heat shock protein levels in U266 cells (i) 17-AAG \rightarrow 8-Cl-Ado sequential combination.....	128
Figure 38. Effect of other 8-Cl-Ado and 17-AAG combination sequences on heat shock protein levels in U266 cells (ii) 8-Cl-Ado + 17-AAG simultaneous combination.....	131
Figure 39. Effect of 8-Cl-Ado and 17-AAG alone and in combination on GRP protein levels in MM.1S cells.....	134
Figure 40. 8-Cl-Ado and 17-AAG alone and in combination did not affect GRP protein levels in MM.1S cells.....	136
Figure 41. Effect of 8-Cl-Ado and 17-AAG alone and in combination on STAT3, Raf-1, and Akt client protein levels in MM.1S, RPMI-8226, and U266 cells	139
Figure 42. Combination of 8-Cl-Ado followed by 17-AAG decreased STAT3 expression levels in MM.1S, RPMI-8226, and U266 cells	142

Figure 43. Combination of 8-Cl-Ado followed by 17-AAG decreased Raf-1 expression levels in MM.1S, RPMI-8226, and U266 cells	145
Figure 44. Combination of 8-Cl-Ado followed by 17-AAG decreased Akt expression levels in MM.1S, RPMI-8226, and U266 cells	147
Figure 45. Effect of other 8-Cl-Ado and 17-AAG combination sequences on STAT3, Raf-1, and Akt client protein levels in U266 cells	150
Figure 46. Effect of other 8-Cl-Ado and 17-AAG combination sequences on STAT3, Raf-1, and Akt client protein levels in U266 cells (i) 17-AAG → 8-Cl-Ado sequential combination.....	153
Figure 47. Effect of other 8-Cl-Ado and 17-AAG combination sequences on STAT3, Raf-1, and Akt client protein levels in U266 cells (ii) 8-Cl-Ado+17-AAG simultaneous combination.....	155
Figure 48. 8-Cl-Ado and 17-AAG alone or in combination did not affect STAT3 transcript levels in MM.1S and RPMI-8226 cells.....	159
Figure 49. 8-Cl-Ado and 17-AAG alone or in combination did not affect Raf-1 transcript levels in MM.1S and RPMI-8226 cells.....	161
Figure 50. 8-Cl-Ado and 17-AAG alone or in combination did not affect Akt transcript levels in MM.1S cells, only effect observed in RPMI-8226 cells for the combination treatment.....	163
Figure 51. Cellular metabolism: accumulation of 8-Cl-Ado cytotoxic triphosphate and concomitant ATP concentration decrease in MM.1S cells	166
Figure 52. Immunoprecipitation and immuno-detection of HSP90α/β and RNA Pol II as a function of concentration	173
Figure 53. Immunoprecipitation and immuno-detection of HSP90α/β and RNA Pol II ..	175

Figure 54. Immunoprecipitation of HSP90 bound to [³ H] 17-AAG in the combination treatment with 8-Cl-Ado	
<i>Effect of 8-Cl-Ado in the binding of [³H] 17-AAG to HSP90</i>	178
Figure 55. Effect of 8-Cl-Ado on 4E-BP1 protein levels in MM.1S cells	182
Figure 56. Effect of 8-Cl-Ado on 4E-BP1 protein levels in U266 cells	185
Figure 57. Cytotoxicity of 8-Cl-Ado followed by 17-AAG in MM cell lines.....	188

List of Tables

Table 1. Heat shock protein family.....	4
Table 2. Increase cytotoxicity of Act D in sequential combination with 17-AAG in MM.1S and RPMI-8226 cells	99
Table 3. Sequential treatment of 8-Cl-Ado followed by 17-AAG reduces 8-Cl-Ado metabolism and ATP accumulation	169
Table 4. Cytotoxicity of 8-Cl-Ado followed by 17-AAG combination sequence in MM cell lines	190
Table 5. Cytotoxicity of 17-AAG followed by 8-Cl-Ado combination sequence in MM cell lines	193
Table 6. Cytotoxicity of 8-Cl-Ado and 17-AAG simultaneous combination in MM cell lines.....	196

Abbreviations

μM	micromolar
17-AAG	17-allylamino-17demethoxygeldanamycin
4E-BP1	4E binding protein
7-AAD	7-amino-actinomycin D
8-Cl-Ado	8-chloro-adenosine
Act D	actinomycin D
ADP	adenosine 5'-diphosphate
Apaf-1	apoptotic protease activating factor 1
ATP	adenosine 5'-triphosphate
Bid	Bcl2 interacting protein
cdc37	cell division cycle 37 protein
CDK	cyclin-dependent kinase
CTP	cytidine 5'-triphosphate
CyP40	cyclophylin 40
DNA	deoxyribonucleic acid
EGR1	early growth response factor 1
eIF4E	eukaryotic translation initiation factor 4E
ER	endoplasmic reticulum
GAPDH	glyceraldehyde -3- phosphate dehydrogenase
GHL	Bacterial Gyrase, HSP90, Histidine Kinase, and MutL Kinase
GRP	glucose regulated protein
GTP	guanosine 5'-triphosphate
HOP	HSP90/HSP70 organizing protein
HPLC	high pressure liquid chromatography

HPRT	hypoxanthine-guanine phosphoribosyltransferase
HSF	heat shock factor
HSP	heat shock protein
IL-6	interleukin-6
IMM	immunophilins
JAK	just another kinase
JNK1	c-Jun N-terminal kinase 1
MAPKAP	mitogen-activated protein kinase-activated protein
mL	milliliter
MM	multiple myeloma
mM	millimolar
mRNA	messenger RNA
mtHSP70	mitochondrial HSP70
mTOR	mammalian target of rapamycin
NF- κ B	nuclear factor κ B
PBS	phosphate buffered saline
PI-3K	phosphatidylinositol-3-kinase
PKC δ	protein kinase c delta
rbS6	ribosomal protein S6
RNA	ribonucleic acid
ROS	reactive oxygen species
RPMI	Roswell Park Memorial Institute medium
rRNA	ribosomal RNA
RT-PCR	reverse transcriptase polymerase chain reaction
SDHA	succinate dehydrogenase complex subunit A
siRNA	small interference RNA

Sp1	specificity protein 1
Src	sarcoma
STAT3	signal transducer and activator of transcription 3
TRAP-1	tumor necrosis factor receptor-associated protein 1
tRNA	transfer RNA
TXN2	thioredoxin 2
UPR	unfolded protein response
UTP	uridine 5'-triphosphate

CHAPTER 1: Introduction

Molecular chaperones

The protein-saturated environment of the cell (approximately 350 g/L) provides a challenging setting for newly synthesized polypeptides to assemble into functional products (Hartl and Hayer-Hartl 2009). Mutations and post-translational events can also give rise to misfolded proteins resulting in toxic intracellular aggregates (Goldberg 2003). A group of specialized proteins, called molecular chaperones, function to assemble polypeptides into proteins, rearrange misfolded proteins or disassemble protein complexes (Hartl and Hayer-Hartl 2002; Hartl and Hayer-Hartl 2009). This set of particular chaperones constitute ~5-10% of the total cellular proteins (Biamonte, Van de Water et al. 2010). The term molecular chaperones was coined in the late 1970s to describe the catalytic role of the nuclear protein nucleoplasmin in the *in vitro* formation of nucleosomes (Laskey, Honda et al. 1978). They were first defined as a group of unrelated proteins that provide transient assistance in protein folding through non-covalent interactions. Molecular chaperones prevent incorrect polypeptide associations but without actually being a component of the final three-dimensional functional protein (Ellis 1993). However, contrary to the accepted notion that protein self-assembly is a spontaneous process that does not require additional molecules, it is now known that most cellular proteins require molecular chaperones for proper folding (Anfinsen 1973; Hartl and Hayer-Hartl 2002). It was later determined that molecular chaperones not only aid in the folding and assembly of unstable proteins but also play a role in protein transport and degradation (Hartl 1996).

Heat shock proteins

In 1962, Ritossa described chromosomal puffing in *Drosophila melanogaster* salivary glands following heat exposure, thus discovering the heat shock response (Ritossa 1996). Later work revealed that exogenous stress, such as increased temperature, induces the expression of only certain specific proteins, while translation of other proteins remains inhibited. This group of induced proteins was subsequently referred to as heat shock proteins (Tissieres, Mitchell et al. 1974). While it was accepted that heat shock proteins protected the cell from stress, the mechanism by which this occurred remained elusive (Ellis 1993). In 1986, Pelham proposed that heat shock proteins could be implicated in protein folding and assembly processes in unstressed as well as stressed cells (Pelham 1986). It has now been established that the heat shock protein family is a group of constitutive and stress-inducible related proteins that act as molecular chaperones assisting in protein folding and stabilization (Hartl and Hayer-Hartl 2002). The heat shock protein family is highly conserved in eukaryotes and prokaryotes. In humans, the heat shock protein (HSP) family is comprised of five subfamilies: HSP100, HSP90, HSP70, HSP60, and the small HSP family (e.g. HSP27) (Table 1) (Kampinga, Hageman et al. 2009).

Table 1. Heat shock protein family

Table 1

Family	Main chaperones in humans	Location	Functions
HSP100	HSP110	Cytosol	Disassembles aggregates
HSP90	HSP90 α HSP90 β GRP94 TRAP-1	Cytosol Cytosol ER Mitochondria	Refolds denatured proteins; antiapoptotic
HSP70	HSP70 HSC70 GRP78 mtHSP70	Cytosol Cytosol ER Mitochondria	Folding of nascent polypeptides; protein transportation; antiapoptotic
HSP60	HSP60	Mitochondria	Regulates protein folding and import
small HSPs	HSP40	Cytosol	Cochaperone activity
	HSP27	Cytosol	Stabilizes cytoskeleton; antiapoptotic

Human heat shock protein subfamilies

HSP100 family

The HSP100 family is composed of four members; three of the isoforms reside in the cytosol and the fourth member is localized in the endoplasmic reticulum (Kampinga, Hageman et al. 2009). To date an HSP100 mitochondrial homologue has not been found in humans (Tatsuta 2009). This family possesses ATPase activity and represses the formation of aggregates prompted by denatured proteins (Maurizi and Xia 2004). Additionally, if aggregation occurs due to the inability of the heat shock proteins to handle an overwhelming amount of denatured proteins, HSP100 family proteins have the ability to facilitate the resolubilization of aggregates (Glover and Tkach 2001). The HSP100 family is highly homologous to HSP70 chaperones, and a longer middle domain linker between the N- and C-terminal domains distinguishes HSP100 from the latter (Polier, Dragovic et al. 2008; Kampinga, Hageman et al. 2009). Recent research suggests that HSP100 proteins can also act as ATP/ADP exchange factors and cooperate in protein folding in concert with HSP70 (Dragovic, Broadley et al. 2006; Polier, Dragovic et al. 2008).

HSP70 family

The HSP70 family is comprised of four homologues. There are two HSP70 isoforms in the cellular cytosol, the stress-inducible HSP70 and the constitutive HSC70. The cytosolic isoforms assist and facilitate the folding of newly synthesized polypeptides and prevent and disassemble protein aggregates (Hartl 1996; Hartl and Hayer-Hartl 2002). The chaperone activity of HSP70 and HSC70 is accomplished in an ATP-dependent manner (Hartl 1996; Dragovic, Broadley et al. 2006; Polier, Dragovic et al. 2008). In addition, HSP70 and HSC70 are important members of the cochaperone protein complex that modulate HSP90 activity (Pratt and Toft 2003).

The other two members of the HSP70 family are restricted to the endoplasmic reticulum and the mitochondria. Proper folding, assembly, and post-translational modifications of proteins occur in the endoplasmic reticulum. The endoplasmic reticulum HSP70 isoform, glucose-regulated protein 78 (GRP78/Bip), maintains homeostasis of protein assembly in this cellular structure with the assistance of other quality-control factors (Sitia and Braakman 2003). Aggregated proteins in the endoplasmic reticulum perturb protein quality control triggering the unfolded protein stress response (UPR) resulting in the synthesis of GRP78/Bip (Kim, Eri et al. 2006). Mitochondrial HSP70 chaperone (mtHSP70) is contained in the mitochondrial matrix and is required for the folding and translocation of nascent proteins (Hartl 1996; Tatsuta 2009). The ATPase activity of mtHSP70 chaperone allows it to bind, fold, and release a newly synthesized or partially folded protein.

HSP60 family

The molecular chaperones in this family are also referred as chaperonins. HSP60 protein is localized to the mitochondria although small levels of this chaperone have been detected outside this compartment in some tissue-specific cells (Samali, Cai et al. 1999; Tatsuta 2009). HSP60 forms large hetero-oligomeric complexes (approximately 800 kDa) with the cochaperone HSP10, promoting maturation of partially folded polypeptides and preventing protein aggregation (Kampinga, Hageman et al. 2009; Tatsuta 2009). The assembly and proper folding of proteins takes place inside the cage-like HSP60•HSP10 complex and is carried out in an ATP-dependent manner (Hartl 1996; Hartl and Hayer-Hartl 2009).

Small heat shock protein family

This subfamily is composed of heat shock proteins of low molecular weight (12-48 KDa in their monomeric form). HSP40 is a cochaperone that stimulates ATPase activity of HSP70 and facilitates the binding of nascent or denatured polypeptides (Qiu, Shao et al. 2006). HSP40 has a critical role in binding and uploading the client proteins onto HSP90 for their proper folding in the chaperone cycle (Pratt and Toft 2003). HSP27 is a heat shock protein that protects the cell from protein aggregates in an ATP-independent manner (Ehrnsperger, Graber et al. 1997). HSP27 can form homo-oligomers of up to 1000 KDa. Careful biochemical studies elucidated that the HSP27 oligomeric complex possesses chaperone capabilities (Shashidharamurthy, Koteiche et al. 2005). HSP27 in the multimer complex can be phosphorylated at different serine residues by MAPKAP kinase-2 and -3, which are serine/threonine protein kinases activated in response to stress, resulting in the formation of dimeric HSP27 (Rouse, Cohen et al. 1994; Vertii, Hakim et al. 2006). Therefore, the dephosphorylation of dimeric HSP27 subunits triggers the formation of the large homo-oligomer (Vertii, Hakim et al. 2006). Aside from the chaperone properties of HSP27 in its oligomeric form, the dimeric subunits play a role in the integrity of the cytoskeleton. HSP27 can inhibit the polymerization of actin by acting as a capping protein (Landry and Huot 1995; Mounier and Arrigo 2002). Another heat-inducible small heat shock protein of importance is α B-crystallin. Similar to HSP27, α B-crystallin plays an essential role in maintaining the integrity of the cytoskeleton and its phosphorylation state is regulated by MAPK AP kinase-2 (Liang and MacRae 1997; Mounier and Arrigo 2002).

HSP90 family

The mammalian HSP90 family consists of four homologues that reside in different compartments of the cell. The glucose-regulated protein 94 (GRP-94) and the tumor necrosis factor receptor-associated protein 1 (TRAP-1) are localized in the endoplasmic

reticulum (ER) and mitochondria, respectively. GRP94 is an ATP-dependent molecule that chaperones only a few known substrates without the assistance of cochaperones (Ostrovsky, Makarewich et al. 2009). This abundant endoplasmic reticulum chaperone is upregulated due to drop in glucose levels, hypoxia, or the homeostatic disruption of the calcium stores in the cell. GRP94 maintains ER-protein homeostasis making it a central player in the ER-associated degradation pathway that is part of the unfolded protein response (UPR) (Kim, Emi et al. 2006; Ostrovsky, Ahmed et al. 2009).

The two isoforms that reside in the cytosol are the inducible HSP90 alpha and the constitutive HSP90 beta. The cytosolic HSP90 α/β is the most abundant chaperone in the cell. Constitutively, it accounts for approximately 1-2% of the cytosolic proteins. An increase in the levels of this chaperone is further observed when the cell is subjected to physiological stress (including hypoxia, heat, and heavy metals) (Whitesell and Lindquist 2005).

HSP90 and cancer

HSP90 is essential in the stabilization and functional conformation of stress-denatured client oncoproteins, however, it is not required for the folding of most nascent polypeptides (Nathan, Vos et al. 1997). HSP90 is known to regulate over 200 proteins, including kinases and cell cycle regulators (updated list of HSP90 client proteins and interactors by Dr. Picard, <http://www.picard.ch/downloads/HSP90interactors.pdf>). In cancer cells, HSP90 constitutes 4-6% of the total protein found in the cell (Kamal, Thao et al. 2003; Brandt and Blagg 2009). The buffering effects of HSP90 in malignant cells allow the cells to withstand and thrive in the highly deregulated and otherwise cytotoxic tumor environment. For example, a protein can become misfolded due to oxidative damage caused by reactive oxygen species (ROS) to the ligand binding clefts, which are hydrophobic openings that allow the binding of substrates such as heme or ATP in the interior of the protein (Pratt, Morishima et al. 2010). Due to the dynamic state of these clefts, hydrophobic aminoacid

residues buried inside the protein become exposed facilitating their oxidation by ROS species resulting in further opening of the cleft which may result in protein unfolding (Shchepinov 2007; Pratt, Morishima et al. 2008; Pratt, Morishima et al. 2010). Therefore, ligand binding clefts are sites of conformational instability that are regulated by HSP90 in order to prevent further unfolding and maintain protein function (Pratt, Morishima et al. 2008; Pratt, Morishima et al. 2010). Since HSP90 is an indispensable chaperone in the maturation of denatured client oncoproteins, it is an attractive therapeutic target. Inhibition of its re-folding activity would result in the simultaneous downregulation of signaling cascades. Due to the importance of HSP90 in the function of oncoproteins and the progression of cancer, several small molecule inhibitors have been developed (Sharp and Workman 2006; Biamonte, Van de Water et al. 2010).

HSP90 overexpression and non-oncogene addiction

Oncogene addiction is characterized by the dependence that tumor cells develop on some genes capable of transformation and maintenance of the malignant phenotype (Weinstein and Joe 2008). In contrast, non-oncogene addiction is defined as the dependence that tumor cells develop for some non-oncoproteins (such as HSP90) for their ability to help tumor cells in adapting and thriving in a highly deregulated tumorigenic environment (Luo, Solimini et al. 2009). Overexpression of HSP90 does not drive transformation of cells; rather its deregulated expression complements the transformed phenotype. The ability of HSP90 to bind to denatured proteins and aid their refolding allows this chaperone to buffer the highly deregulated signaling cascades that drive oncogenesis in tumor cells (Bagatell and Whitesell 2004). Therefore, HSP90 is of particular importance in the maintenance of the tumorigenic phenotype. A review by Hanahan and Weinberg described the six hallmarks of cancer (evasion of apoptosis, insensitivity to antigrowth signals, limitless replicative potential, tissue invasion and metastasis, sustained

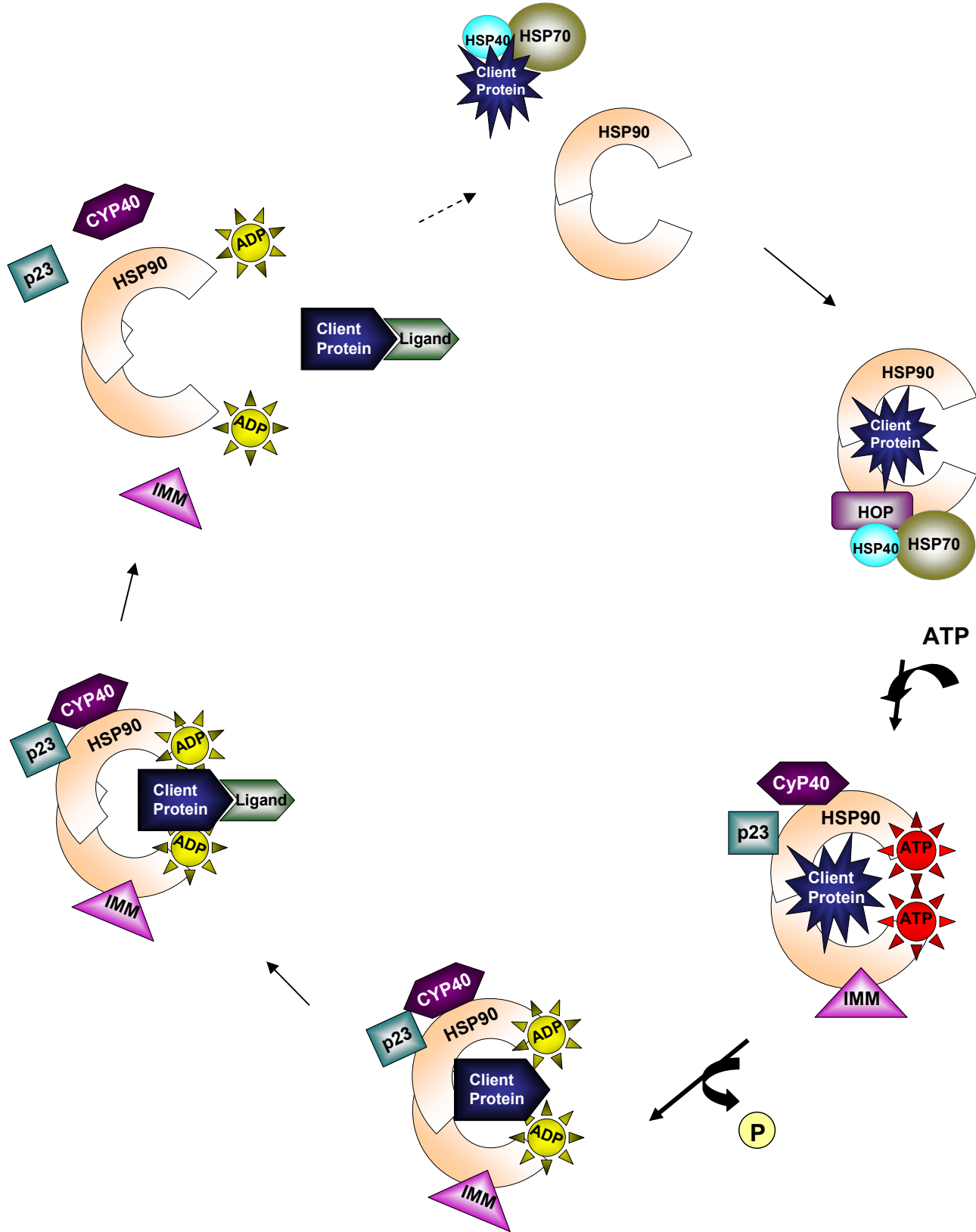
angiogenesis, self-sufficiency in growth signals), featuring specific alterations acquired by malignant cells and examples of oncoproteins that drove and sustained cellular transformation (Hanahan and Weinberg 2000). Interestingly, these traits are driven by several HSP90 client oncoproteins, hence, HSP90 chaperones the oncoproteins that characterize the malignant phenotype (Sharp and Workman 2006; Neckers 2007).

HSP90 chaperone cycle

HSP90 chaperone activity is an ATP-dependent process (Prodromou, Roe et al. 1997; Obermann, Sondermann et al. 1998; Wandinger, Richter et al. 2008). A denatured client protein is recognized by cochaperones HSP70 and HSP40 priming it in preparation for loading onto HSP90 (Figure 1) (Pratt and Toft 2003). Transfer of the client protein to HSP90 is facilitated by the cochaperone HSP90/HSP70 organizing protein (HOP) (Smith, Sullivan et al. 1993; Onuoha, Coulstock et al. 2008). Once the unfolded client interacts with HSP90, ATP binds to the ATP binding pocket in HSP90 and subsequent cochaperones bind to the client•HSP90 complex, facilitating its stabilization. For example, if the client protein is a glucocorticoid receptor, cochaperones include p23, immunophilins (IMM), and CyP40 (Pratt and Toft 2003; Whitesell and Lindquist 2005). If the client substrate is a kinase, a different set of cochaperones, such as cdc37, interact with HSP90 (Roe, Ali et al. 2004). Once the mature complex is assembled, a change in HSP90 conformation triggers ATP hydrolysis catalyzing the maturation of the client protein (Whitesell and Lindquist 2005; Biamonte, Van de Water et al. 2010). Once in the proper folded state, the client protein is functional and able to interact with ligands, in the case of glucocorticoid receptors, or phosphorylate a substrate, in the case of kinases. Interaction of the client protein with its ligand or phosphorylation of its substrate triggers the dissociation of the HSP90 complex (Whitesell and Lindquist 2005; Wandinger, Richter et al. 2008). Due to the significance of proper HSP90 chaperone function in oncoprotein stability, several small molecules have

Figure 1. HSP90 chaperone cycle

Figure 1



been synthesized to down-regulate numerous signaling cascades simultaneously (Sharp and Workman 2006; Kim, Alarcon et al. 2009; Biamonte, Van de Water et al. 2010) .

HSP90 inhibition

Given the importance of the HSP90 chaperone cycle in the stability of oncoproteins, several inhibitors of HSP90 have been identified including natural products. Two examples are the ansamycins geldanamycin and herbimycin A. These two ansamycins are produced by the strain *Streptomyces* and it was discovered that they possessed antibiotic activity more than thirty years ago (DeBoer, Meulman et al. 1970; Omura, Iwai et al. 1979). Originally, geldanamycin and herbimycin A were thought to be Src kinase inhibitors (Uehara, Hori et al. 1985; Uehara, Hori et al. 1986). Even though several studies demonstrated that this was an erroneous observation, it was later determined that these agents affect protein turnover of Src and other kinases. Still, the mechanism of action by which these two drugs acted remained elusive (Takahashi, Suzuki et al. 1992; Whitesell, Shifrin et al. 1992; Miller, DiOrio et al. 1994). In 1994, Whitesell et. al. described a mechanism reconciling these observations by discovering HSP90 as a modulator of substrate activity (Whitesell, Mimnaugh et al. 1994).

HSP90 belongs to the GHKL (Bacterial Gyrase, HSP90, Histidine Kinase, and MutL Kinase) family of ATPases (Dutta and Inouye 2000). The N-terminal ATP/ADP-binding pocket contains an unusual adenine-nucleotide-binding motif known as the Bergerat fold (Prodromou, Roe et al. 1997; Dutta and Inouye 2000). Interestingly, the ATP-pocket in other kinases or even HSP70 has no resemblance to the Bergerat pocket in HSP90. Geldanamycin inhibits the chaperone function of HSP90 by mimicking ATP and occupying its place in the N-terminal ATP-ADP-binding pocket (Prodromou, Roe et al. 1997). Hence, geldanamycin is a competitor of endogenous ATP binding. Since ATP binding to HSP90 is necessary for refolding and stabilization of client proteins, binding of geldanamycin hinders

the chaperone activities of HSP90 (Prodromou, Roe et al. 1997; Neckers and Neckers 2002). As a result, HSP90 client substrates are not properly folded or stabilized. Since the aggregation of unfolded proteins is deleterious in cells, the client oncoproteins are tagged with ubiquitin and destined for proteasomal degradation (Neckers and Neckers 2002).

Due to the special characteristics and properties of HSP90, several small molecule inhibitors that compete for the ATP pocket in this chaperone have been developed. The pursuit for improved HSP90 inhibitors was prompted by the unacceptable hepatotoxicity and poor solubility exhibited by the first HSP90 inhibitors (Supko, Hickman et al. 1995). Geldanamycin derivatives, 17-allylamino-17-geldanamycin (17-AAG), its hydroquinone form (IPI-504), and also fully synthetic inhibitors (such as the purine scaffold BIIB021) are such examples (Kim, Alarcon et al. 2009; Biamonte, Van de Water et al. 2010).

17-AAG

Although geldanamycin, the first HSP90 inhibitor, did not enter clinical trials due to its lack of solubility and unwanted side effects, it provided a proof-of-principal for HSP90 inhibition (Supko, Hickman et al. 1995). Geldanamycin contained potent anticancer activity however its severe liver toxicity and unstable reactivity prompted the development of still potent but more stable and safer derivatives such as 17-AAG (Schnur, Corman et al. 1995; Supko, Hickman et al. 1995; Solit, Zheng et al. 2002). 17-AAG, is a semisynthetic ATP competitive inhibitor of HSP90 (Figure 2) (Schnur, Corman et al. 1995). Similarly to geldanamycin, 17-AAG binds to the ATP pocket in HSP90. It mimics the C-shape conformation that the endogenous substrates ATP/ADP adopt in the Bergerat ATP-binding fold (Prodromou, Roe et al. 1997). Binding of 17-AAG to the ATP pocket in HSP90 results in an immature HSP90•client complex (Figure 3). Hence, the HSP90 inhibitor interrupts the maturation and proper folding of the client protein by HSP90 leading to the proteasomal degradation of the

Figure 2. Structure of 17-(Allylamino)-17-geldanamycin

Figure 2

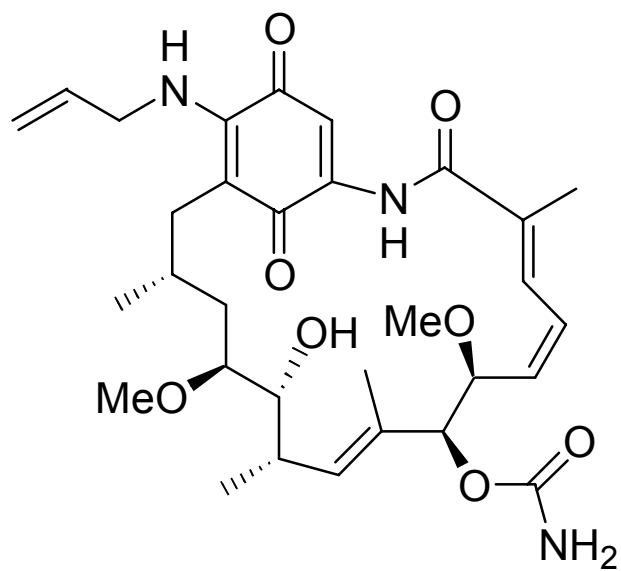
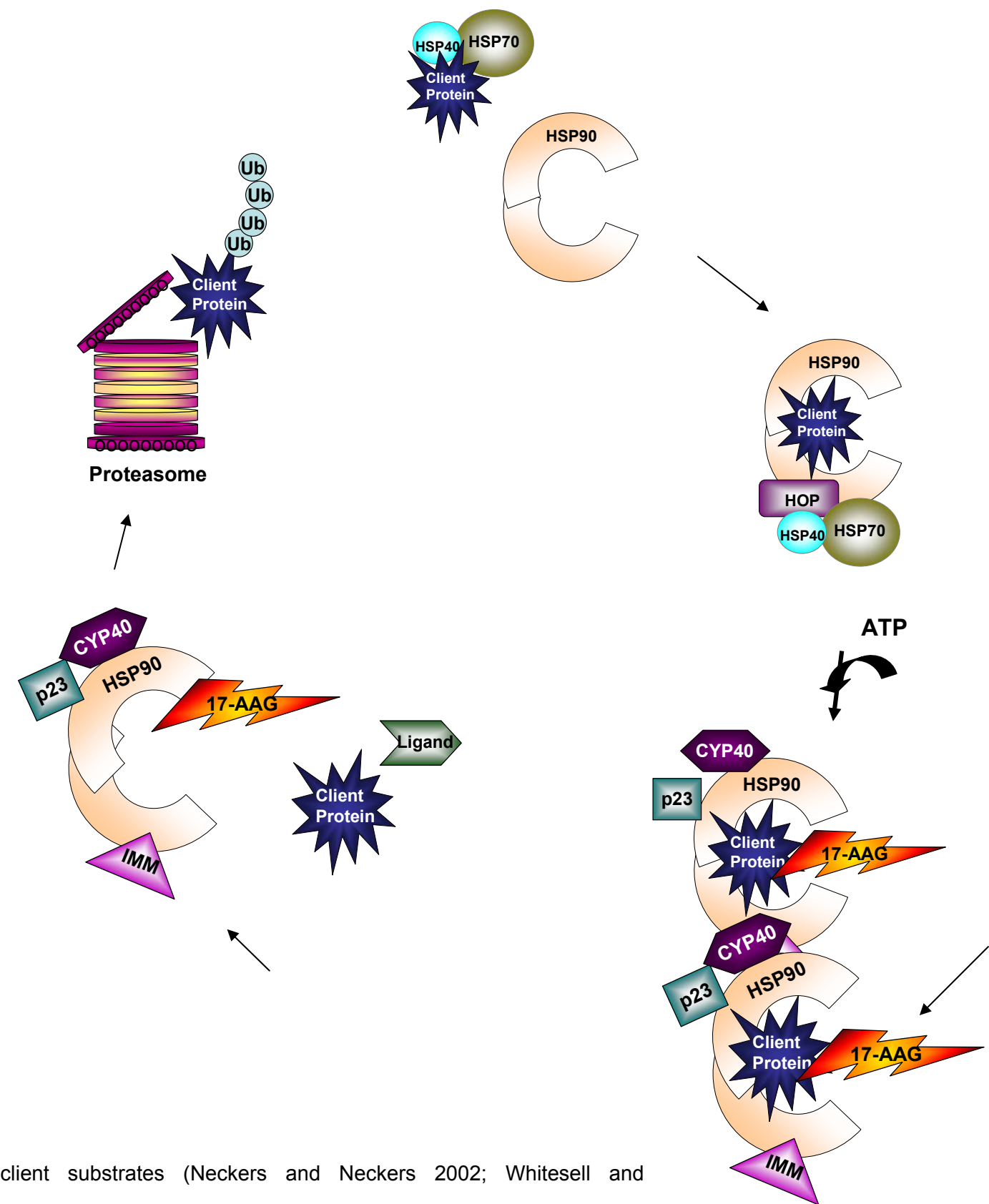


Figure 3. Inhibition of HSP90 chaperone function by 17-AAG

Figure 3



client substrates (Neckers and Neckers 2002; Whitesell and

Lindquist 2005). *In vitro* and *in vivo* studies showed the antitumor activity comes from the ability of 17-AAG to lead to degradation of several client proteins (Schnur, Corman et al. 1995; Schulte and Neckers 1998; Solit, Zheng et al. 2002). Promising preclinical data with 17-AAG prompted the first clinical trial in 1999, making it the first HSP90 inhibitor in phase I trials (Biamonte, Van de Water et al. 2010). However, binding of 17-AAG or any other HSP90 inhibitor, to the ATP pocket of the chaperone elicits a stress response resulting in the transcription and translation of heat shock proteins (Bagatell, Paine-Murrieta et al. 2000). Importantly, some studies have elucidated some of the heat shock proteins, such as HSP90, HSP70, and HSP27 possess antiapoptotic properties (Beere, Wolf et al. 2000; Pandey, Farber et al. 2000; Pandey, Saleh et al. 2000). Clinical trial pharmacodynamic studies with 17-AAG confirmed a similar depletion of client proteins and sustained elevation of HSP70 protein levels (Banerji, O'Donnell et al. 2005).

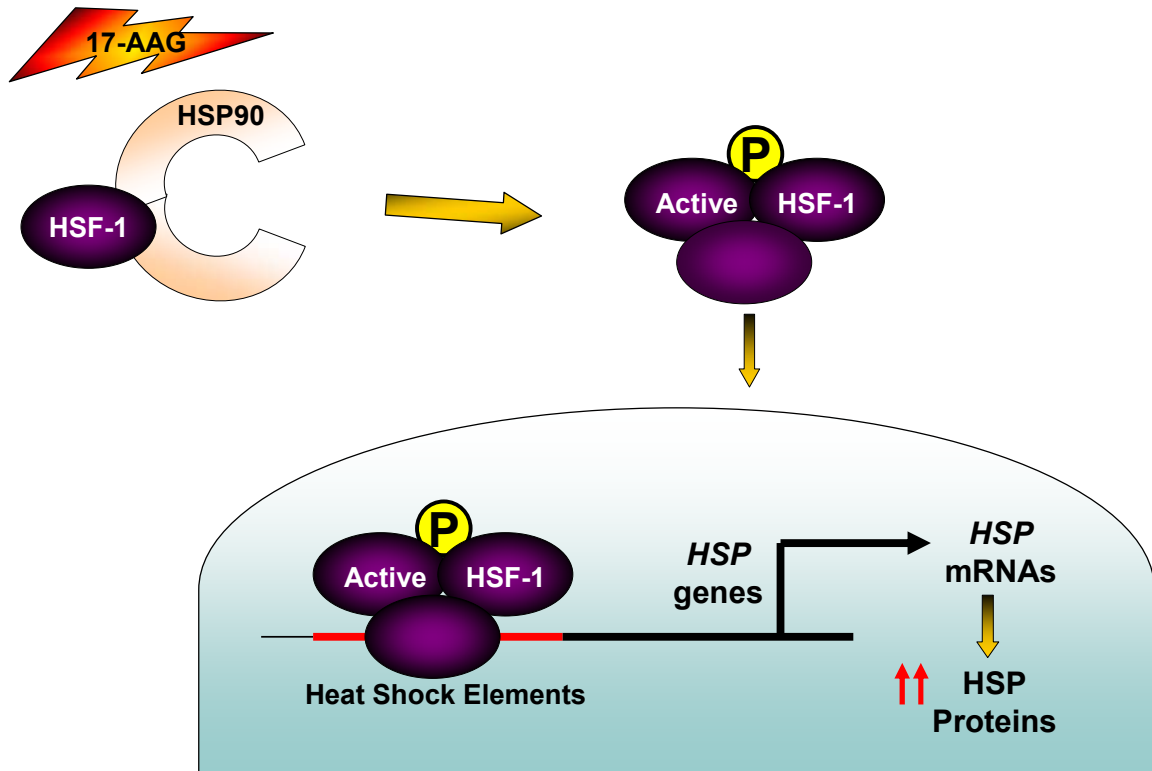
Heat shock factor-1 and heat shock protein stress-regulated response

Heat Shock Factor-1 (HSF-1) is a transcription activator of all heat shock protein genes (Voellmy 1994). Under basal physiological conditions, HSP90 and other cochaperones that are part of the repressing complex, such as p23 and the immunophilin CyP40, are bound to the transcription factor HSF-1, regulating its activation (Zou, Guo et al. 1998; Freeman, Borrelli et al. 1999; Guo, Guettouche et al. 2001). Other heat shock factor members that have been identified in humans are HSF-2 and HSF-4 (He, Soncin et al. 2003). HSF-4 is not known to be involved in the heat shock stress response, however HSF-2 can trigger heat shock protein transcription in response to cellular stress other than heat (He, Soncin et al. 2003; Trinklein, Chen et al. 2004). For example, the HSF-2 isoform HSF-2A, cooperates with HSF-1 in heat shock protein gene transcription (He, Soncin et al. 2003). The presence of stress inducers in the cell triggers the release of HSF-1 from its constitutive repressing complex triggering transcription of the heat shock proteins. Common

stress inducers include heat, reactive oxygen species, nutrient deprivation, hypoxia, low pH, infection, small molecules and aggregated, denatured, and damaged proteins (Ananthan, Goldberg et al. 1986; Zaarur, Gabai et al. 2006). Studies have also reported that tumor cells can circumvent the requirement of a stress trigger to activate HSF-1 under non-stress conditions (Khaleque, Bharti et al. 2005; Ciocca, Gago et al. 2006). Of particular significance, in healthy non-stressed cells, HSF-1 is inactive and does not participate in basal heat shock protein transcription to a noticeable extent (Kingston, Schuetz et al. 1987; Hensold, Hunt et al. 1990). Once released, HSF-1 undergoes trimerization and phosphorylation resulting in the active conformation of the HSF-1 trimeric complex (Figure 4) (Wu 1995; Cotto, Kline et al. 1996). The tyrosine kinases caseine kinase 2 and polo-like kinase 1 phosphorylate the HSF-1 activation site residues threonine 142 and serine 419, respectively (Soncin, Zhang et al. 2003; Kim, Yoon et al. 2005). Once activated the HSF-1 trimer translocates to the nucleus where it binds the heat shock elements present in the promoter of the heat shock protein genes. Binding of HSF-1 triggers multiple rounds of heat shock protein transcription resulting in an overexpression of heat shock proteins in the cell (Baler, Dahl et al. 1993).

Figure 4. Heat shock proteins transcription induction by HSF-1 transcription factor

Figure 4



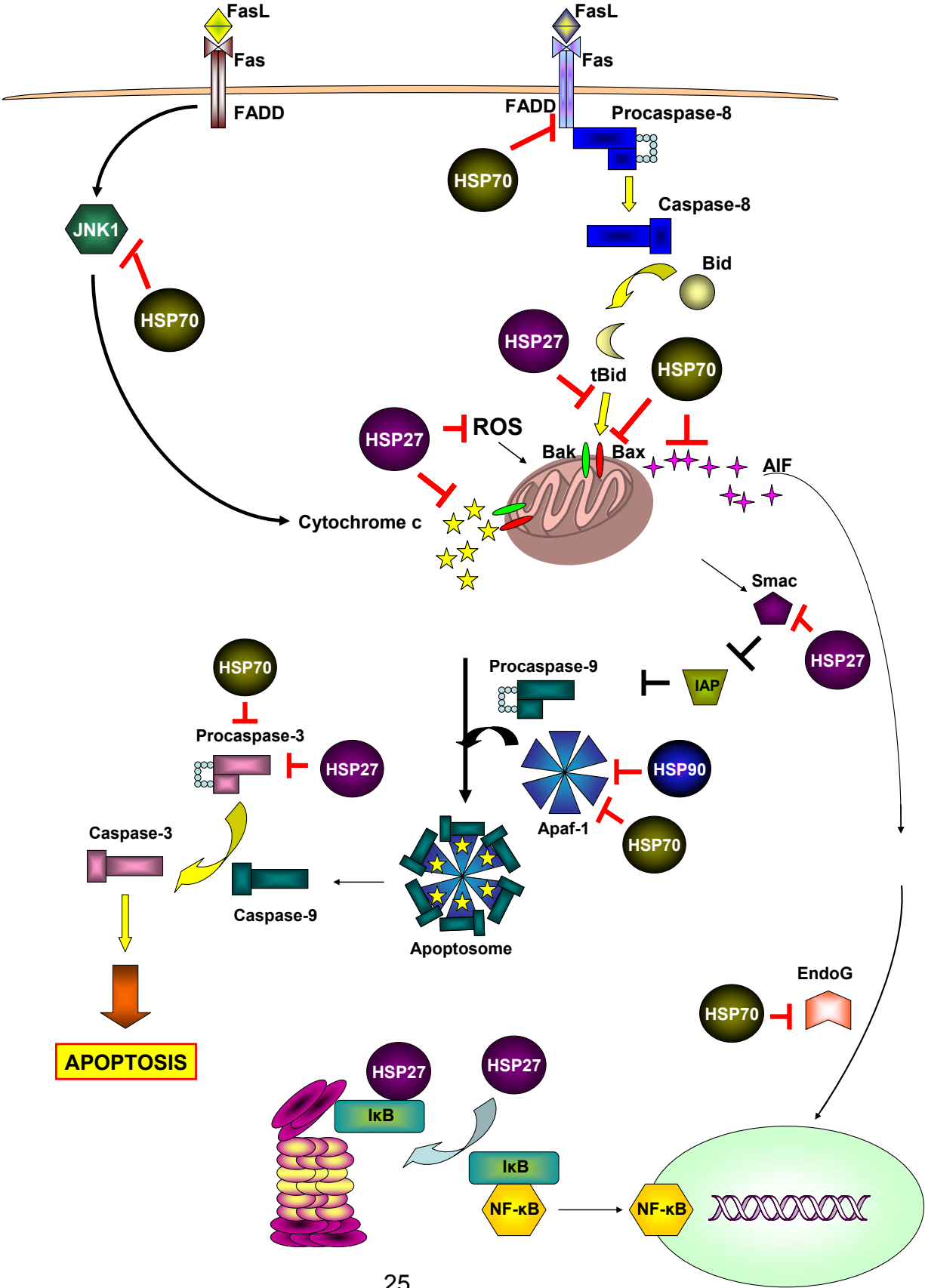
Antiapoptotic heat shock proteins

Certain heat shock proteins play a role in hindering the apoptotic process. Investigations in this area have explained the responsible protective mechanisms by which heat shock proteins can confer cell survival (Figure 5). For example, HSP90 binds to Apaf-1 protein blocking its oligomerization with cytochrome c and procaspase-9, thus inhibiting the formation of the apoptosome, cleavage of procaspase-9 and downstream activation of procaspase-3 (Pandey, Saleh et al. 2000).

Investigations of the prosurvival functions of HSP70 have demonstrated that it negatively regulates apoptosis by inhibiting caspase-dependent and caspase-independent apoptotic pathways. Inducible *HSP70* knockout studies in cells demonstrate that the abrogation of this protein can sensitize the cells to a variety of cytotoxic insults inducing apoptosis (Schmitt, Parcellier et al. 2003). In accordance to this finding, an augmentation of HSP70 levels in the cell blocks the apoptotic pathway c-Jun N-terminal kinase (JNK1). JNK1 positively regulates apoptosis by inducing cytochrome c release from the mitochondria and activating BH3-only proapoptotic proteins (Lei, Nimnual et al. 2002). HSP70 binds and inhibits JNK1 hindering its pro-apoptotic function (Park, Lee et al. 2001). HSP70 can also prevent Bax translocation to the mitochondria blocking mitochondrial membrane permeabilization (Stankiewicz, Lachapelle et al. 2005). Similar to HSP90, HSP70 has also been reported to inhibit apoptosome formation by binding to Apaf-1 and hindering its oligomerization in the presence of procaspase-9 and cytochrome c (Beere, Wolf et al. 2000; Saleh, Srinivasula et al. 2000). Moreover, this chaperone also appears to directly associate with procaspases-3 and -7 suppressing their activation (Komarova, Afanasyeva et al. 2004). HSP70 can also inhibit Fas-mediated apoptosis ultimately inhibiting mitochondrial membrane depolarization (Clemons, Buzzard et al. 2005). Proteins belonging to the caspase-independent cascade, such as the apoptosis-inducing factor (AIF), can also be

Figure 5. Antiapoptotic heat shock proteins

Figure 5



bound by HSP70 thus inhibiting their function (Ravagnan, Gurbuxani et al. 2001; Gurbuxani, Schmitt et al. 2003). AIF resides in the intracellular space of the mitochondria, which upon death stimuli is released to the cytosol and subsequently translocated to the nucleus where it induces chromatin condensation, one of the hallmarks of apoptosis (Susin, Lorenzo et al. 1999). HSP70 can also sequester endonuclease G, another mitochondrial resident, inhibiting its DNA-cleaving capabilities (Kalinowska, Garncarz et al. 2005).

HSP27 is another highly overexpressed heat shock protein that confers a cytoprotective effect against cancer therapy. This antiapoptotic chaperone appears to block apoptosis in prostate cell lines through inhibition of caspase-3 proteolysis as suggested by studies where HSP27 is silenced using small interference RNA (Rocchi, Jugpal et al. 2006). Studies have found that HSP27 not only sequesters important players in the mitochondrial apoptotic pathway such as cytochrome c and second mitochondria-derived activator of caspases, but also directly complexes with procaspase-3 repressing its activation (Pandey, Farber et al. 2000; Paul, Manero et al. 2002; Chauhan, Li et al. 2003). HSP27 can also hinder apoptosis even when no direct interaction is occurring with the pro-apoptotic proteins, for example, changes in HSP27 expression levels contribute to altered intracellular localization of the pro-apoptotic protein Bid (Paul, Manero et al. 2002). Additionally, HSP27 protects the cell against oxidative stress by reducing the levels of intracellular ROS species (Wyttenbach, Sauvageot et al. 2002; Lee, Lee et al. 2005). Radiation treatment induces mitochondrial-generated ROS species. The protein kinase c delta (PKC δ) has been implicated to have proapoptotic functions in the cell. PKC δ phosphorylates p38 MAP kinase which facilitates mitochondrial-mediated ROS generation and caspase-dependent apoptosis. In radiated cells, HSP27 inhibited activation of PKC δ (Lee, Lee et al. 2005). Unlike the other cytoprotective heat shock proteins, HSP27 has an important role in the stability of the actin network critical for the integrity of the cytoskeleton (Landry and Huot 1995; Mounier and Arrigo 2002). It has been suggested that cytoskeleton

disruption and release of cytochrome c through mitochondria-induced apoptosis are connected, however this cell death mechanism is abrogated by HSP27 overexpression (Paul, Manero et al. 2002).

Aside from its cytoprotective role in the mitochondrial pathway, HSP27 interacts with Akt kinase and regulates its kinase activity, negatively affecting apoptosis (Rane, Pan et al. 2003). Another important cytoprotective property of HSP27 is its ability to regulate the activity of the transcription factor nuclear factor κ B (NF- κ B). NF- κ B triggers the transcription of pro-survival proteins when activated, and in the cytosol its activity is kept repressed when complexed with its inhibitory protein I κ B α . HSP27 binds to the repressor I κ B α accelerating its ubiquitination and proteasomal degradation relieving the inhibitory effect on NF- κ B (Parcellier, Schmitt et al. 2003). In a similar manner, HSP27 promotes the ubiquitination and degradation of the cyclin-dependent kinase inhibitor p27 circumventing cell cycle arrest (Parcellier, Brunet et al. 2006).

In addition to these antiapoptotic cytosolic heat shock proteins, other chaperones localized in some cellular compartments possess cytoprotective properties. HSP90 and HSP70 endoplasmic reticulum homologues, GRP94 and GRP74, respectively, are known to provide cytoprotection from stress conditions that otherwise could have resulted in cell death (Reddy, Lu et al. 1999; Reddy, Mao et al. 2003; Ostrovsky, Ahmed et al. 2009). The mitochondrial HSP90 homologue TRAP-1 can protect the cells in tumorigenic tissue from apoptotic stimuli. For example, TRAP-1 protects the cell from mitochondria-mediated apoptosis induced by oxidative stress (Montesano Gesualdi, Chirico et al. 2007). TRAP-1 and HSP90 are overexpressed in the mitochondria of tumor cells in contrast to their low levels in mitochondria of non-malignant cells (Kang, Plescia et al. 2007). Interestingly, TRAP-1 appears to lack the client protein chaperone capabilities of its cytosolic paralog. Even though TRAP-1 has ATPase activity, it is not known to form stable complexes with any cochaperone. This renders TRAP-1 incapable of promoting client protein maturation (Felts,

Owen et al. 2000). However, in association with HSP90, both chaperones can bind to cyclophilin D inhibiting its pore-forming function in mitochondrial permeability transition and therefore block mitochondria-induced cell death. New classes of small molecule inhibitors, such as the GA-mitochondrial matrix inhibitors (gamitrinibs), are currently being developed to directly target HSP90 in the mitochondria of tumor cells and disrupt HSP90 association with TRAP-1 and cyclophilin D (Kang, Plescia et al. 2009).

Proapoptotic heat shock proteins

In contrast to the antiapoptotic properties of some heat shock proteins, there is also at least one chaperone that positively regulates apoptosis by modulating caspase activation. Via its chaperone activity, HSP60 can accelerate the proteolytic activation of procaspase-3 through caspase 6 stimulating the apoptotic process (Xanthoudakis, Roy et al. 1999). Although HSP60 can act alone in stimulating apoptosis, another study found that this chaperone can also be found in complex with HSP10 and procaspase-3 in the mitochondria activating procaspase-3 in the presence of cytochrome c and dATP (Samali, Cai et al. 1999). To reconcile the fact that HSP60 resides in the mitochondrial matrix and heat shock proteins are not known to play a role in the release of cytochrome c and subsequent caspase activation, it was suggested that in the late stage of apoptosis, mitochondria integrity is lost releasing its molecular content (such as HSP60) into the cytosol efficiently activating the caspase cascade (Samali, Cai et al. 1999). Interestingly, although HSP90 has been mainly associated with cell death repression, it is important to note that HSP90 expression can also exert proapoptotic properties in specific cell culture settings. For example, the proapoptotic protein JNK1 is a HSP90 client protein. Leukemic cells treated with the anticancer drug edelfosine need continual activation of JNK1 to undergo cell death. Treatment with HSP90 inhibitors diminished edelfosine-mediated cytotoxicity in these cells (Nieto-Miguel, Gajate et al. 2008).

Heat shock protein overexpression and cytotoxicity resistance

The antiapoptotic nature of the heat shock proteins allows the cell to evade cell death and become resistant to therapeutic agents. Multiple studies have reported that heat shock protein overexpression facilitates resistance to chemotherapeutic agent-induced cytotoxicity in various malignancies. HSP90 is overexpressed in Ewing sarcoma promoting resistance to insulin-like growth factor 1 receptor treatment (Martins, Ordonez et al. 2008). Induction of HSP70 in geldanamycin- or 17-AAG-treated leukemic cells conferred cell death resistance to doxorubicin (Demidenko, Vivo et al. 2006). HSP70 protein induction and accumulation occurs with 5-fluorouracil treatment in colorectal cancer cell lines protecting these malignant cells from apoptosis (Grivicich, Regner et al. 2007). Transfection and overexpression of HSP27 in colorectal cancer cells prevented doxorubicin- and cisplatin-induced cell death (Garrido, Ottavi et al. 1997). Studies have also reported that increased HSP27 protein levels block the cytotoxic effects of staurosporine and dexamethasone (Mehlen, Schulze-Osthoff et al. 1996; Chauhan, Li et al. 2003). Overexpression of endoplasmic reticulum chaperones, GRP94 and GRP78, can promote protection and cell survival from topoisomerase inhibitors (Reddy, Lu et al. 1999; Reddy, Mao et al. 2003).

In accordance to their cytoprotective effect, silencing of HSP90, HSP70, HSP27, or GRP94 protein expression results in sensitization to chemotherapeutic agents and induction of cell death (Reddy, Lu et al. 1999; Guo, Rocha et al. 2005; Rocchi, Jugpal et al. 2006; Aghdassi, Phillips et al. 2007; Chatterjee, Jain et al. 2007; Martins, Ordonez et al. 2008). Similarly, dual siRNA targeting of heat shock protein genes induces apoptosis in transformed cells (Powers, Clarke et al. 2008). Inability of a molecular chaperone to perform its chaperoning functions can result in loss of its cytoprotective capabilities. Mutations to the ATP-pocket in GRP78 resulted in abrogation of its antiapoptotic properties and sensitization to cytotoxic agents (Reddy, Mao et al. 2003).

The important chaperone function that HSP90 has in sustaining the functional conformation of several client oncoproteins makes it an attractive therapeutic target. As previously mentioned, the inhibition of HSP90 results in an elevation of antitapoptotic heat shock proteins (Bagatell, Paine-Murrieta et al. 2000). Evasion of the stress response that is elicited by inhibition of HSP90 is desirable. In order to circumvent the heat shock protein stress response inhibitors for chaperones other than HSP90 are currently being developed (Leu, Pimkina et al. 2009).

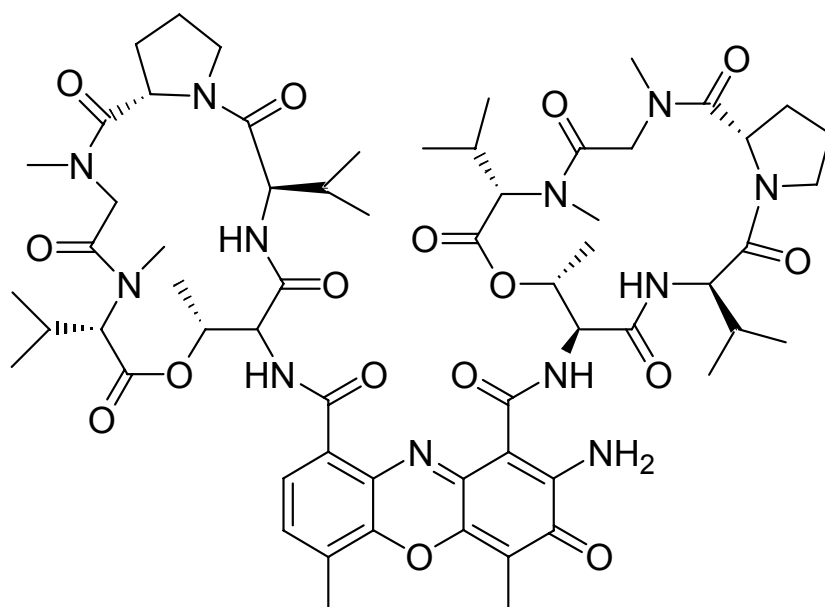
Another approach to block activation of the heat shock stress response could be through transcription and/or translation inhibition. Agents that can target transcription and/or translation could be use in combination with HSP90 inhibitors. This will abrogate augmentation of cytoprotective heat shock proteins or decrease levels of client proteins resulting in increase cytotoxicity. The transcription inhibitor Actinomycin C (Act D) and the ribonucleoside analogue 8-Chloro-Adenosine (8-Cl-Ado) are two examples of such agents.

Actinomycin D

The actinomycin family member Act D is one of the first antibiotics that was determined to posses anti-neoplastic activity (Figure 6) (Woodruff and Waksman 1960). This drug is isolated from the soil bacteria *Streptomyces* and was introduced in the clinic for the treatment of tumors in 1954 (Farber, Pinkel et al. 1956). Currently, this drug is mostly used in the clinic against various pediatric malignancies (Estlin and Veal 2003; Veal, Cole et al. 2005). Act D is an established transcription inhibitor that induces cytotoxicity by inhibiting global RNA synthesis (Perry and Kelley 1970). Act D acts by binding and intercalating into DNA (Gniazdowski, Denny et al. 2003). Its phenoxazone ring intercalates between bases and the peptide substituents bind to the minor groove of DNA, thus blocking the binding of RNA polymerase II and subsequently inhibiting RNA elongation (Sobell 1985; Gniazdowski, Denny et al. 2003).

Figure 6. Structure of Actinomycin D

Figure 6



8-Chloro-Adenosine

8-Chloro-Adenosine (8-Cl-Ado) is a ribonucleoside analog reported to cause *in vitro* cytotoxicity in several solid and hematological malignancies (Figure 7) (Zhang, Zheng et al. 1998; Gandhi, Ayres et al. 2001; Wang, Liu et al. 2004; Balakrishnan, Stellrecht et al. 2005; Gu, Zhang et al. 2006; Dennison, Balakrishnan et al. 2009; Stellrecht, Ayres et al. 2009; Yang, Jia et al. 2009). Unlike the DNA-directed analogs that are metabolized to the triphosphate derivative and incorporated into DNA during replication, 8-Cl-Ado is phosphorylated to the triphosphate and incorporated into RNA (Figure 8) (Stellrecht, Rodriguez et al. 2003). This ribonucleoside analog, is mono-phosphorylated by adenosine kinase and further phosphorylated to the di- and triphosphate forms by mono- and diphosphate kinases, respectively (Gandhi, Ayres et al. 2001). Unlike the metabolism of conventional nucleosides, the diphosphate compound 8-Cl-ADP, can also be phosphorylated to the cytotoxic 8-Cl-ATP by ATP synthase (Chen, Nowak et al. 2009).

8-Cl-Ado is believed to cause cellular toxicity through various mechanisms of action. Upon phosphorylation to its triphosphate form, 8-Cl-Ado is incorporated into RNA, with approximately 4.5 fold preferential incorporation into mRNA, causing mRNA synthesis inhibition (Stellrecht, Rodriguez et al. 2003). Stability of mRNA is further hindered by the ability of 8-Cl-ATP to inhibit polyadenylation by poly(A)polymerase (Chen and Sheppard 2004; Chen, Du-Cuny et al. 2010). Additionally, treatment of cells with 8-Cl-Ado results in a decrease of the endogenous cellular ATP pool with a concomitant increase in 8-Cl-ATP levels (Gandhi, Ayres et al. 2001). The metabolism of 8-Cl-Ado to its triphosphate form is achieved through distinct mechanisms. An abundant nucleoside kinase, adenosine kinase, was found to have high substrate specificity for this drug allowing 8-Cl-ATP to accumulate as high as 700 μM in multiple myeloma cells (Gandhi, Ayres et al. 2001). Given that 8-Cl-ATP is an ATP analog, it has been proposed that the diphosphate form of 8-Cl-Ado can serve as a substrate for ATP synthase and 8-Cl-ATP can act as a potential inhibitor of this enzyme

Figure 7. Structure of 8-Chloro-Adenosine

Figure 7

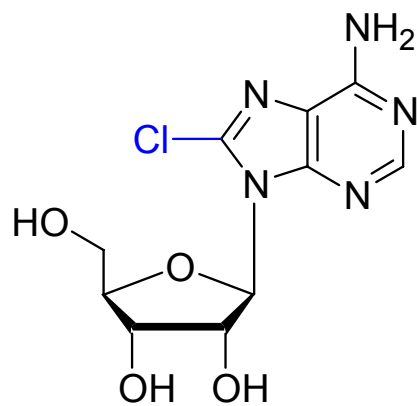
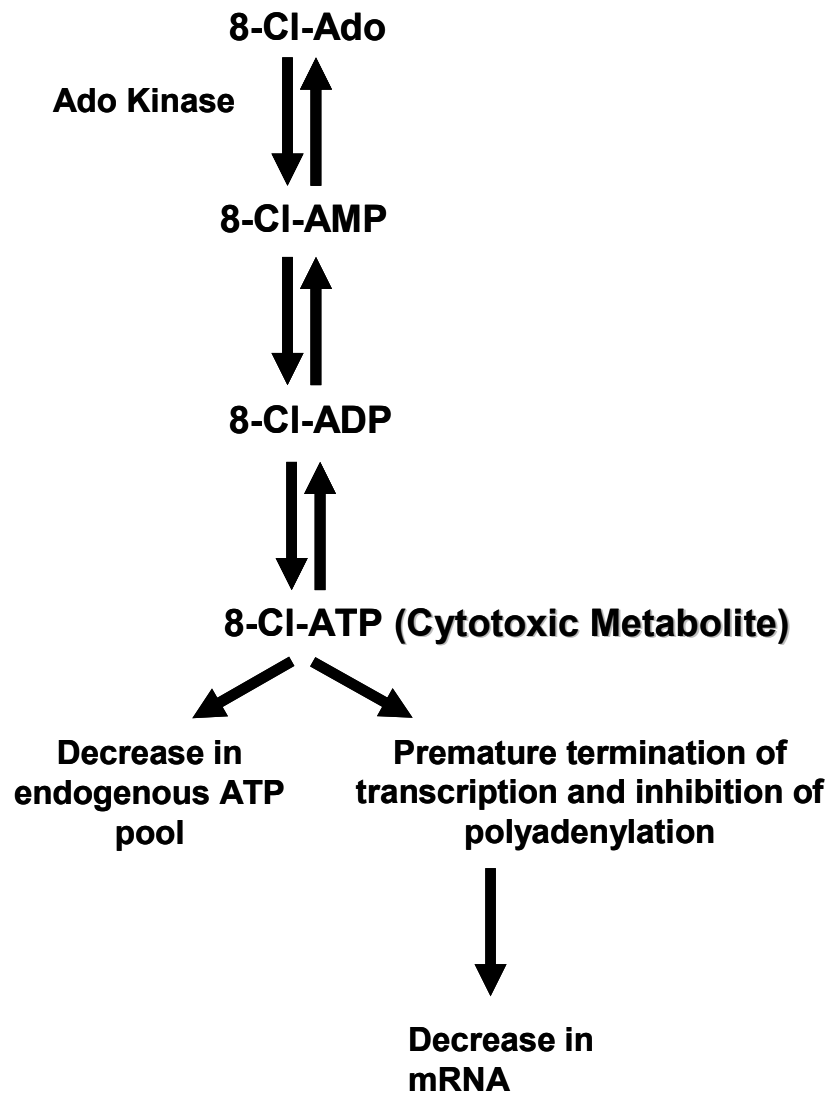


Figure 8. Metabolism of 8-Cl-Ado

Figure 8



(Chen, Nowak et al. 2009). Additionally, a recent study attributed the decline of cellular ATP to the succinylation of 8-Cl-Ado that results in the depletion of fumarate, an intermediate in the Krebs cycle, potentially affecting the production of ATP by oxidative phosphorylation (Dennison, Ayres et al. 2010). Due to the decline of cellular bioenergetics, this drug activates the mTOR/Akt autophagy pathways as a survival strategy in some tumor cell lines (Stellrecht, unpublished data). 8-Cl-Ado is currently in a phase I clinical trial for the treatment of chronic lymphocytic leukemia.

Multiple myeloma

HSP90 has been found to be overexpressed in several solid tumors and hematological malignancies including multiple myeloma (Bagatell and Whitesell 2004; Whitesell and Lindquist 2005; Chatterjee, Jain et al. 2007). Multiple myeloma is an indolent cancer of the plasma cell that is resistant to several chemotherapeutic agents (Dalton, Bergsagel et al. 2001). This hematological malignancy is characterized by high levels of monoclonal immunoglobulins (paraprotein) in the serum and/or urine, accumulation of plasma cells in the bone marrow and osteolytic lesions (Kuehl and Bergsagel 2002). At present, multiple myeloma is an incurable malignancy with a median survival of 3-5 years (Tassone, Tagliaferri et al. 2006). According to the 2009 cancer statistics, it was estimated that 20,580 individuals were diagnosed with multiple myeloma and 10,580 deaths from this disease occurred in this year in the United States alone (Jemal, Siegel et al. 2009). The first case report and description of multiple myeloma was presented by Dr. Solly in 1844 (Engelhardt and Mertelsmann 2006). However, it was not until 1962 that clinical investigators reported that the outcome of multiple myeloma patients could be improved with the alkylating agent melphalan (Bergsagel, Sprague et al. 1962). Traditional therapies for multiple myeloma have included other alkylating agents (cyclophosphamide), steroids (prednisolone, dexamethasone), and stem cell transplantation (Terpos, Rahemtulla et al.

2005). A major obstacle in the treatment of multiple myeloma is the acquired resistance to therapeutic agents that patients develop resulting in relapse of the disease (Dalton, Bergsagel et al. 2001). However, new treatments have recently surfaced. The proteasome inhibitor bortezomib (Velcade) was approved in 2003 and the immunomodulatory drugs, thalidomide (Thalomid) and lenalidomide (Revlimid), were approved in 2006 for the treatment of multiple myeloma (Rajkumar, Richardson et al. 2005; Strobeck 2007). Additional emerging anti-myeloma drugs include HSP90 inhibitors such as 17-AAG, histone deacetylase inhibitors, an Akt inhibitor, and monoclonal antibodies (Jagannath, Kyle et al. 2010).

Multiple myeloma is now perceived as a disease that arises due to genetic lesions involving translocations between immunoglobulin enhancers and oncogenes in addition to alterations in proliferation and survival signaling pathways (Bommert, Bargou et al. 2006). This malignancy is further fueled by the interaction between multiple myeloma cells and bone marrow stromal cells leading to enhanced expression and secretion of cytokines such as interleukin-6 (IL-6) that activate signaling cascades, which promote proliferation and resistance to apoptosis (Hideshima, Podar et al. 2005). Pathways that play a role in the biology of multiple myeloma and are activated due to cytokine secretion include PI-3K/Akt/mTOR, IKK/NF- κ B, Ras/Raf/MAPK as well as JAK/STAT3 cascades (Mitsiades, Mitsiades et al. 2006). Consequently, these pathways promote tumorigenesis by hindering the activation of proapoptotic proteins, upregulating antiapoptotic proteins and stimulating angiogenesis (Chng, Lau et al. 2005; Mitsiades, Mitsiades et al. 2006). Interaction of multiple myeloma cells with their milieu result in the upregulation of heat shock proteins which are necessary for the stabilization and functional conformation of proliferative and antiapoptotic proteins (Hideshima, Mitsiades et al. 2007). Disruption of cellular signaling networks is therefore desired when combining therapeutic agents.

Significance

Due to the chaperoning capabilities that HSP90 displays in sustaining tumorigenic cells, efforts to develop specific inhibitors for HSP90 have been pursued. HSP90 binds to partially folded client oncoproteins facilitating their refolding to a functional conformation state. Simultaneous downregulation of the client oncoproteins is achieved when the chaperone HSP90 is inhibited. Because this was a newly identified target, efforts to develop and test HSP90 inhibitors in preclinical and clinical settings were performed with large expectations. However, induction of antiapoptotic heat shock proteins and cell death resistance is an undesirable consequence stimulated by HSP90 inhibition. Hence, abrogation of the stress response is desired when using small molecules that target HSP90. The work in this dissertation investigates whether agents that inhibit transcription and/or translation can either abrogate the induction of heat shock proteins at the transcript or expression level or decrease client protein transcript and expression levels resulting in increase cytotoxicity.

HSP90 is overexpressed in several malignancies including multiple myeloma (Bagatell and Whitesell 2004; Whitesell and Lindquist 2005; Chatterjee, Jain et al. 2007). Multiple myeloma is a complex disease driven by multiple survival and proliferative signaling cascades that like many other neoplasms, relies on the chaperone HSP90 to remain functional. This malignancy was used as a model to evaluate the biological effect of the HSP90 inhibitor 17-AAG in combination with the transcription inhibitor Act D or the ribonucleoside analog 8-Cl-Ado, which inhibits transcription, translation and decreases cellular bioenergy. These combination strategies were designed as proof-of-principle in the utilization of these clinically used agents in conjunction with HSP90 inhibitors such as 17-AAG in the abrogation of the heat shock stress response or client protein downregulation.

CHAPTER 2: Materials and Methods

Cell lines

The cell line MM.1S was obtained from the laboratory of Drs. Nancy Krett and Steve Rosen (Robert H. Laurie Comprehensive Cancer Center, Northwestern University, Chicago, IL). The cell lines U266 and RPMI-8226 were obtained from the laboratory of Dr. William S. Dalton (H. Lee Moffitt Cancer Center and Research Institute, Tampa, FL). The MM (multiple myeloma) cell lines were maintained in RPMI 1640 (Life Technologies, Inc, Grand Island, NY) supplemented with 10% heat-inactivated fetal bovine serum (Fisher Scientific, Pittsburgh, PA) in the presence of 5% CO₂ at 37°C. Cells were routinely tested for *Mycoplasma* infection using a commercially available kit (Gen-Probe Inc, San Diego, CA). Approximate doubling times for MM.1S, U266, and RPMI-8226 are 48, 36, and 24 hours, respectively.

Materials

Actinomycin D (Act D) and 17-(Allylamino)-17-demethoxygeldanamycin (17-AAG) were purchased from Sigma-Aldrich Co. (St Louis, MO). Drugs were dissolved in dimethylsulfoxide at a concentration of 1000 µg/mL for Act D, and 1mM for 17-AAG. 8-Chloro-adenosine (8-Cl-Ado) was obtained from Dr. Vishnuvajjala Rao (Drug Development Branch, National Cancer Institute, Bethesda, MD) and it was dissolved in Milli-Q water (Millipore Corp., Billerica, MA) at a concentration of 10 mM. Aliquots were prepared for all drugs and stored at -20°C.

RNA synthesis

Global RNA synthesis was measured using [5, 6-³H]-uridine incorporation (37.2 Ci/mmol; Moraveck Biochemical Inc, Brea, CA). MM cells were left untreated or treated for

4, 8, and 12 hours with 0.05 µg/mL Act D. Thirty minutes prior to the end of incubation, the cells were labeled with [5, 6-³H]-uridine (1µCi/mL) at 37°C. MM cells were also left untreated or treated for 4 and 8 with 10 µM 8-Cl-Ado. One hour before the end of incubation, the cells were labeled with [5, 6-³H]-uridine (1µCi/mL) at 37°C. The labeled samples were harvested, washed with 10 mL of cold PBS and transferred to glass fiber filters (Whatman Inc, Clifton, NJ) using a Millipore vacuum manifold (Fisher Scientific, Pittsburgh, PA). The filters were then washed twice with 5mL of cold 0.4 N perchloric acid and rinsed once with 70% ethanol. The filters were dried overnight and transferred to scintillation vials containing 7 mL of High flash point cocktail scintillation fluid (Research Products International Corp, Mount Prospect, IL). The radioactivity on the filters was quantified by a liquid scintillation counter (Packard, Ramsey, MN). Data were expressed as a percentage of untreated control.

Isolation of RNA and quantitative real time RT-PCR

Total RNA was isolated using the RNeasy Mini kit (Qiagen, Valencia, CA) according to manufacturer's instructions. RNA concentration measurement was performed using the PowerWave XS Microplate Spectrometer and KC4 Data Analysis software (BioTek Instruments Inc, Winooski, VT). The relative transcript levels of gene expression were assessed using TaqMan One Step RT-PCR master mix reagents (Applied Biosystems, Foster City, CA) on an ABI prism 7900HT Sequence Detection System. Predesigned primers and TaqMan probes for thioredoxin 2 (TXN2), glyceraldehyde -3- phosphate dehydrogenase (GAPDH), HSP90α (HS00743767_sH), HSP90β (HS00607336_gH), HSP70 (HS00359147_s1), HSC70 (HS01683591_g1), HSP27 (HS00356629_g1), HSF-1 (HS01027619_m1), Akt1 (HS00920503_m1), STAT-3 (HS01047579_m1), and Raf-1 (HS00991918_m1) were purchased from Applied Biosystems. Contaminating DNA was removed from RNA preparations by using a commercially available DNA-free DNase

treatment and removal kit (Ambion, Austin, TX). To verify the absence of DNA in each RNA sample, a control reaction without reverse transcriptase was performed. Relative levels of HSP gene expression were determined by using standard curves and normalized either with the endogenous gene TXN2 or GAPDH. Experiments were done in triplicate and the results were plotted as fold change in comparison to untreated MM cells.

Protein extraction and immunoblot assays

Exponentially growing MM.1S, U266, and RPMI-8226 cells were treated with the various drugs as indicated. Cells were grown to a concentration of 5×10^5 cells per mL in 10 mL total per condition. Samples were harvested, centrifuged at 1,500 rpm for 5 minutes, and washed twice with PBS. Cells were lysed using one tablet of Complete Mini Protease Inhibitor Cocktail and one tablet of PhosSTOP Phosphatase Inhibitor Cocktail Tablets (Roche, Indianapolis, IN) in 10 mL of M-PER Mammalian Protein Extraction Reagent manufactured by Pierce (Rockford, IL). Lysates were centrifuged at 10,000 rpm for 10 minutes at 4°C and the supernatant collected and transferred to a different tube. Protein concentration was determined by DC protein assay (Bio-Rad Laboratories, Hercules, CA) per the manufacturer instructions. Quantitation of protein concentration was performed using the PowerWave XS Microplate Spectrometer and KC4 Data Analysis software (BioTek Instruments Inc.). Forty five µg of protein was mixed with 4X reducing agent and lysis buffer and boiled at 96°C for 10 minutes. For immunoblot analysis, protein samples were eletrophoresed on Criterion Bis-Tris Gels using the XT MOPS buffer kit (Bio-Rad Laboratories) for 2 hrs at 100 volts and transferred to NitroBind pure-nitrocellulose membranes (Osmotics Inc., Gloucester, MA) at 100V for 1 hr at 4°C. Membranes were then blocked with blocking buffer (LI-COR Biosciences, Lincoln, NE) for 1 hour at room temperature and probed for the indicated primary antibodies diluted in blocking buffer for 2 hours at room temperature. The membranes were washed three times with PBS-0.1%

Tween 20 for 5 minutes each and incubated with the secondary fluorescent antibody for 1 hour at room temperature. The same washing procedure was performed after this incubation. Immunoblots were imaged and quantified using Odyssey Infrared Imaging System (LI-COR Biosciences). Primary antibodies were purchased from the following sources: GRP78 (BiP), HSP90 α/β , HSP70, HSC70, HSP27, and HSF-1 (Stressgen, Ann Harbor, MI); Grp94 (2H3) (Abcam Inc, Cambridge, MA); STAT3 (124H6), Akt, and GAPDH (Cell Signaling Technology, Beverly, MA); c-Raf, BD Biosciences Pharmingen (San Jose, CA); β -actin (AC-15) (Sigma, Saint Louis, MO); RNA Polymerase II 8WG16 (Covance, Berkeley, CA); Alexa-Fluor 680 goat anti-mouse IgG, and Alexa-Fluor 800 goat anti-rabbit IgG (Molecular Probes, Eugene, OR).

Immunoprecipitation of HSP90 protein bound to [3 H] 17-AAG

Radioactive [allylamino-2, 3- 3 H]-17-AAG was synthesized by Moravsek Biochemicals. MM.1S cells (1×10^6 cells in 40 mL) were incubated with 0.5 μ M [allylamino-2, 3- 3 H]-17-AAG alone or the simultaneous combination of 0.5 μ M [allylamino-2, 3- 3 H]-17-AAG plus 10 μ M 8-Cl-Ado for 20 hours. Each condition was performed in duplicate. At the end of treatment period, cells were harvested and centrifuged at 1,500 rpm for 5 minutes, and washed once with PBS. Cells were lysed by sonication with one tablet of Complete Mini Protease Inhibitor Cocktail (Roche) and one tablet of PhosSTOP Phosphatase Inhibitor Cocktail Tablets (Roche) in 10mL $\frac{1}{2}$ X RIPA buffer (Upstate Biotechnology, Billerica, MA). The lysate was centrifuged at 10,000 rpm for 10 minutes at 4°C and the supernatant was collected and transferred to a 1.5 mL microcentrifuge tube. Each sample was precleared with 3% FBS-blocked Protein G Plus/Protein A-Agarose (Calbiochem EMD Biosciences, Gibbstown, NJ) for 20 minutes at 4°C. The blocked Protein G Plus/Protein A-Agarose solution was spun down and washed 3 times with cold $\frac{1}{2}$ X RIPA buffer before being used. The precleared lysates were spun down at 10,000 rpm for 1 minute at 4°C and supernatant

transferred to a new 1.5 mL microcentrifuge tube. Protein concentration was determined by DC protein assay (Bio-Rad) and quantified using the PowerWave XS Microplate Spectrometer and KC4 Data Analysis software (BioTek Instruments Inc.). Following this, 1 mg of protein per treatment sample was incubated for 2 hours at 4°C with either 20 µg of IgG mouse antibody (Santa Cruz Biotechnology, Santa Cruz, CA); 20 µg of HSP90α/β (Stressgen); or 5 µg of RNA Polymerase II 8WG16 (Covance) used as a negative control for possible [allylamino-2, 3-³H]-17-AAG binding. A fourth tube for each duplicate of each treatment containing only 1 mg of protein and ½ X RIPA buffer was also incubated under the same conditions. All samples were adjusted to 500 µL using ½ X RIPA buffer with the cocktail inhibitor tablets. After this incubation, 40 µL of Protein G Plus/Protein A-Agarose was added to each tube and allowed to incubate for 1 hour at 4°C. Samples were then centrifuged at 10,000 rpm for 1 minute at 4°C, the supernatant transferred to a new 1.5 mL microcentrifuged tube, and the immuno-radiolabeled precipitants washed twice with 1 mL of ½ X RIPA buffer. The 2 mL washes for each sample were not discarded, but set aside in 15 mL conical tubes. The [allylamino-2, 3-³H]-17-AAG contained in each sample condition was then analyzed by transferring the immuno-radiolabeled precipitants to scintillation vials containing 7 mL of High flash point cocktail scintillation fluid (Research Products International Corp).

In order to follow the material balance, the collected supernatant and 2 mL washes of each sample were also transferred to scintillation vials containing 7 mL of scintillation fluid. The radioactivity was quantified by a liquid scintillation counter (Packard).

The immunoprecipitation of untreated MM.1S cells was also done as described above followed by immunoblotting of HSP90α/β and RNA Polymerase II 8WG16 as previously mentioned in order to corroborate the assayed proteins were being pull down.

Annexin V cell death assay

MM cells were treated with the indicated combinations of drugs and time points. After treatment, cells (approximately 1×10^6 cells per condition) were harvested and spun down at 1,500 rpm for 5 minutes and washed twice with cold PBS. Samples were resuspended in 500 μ L 1X Annexin V binding buffer (BD Biosciences Pharmingen) and incubated with 5 μ L (0.25 μ g) 7-AAD (BD Biosciences Pharmingen) and 5 μ L (25 μ g) Annexin V-FITC (BD Biosciences Pharmingen) for 15 minutes in the dark at room temperature. Total cell death was analyzed using the BD FACSCalibur system (BD Biosciences Pharmingen). The endogenous cell death was subtracted from all the conditions, and the expected percentage of cells surviving after treatment with the combination was calculated using the fractional two-drug combinational analysis. To compare the expected and observed (Annexin V/7-AAD staining) levels of cell death for the different combinations, we first calculated the expected level of cell survival for the combination treatments. For example, the percentage of cells surviving 17-AAG treatment ($100\% - X\%$ Annexin V/7-AAD staining) was multiplied by the percentage of cells surviving Act D treatment ($100\% - X\%$ Annexin V/7-AAD staining) divided by 100. With this calculation, a comparison of the expected cell death versus the observed cell death was made for all the different drug combinations.

Perchloric acid extraction of intracellular nucleotides

MM cells were seeded at 5×10^5 cells per mL in 10 mL and treated with 8-Cl-Ado alone or 8-Cl-Ado and 17-AAG in combination as indicated. Cells were harvested after treatment and transferred to a 15 mL conical tube to be centrifuged at 1,500 rpm for 5 minutes at 4°C. The media was aspirated and the cells were resuspended in 10 mL of cold PBS, spun down at 1,500 rpm for 5 minutes at 4°C and PBS aspirated. After this washing procedure was performed twice, the cells were resuspended in 250 μ L of cold Milli-Q water

and 250 μ L of cold 0.8 N perchloric acid (PCA) was added to the suspended cells while gently vortexing. In order to lyse the cells, they were allowed to incubate for 5 minutes on ice. The samples were centrifuged at 1,500 rpm for 5 minutes at 4°C and the supernatant (nucleotides in PCA solution) was transferred to another 15 mL conical tube stored on ice. A second extraction was performed on the pelleted cell debris and nuclei by resuspending pellet in 250 μ L of cold 0.4 N PCA while gently vortexing and incubating on ice for 5 minutes. The sample was centrifuged at 1500 rpm for 5 minutes at 4°C. The supernatant from this second extraction was then added to the first extraction contained in the 15 mL conical tube stored on ice. In order to neutralize the PCA in the nucleotide solution, 10 N potassium hydroxide was added carefully to the 15 mL tube until a pH of 6-7 was achieved when tested with Hydrion pH test paper (Micro Essential Laboratory, Brooklyn, NY). The neutralized solution was centrifuged at 1,500 rpm for 5 minutes at 4°C. The supernatant was removed using a Hamilton glass syringe while taking care to avoid the pelleted salts. The sample was transferred to a 1.5 mL microcentrifuge tube; the volume was adjusted to 1 mL with Milli-Q water and stored at -20°C.

Intracellular nucleotide quantitation by HPLC

Nucleotide separation and quantitation were performed using high pressure liquid chromatography (HPLC). The neutralized PCA extracts were applied to an anion-exchange Partisil-10 SAX column at a flow rate of 1.5 mL per minute using a Waters 2697 Separations Module (Waters Corp., Milford, MA). The nucleotides were eluted with a 60 minute concave gradient from 60% 0.005 M $\text{NH}_4\text{H}_2\text{PO}_4$ (pH 2.8) and 40% 0.75 M $\text{NH}_4\text{H}_2\text{PO}_4$ (pH 3.7) to 100% 0.75 M $\text{NH}_4\text{H}_2\text{PO}_4$ (pH 3.7). Buffer solutions were prepared using HPLC reagent grade products, pH adjusted, and the solution filtered through a Millipore Type HA 0.45 μ M filter disc.

The column eluate was monitored by UV absorption at 257 nm with a Waters 2487 Dual λ Absorbance Detector and the nucleotide triphosphates were quantified by electronic integration with reference to standards for CTP, GTP, UTP, ATP, and 8-Cl-ATP. In order to quantitate the levels of radioactive 8-Cl-Ado and its metabolites, the HPLC was done using a Radiomatic Flow-through HPLC system (Packard, Downers Grove, IL). The cytotoxic analog triphosphate (8-Cl-ATP) was measured by comparing its retention profile and absorption spectrum with a standard.

The intracellular concentration of nucleotides of each sample was calculated from the measured number of cells and mean cell volume at the time of cell harvest. The cell number and volume was determined using the Beckman Coulter particle count and size analyzer.

Statistical analysis. One-tailed paired Student's *t*-test analyses were done using GraphPad Prism (GraphPad Software, San Diego, CA).

CHAPTER 3: Results

The chaperone HSP90 facilitates the refolding of denatured client oncoproteins. Inhibition of HSP90 chaperone activity by 17-AAG results in the proteasomal degradation of the client proteins. However, 17-AAG elicits a stress response causing the induction of antiapoptotic heat shock proteins leading to cell death resistance. Based on this, it was hypothesized that the mechanism-based combination of 17-AAG with agents that target antiapoptotic heat shock proteins and client proteins will result in an increase in cytotoxicity in multiple myeloma cells.

To investigate the cytotoxic effects of agents that inhibit transcription or translation in combination with 17-AAG, experiments were performed and divided into two aims.

AIM 1: Actinomycin D

17-AAG treatment results in a dose-dependent increase in heat shock proteins in MM.1S and RPMI-8226 cells

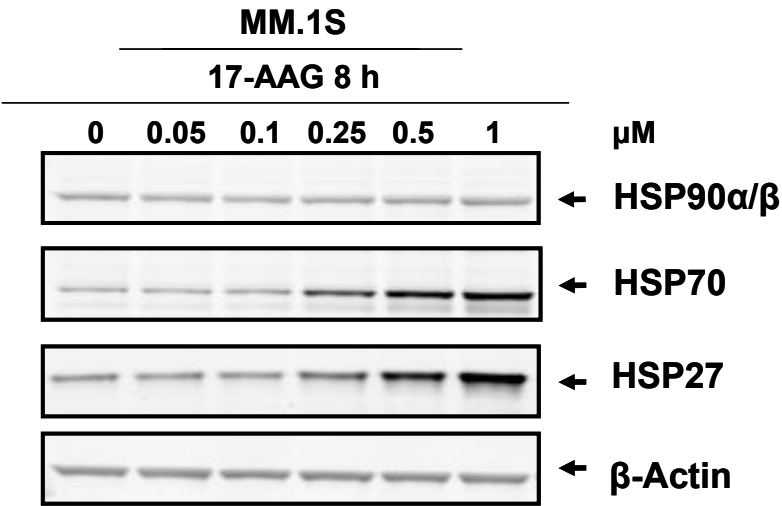
The HSP90 inhibitor, 17-AAG, induces the transcription of heat shock proteins in the cell (Bagatell, Paine-Murrieta et al. 2000). To determine the extent of 17-AAG induction of heat shock proteins in MM cells, a 17-AAG dose-response experiment was performed. MM.1S and RPMI-8226 cells were incubated with escalating doses of 17-AAG for 8 hours (Figure 9). Protein lysates were prepared and immunoblots were performed and subsequently analyzed for HSP90 α/β , HSP70, and HSP27 proteins. The housekeeping protein β -actin was used as a loading control. Early induction of HSP70 and HSP27 protein levels were observed with 0.25 μ M 17-AAG in both cell lines. In contrast, constitutive/stress-induced HSP90 levels did not change in either MM.1S or RPMI-8226 cells.

Figure 9. 17-AAG treatment results in a dose-dependent increase in heat shock proteins in MM.1S and RPMI-8226 cells

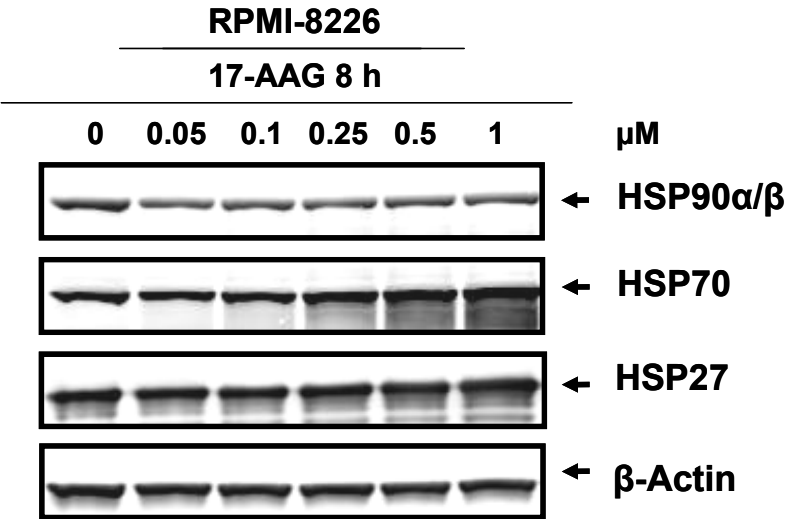
Cells were treated for 8 hours with 17-AAG at the indicated doses. Protein extracts were analyzed by immunoblot for inducible HSP90 α and constitutive HSP90 β , inducible HSP70, HSP27, and the loading control β -actin for MM.1S (A) as well as in RPMI-8226 cells (B).

Figure 9

A



B



17-AAG treatment results in a time-dependent increase in heat shock proteins in MM.1S and RPMI-8226 cells

To analyze time-dependent augmentation of heat shock proteins, MM cells were also treated with 0.5 μ M 17-AAG for 2, 4, 8, 12, and 24 hours and analyzed for protein expression of HSP90 α / β , HSP70, HSP27, and β -actin via immunoblots (Figure 10). Induction of HSP70 and HSP27 protein levels was observed as early as 4 hours in both MM.1S and RPMI-8226 cell lines. This level was either maintained or further increased with time. Conversely, HSP90 α / β levels remained fairly constant throughout the 24 hour treatment. The maximum concentration of DMSO at the highest 17-AAG dose (1 μ M) was 0.1%, and at this level of DMSO alone there was no change in the protein levels of any of the heat shock proteins. Based on the dose-response and time-dependent experiments, 0.5 μ M 17-AAG treatment for 8 hours was identified to test in combination with the transcription inhibitor Act D. The selected 17-AAG concentration is achievable in the clinic (Banerji, O'Donnell et al. 2005).

Act D treatment results in a dose-dependent decrease in heat shock proteins in MM.1S and RPMI-8226 cells

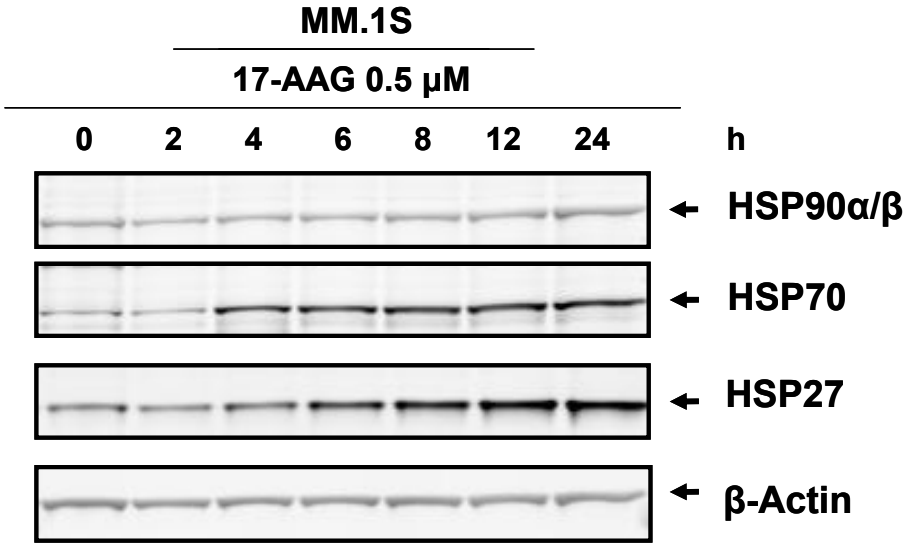
Act D is an established transcription inhibitor (Gniazdowski, Denny et al. 2003). In order to determine if Act D was able to diminish endogenous levels of heat shock proteins, cells were treated with escalating concentrations of Act D for 12 hours (Figure 11). Cells were harvested following treatment, and analyzed for HSP90 α / β , HSP70, HSP27, and β -actin protein levels via immunoblots. HSP27 protein expression was more sensitive to Act D when compared to the other heat shock proteins in both cell lines.

Figure 10. 17-AAG treatment results in a time-dependent increase in heat shock proteins in MM.1S and RPMI-8226 cells

Cells were treated with 0.5 μ M 17-AAG for the indicated times. Immunoblot analyses were performed to detect for inducible HSP90 α and constitutive HSP90 β , inducible HSP70, HSP27, and the loading control β -actin for MM.1S (A) as well as for RPMI-8226 cells (B).

Figure 10

A



B

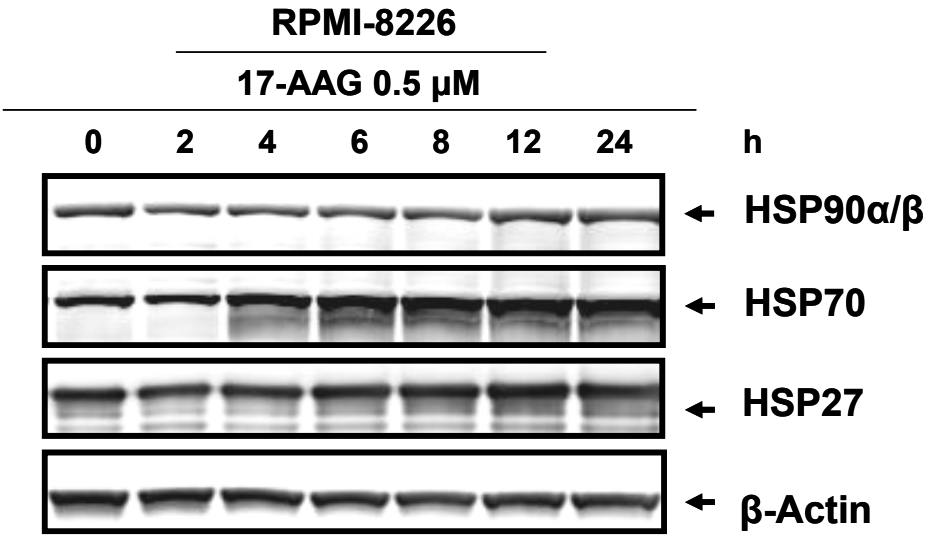
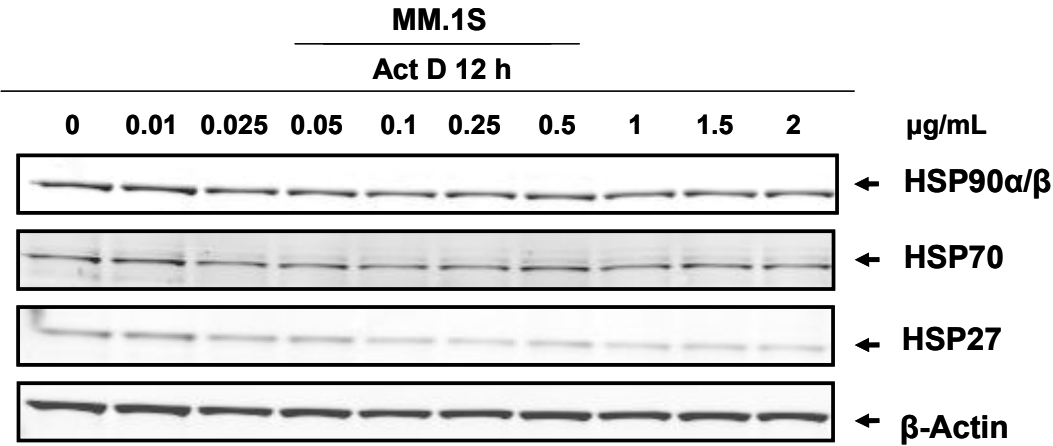


Figure 11. Act D treatment results in a dose-dependent decrease in heat shock proteins in MM.1S and RPMI-8226 cells

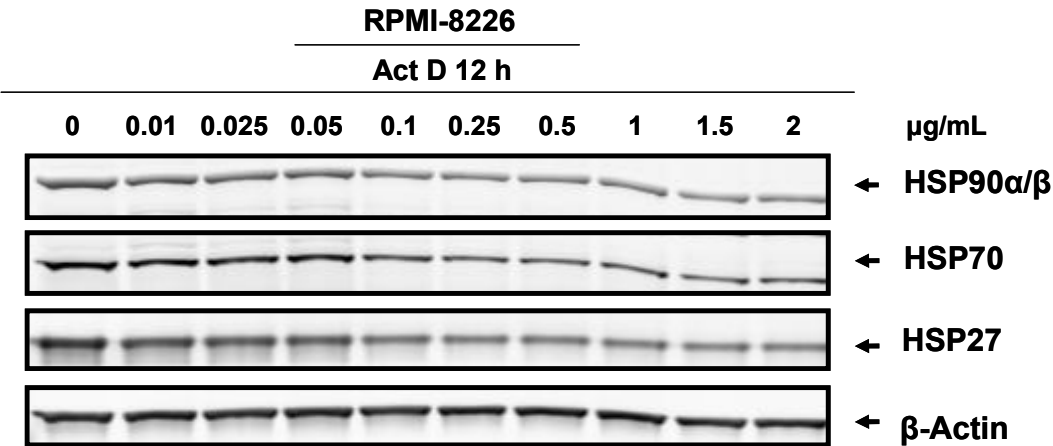
Cells were treated for 12 hours with Act D at the indicated doses. Protein extracts were analyzed by immunoblot for inducible HSP90 α and constitutive HSP90 β , inducible HSP70, HSP27, and the loading control β -actin for MM.1S (A) as well as in RPMI-8226 cells (B).

Figure 11

A



B



Act D treatment results in a time-dependent decrease in heat shock proteins in MM.1S and RPMI-8226 cells

To determine time-dependent changes, cells were treated with 0.05 µg/mL Act D for different time-points (Figure 12). Cells were harvested, immunoblot assays performed and analyzed for HSP90α/β, HSP70, HSP27 and the loading control β-actin. There was an evident reduction on all heat shock protein levels in MM.1S and RPMI-8226 by 30 minutes. This decline was maintained throughout the 24-hour treatment time. Since a longer treatment period was going to be needed to assess cytotoxicity of this agent, 0.05 µg/mL Act D treatment for 12 hours was selected to combine with 0.5 µM 17-AAG for 8 hours. The chosen concentration of Act D is attainable in the clinic (Veal, Cole et al. 2005).

Inhibition of global RNA synthesis by Act D in MM.1S and RPMI-8226 cells

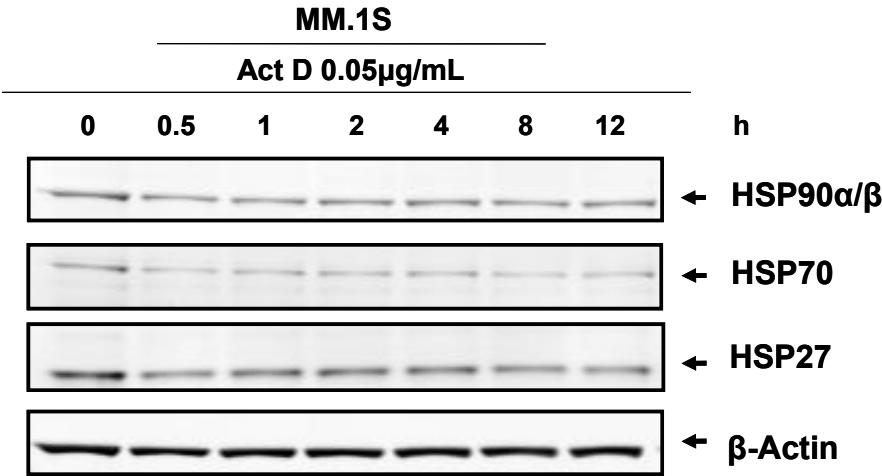
To determine if transcription inhibitor Act-D was able to reduce global RNA synthesis in both MM cell lines, a radioactive [³H]-uridine incorporation assay was performed. Cells were incubated with 0.05 µg/mL Act D for 4, 8, and 12 hours (Figure 13). Radiolabeled uridine isotope (1 µCi) was added to each experiment condition 30 minutes before the end of treatment. Cells were then harvested and total RNA was extracted. The levels of incorporated radiolabeled uridine were normalized to the untreated control. Each time point was performed in triplicate in three independent experiments conducted for each cell line. In MM.1S cells there was a 55, 70 and 80% global RNA inhibition at 4, 8, and 12 hours, respectively. RPMI-8226 cells were more sensitive to the transcription inhibitor Act D, suppressing global RNA by 70, 80 and 90% at 4, 8, and 12 hours, respectively.

Figure 12. Act D treatment results in a time-dependent decrease in heat shock proteins in MM.1S and RPMI-8226 cells

Cells were treated with 0.05 µg/mL Act D for the indicated times. Immunoblot analyses were performed to detect for inducible HSP90α and constitutive HSP90β, inducible HSP70, HSP27, and the loading control β-actin for MM.1S (A) as well as in RPMI-8226 cells (B).

Figure 12

A



B

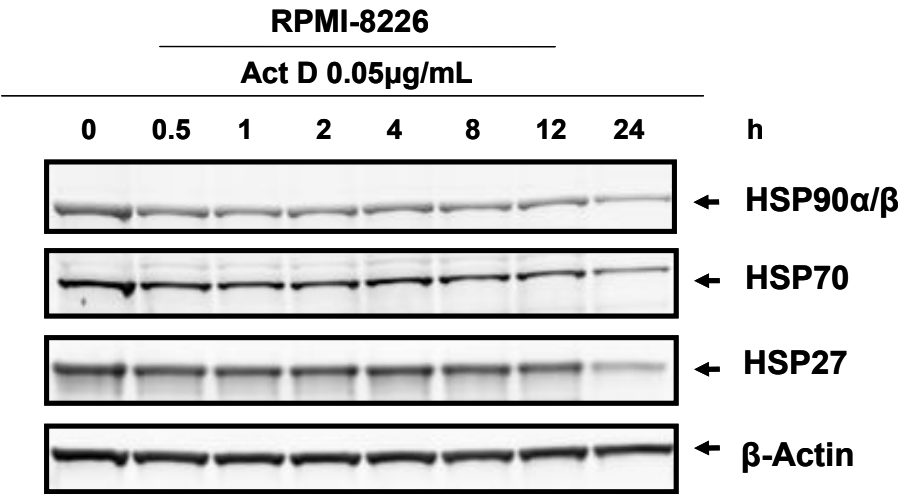
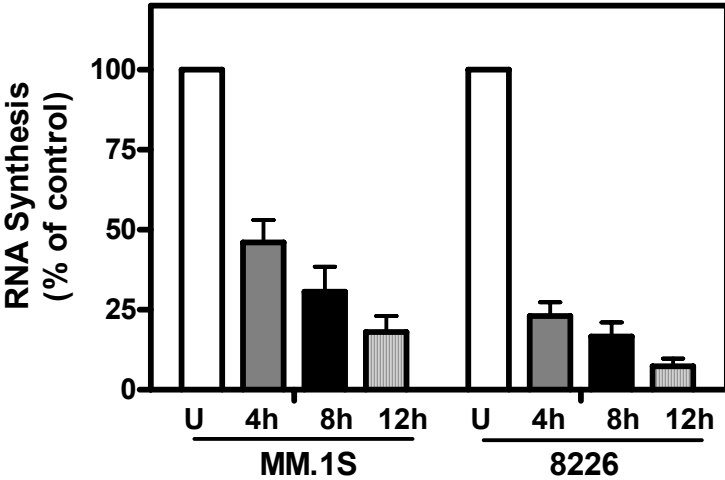


Figure 13. Inhibition of global RNA synthesis by Act D

MM.1S and RPMI-8226 cells were treated with 0.05 µg/mL Act D for the indicated time points, then incubated with [³H]uridine for the last 0.5 hour. Each column is plotted as the percentage of untreated control and represents the mean and SD of three independent experiments (62751±13970 DPM/ 5 x 10⁷ cells in untreated MM.1S cells and 74718±23476 DPM/ 5 x 10⁷ cells in untreated RPMI-8226 cells).

Figure 13



Inhibition of global RNA synthesis by Act D in combination with 17-AAG in MM.1S and RPMI-8226 cells

The HSP90 inhibitor, 17-AAG, elicits a stress response in the cell inducing the transcription of antiapoptotic heat shock proteins resulting in resistance to therapy and cell death (Bagatell, Paine-Murrieta et al. 2000; Beere, Wolf et al. 2000; Pandey, Farber et al. 2000; Pandey, Saleh et al. 2000). To evaluate if Act D could abrogate the 17-AAG-mediated induction of heat shock protein mRNA levels, a combination experiment was designed. The mechanism of action of Act D is to intercalate in the DNA and block elongation by RNA Pol II (Sobell 1985). A sequential combination where the transcription inhibitor was added first was chosen to allow time to Act D to intercalate and block transcription before addition of 17-AAG (Figure 14). MM cells were either not treated or treated with 0.5 μ M 17-AAG alone for 8 hours, a combination treatment with 0.05 μ g/mL Act D added first for 4 hours followed by 0.5 μ M 17-AAG for 8 hours, or 0.05 μ g/mL Act D alone for 12 hours. Radiolabeled uridine isotope (1 μ Ci) was added to each experiment condition 30 minutes before the end of treatment (Figure 15). Cells were then harvested and total RNA was extracted. The levels of incorporated radiolabeled uridine were normalized to the untreated control. Each time point was performed in triplicate in three independent experiments conducted for each cell line. MM.1S cells were sensitive to 17-AAG, suppressing global RNA by 40% compared to the untreated control. There was an 80% global RNA inhibition with Act D as a single agent and a 90% suppression of RNA synthesis with the combination treatment. RPMI-8226 cells treated with 17-AAG resulted in less than 10% inhibition of RNA synthesis. The combination condition and Act D treatment suppressed global RNA synthesis by 90% when compared to the untreated control.

Figure 14. Drug schedule for Act D and 17-AAG combination treatment

MM cells were either left untreated or treated with 0.5 μ M 17-AAG for 8 hours, the combination of Act D for 4 hours and then 17-AAG for 8 hours, or 0.05 μ g/mL Act D for 12 hours.

Figure 14

Drug schedule

Untreated control

17-AAG for 8 hours

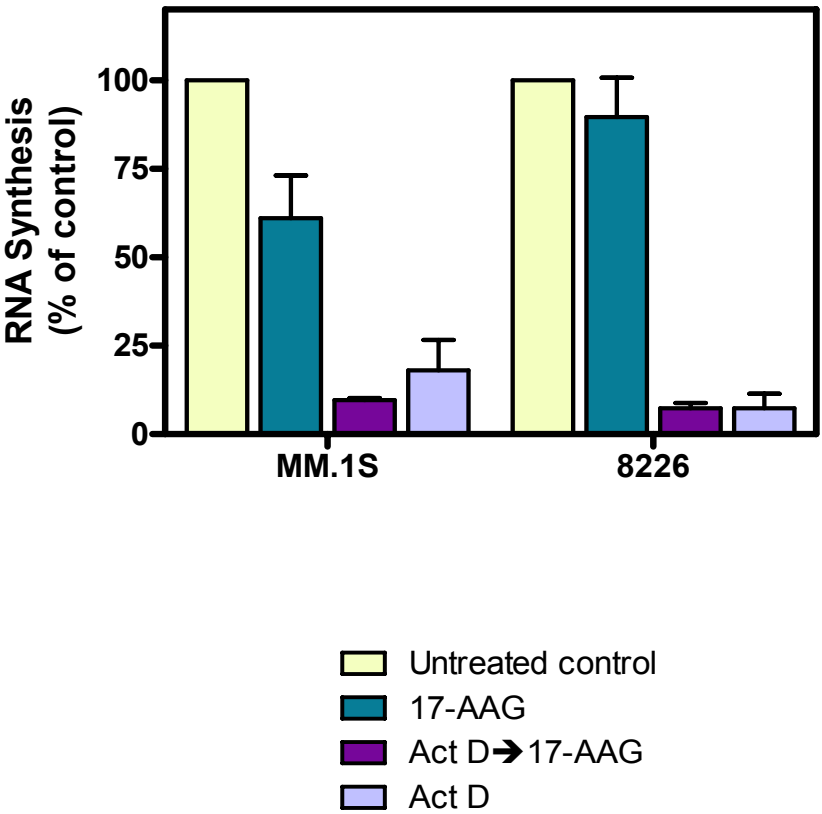
Act D 4 hours → 17-AAG 8 hours = 12 hours

Act D for 12 hours

Figure 15. Inhibition of global RNA synthesis by Act D

MM.1S and RPMI-8226 cells were either not treated or treated with 0.5 μ M 17-AAG for 8 hours, 0.05 μ g/mL Act D for 12 hours, or the combination of Act D for 4 hours and then 17-AAG for 8 hours. Condition treatments were then incubated with [3 H]uridine for the last 0.5 hour. Each column is plotted as the percentage of untreated control and represents the mean and SD of three independent experiments (62751 \pm 13970 DPM/ 5×10^7 cells in untreated MM.1S cells and 74718 \pm 23476 DPM/ 5×10^7 cells in untreated RPMI-8226 cells).

Figure 15



Effect of Act D and 17-AAG alone and in sequential combination on heat shock protein mRNA levels in MM.1S and RPMI-8226 cells

While uridine incorporation assay measures global RNA synthesis, it does not measure transcription induction of the specific heat shock proteins. Therefore, real time RT-PCR was performed to measure transcript levels of stress-inducible *HSP90α*, constitutive *HSP90β*, stress-inducible *HSP70*, constitutive *HSC70*, *HSP27* and *HSF-1* in the treated MM cells. MM cells were either not treated or treated with 0.5 μM 17-AAG alone for 8 hours, a combination treatment with 0.05 μg/mL Act D added first for 4 hours followed by 0.5 μM 17-AAG for 8 hours, or 0.05 μg/mL Act D alone for 12 hours. Cells were harvested following drug treatment and RNA isolated for each condition as described in materials and methods. Condition treatments were normalized using the housekeeping gene *TXN2* and the data plotted as fold change in comparison to the untreated control. Three independent experiments with each condition treatment done in triplicate were performed.

Act D diminished constitutive and stress-inducible *HSP90* mRNA induced by 17-AAG in MM.1S and RPMI-8226 cells

Specific probes were used to detect levels of the stress-inducible *HSP90α* and constitutive *HSP90β* human isoforms (Figure 16). *HSP90α* mRNA levels were increased following 17-AAG treatment by 3- and 4-fold in MM.1S and RPMI-8226, respectively (Figure 16A). Act D treatment alone decreased the endogenous levels of *HSP90α* transcripts compared to the untreated control in both cell lines. In the combination treatment, Act D was only able to abrogate the 17-AAG-induced *HSP90α* in a statistically significant manner in RPMI-8226. In MM.1S cells, the addition of Act D diminished 17-AAG-induced *HSP90α* transcript levels by 30%.

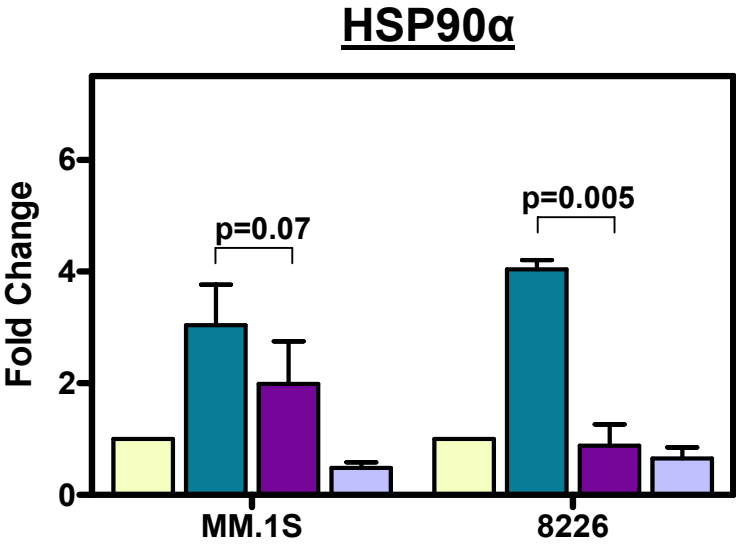
In contrast to the stress-inducible isoform of *HSP90α*, the constitutive *HSP90β* mRNA levels were induced in MM.1S and RPMI-8226 cells by less than 2-fold and by 2.5-

Figure 16. Act D diminished constitutive and stress-inducible HSP90 mRNA induced by 17-AAG in MM.1S and RPMI-8226 cells

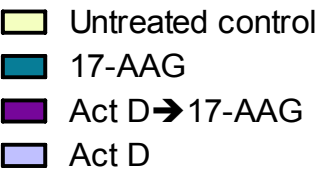
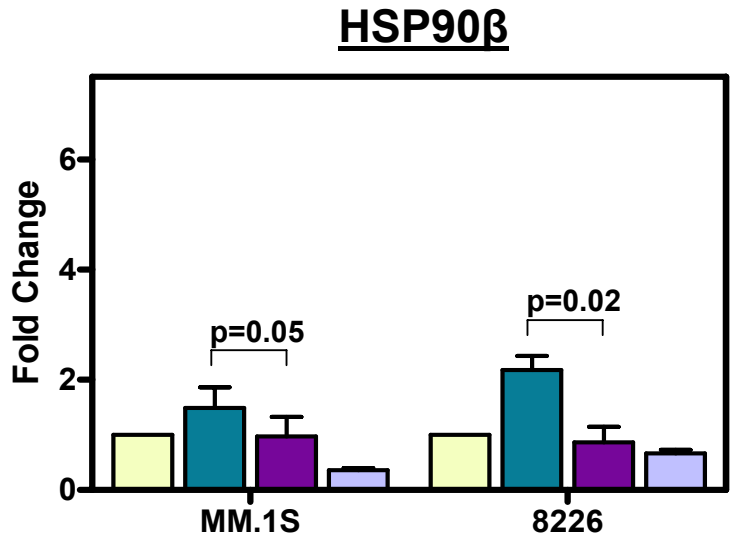
Cells were either not treated or treated with 0.5 μ M 17-AAG for 8 hours, 0.05 μ g/mL Act D for 12 hours, or the combination of Act D for 4 hours and then 17-AAG for 8 hours. Total RNA was isolated and inducible HSP90 α (A) and constitutive HSP90 β (B) mRNA levels were measured using real-time RT-PCR. TXN2 was used as the endogenous gene for normalization. mRNA levels are represented as fold change in comparison with the untreated control. Each column represents the mean and SD of triplicate experiments. Statistical significance ($p < 0.05$) comparing 17-AAG alone with the combination condition is shown.

Figure 16

A



B



fold, respectively (Figure 16B). This induction was reduced to basal levels as compared to the untreated control when both cell lines were treated with the combination treatment. Therefore, Act D was able to diminish the induction of *HSP90β* mRNA levels when cells are treated with the HSP90 inhibitor. The difference between *HSP90β* levels in the 17-AAG and the combination treatment were statistically significant ($p < 0.05$). Act D treatment as a single agent also resulted in a lessening of this transcript by more than 50% when compared to the untreated control in both cell lines.

Act D diminished constitutive *HSC70* but not stress-inducible *HSP70* mRNA induced by 17-AAG in MM.1S and RPMI-8226 cells

The specific levels of the stress-inducible *HSP70* and constitutive *HSC70* human isoforms were also evaluated (Figure 17). *HSP70* mRNA levels were induced as expected with 17-AAG treatment alone in both cell lines (Figure 17A). However, the 4- and 6-fold level induction measured for MM.1S and RPMI-8226 cells, respectively, was not diminished by addition of Act D in the combination condition. In fact, a statistically significant increase was measured for the combination treatment compared to 17-AAG as a single agent in RPMI-8226. Moreover, the transcription inhibitor by itself did not reduce the endogenous levels of this transcript in either cell line.

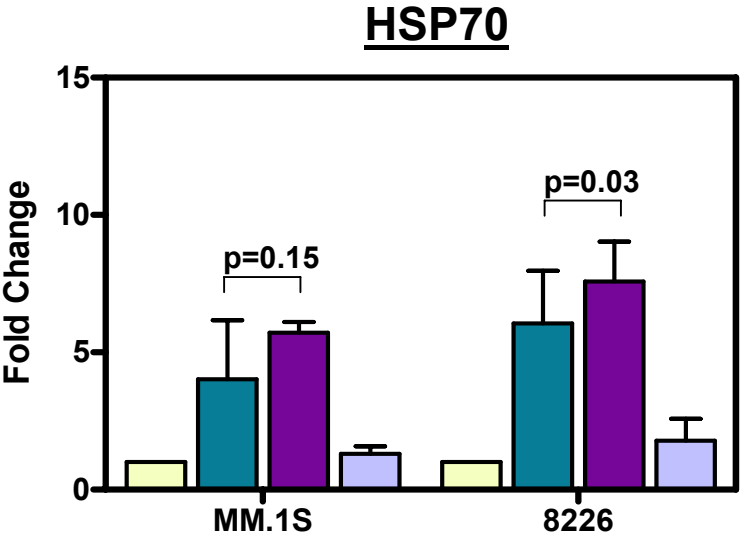
Although *HSC70* mRNA was also induced with 17-AAG treatment, it was not to the same extent as with its stress-inducible homologue *HSP70* (Figure 17B). 17-AAG treatment augmented *HSC70* transcript levels by 2- and approximately 4-fold in MM.1S and RPMI-8226 cells, respectively. This effect however, was blocked by adding Act D first followed by 17-AAG in the combination condition. *HSC70* levels in the combination treatment were similar to the transcript levels in the untreated control, which was detected to be statistically significant. In addition, endogenous *HSC70* mRNA levels were diminished by 90% with Act D treatment alone.

Figure 17. Act D diminished constitutive HSC70 but not stress-inducible HSP70 mRNA induced by 17-AAG in MM.1S and RPMI-8226 cells

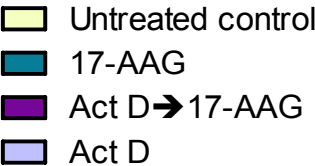
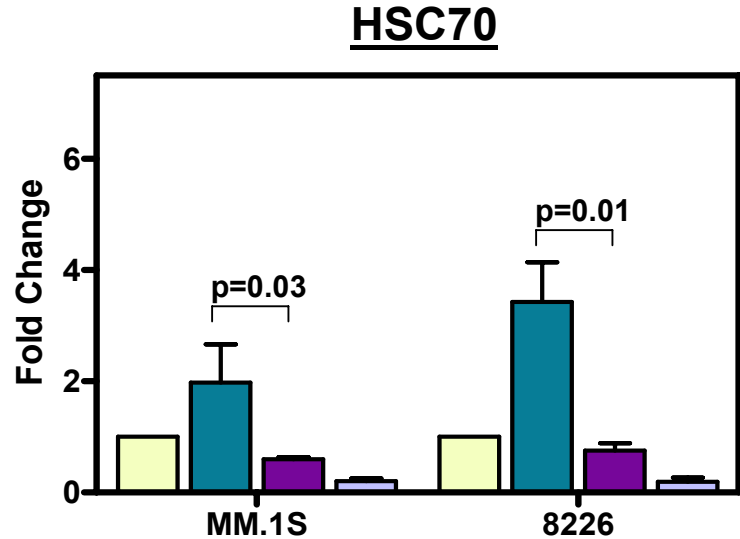
Cells were either not treated or treated with 0.5 μ M 17-AAG for 8 hours, 0.05 μ g/mL Act D for 12 hours, or the combination of Act D for 4 hours and then 17-AAG for 8 hours. Total RNA was isolated and inducible HSP70 (A) and constitutive HSC70 (B) mRNA levels were measured using real-time RT-PCR. TXN2 was used as the endogenous gene for normalization. mRNA levels are represented as fold change in comparison with the untreated control. Each column represents the mean and SD of triplicate experiments. Statistical significance ($p < 0.05$) comparing 17-AAG alone with the combination condition is shown.

Figure 17

A



B



Act D diminished *HSP27* mRNA induced by 17-AAG in MM.1S and RPMI-8226 cells

The specific levels of *HSP27* were also quantified (Figure 18). *HSP27* levels were induced with 17-AAG treatment by 20-fold in MM.1S cells but only induced 10-fold with the combination treatment. This suggests that Act D was able to partially block induction of this transcript when added before 17-AAG. In RPMI-8226 cells, 17-AAG treatment alone induced *HSP27* mRNA levels by 10-fold. This was abrogated by Act D in the combination treatment since only a 2-fold induction of *HSP27* transcript was measured for this condition. Unlike the decrease observed in MM.1S cells, the reduction of *HSP27* mRNA levels for the combination treatment in RPMI-8226 was statistically significant when compared to 17-AAG treatment alone. Also, Act D as a single agent reduced *HSP27* transcript levels by 50% compared to the untreated control in both cell lines.

Act D diminished *HSF-1* mRNA in MM.1S and RPMI-8226 cells

Following cellular stress, the transcription factor *HSF-1* is released from *HSP90* and subsequently phosphorylated by cytoplasmic kinases. Once in the hyperphosphorylated state, *HSF-1* trimerizes and translocates to the nucleus binding DNA and triggering transcription of heat shock proteins (Wu 1995). Contrary to heat shock proteins mRNA levels, *HSF-1* transcript levels were not increased following the addition of 17-AAG in either cell line (Figure 19). However, Act D alone or in combination diminished the basal *HSF-1* mRNA levels by 50% in both MM cell lines. The difference between the *HSF-1* transcripts measured for 17-AAG alone and the combination treatment was statistically significant in both MM cell lines.

Taken together, these results indicate that in MM.1S cells the heat shock protein mRNA 17-AAG-mediated induction was abrogated by Act D in a statistically significant manner for the constitutive heat shock protein transcripts (*HSP90 β* and *HSC70*) and the

Figure 18. Act D diminished HSP27 mRNA induced by 17-AAG in MM.1S and RPMI-8226 cells

Cells were either not treated or treated with 0.5 μ M 17-AAG for 8 hours, 0.05 μ g/mL Act D for 12 hours, or the combination of Act D for 4 hours and then 17-AAG for 8 hours. Total RNA was isolated and HSP27 mRNA levels were measured using real-time RT-PCR. TXN2 was used as the endogenous gene for normalization. mRNA levels are represented as fold change in comparison with the untreated control. Each column represents the mean and SD of triplicate experiments. Statistical significance ($p < 0.05$) comparing 17-AAG alone with the combination condition is shown.

Figure 18

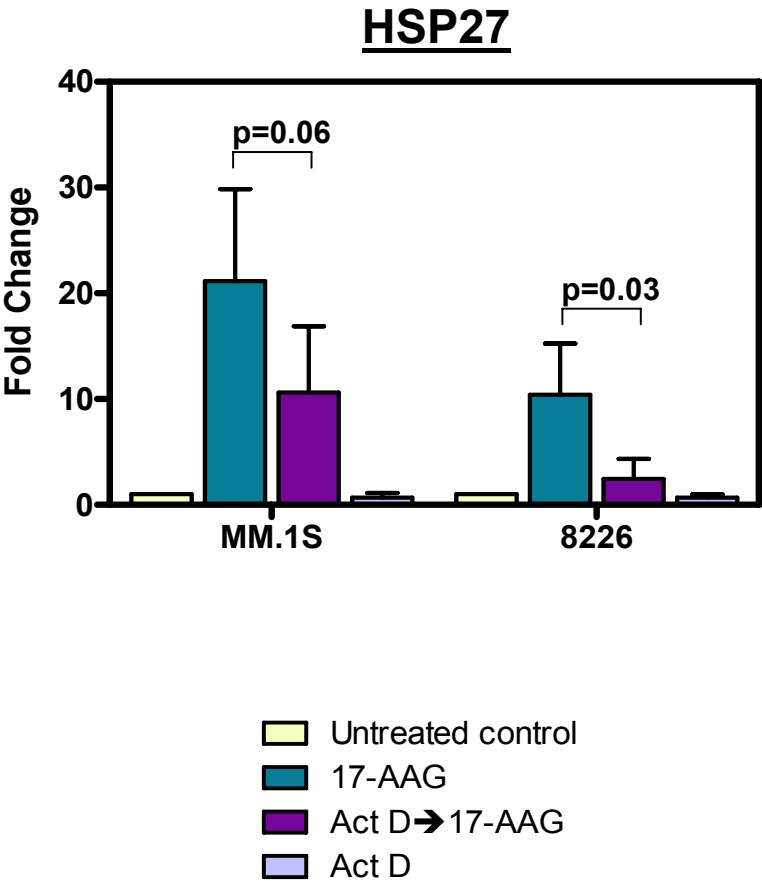
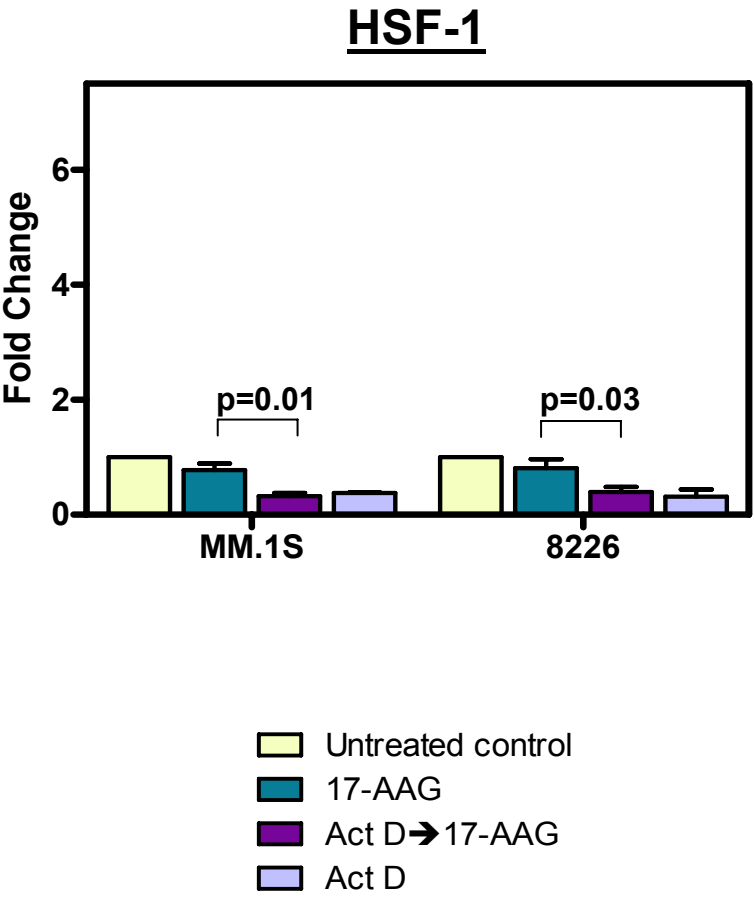


Figure 19. Act D diminished HSF-1 mRNA in MM.1S and RPMI-8226 cells

Cells were either not treated or treated with 0.5 μ M 17-AAG for 8 hours, 0.05 μ g/mL Act D for 12 hours, or the combination of Act D for 4 hours and then 17-AAG for 8 hours. Total RNA was isolated and HSF-1 mRNA levels were measured using real-time RT-PCR. TXN2 was used as the endogenous gene for normalization. mRNA levels are represented as fold change in comparison with the untreated control. Each column represents the mean and SD of triplicate experiments. Statistical significance ($p < 0.05$) comparing 17-AAG alone with the combination condition is shown.

Figure 19



transcription factor *HSF-1*. In RPMI-8226 cells, Act D abrogated the 17-AAG-mediated induction of all heat shock protein transcripts in a statistically significant manner except for *HSP70* mRNA. Act D also reduced the levels of the transcription factor *HSF-1*.

Act D diminished 17-AAG-mediated induction of heat shock protein and HSF-1 expression levels in MM.1S and RPMI-8226 cells

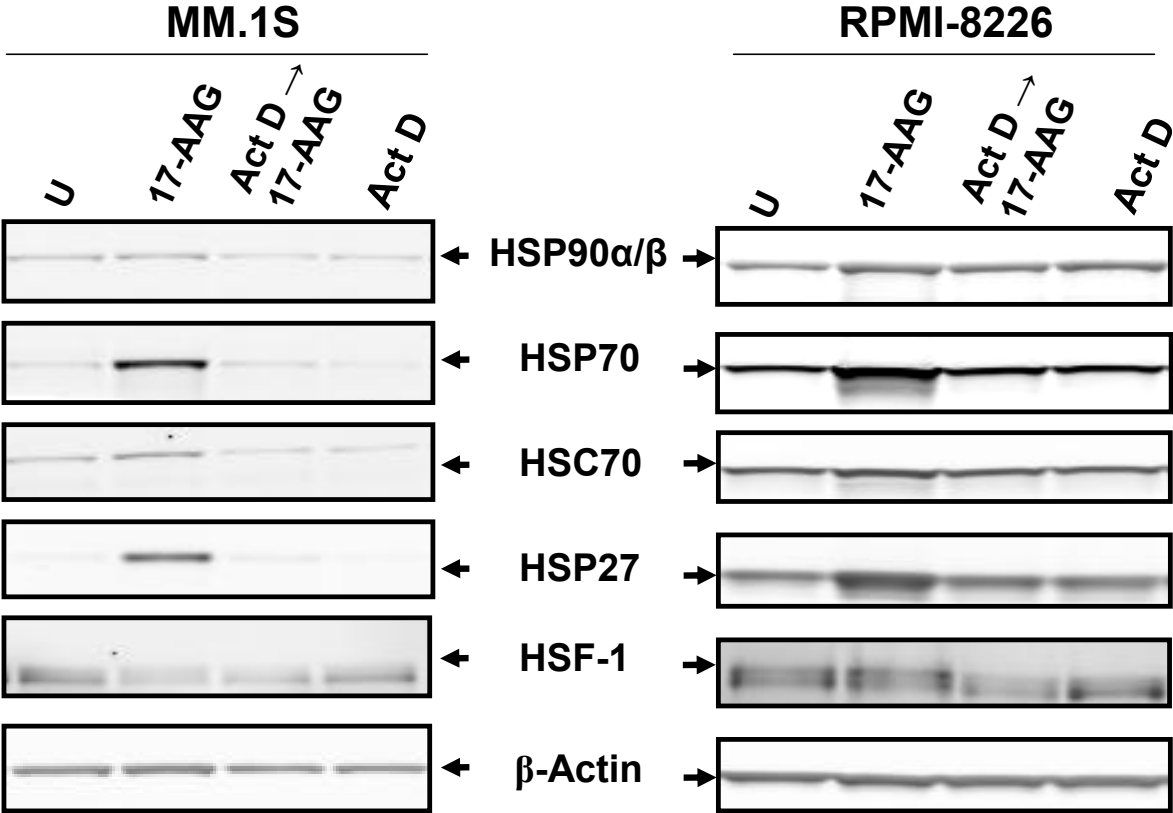
To determine if the decrease in mRNA transcripts results in decreased protein levels, immunoblot analyses were performed to assess if Act D and 17-AAG combination treatment resulted in heat shock protein expression decrease. The same sequential combination treatment used in the analysis of heat shock protein transcript levels was followed. MM cells were either not treated or treated with 0.5 μ M 17-AAG alone for 8 hours, a combination treatment with 0.05 μ g/mL Act D added first for 4 hours followed by 0.5 μ M 17-AAG for 8 hours, or 0.05 μ g/mL Act D alone for 12 hours. The cells were harvested following drug treatment and analyzed for HSP90 α / β , HSP70, HSC70, HSP27, HSF-1 and the loading control β -actin via immunoblots (Figure 20). In both cell lines there was an induction of all heat shock proteins when treated with 17-AAG. However, the levels of the transcription factor HSF-1 remained at endogenous levels when compared to the untreated condition. Treatment with Act D alone did not cause a further reduction of endogenous heat shock proteins or HSF-1. Addition of Act D at the beginning in the combination treatment though was able to abrogate the stress response triggered by 17-AAG treatment. The expression of the heat shock proteins and HSF-1 was maintained at endogenous levels with the combination of both agents.

To quantify the abrogation by Act D of 17-AAG-mediated inducible and constitutive heat shock protein and HSF-1 expression in the combination treatment, three independent immunoblots were completed for each MM cell line. The same sequential combination

Figure 20. Act D diminished 17-AAG-mediated induction of heat shock protein and HSF-1 expression levels in MM.1S and RPMI-8226 cells

Cells were either not treated (U) or treated with 0.5 μ M 17-AAG for 8 hours, 0.05 μ g/mL Act D for 12 hours, or the combination of Act D for 4 hours and then 17-AAG for 8 hours. Heat shock protein and HSF-1 protein levels for these conditions were visualized on immunoblots using antibodies for inducible HSP90 α and constitutive HSP90 β , inducible HSP70, constitutive HSC70, HSP27, HSF-1, and the loading control β -actin for MM.1S and RPMI-8226 cells.

Figure 20



design and analysis was performed. Stress-inducible and constitutive heat shock proteins and HSF-1 levels were normalized with the endogenous control β -actin and the fold change was compared to the untreated control for each protein. The p value compares the treatment with 17-AAG alone and the combination treatment (Figure 21, 22, 23 and 24).

Act D diminished 17-AAG-mediated induction of HSP90 α / β expression levels in MM.1S and RPMI-8226 cells

In MM.1S cells, HSP90 α / β levels were increased by two fold following 17-AAG treatment (Figure 21). Act D alone did not affect the expression of stress-inducible/constitutive HSP90; however in the combination treatment the transcription inhibitor abrogated the induction of HSP90 α / β protein levels. The decrease in the combination treatment was not statistically different from the 17-AAG-induced HSP90 α / β levels. In RPMI-8226 cells, HSP90 α / β levels were only slightly increased with the HSP90 inhibitor 17-AAG (Figure 21). Levels in the combination treatment remained at endogenous levels as well with Act-D treatment as a single agent. There is however, a statistically significant difference in the HSP90 α / β protein levels between 17-AAG and the combination treatment.

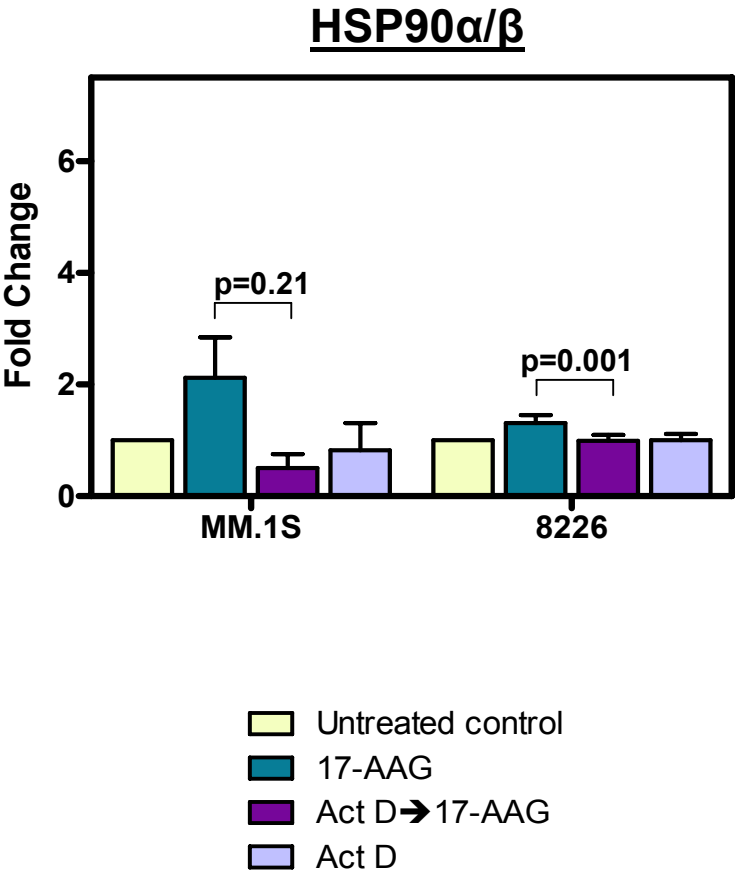
Act D diminished 17-AAG-mediated induction of constitutive HSC70 and stress-inducible HSP70 expression levels in MM.1S and RPMI-8226 cells

In the cell line MM.1S, the protein levels of stress-inducible HSP70 were increased by 10-fold with 17-AAG alone but no significant change was observed for Act D treatment alone (Figure 22A). The combination treatment resulted in a lesser induction of HSP70 protein levels but this was not diminished to endogenous levels nor was it statistically significant. Conversely, the constitutive levels of HSC70 were only induced 2-fold with the HSP90 inhibitor, which was abrogated by Act D in the combination treatment in a

Figure 21. Act D diminished 17-AAG-mediated induction of HSP90 α / β expression levels in MM.1S and RPMI-8226 cells

Immunoblot analysis was performed in triplicate and quantified using Odyssey infrared imaging system application software (version 1.2). Protein levels for HSP90 α / β were normalized to β -actin. Data represents three independent immunoblots plotted as means plus SD. Statistical significance ($p < 0.05$) comparing 17-AAG alone with the combination condition is shown.

Figure 21



statistically significant manner (Figure 22B). HSP70 expression was induced by less than 5-fold in RPMI-8226 cell line when treated with the HSP90 inhibitor (Figure 22A). And although HSP70 levels in the combination treatment were close to endogenous levels, this difference between the two treatments was not statistically significant. The constitutive levels of the HSP70 homologue, HSC70, were not substantially increased with 17-AAG treatment (Figure 22B). However the combination treatment abrogated this slight induction in a statistically significant manner.

Act D diminished 17-AAG-mediated induction of HSP27 expression levels in MM.1S and RPMI-8226 cells

In MM.1S cells, HSP27 protein levels were increased with 17-AAG by 10-fold and although the combination of Act D and 17-AAG maintained the levels of this chaperone close to endogenous levels, the results were not statistically significant (Figure 23). In RPMI-8226 cells, HSP27 protein levels were also induced following 17-AAG treatment, which was abrogated by Act D in the combination treatment and was statistically significant (Figure 23).

Act D in combination with 17-AAG diminished HSF-1 expression levels in MM.1S and RPMI-8226 cells

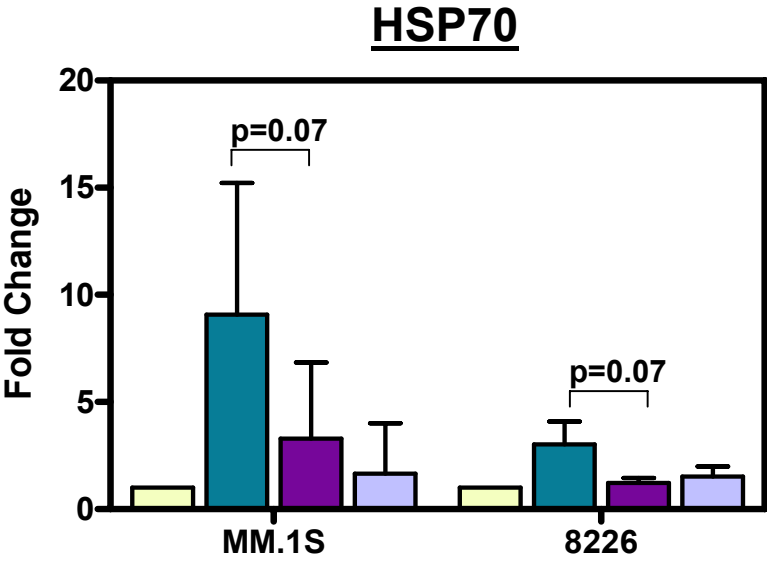
Finally, HSF-1 expression levels were also measured for each condition treatment showing some statistically significant decrease in the combination treatment compared to the levels in the 17-AAG treatment condition in MM.1S cells (Figure 24). In RPMI-8226 cells, HSF-1 protein levels remained at endogenous levels under all conditions, except the combination treatment (Figure 24). A 50% reduction in HSF-1 protein compared to the untreated control was measured in the combination condition, which was statistically significant ($p < 0.05$).

Figure 22. Act D diminished 17-AAG-mediated induction of constitutive HSC70 and stress-inducible HSP70 expression levels in MM.1S and RPMI-8226 cells

Immunoblot analysis was performed in triplicate and quantified using Odyssey infrared imaging system application software (version 1.2). Protein levels for stress-inducible HSP70 (A) and constitutive HSC70 (B) were normalized to β -actin. Data represents three independent immunoblots plotted as means plus SD. Statistical significance ($p < 0.05$) comparing 17-AAG alone with the combination condition is shown.

Figure 22

A



B

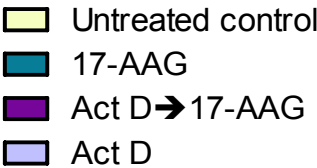
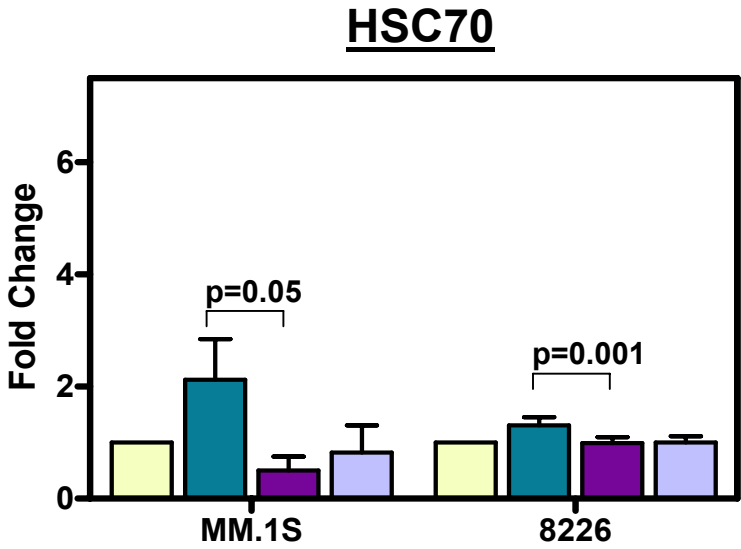


Figure 23. Act D diminished 17-AAG-mediated induction of HSP27 expression levels in MM.1S and RPMI-8226 cells

Immunoblot analysis was performed in triplicate and quantified using Odyssey infrared imaging system application software (version 1.2). Protein levels for HSP27 were normalized to β -actin. Data represents three independent immunoblots plotted as means plus SD. Statistical significance ($p < 0.05$) comparing 17-AAG alone with the combination condition is shown.

Figure 23

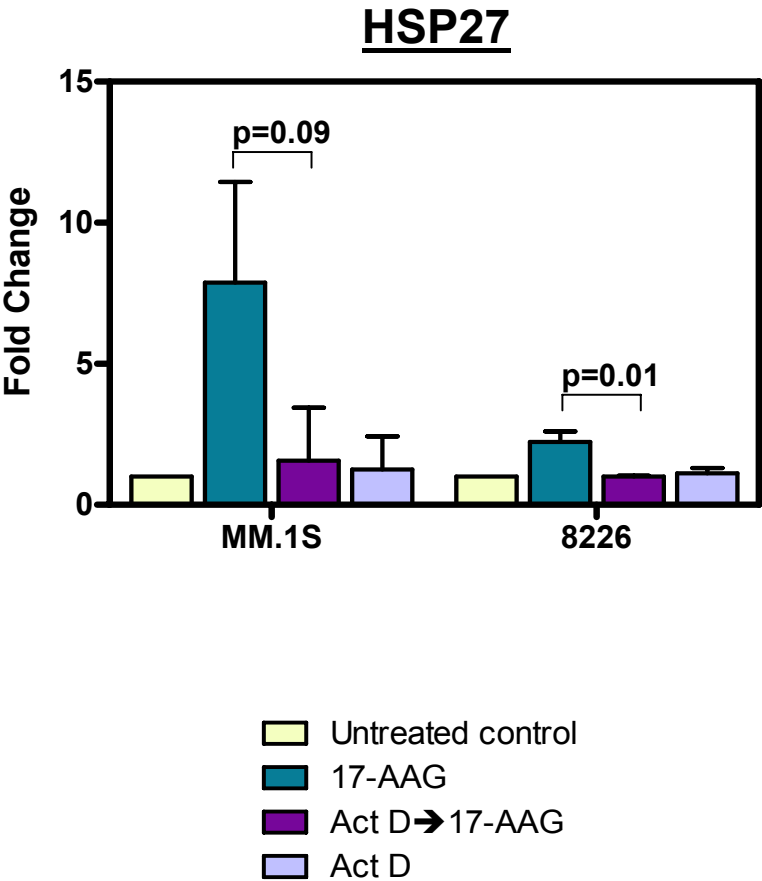
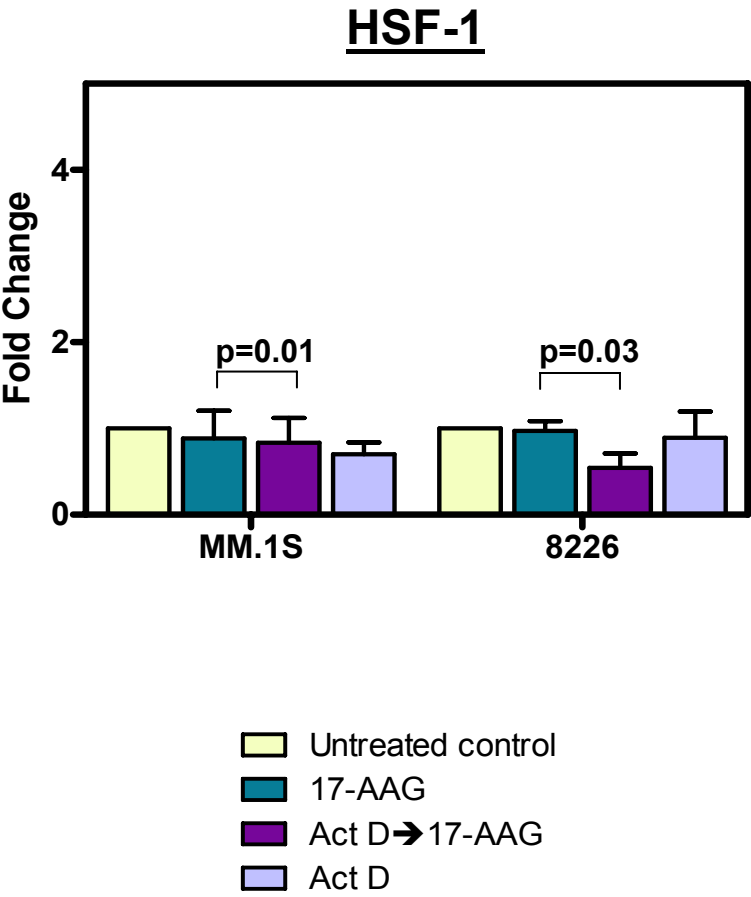


Figure 24. Act D in combination with 17-AAG diminished HSF-1 expression levels in MM.1S and RPMI-8226 cells

Immunoblot analysis was performed in triplicate and quantified using Odyssey infrared imaging system application software (version 1.2). Protein levels for HSF-1 were normalized to β -actin. Data represents three independent immunoblots plotted as means plus SD. Statistical significance ($p < 0.05$) comparing 17-AAG alone with the combination condition is shown.

Figure 24



In summary, in MM.1S cells even when Act D was able to abrogate the induction of heat shock protein expression by 17-AAG treatment, this reduction was only statistically significant for the constitutive HSC70 (Figure 22B). In contrast, in RPMI-8226 cells, Act D abrogated the 17-AAG-mediated induction of all heat shock proteins and HSF-1 protein levels in a statistically significant manner except for the stress-inducible HSP70 (Figure 22A). Moreover, the expression levels of HSF-1 were diminished in both cell lines in a statistically significant manner when compared to 17-AAG treatment alone (Figure 24).

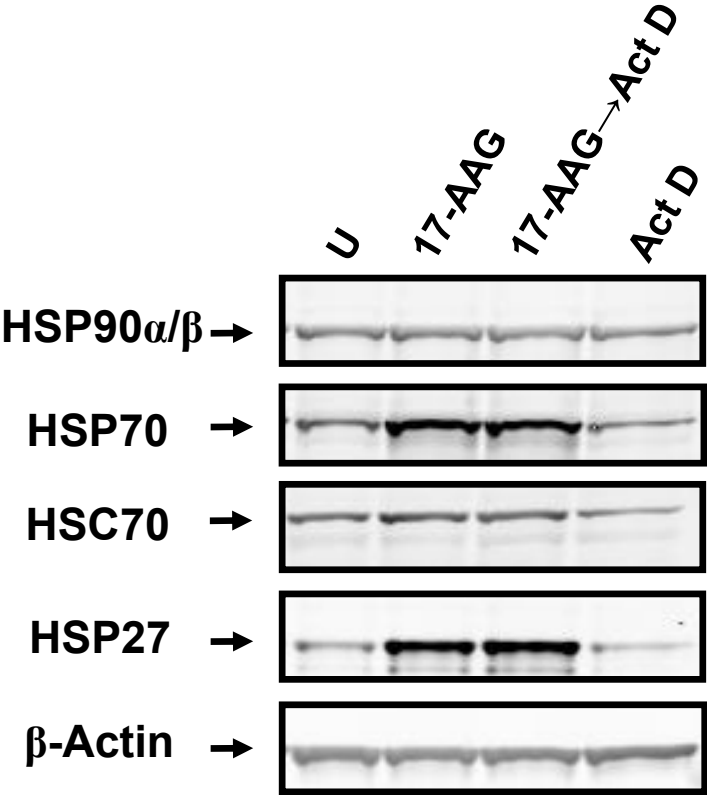
Heat shock protein levels are not diminished in the sequential combination of 17-AAG followed by Act D in MM.1S cells

Published reports of 17-AAG described that this agent needs to be added in a sequential manner in order to circumvent the induction of antiapoptotic heat shock proteins (Guo, Rocha et al. 2005; Demidenko, Vivo et al. 2006). In accordance with this, immunoblot analysis of an experiment where 0.5 μ M 17-AAG was added first followed by addition of 0.05 μ g/mL Act D, did not indicate reduction of any of the heat shock proteins or HSF-1 expression (Figure 25). As expected, treatment with 17-AAG induced the expression of all heat shock proteins in MM.1S cells. Act D as a single agent reduced the levels of all heat shock proteins. However, when the cells were treated first with 17-AAG followed by Act D in the combination condition, there was no abrogation of any of the heat shock protein levels. The expression of all constitutive and stress-inducible heat shock proteins remained similar to the levels observed for 17-AAG treatment as a single agent. This result further confirms that 17-AAG needs to be added after treatment with the transcription inhibitor Act D in order to block the stress response elicited by the HSP90 inhibitor.

Figure 25. Heat shock protein levels are not diminished in the sequential combination of 17-AAG followed by Act D in MM.1S cells

Cells were either left untreated (U) or treated with 0.5 μ M 17-AAG for 12 hours, 0.05 μ g/mL Act D for 4 hours, or the sequential combination of 17-AAG for 8 hours and then Act D for 4 hours. Heat shock protein levels under these conditions were determined via immunoblot analysis for inducible HSP90 α and constitutive HSP90 β , inducible HSP70, constitutive HSC70, HSP27, and the loading control β -actin for MM.1S cells.

Figure 25



Increased cytotoxicity of Act D in sequential combination with 17-AAG in MM.1S and RPMI-8226 cells

To determine if the combination of Act D and 17-AAG could result in increased cytotoxicity, Annexin V/7-AAD assay was performed. Plotted data represent the mean of three different experiments for each cell line. The endogenous cell death was subtracted from each condition. Endogenous cell death in MM.1S cells was around 10 to 15% and in RPMI-8226 it ranged from 15 to 20%. In order to dilute the drugs, the concentration of DMSO in 0.5 μ M 17-AAG was 0.05% and in 0.05 μ g/mL Act D was 0.005%. Therefore, the combination treatment contained less DMSO concentration than the established non-cytotoxic and tolerated amount by cells (<0.1%).

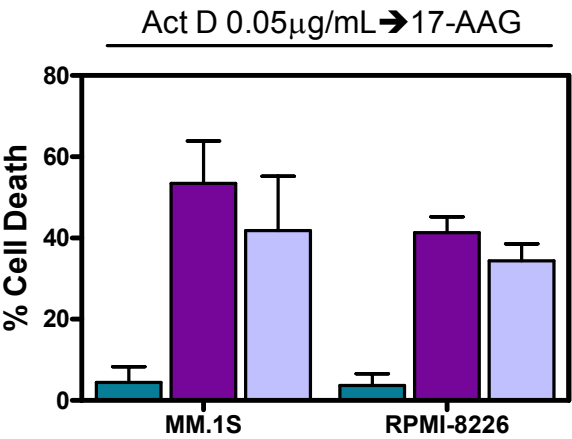
MM cells were treated with the previously mentioned sequential combination schedule. MM cells were either not treated or treated with 0.5 μ M 17-AAG alone for 8 hours, a combination treatment with 0.05 μ g/mL Act D added first for 4 hours followed by 0.5 μ M 17-AAG for 8 hours, or 0.05 μ g/mL Act D alone for 12 hours. Eight-hour treatment with 0.5 μ M 17-AAG resulted in 5 and 4% cell death in MM.1S and RPMI-8226 cells, respectively. When cells were treated with 0.05 μ g/mL Act D, there was 38% cell death in MM.1S cells and 34% cell death in RPMI-8226 cells (Figure 26A). The sequential combination of 0.05 μ g/mL Act D and 17-AAG resulted in 49 and 41% cell death for MM.1S and RPMI-8226 cells, respectively. Since these results suggested an additive effect when both drugs were combined, lower concentrations (0.01 and 0.025 μ g/mL) of Act D for 12 hours, alone or in combination with 0.5 μ M 17-AAG, were tested for cytotoxicity in MM.1S and RPMI-8226 cells (Figure 26B and C). MM cells treated with 17-AAG resulted in less than 5% cytotoxicity. MM.1S cells treated with 0.01 and 0.025 μ g/mL Act D for 12 hours caused 7 and 30% cytotoxicity, respectively. In the combination condition, there was 11% (0.01 μ g/mL Act D) and 37% (0.025 μ g/mL Act D) cell death in MM.1S cells. RPMI-8226 cells treated with 0.01 and 0.025 μ g/mL Act D for 12 hours resulted in 11 and 30%

Figure 26. Increase cytotoxicity of Act D in sequential combination with 17-AAG in MM.1S and RPMI-8226 cells

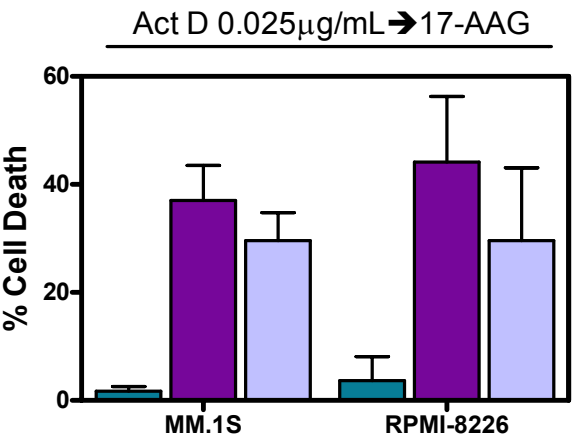
Percentages of cell death in untreated cells or cells treated with 0.5 μ M 17-AAG for 8 hours, (0.05 μ g/mL (A), .025 μ g/mL (B), or 0.01 μ g/mL (C)) Act D for 12 hours, or the combination of (0.05 μ g/mL, .025 μ g/mL, or 0.01 μ g/mL) Act D for 4 hours followed by 17-AAG for 8 hours. Flow cytometry was performed to measure cell death, which was determined as the percentage of cells staining positive for Annexin V/7-AAD after subtracting the percentage of endogenous cell death. The plots represent mean and SD from triplicate experiments.

Figure 26

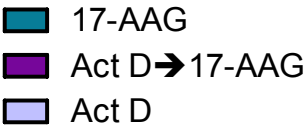
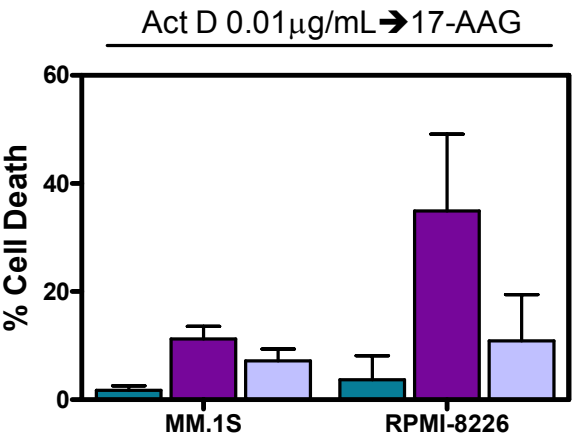
A



B



C



cytotoxicity, in that order. In the combination condition, there was 35% (0.01 µg/mL Act D) and 44% (0.025 Act D µg/mL) cell death in RPMI-8226 cells.

A fractional two-drug combination analysis as described in materials and methods was performed (Table 2). This analysis determines if the observed cell death obtained with annexin V/7-AAD binding assay is more than the calculated expected cell death for the combination treatment. For example, for the combination condition with 0.05 µg/mL Act D and 0.5 µM 17-AAG, the calculated expected cytotoxicity for the combination condition was 41 and 37% in MM.1S and RPMI-8226 cells, respectively. When comparing the observed (measured) cell death against the expected (calculated) cell death, the measured cytotoxicity for the combination condition was more than the expected cell death for the same condition. However, student's *t*-test analysis shows statistically significant difference only in RPMI-8226 cell line between the expected and observed cell death values (MM.1S, $p = 0.183$; RPMI-8226, $p = 0.049$). Calculation of the expected value for the combination of Act D (0.01 µg/mL and 0.025 µg/mL) with 0.5 µM 17-AAG showed that the observed (actual) cell death was higher. Student's *t*-test analysis shows that this difference is statistically significant. (MM.1S, $p = 0.059$ [0.01 µg/mL Act D], $p = 0.015$ [0.025 µg/mL]; RPMI-8226, $p = 0.003$ [0.01 µg/mL Act D], $p = 0.019$ [0.025 µg/mL]).

Taken together, there was a statistically significant increase in cytotoxicity with the combination treatment for all Act D concentrations for RPMI-8226 cell line. However, in MM.1S cells a significant increase in cytotoxicity was only measured for the combination treatment using the lowest Act D concentrations (0.01 µg/mL and 0.025 µg/mL).

Table 2. Increase cytotoxicity of Act D in sequential combination with 17-AAG in MM.1S and RPMI-8226 cells

Cells were either left untreated or treated with 0.5 μ M 17-AAG for 8 hours, (0.05 μ g/mL, .025 μ g/mL, or 0.01 μ g/mL) Act D for 12 hours, or the combination of (0.05 μ g/mL, .025 μ g/mL, or 0.01 μ g/mL) Act D for 4 hours followed by 17-AAG for 8 hours. Flow cytometry was performed to measure cell death, which was determined as the percentage of cells staining positive for Annexin V/7-AAD after subtracting the percentage of endogenous cell death. The expected percent survival for the combination condition was calculated following the fractional two-drug combination analysis. Statistical significance ($p < 0.05$) comparing 17-AAG alone with the combination condition is shown.

Table 2

	17-AAG	Act D	Combination	
MM.1S	0.5 μM	0.05 μg/mL	<i>Expected</i>	<i>Observed</i>
Cell Death	5	38	41	49
Cell Survival	95	62	59	
				<i>p = 0.183</i>
RPMI-8226	0.5 μM	0.05 μg/mL	<i>Expected</i>	<i>Observed</i>
Cell Death	4	34	37	41
Cell Survival	96	66	63	
				<i>p = 0.049</i>
MM.1S	0.5 μM	0.025 μg/mL	<i>Expected</i>	<i>Observed</i>
Cell Death	2	30	31	37
Cell Survival	98	70	69	
				<i>p = 0.015</i>
RPMI-8226	0.5 μM	0.025 μg/mL	<i>Expected</i>	<i>Observed</i>
Cell Death	4	30	32	44
Cell Survival	96	70	68	
				<i>p = 0.019</i>
MM.1S	0.5 μM	0.01 μg/mL	<i>Expected</i>	<i>Observed</i>
Cell Death	2	7	9	11
Cell Survival	98	93	91	
				<i>p = 0.059</i>
RPMI-8226	0.5 μM	0.01 μg/mL	<i>Expected</i>	<i>Observed</i>
Cell Death	4	11	14	35
Cell Survival	96	89	86	
				<i>p = 0.003</i>

AIM 2: 8-Chloro-Adenosine

Inhibition of global RNA synthesis by 8-Cl-Ado in MM.1S and RPMI-8226 cells

The ribonucleoside analogue 8-Cl-Ado has different mechanisms of action that include inhibition of RNA synthesis and reduction of the cellular ATP pool (Gandhi, Ayres et al. 2001; Stellrecht, Rodriguez et al. 2003). To investigate if 8-Cl-Ado could diminish RNA synthesis in MM cells, a [³H]uridine incorporation assay was performed (Figure 27). MM.1S and RPMI-8226 cells were incubated with 10 µM 8-Cl-Ado for 4 and 8 hours, then radioactive uridine (1µCi) was added to cell cultures in the last hour before harvesting the cells. Cells were processed as described in materials and methods and the levels of radioactivity were measured and normalized to the untreated control. Three independent experiments for each condition in triplicate were performed. MM.1S cell line was more sensitive to the actions of 8-Cl-Ado than RPMI-8226. A 25% decrease in global RNA synthesis was observed after 4 hours, further decreasing to 50% after 8 hours. Treatment with 8-Cl-Ado in RPMI-8226 cells caused only a 25% inhibition at both time points compared to control.

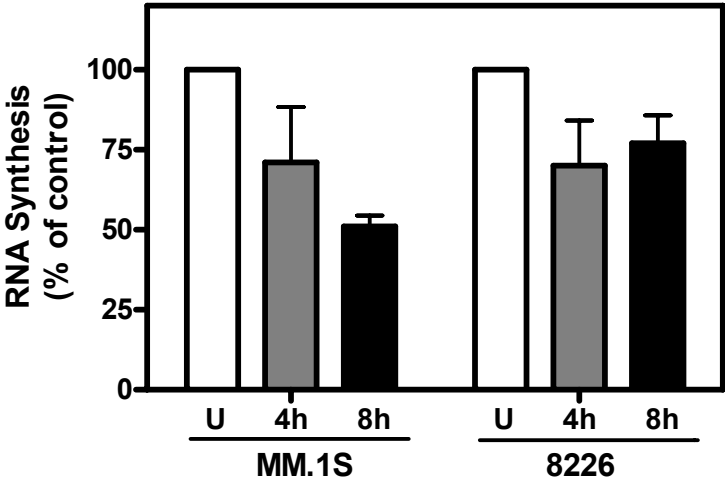
Effect of 8-Cl-Ado and 17-AAG alone and in sequential combination on heat shock protein mRNA levels in MM.1S and RPMI-8226 cells

The nucleoside analogue 8-Cl-Ado is phosphorylated into its cytotoxic triphosphate 8-Cl-ATP, which gets incorporated into RNA during transcription (Stellrecht, Rodriguez et al. 2003). Once incorporated into RNA, poly(A) polymerase is unable to synthesize poly(A) tails on RNA primers with 3'-terminal 8-Cl-AMP residues. In addition, 8-Cl-ATP inhibits ATP-dependent poly(A) tail synthesis, and thus as a consequence mRNA processing is inhibited (Chen and Sheppard 2004; Chen, Du-Cuny et al. 2010). To determine if the transcription inhibitory actions of 8-Cl-Ado could abrogate the 17-AAG-mediated induction

Figure 27. Inhibition of global RNA synthesis by 8-Cl-Ado

MM.1S and RPMI-8226 cells were treated with 10 μ M 8-Cl-Ado for the indicated time points and labeled with [3 H]uridine for 1 hour before the end of treatment. Each column is plotted as the percentage of untreated control and represents the mean and SD of three independent experiments each done in triplicate.

Figure 27



of HSP mRNA levels, the transcript levels for heat shock proteins were measured using real time RT-PCR. A sequential combination treatment was designed to verify if 8-Cl-Ado could block transcription of antiapoptotic heat shock proteins. MM cells were left untreated or treated with 0.5 μ M 17-AAG alone for 8 hours, a combination treatment where 10 μ M 8-Cl-Ado was added first and 12 hours later 0.5 μ M 17-AAG was added for 8 hours, or 10 μ M 8-Cl-Ado for 20 hours alone (Figure 28). Cells were harvested and then RNA was isolated for each condition. Primers and probes specific for the heat shock protein genes were used. The housekeeping gene GAPDH was used for normalization and the data plotted as fold change in comparison to the untreated control. Three independent experiments for each condition treatment were performed in triplicate.

8-Cl-Ado did not diminish constitutive and stress-inducible *HSP90* mRNA induced by 17-AAG in MM.1S and RPMI-8226 cells

Transcript levels for the stress-inducible *HSP90 α* and constitutive *HSP90 β* isoforms were measured in both MM cell lines under the conditions previously described (Figure 29). *HSP90 α* transcript levels in MM.1S and RPMI-8226 cells were induced with 17-AAG treatment by approximately 3-fold (Figure 29A). However, this induction persisted with the combination treatment in both cell lines, which implies that 8-Cl-Ado was not able to abrogate the *HSP90 α* -induction elicited by 17-AAG. The constitutive *HSP90 β* mRNA levels were induced to a lesser degree than the stress-inducible homologue transcript levels with 17-AAG treatment in MM.1S and RPMI-8226 cells (Figure 29B). Yet, it was not abrogated in the combination treatment by 8-Cl-Ado. No statistical significant difference was calculated for the heat shock protein mRNA levels in the combination treatment or 17-AAG treatment alone. The treatment with 8-Cl-Ado as a single agent did not result in further decrease in the basal levels of any of the inducible or constitutive *HSP90* transcript levels.

Figure 28. Drug schedule for 8-Cl-Ado and 17-AAG combination treatment

Cells were either not treated or treated with 0.5 μ M 17-AAG for 8 hours, the combination of 8-Cl-Ado for 12 hours followed by 17-AAG for 8 hours, or 10 μ M 8-Cl-Ado for 12 hours.

Figure 28

Drug schedule

Untreated control

17-AAG for 8 hours

8-Cl-Ado 12 hours  17-AAG 8 hours = 20 hours

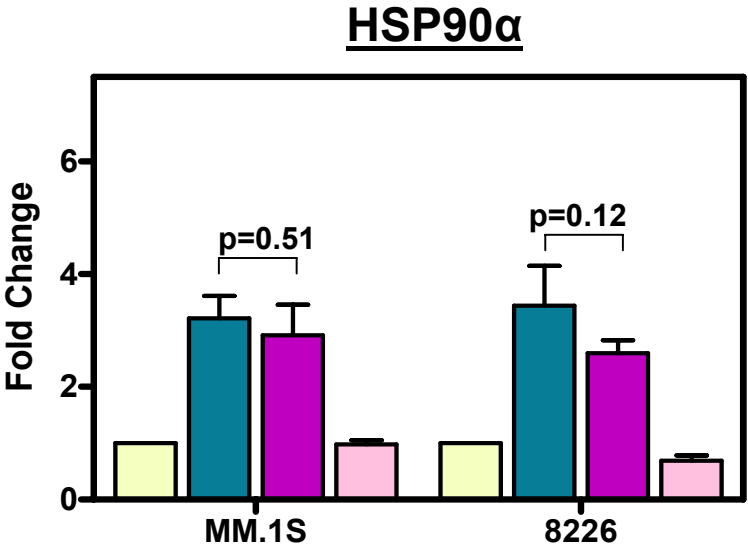
8-Cl-Ado for 20 hours

Figure 29. 8-Cl-Ado did not diminish constitutive and stress-inducible *HSP90* mRNA induced by 17-AAG in MM.1S and RPMI-8226 cells

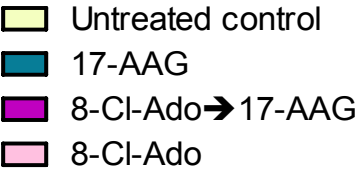
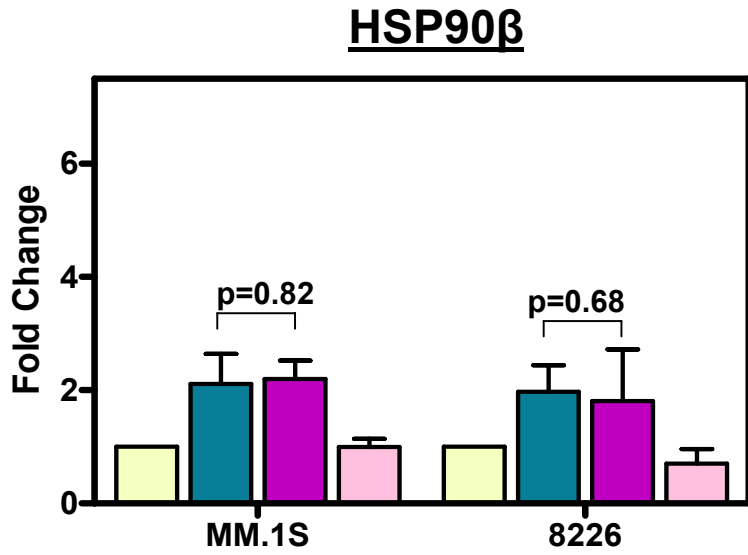
Cells were either not treated or treated with 0.5 μ M 17-AAG for 8 hours, 10 μ M 8-Cl-Ado for 12 hours, or the combination of 8-Cl-Ado for 12 hours followed by 17-AAG for 8 hours. After RNA was isolated, inducible HSP90 α (A) and constitutive HSP90 β (B) mRNA levels were measured using real-time RT-PCR technique. GAPDH was used as the endogenous gene for normalization. mRNA levels are plotted as fold change in comparison with the untreated control. Each column represents the mean and SD of triplicate experiments. Statistical significance ($p < 0.05$) comparing 17-AAG alone with the combination condition is shown.

Figure 29

A



B



8-Cl-Ado did not diminish constitutive *HSC70* or stress-inducible *HSP70* mRNA induced by 17-AAG in MM.1S and RPMI-8226 cells

The levels of stress-inducible *HSP70* and constitutive *HSC70* human isoforms were also quantified (Figure 30). Treatment with 17-AAG triggered the elevation of *HSP70* mRNA levels in both cell lines by less than 3-fold (Figure 30A). Unexpectedly, the combination treatment further elevated the levels of *HSP70* by 13- and 4-fold in MM.1S and RPMI-8226 cells, respectively, in a statistically significant fashion. Treatment with 8-Cl-Ado alone resulted in increase mRNA levels of *HSP70* by 2-fold compared to the untreated control. This induction was absent in RPMI-8226 cells, and the transcripts of *HSP70* remained at basal levels following treatment with 8-Cl-Ado alone. In contrast, constitutive *HSC70* mRNA levels were induced equally in cells treated with 17-AAG alone and with the combination, by less than 3-fold in both cell lines (Figure 30B). The ribonucleoside analog did not affect the endogenous levels of constitutive *HSC70* in either cell line. Hence, treatment with 8-Cl-Ado alone did not abolish the stress response elicited by 17-AAG.

8-Cl-Ado did not diminish *HSP27* mRNA induced by 17-AAG in MM.1S and RPMI-8226 cells

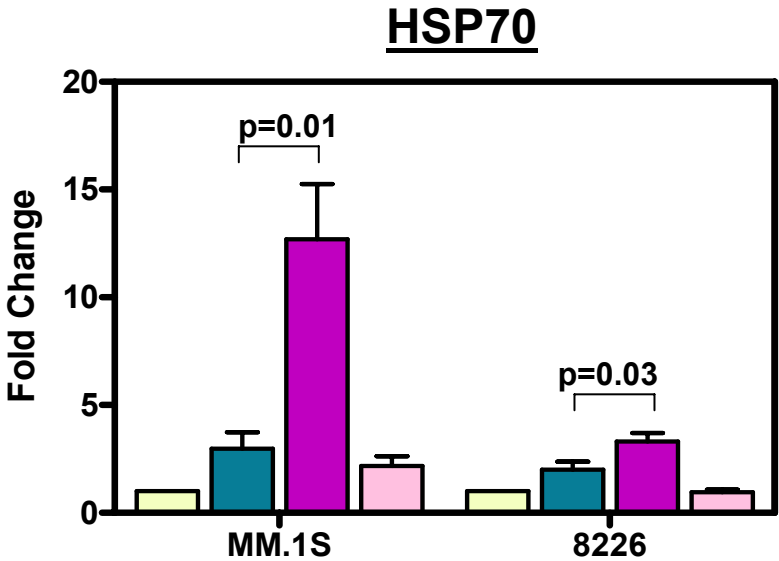
Finally, *HSP27* mRNA levels were measured in MM cells treated under the conditions previously described (Figure 31). Similar to the stress-inducible *HSP70*, the mRNA levels of *HSP27* were further induced in the combination treatment of 8-Cl-Ado and 17-AAG by 25-fold compared to the 9-fold induction measured with 17-AAG by itself in MM.1S cells. The augmentation in the levels of *HSP27* mRNA for the combination treatment was determined to be statistically different from 17-AAG treatment as a single agent. These unexpected results were not observed for RPMI-8226 cells, and treatment with 17-AAG alone resulted in an 8-fold increase of *HSP27* transcript levels that remained the same in the combination treatment. While the results were quantitatively different in

Figure 30. 8-Cl-Ado did not diminish constitutive *HSC70* or stress-inducible *HSP70* mRNA induced by 17-AAG in MM-1S and RPMI-8226 cells

Cells were either not treated or treated with 0.5 μ M 17-AAG for 8 hours, 10 μ M 8-Cl-Ado for 12 hours, or the combination of 8-Cl-Ado for 12 hours followed by 17-AAG for 8 hours. After RNA was isolated, inducible HSP70 (A) and constitutive HSC70 (B) mRNA levels were measured using real-time RT-PCR technique. GAPDH was used as the endogenous gene for normalization. mRNA levels are plotted as fold change in comparison with the untreated control. Each column represents the mean and SD of triplicate experiments. Statistical significance ($p < 0.05$) comparing 17-AAG alone with the combination condition is shown.

Figure 30

A



B

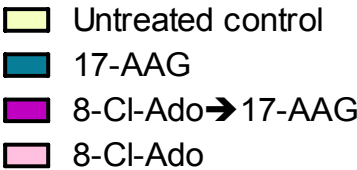
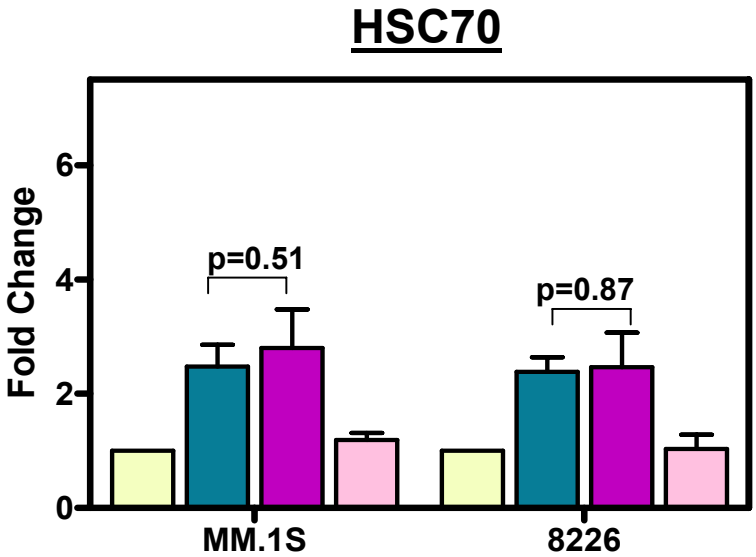
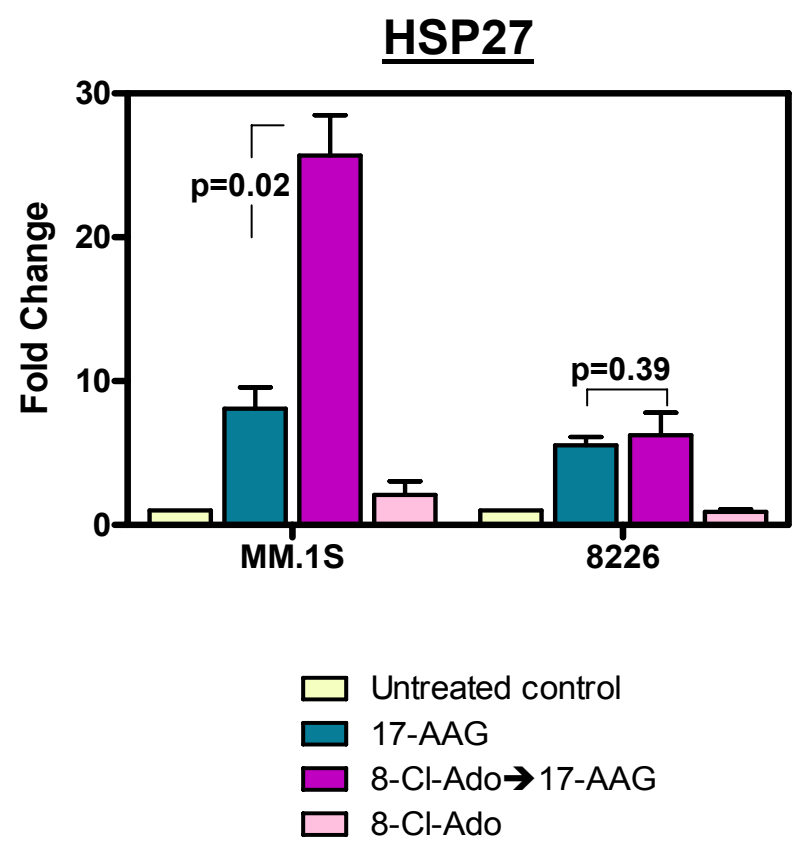


Figure 31. 8-Cl-Ado did not diminish *HSP27* mRNA induced by 17-AAG in MM.1S and RPMI-8226 cells

Cells were either not treated or treated with 0.5 μ M 17-AAG for 8 hours, 10 μ M 8-Cl-Ado for 12 hours, or the combination of 8-Cl-Ado for 12 hours followed by 17-AAG for 8 hours. After RNA was isolated, *HSP27* mRNA levels were measured using real-time RT-PCR technique. GAPDH was used as the endogenous gene for normalization. mRNA levels are plotted as fold change in comparison with the untreated control. Each column represents the mean and SD of triplicate experiments. Statistical significance ($p < 0.05$) comparing 17-AAG alone with the combination condition is shown.

Figure 31



both cell lines, qualitatively they were similar as 8-Cl-Ado addition did not decrease *HSP27* mRNA levels.

Effect of 8-Cl-Ado and 17-AAG alone and in combination on heat shock protein levels in MM.1S, RPMI-8226, and U266 cells

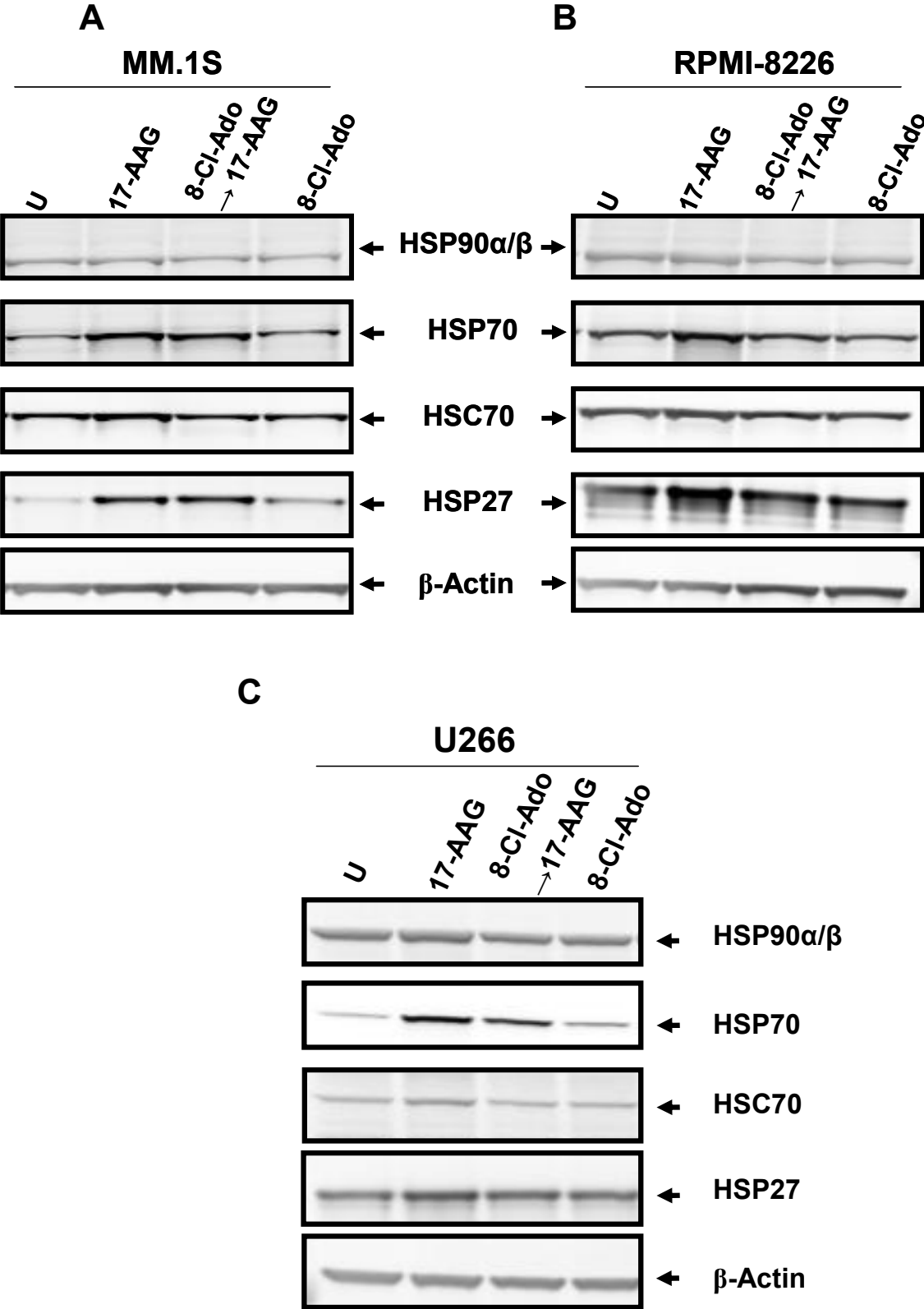
Immunoblot analysis to detect for heat shock protein expression was performed to determine if the observed increase in inducible heat shock protein transcripts following treatment with 8-Cl-Ado and 17-AAG in combination were obtained at the heat shock protein expression level (Figure 32). The same sequential combination treatment was followed. MM cells were left untreated or treated with 0.5 μ M 17-AAG alone for 8 hours; a combination treatment where 10 μ M 8-Cl-Ado was added first and 12 hours later 0.5 μ M 17-AAG was added for 8 hours; or 10 μ M 8-Cl-Ado alone for 20 hours. The cells were harvested at the indicated time points, and immunoblot analysis for HSP90 α/β , HSP70, HSC70, and HSP27 proteins were performed using β -actin as a loading control. As anticipated, HSP70 and HSP27 protein levels were increased with 17-AAG treatment in all three cell lines (Figure 32). Similar to heat shock protein transcript levels, 17-AAG-induced expression of heat shock proteins was not abrogated by 8-Cl-Ado addition in the combination treatment. Treatment of 8-Cl-Ado alone did not affect the endogenous levels of heat shock proteins in any cell line.

To quantify inducible and constitutive heat shock protein expression for 8-Cl-Ado, 17-AAG, and the combination treatment, three independent immunoblots were completed for each MM cell line. The same sequential combination design and analysis was followed. Stress-inducible and constitutive heat shock proteins were normalized with the endogenous control β -actin and the fold change for each heat shock protein plotted in comparison to the untreated control. Statistical analysis was performed and the *p* value is indicated comparing the treatment with 17-AAG alone and the combination treatment.

Figure 32. Effect of 8-Cl-Ado and 17-AAG alone and in combination on heat shock protein levels in MM.1S, RPMI-8226, and U266 cells

Cells were either not treated or treated with 0.5 μ M 17-AAG for 8 hours, 10 μ M 8-Cl-Ado for 12 hours, or the combination of 8-Cl-Ado for 12 hours followed by 17-AAG for 8 hours. Immunoblot analyses were performed to detect heat shock protein levels for these conditions using antibodies for inducible HSP90 α and constitutive HSP90 β , inducible HSP70, constitutive HSC70, HSP27, and the loading control β -actin for MM.1S (A), RPMI-8226 (B) and U266 (C) cells.

Figure 32



8-Cl-Ado and 17-AAG did not affect HSP90 α / β expression levels in MM.1S or RPMI-8226, only in U266 cells

In MM.1S cells, HSP90 α / β protein levels were not induced following 17-AAG treatment although 8-Cl-Ado was able to diminish the endogenous levels of this protein by 50% alone and in the combination treatment (Figure 33). In RPMI-8226 cells, HSP90 α / β protein levels were not significantly affected with any of the condition treatments. In U266 cells, protein levels for constitutive/stress-inducible HSP90 were not increase by 17-AAG treatment. Similar levels of reduction were obtained for HSP90 α / β with the combination treatment and 8-Cl-Ado treatment alone. A statistically significant decrease of heat shock protein expression in the combination treatment versus 17-AAG alone was only obtained for HSP90 α / β protein levels in U266 cells.

8-Cl-Ado did not diminish 17-AAG-mediated induction of constitutive HSC70 and stress-inducible HSP70 expression levels in MM.1S and RPMI-8226 cells, only in U266 cells

In MM.1S cells, stress inducible levels of HSP70 were increased by more than 10-fold with 17-AAG treatment, however 8-Cl-Ado was unable to abrogate this induction in the combination sequence (Figure 34A). The constitutive levels of HSC70 were not changed in a noticeable way for any condition treatment (Figure 34B). In RPMI-8226 cells, there was no significant change in HSP70 and HSC70 levels under any of the conditions assessed (Figure 34A and B). In U266 cells, HSP70 expression was induced by 5-fold with 17-AAG, which was diminished 50% by 8-Cl-Ado in the combination treatment (Figure 34A). Endogenous levels on HSP70 were not altered following 8-Cl-Ado treatment as a single agent. When cells where treated with 17-AAG alone, constitutive HSC70 levels were induced to a minimal extent (Figure 34B). HSC70 protein levels in the combination treatment and 8-Cl-Ado treatment were diminished approximately by 50% in MM.1S and U266 cells when compared to the untreated control, and no change was observed in RPMI-

Figure 33. 8-Cl-Ado did not affect HSP90 α / β expression levels in MM.1S or RPMI-8226, only in U266 cells

Immunoblot assays were performed in triplicate and quantified using Odyssey infrared imaging system application software (version 1.2). Protein levels for HSP90 α / β were normalized to β -actin. Data represents three independent immunoblots plotted as means plus SD. Statistical significance ($p < 0.05$) comparing 17-AAG alone with the combination condition is shown.

Figure 33

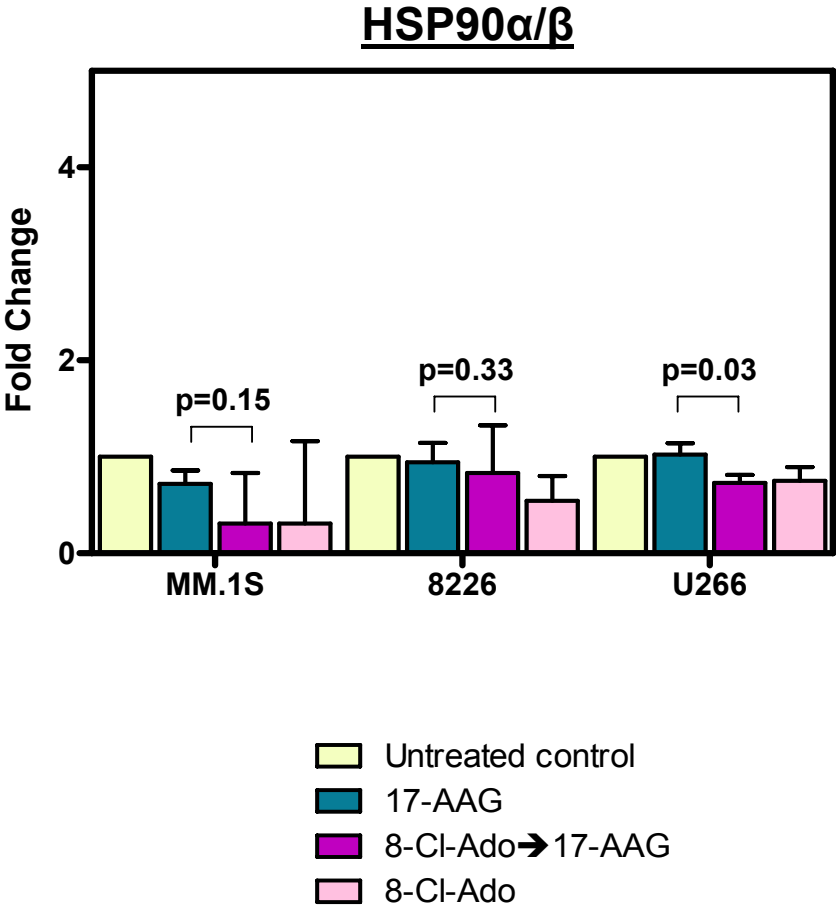
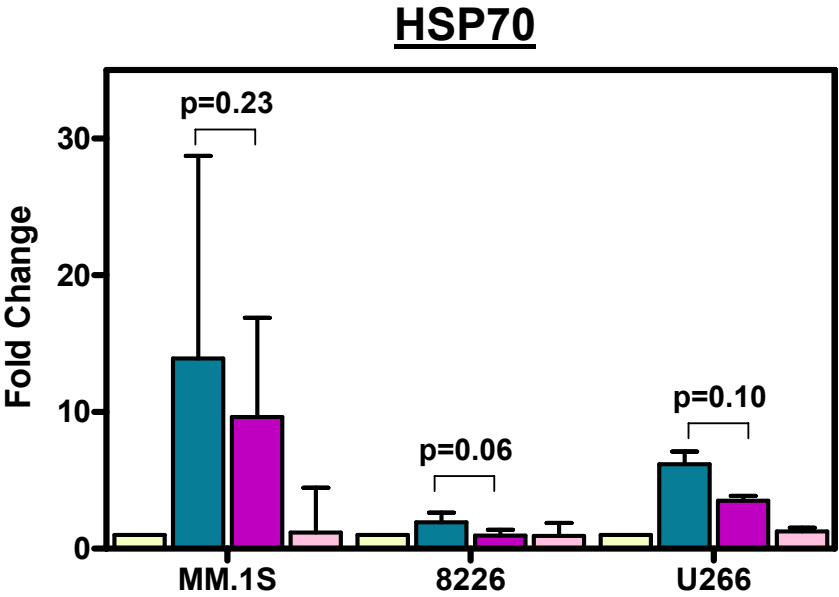


Figure 34. 8-Cl-Ado did not diminish 17-AAG-mediated induction of constitutive HSC70 and stress-inducible HSP70 expression levels in MM.1S or RPMI-8226, only in U266 cells

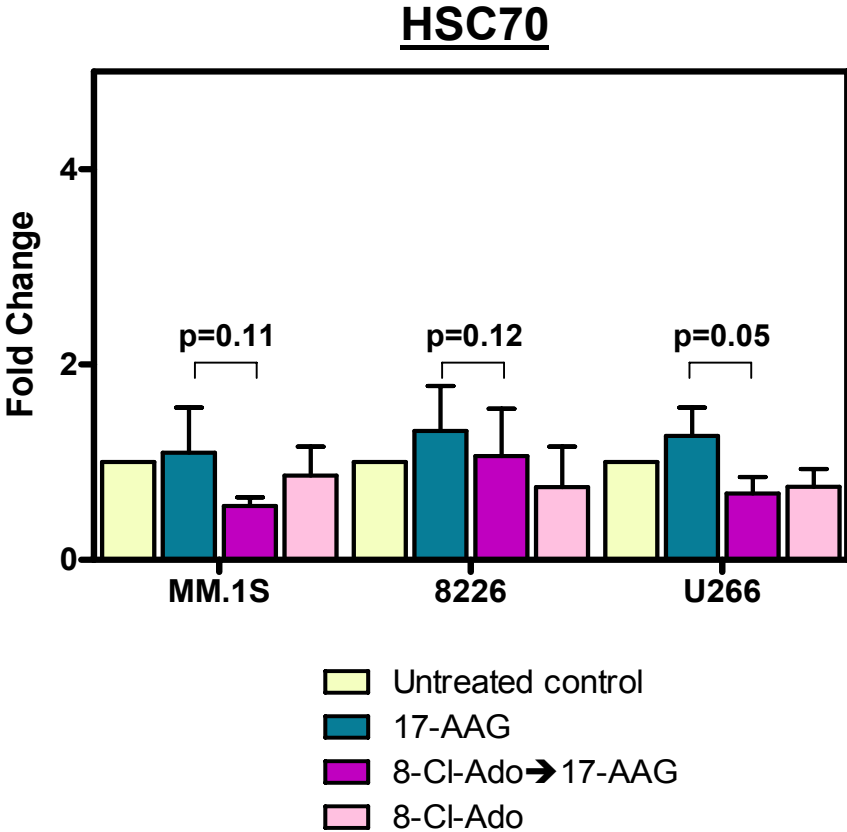
Immunoblot assays were performed in triplicate and quantified using Odyssey infrared imaging system application software (version 1.2). Protein levels for inducible HSP70 (A) and constitutive HSC70 (B) were normalized to β -actin. Data represents three independent immunoblots plotted as means plus SD. Statistical significance ($p < 0.05$) comparing 17-AAG alone with the combination condition is shown.

Figure 34

A



B



8226 cells. A statistically significant decrease of heat shock protein expression in the combination treatment versus 17-AAG alone was only obtained for constitutive HSC70 protein levels in U266 cells.

8-Cl-Ado did not diminish 17-AAG-mediated induction of HSP27 expression levels in MM.1S, RPMI-8226, or U266 cells

Finally, HSP27 levels in MM.1S cells were induced by 15-fold following 17-AAG treatment compared to the untreated control, and this level of induction remained the same in the combination treatment (Figure 35). Similar to induction of HSP27 transcript levels (Figure 31), treatment with 8-Cl-Ado alone also caused an increased of HSP27 protein by 4-fold in MM.1S cell line. In RPMI-8226 cells, HSP27 expression levels resulted in a 4-fold increase with 17-AAG treatment, which was not diminished by 8-Cl-Ado in the combination condition. In the cell line U266, HSP27 expression remained constant with the different treatments and treatment with 8-Cl-Ado alone did not affect HSP27 expression.

Taken together, these immunoblot assays indicated that 8-Cl-Ado was not able to abrogate 17-AAG-mediated induction of heat shock proteins. The *p* values comparing 17-AAG treatment alone and 8-Cl-Ado in combination with 17-AAG treatment resulted in no statistical significant difference for any of the heat shock proteins in any cell line except for HSP90 α/β and constitutive HSC70 in U266 cells (Figures 33 and 34B)).

Effect of other 8-Cl-Ado and 17-AAG combination sequences on heat shock protein levels in U266 cells

In order to elucidate whether the sequence of 8-Cl-Ado and 17-AAG in the combination treatment had a different effect on heat shock protein expression, two other combinations were tested in U266 cells (Figure 36). In the first combination sequence

Figure 35.8-CI-Ado did not diminish 17-AAG-mediated induction of HSP27 expression levels in MM.1S, RPMI-8226, or U266 cells

Immunoblot assays were performed in triplicate and quantified using Odyssey infrared imaging system application software (version 1.2). Protein levels for HSP27 were normalized to β -actin. Data represents three independent immunoblots plotted as means plus SD. Statistical significance ($p < 0.05$) comparing 17-AAG alone with the combination condition is shown.

Figure 35

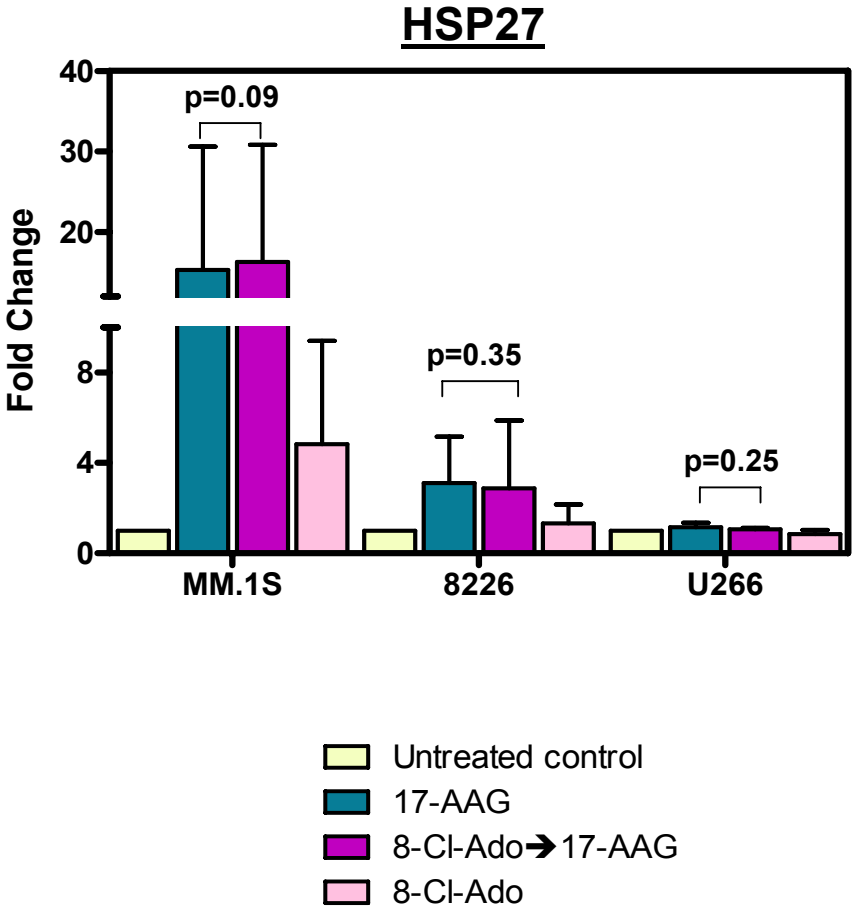
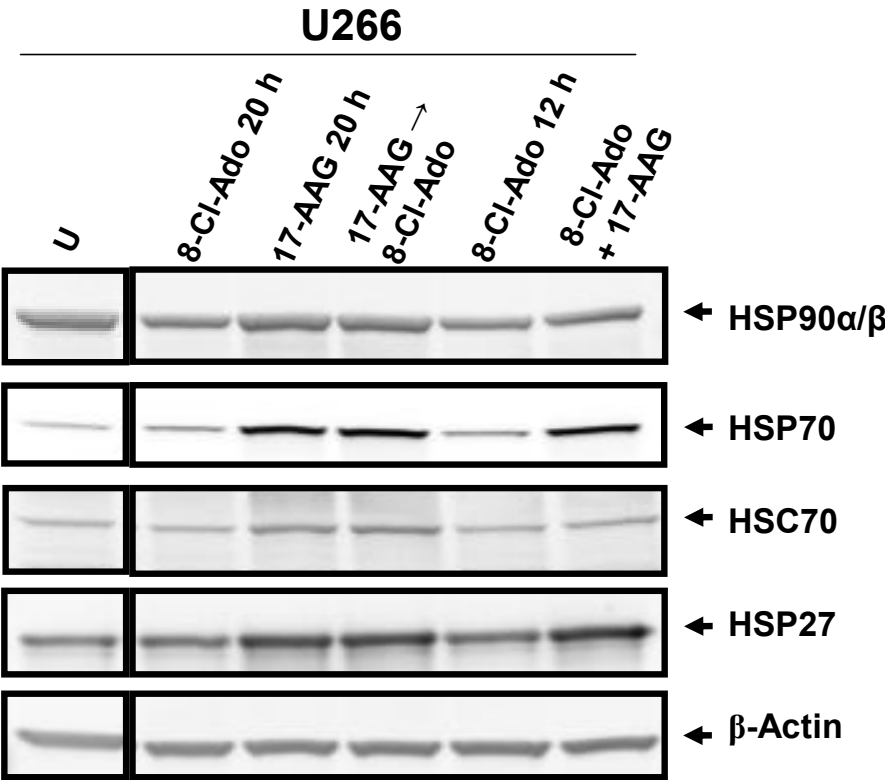


Figure 36. Effect of other 8-Cl-Ado and 17-AAG combination sequences on heat shock protein levels in U266 cells

Cells were either left untreated (U) or treated with 10 μ M 8-Cl-Ado for 20 hours, 0.5 μ M 17-AAG for 20 hours, the combination of 17-AAG for 12 hours followed 8-Cl-Ado for 8 hours, 10 μ M 8-Cl-Ado for 12 hours, or combination of 8-Cl-Ado and 17-AAG added simultaneously for 20 hours. Immunoblot analyses were performed to detect protein levels for inducible/constitutive HSP90 α / β , inducible HSP70, constitutive HSC70, HSP27, and the loading control β -actin in U266 cells.

Figure 36



tested, cells were treated with 0.5 μ M 17-AAG for 20 hours alone, treated first with 0.5 μ M 17-AAG for 8 hours followed by 10 μ M 8-Cl-Ado for 12 hours for the combination treatment, or treated with 10 μ M 8-Cl-Ado for 12 hours alone. For the second combination condition, 10 μ M 8-Cl-Ado and 0.5 μ M 17-AAG were added simultaneously for 20 hours, and the two parallel conditions with the single agents alone were included. Cells were harvested at the end of each treatment time point, and immunoblot analysis for HSP90 α / β , HSP70, HSC70, and HSP27 proteins were performed using β -actin as a loading control. As expected, addition of 17-AAG to the conditions triggered induction of heat shock protein expression in U266 cells. However, 8-Cl-Ado was not able to diminish this induction in any of the combination sequences. By itself, 8-Cl-Ado treatment did not result in any change in heat shock protein levels.

To quantify these results, three different immunoblots were performed for the three different condition treatments in U266 cells. The same sequential and simultaneous combination designs were tested and immunoblot analysis were performed. Stress-inducible and constitutive heat shock proteins were normalized with the endogenous control β -actin and the fold change for each heat shock protein plotted in comparison to the untreated control. The *p* value compares 17-AAG treatment alone versus the combination treatment.

(i) 17-AAG \rightarrow 8-Cl-Ado sequential combination

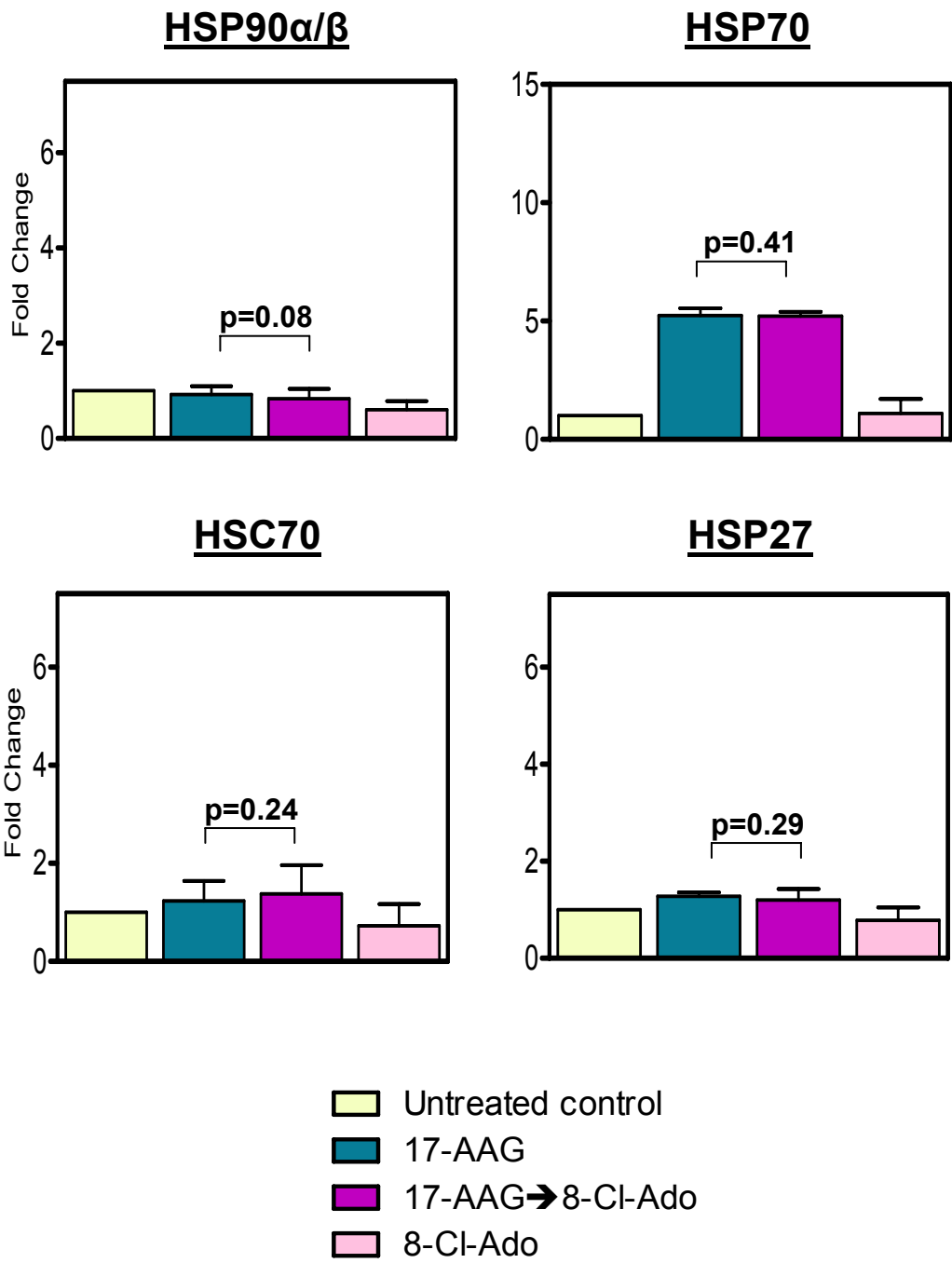
U266 cells were left untreated or treated with 0.5 μ M 17-AAG for 20 hours alone, 10 μ M 8-Cl-Ado for 12 hours alone, or treated first with 0.5 μ M 17-AAG for 8 hours followed by 10 μ M 8-Cl-Ado for 12 hours. Immunoblot analysis indicated that HSP90 α / β protein levels remained at endogenous levels after 17-AAG or combination treatment (Figure 37). On the other hand, 8-Cl-Ado as a single treatment diminished HSP90 α / β levels by 50% in comparison to the untreated control. Inducible HSP70 protein levels were induced by 5-fold

Figure 37. Effect of other 8-Cl-Ado and 17-AAG combination sequences on heat shock protein levels in U266 cells

(i) 17-AAG → 8-Cl-Ado sequential combination

U266 cells were left untreated or treated with 0.5 μ M 17-AAG for 20 hours, the sequential combination of 0.5 μ M 17-AAG for 8 hours followed by 10 μ M 8-Cl-Ado for 12 hours, or 10 μ M 8-Cl-Ado for 12 hours. Immunoblot assays were performed in duplicate and quantified using Odyssey infrared imaging system application software (version 1.2). Protein levels for HSP90 α/β , inducible HSP70, constitutive HSC70, and HSP27 were normalized to β -actin. Data represents two independent immunoblots plotted as means plus SD. Statistical significance ($p < 0.05$) comparing 17-AAG alone with the combination condition is shown.

Figure 37



following 17-AAG treatment alone or in combination with 8-Cl-Ado compared to the untreated control. This suggests that the transcription inhibitory actions of the nucleoside analogue, 8-Cl-Ado, could not block 17-AAG-regulated HSP70 transcription-induction. Treatment with 8-Cl-Ado as a single agent did not affect HSP70 protein levels. Constitutive HSC70 expression levels remained similar to endogenous levels as measured in the untreated control after 17-AAG and 8-Cl-Ado treatments as single agents or in combination. Similarly, HSP27 levels were not changed following the addition of either 17-AAG or 8-Cl-Ado alone, nor in their combination treatment. The calculated *p* values for all heat shock proteins did not indicate a statistical difference between 17-AAG as a single treatment or its sequential combination with 8-Cl-Ado.

(ii) 8-Cl-Ado + 17-AAG simultaneous combination

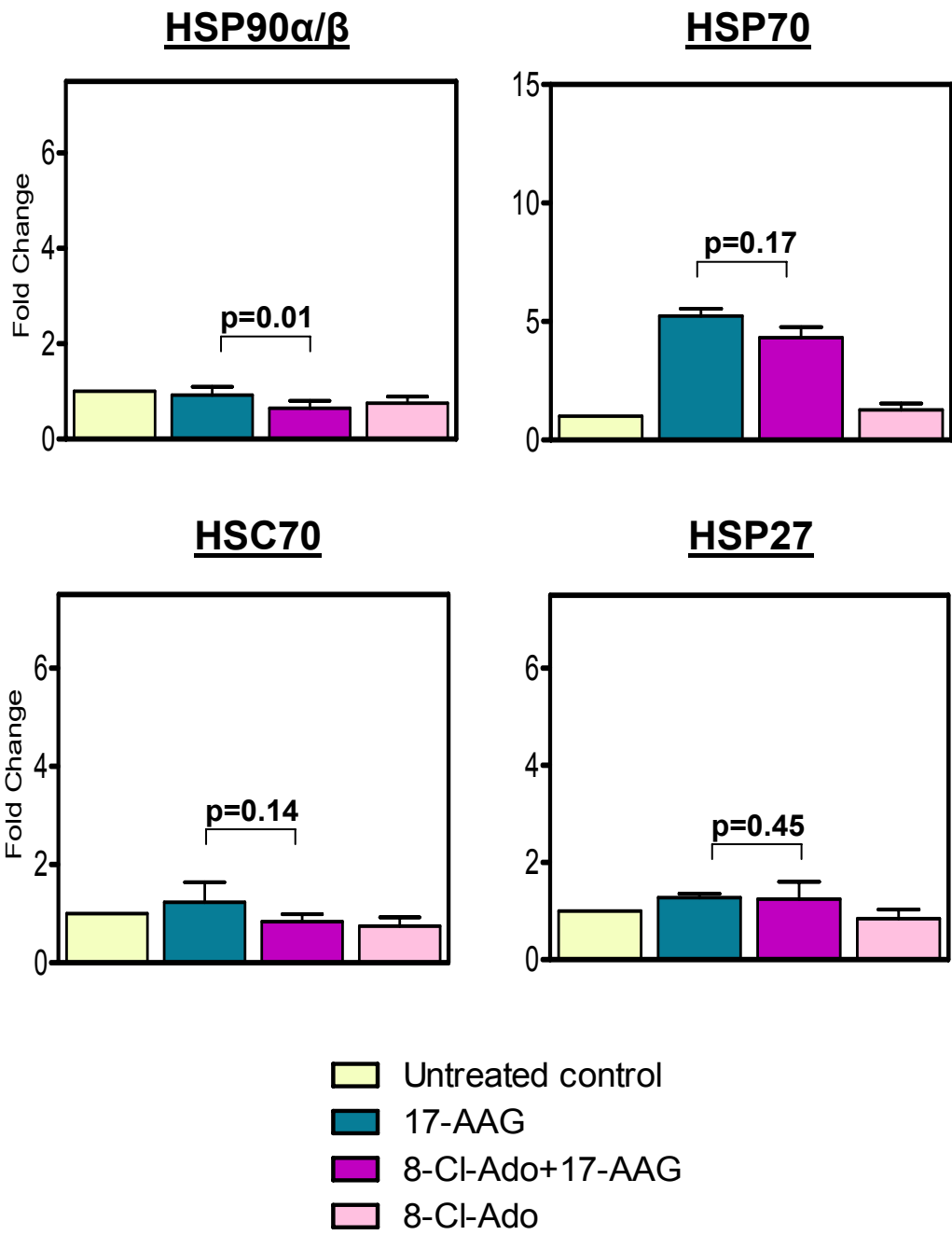
U266 cells were left untreated or treated with 10 μ M 8-Cl-Ado for 20 hours alone, 0.5 μ M 17-AAG for 20 hours by itself, or treated simultaneously with 10 μ M 8-Cl-Ado and 0.5 μ M 17-AAG for 20 hours. HSP90 α/β protein levels were not induced with 17-AAG or 8-Cl-Ado treatment as single agents (Figure 38). Expression of this chaperone was diminished by 50% in the combination treatment when compared to 17-AAG treatment. HSP70 levels were induced by 5-fold with addition of 17-AAG alone. This increase however was not blocked in the combination treatment, resulting also in a similar 5-fold induction of HSP70 protein levels. In contrast, HSC70 levels were not changed after addition of any of the agents by themselves or in combination. In a similar manner, HSP27 remained at endogenous levels comparable to the untreated control after treatment with 17-AAG or 8-Cl-Ado alone or in combination. When 17-AAG alone and the combination were compared, only the difference in HSP90 α/β expression was found to be statistically significant.

Figure 38. Effect of other 8-Cl-Ado and 17-AAG combination sequences on heat shock protein levels in U266 cells

(ii) 8-Cl-Ado + 17-AAG simultaneous combination

U266 cells were left untreated or treated with 0.5 μ M 17-AAG for 20 hours, the simultaneous combination of 0.5 μ M 17-AAG and 10 μ M 8-Cl-Ado for 20 hours, or 10 μ M 8-Cl-Ado for 20 hours. Immunoblot assays were performed in duplicate and quantified using Odyssey infrared imaging system application software (version 1.2). Protein levels for HSP90 α/β , inducible HSP70, constitutive HSC70, and HSP27 were normalized to β -actin. Data represents two independent immunoblots plotted as means plus SD. Statistical significance ($p < 0.05$) comparing 17-AAG alone with the combination condition is shown.

Figure 38



In summary, addition of 8-Cl-Ado in any of the two different combination sequences in U266 cells did not result in a reduction of the heat shock protein levels induced by 17-AAG treatment.

Effect of 8-Cl-Ado and 17-AAG alone and in combination on GRP protein levels in MM.1S cells

Diminishing the bioenergetic pool levels of the cell is one of the mechanisms by which 8-Cl-Ado exerts cytotoxicity (Gandhi, Ayres et al. 2001). Glucose deprivation (metabolic homeostatic perturbation) is a strong inducer of endoplasmic reticulum stress triggering the UPR, which results in elevation of GRP78 and GRP94, the HSP homologues in the ER. Although it is not known to what extent ATP depletion is accountable for ER-stress induction (Schroder 2008). It has been reported that treatment with HSP90 inhibitors are able to activate the UPR (Davenport, Moore et al. 2007). Hence, GRP78 and GRP94 protein levels were measured to determine if the combination treatment of 8-Cl-Ado and 17-AAG could affect their endogenous levels (Figure 39). MM.1S cells were left untreated or treated with 0.5 μ M 17-AAG for 8 hours, 10 μ M 8-Cl-Ado for 20 hours, or the combination of 8-Cl-Ado for 12 hours and then 17-AAG for 8 hours. Cells were harvested at the end of each treatment and immunoblots were performed to detect for GRP94 and GRP78 protein levels as well as β -actin. Compared to the untreated control, no noticeable changes in the levels of these ER chaperones were observed for any condition treatment. In order to establish if reproducible results could be obtained, three independent immunoblots were performed (Figure 40). GRP protein levels were normalized against β -actin and plotted as fold change in comparison to the untreated control. The *p* value compares 17-AAG treatment alone and the sequential combination treatment. GRP94 and GRP78 levels remained similar to endogenous levels in the untreated control regardless of 17-AAG and 8-

Figure 39. Effect of 8-Cl-Ado and 17-AAG alone and in combination on GRP protein levels in MM.1S cells

Cells were not treated (U) or treated with 0.5 μ M 17-AAG for 8 hours, 10 μ M 8-Cl-Ado for 20 hours, or the combination of 8-Cl-Ado for 12 hours followed by 17-AAG for 8 hours. Immunoblot analysis were performed to evaluate GRP protein levels for these conditions using antibodies for GRP94, GRP78, and the loading control β -actin in MM.1S cells.

Figure 39

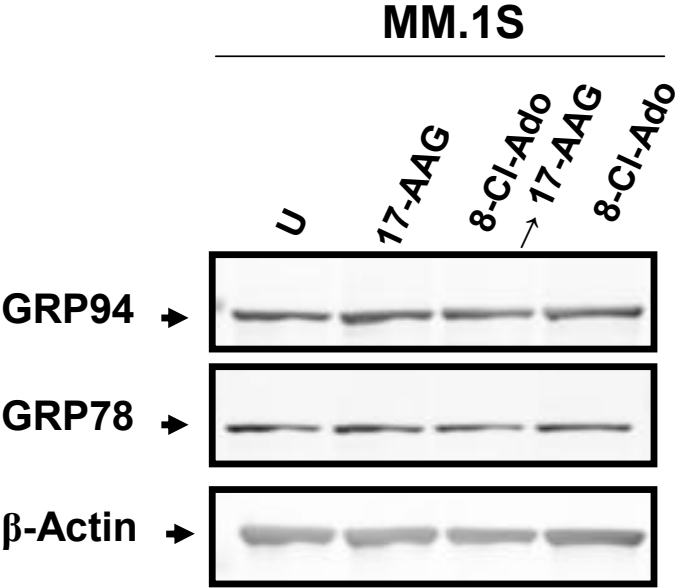
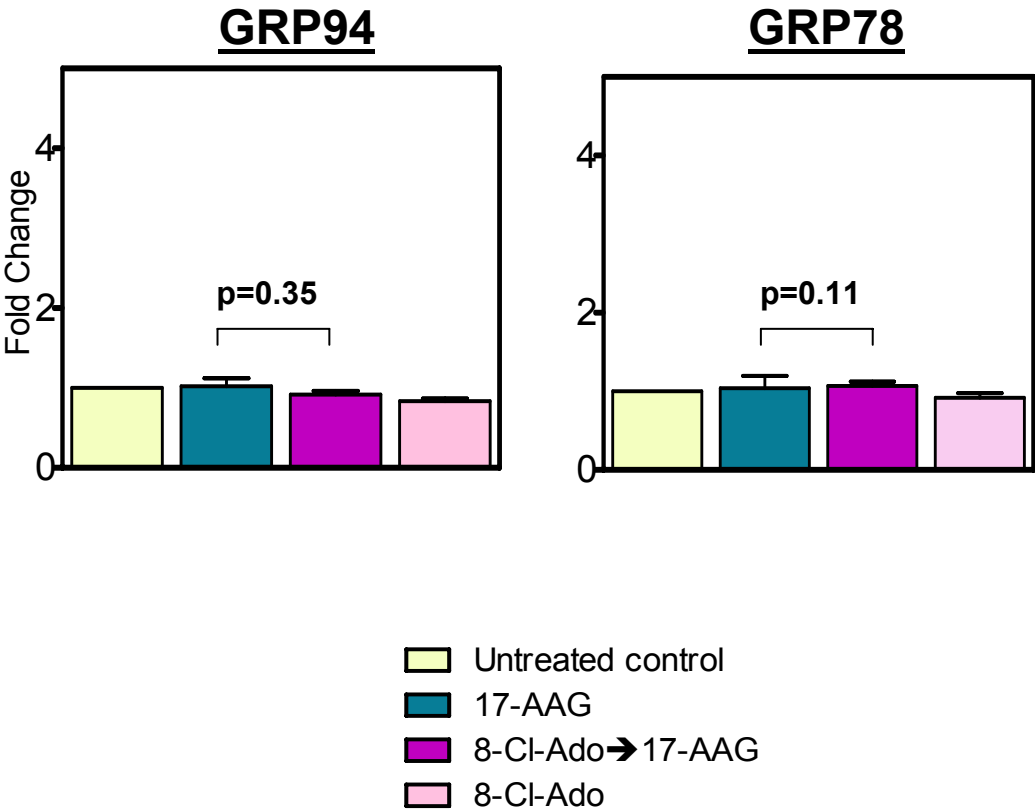


Figure 40. 8-Cl-Ado and 17-AAG alone and in combination did not affect GRP protein levels in MM.1S cells

Immunoblot assays were performed in triplicate and quantified using Odyssey infrared imaging system application software (version 1.2). Protein levels for GRP94 and GRP78 were normalized to β -actin. Data represents three independent immunoblots plotted as means plus SD. Statistical significance ($p < 0.05$) comparing 17-AAG alone with the combination condition is shown.

Figure 40



Cl-Ado treatments. As expected, the calculated p value comparing 17-AAG treatment alone and the sequential combination condition showed no statistical significance.

Effect of 8-Cl-Ado and 17-AAG alone and in combination STAT3, Raf-1, and Akt client protein levels in MM.1S, RPMI-8226, and U266 cells

Notorious oncoproteins, such as STAT-3, Raf-1, and Akt, are part of redundant signaling cascades. 17-AAG and other HSP90 inhibitors are unique in their ability to simultaneously downregulate numerous client oncoprotein substrates by increasing their turnover rate (Neckers and Neckers 2002). 8-Cl-Ado can inhibit transcription and translation processes due to its actions not only on RNA incorporation and termination but also on the decrease of endogenous ATP pool levels (Gandhi, Ayres et al. 2001; Stellrecht, Rodriguez et al. 2003; Chen, Nowak et al. 2009). To investigate if the combination of both agents could further decrease the levels of client oncoproteins in the cells through their different mechanisms of action, immunoblot analysis using antibodies against STAT-3, Raf-1, Akt, and the loading control β -actin were performed (Figure 41). Cells were left untreated or treated with 0.5 μ M 17-AAG for 8 hours, 10 μ M 8-Cl-Ado for 20 hours, or the combination of 8-Cl-Ado for 12 hours and then 17-AAG for 8 hours.

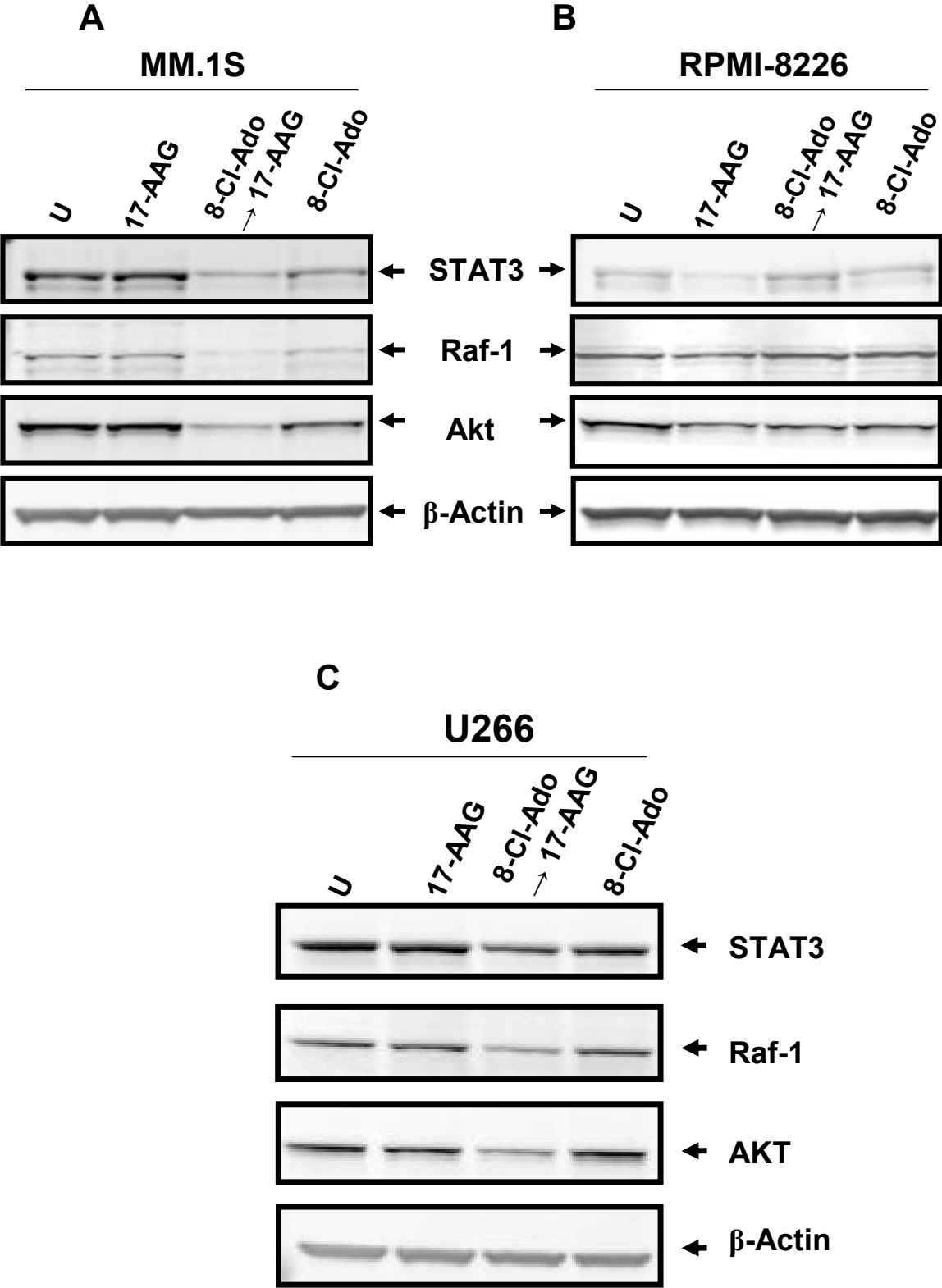
In MM.1S cells, 17-AAG treatment as single agent caused a minimal decrease in all client protein levels. 8-Cl-Ado treatment by itself decreased client protein expression no more than 40%. However, the combination of both agents resulted in a drastic decrease (>75%) of STAT-3, Raf-1, and Akt compared to not only the untreated control but also to the single agents (Figure 41A). This effect though, was not observed for Akt protein levels in RPMI-8226 cells. Furthermore, the levels of STAT-3 and Raf-1 client proteins were diminished to some extent with 17-AAG by itself but this reduction was not observed in the combination treatment (Figure 41B). In U266 cells, 8 hour treatment with 17-AAG did not affect protein levels to a considerable degree. In a similar manner, 8-Cl-Ado treatment did

Figure 41. Effect of 8-Cl-Ado and 17-AAG alone and in combination on STAT3, Raf-1, and Akt client protein levels in MM.1S, RPMI-8226, and U266 cells

Cells were not treated (U) or treated with 0.5 μ M 17-AAG for 8 hours, 10 μ M 8-Cl-Ado for 20 hours, or the combination of 8-Cl-Ado for 12 hours followed by 17-AAG for 8 hours.

Immunoblot analyses were performed to detect protein levels for STAT3, Raf-1, Akt, and the loading control β -actin in MM.1S (A), RPMI-8226 (B), and U266 (C) cells.

Figure 41



not affect client protein levels. However, combination of 17-AAG and 8-Cl-Ado resulted in further reduction of STAT-3, Raf-1, and Akt protein levels (Figure 41C).

Three independent immunoblots were performed in order to quantify the decrease of the client proteins observed with the combination treatment. Antibodies raised against STAT-3, Raf-1, Akt and β -actin were utilized. Client protein levels were normalized against β -actin and plotted as fold change in comparison to the untreated control. The p values compare the combination treatment versus the single agents and the untreated condition.

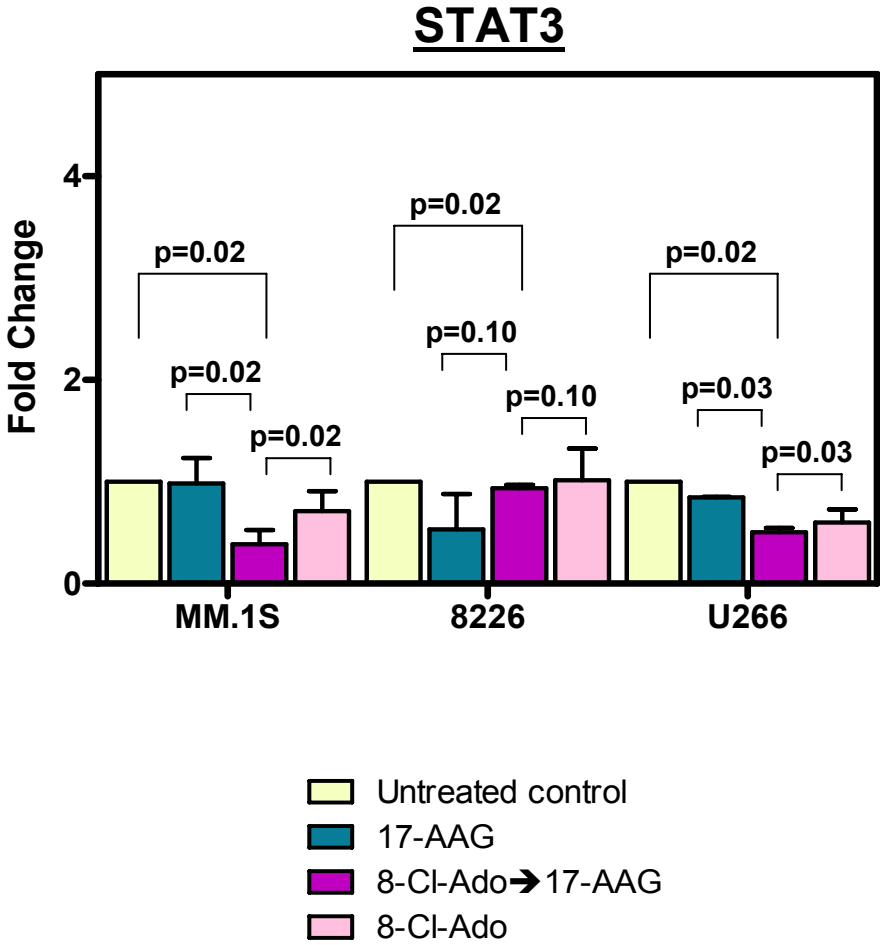
Combination of 8-Cl-Ado followed by 17-AAG decreased STAT3 expression levels in MM.1S, RPMI-8226, and U266 cells

In MM.1S cells, STAT-3 expression levels were not decreased with the 8 hour 17-AAG treatment (Figure 42). 8-Cl-Ado alone only diminished levels by 10%. Conversely, their combination decreased STAT-3 by 60%. The calculated p values showed that this decrease in the combination treatment was statistically significant when compared to single agents and untreated conditions. In RPMI-8226 cells, STAT3 protein levels were decreased by 50% with 17-AAG treatment when compared to the untreated control. 8-Cl-Ado alone or in the combination treatment did not diminish client protein levels in a statistically significant manner (Figure 42). For the U266 cell line, STAT3 expression levels were decreased by 10% when 17-AAG was added to the cells. 8-Cl-Ado was able to cause a 40% decrease of STAT-3 protein levels when compared to the control (Figure 42). The combination of both agents resulted in a reduction of STAT3 levels by 50% when compared to the untreated control. The decrease in the combination condition in comparison to the other treatments was statistically significant ($p < 0.05$).

Figure 42. Combination of 8-Cl-Ado followed by 17-AAG decreased STAT3 expression levels in MM.1S, RPMI-8226, and U266 cells

Immunoblot assays were performed in triplicate and quantified using Odyssey infrared imaging system application software (version 1.2). Protein levels for STAT3 were normalized to β -actin. Data represents three independent immunoblots plotted as means plus SD. Statistical significance ($p < 0.05$) comparing the combination condition with 17-AAG alone, 8-Cl-Ado alone, or the untreated control is shown.

Figure 42



Combination of 8-Cl-Ado followed by 17-AAG decreased Raf-1 expression levels in MM.1S, RPMI-8226, and U266 cells

In MM.1S cells, Raf-1 expression levels were not decreased with the 8 hour 17-AAG treatment (Figure 43). 8-Cl-Ado alone diminished Raf-1 protein levels by 40%. The combination treatment decreased Raf-1 protein levels by 90%. This reduction was statistically significant ($p = 0.006$) when compared to the untreated control. In RPMI-8226 cells, Raf-1 protein levels were only minimally decreased with 17-AAG treatment (Figure 43). Similarly, 8-Cl-Ado alone or in the combination treatment did not diminish client protein levels in a significant manner. In U266 cells, Raf-1 levels were decreased by 10% when 17-AAG was added to the cells (Figure 43). 8-Cl-Ado was able to cause a 20% decrease of Raf-1 protein levels. The combination of both agents resulted in a reduction of 60% when compared to the untreated control, which was statistically significant ($p = 0.03$).

Combination of 8-Cl-Ado followed by 17-AAG decreased Akt expression levels in MM.1S, RPMI-8226, and U266 cells

In MM.1S cells, Akt expression levels were not markedly decreased following 17-AAG treatment (Figure 44). 8-Cl-Ado alone diminished client protein levels by 30%. Their combination decreased Akt protein levels by 80%. The calculated p values showed that this decreased in the combination treatment was statistically significant when compared to single agents and untreated condition. In RPMI-8226 cells, Akt levels were only minimally decreased with 17-AAG (Figure 44). 8-Cl-Ado alone did not affect Akt protein levels; however, the combination treatment diminished client protein levels in a significant manner ($p = 0.04$) when compared to the untreated control. In U266 cells, Akt protein levels were decreased by 10% with 17-AAG. 8-Cl-Ado only caused a 5% decrease in Akt protein levels when compared to the control (Figure 44). The combination of both agents resulted in a

Figure 43. Combination of 8-Cl-Ado followed by 17-AAG decreased Raf-1 expression levels in MM.1S, RPMI-8226, and U266 cells

Immunoblot assays were performed in triplicate and quantified using Odyssey infrared imaging system application software (version 1.2). Protein levels for Raf-1 were normalized to β -actin. Data represents three independent immunoblots plotted as means plus SD. Statistical significance ($p < 0.05$) comparing the combination condition with 17-AAG alone, 8-Cl-Ado alone, or the untreated control is shown.

Figure 43

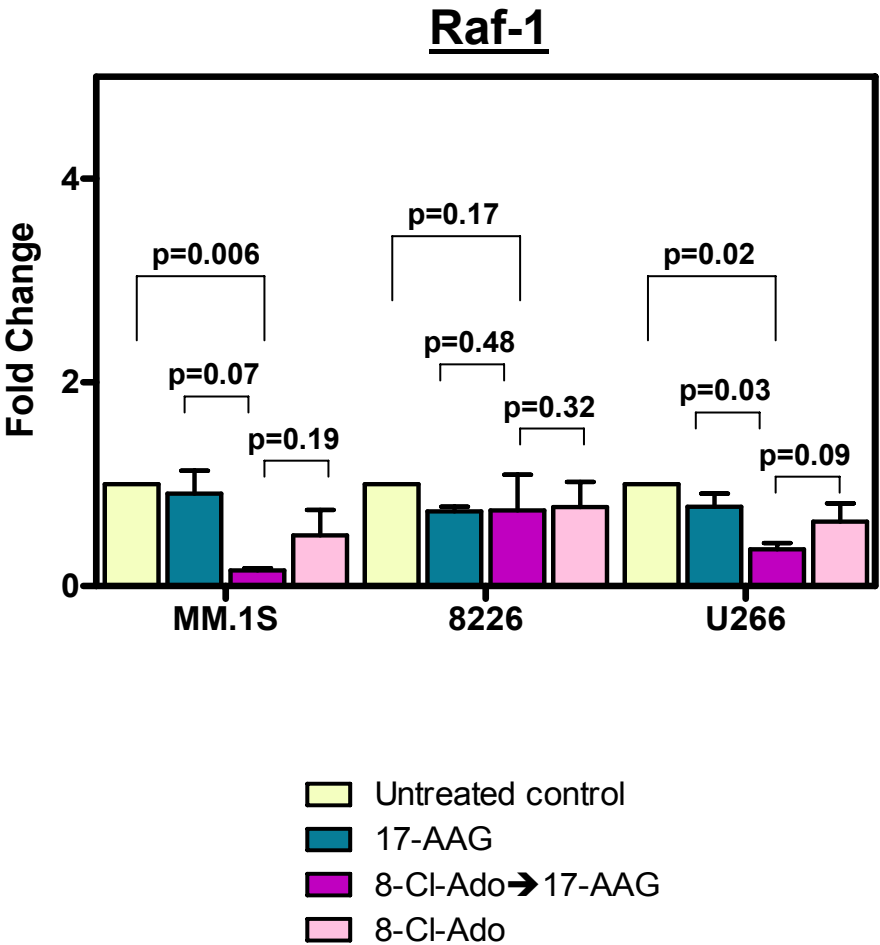
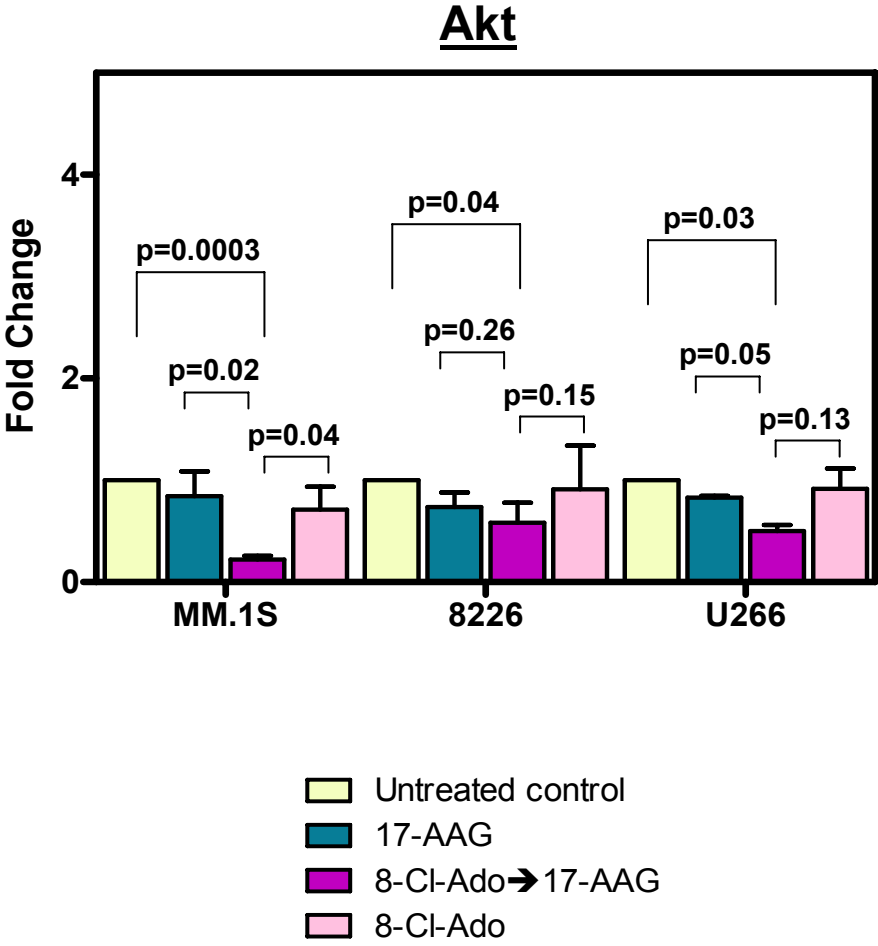


Figure 44. Combination of 8-Cl-Ado followed by 17-AAG decreased Akt expression levels in MM.1S, RPMI-8226, and U266 cells

Immunoblot assays were performed in triplicate and quantified using Odyssey infrared imaging system application software (version 1.2). Protein levels for Akt were normalized to β -actin. Data represents three independent immunoblots plotted as means plus SD. Statistical significance ($p < 0.05$) comparing the combination condition with 17-AAG alone, 8-Cl-Ado alone, or the untreated control is shown.

Figure 44



reduction of 50% Akt, when compared to the untreated control, this reduction was statistically significant ($p = 0.03$).

Effect of other 8-Cl-Ado and 17-AAG combination sequences on STAT3, Raf-1, and Akt client protein levels in U266 cells

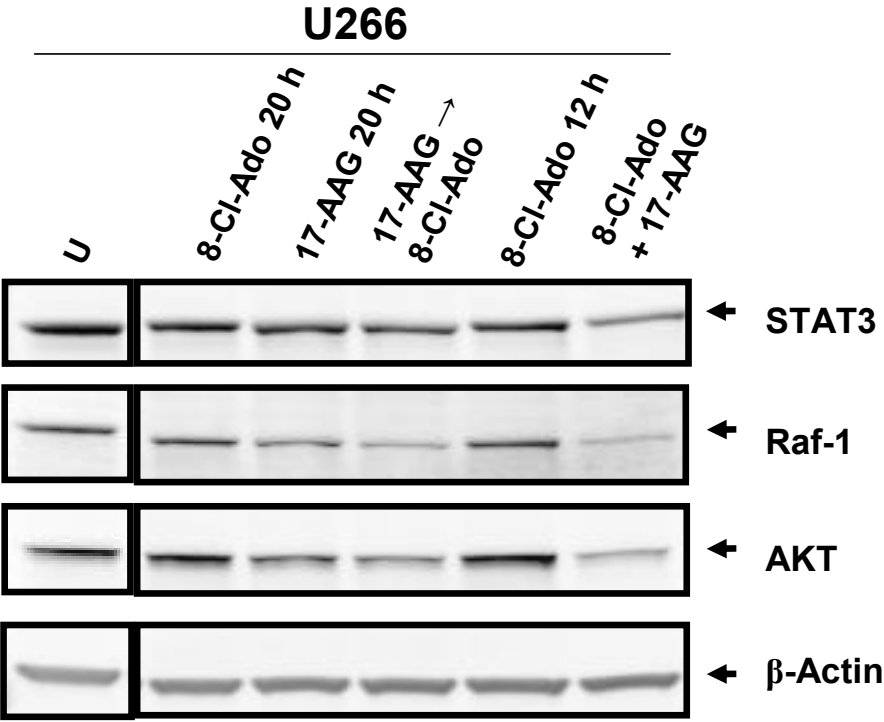
In order to elucidate whether the sequence of the drugs in the combination treatment had a different effect on the client protein levels, two other combination sequences were tested in U266 cells (Figure 45). For the first combination sequence evaluated, cells were treated with 0.5 μM 17-AAG for 20 hours alone, treated first with 0.5 μM 17-AAG for 8 hours and then 10 μM 8-Cl-Ado was added for 12 hours for the combination treatment, or treated with 10 μM 8-Cl-Ado for 12 hours alone. For the second combination condition, 10 μM 8-Cl-Ado and 0.5 μM 17-AAG were added simultaneously for 20 hours, and parallel cultures with the single agents were also treated for 20 hours. The cells were harvested at the end of each treatment, and immunoblot analysis was performed using antibodies against STAT-3, Raf-1, Akt and the loading control β -actin to evaluate changes in those protein levels. As expected, 17-AAG treatment for 20 hours reduced the client protein levels in U266 cell line. 8-Cl-Ado treatment as a single agent was not able to diminish to a noticeable extent of any of the client protein levels. However, both combination treatments lessened STAT-3, Raf-1, and Akt protein levels in a drastic manner. In both condition treatments, all of the client proteins were reduced by more than 60% when compared to the untreated control (Figure 45).

To determine if these were reproducible results, three different immunoblots were performed for the three different condition treatments in U266 cells. The same sequential and simultaneous combination designs were tested and immunoblot analyses were performed (Figure 46 and 47). The levels of client proteins STAT3, Raf-1, and Akt were normalized to β -actin and plotted as fold change in comparison to the untreated control.

Figure 45. Effect of other 8-Cl-Ado and 17-AAG combination sequences on STAT3, Raf-1, and Akt client protein levels in U266 cells

Cells were either left untreated (U) or treated with 10 μ M 8-Cl-Ado for 20 hours, 0.5 μ M 17-AAG for 20 hours, the combination of 17-AAG for 12 hours followed 8-Cl-Ado for 8 hours, 10 μ M 8-Cl-Ado for 12 hours, or combination of 8-Cl-Ado and 17-AAG added simultaneously for 20 hours. Immunoblot analyses were performed to detect protein levels for STAT3, Raf-1, Akt and the loading control β -actin in U266 cells.

Figure 45



The *p* values compare the combination treatment versus the single agents and the untreated condition.

(i) 17-AAG→8-Cl-Ado sequential combination

U266 cells were left untreated or treated with 0.5 μ M 17-AAG for 20 hours alone, treated first with 0.5 μ M 17-AAG for 8 hours followed by 10 μ M 8-Cl-Ado for 12 hours, or treated with 10 μ M 8-Cl-Ado for 12 hours alone. Treatment with 17-AAG for 20 hours alone diminished levels of all client proteins by 50% compared to the endogenous levels in the untreated control (Figure 46). In a similar manner, treatment with the ribonucleoside analogue 8-Cl-Ado resulted in a 50% decrease of STAT-3 and Raf-1 when compared to the untreated control; however, Akt protein levels were unchanged. The combination of both agents reduced all client protein levels in a statistically significant manner by approximately 50% compared to treatment with 17-AAG alone. Hence, compared to the untreated control, the combination condition reduced the levels of the client proteins by 70% or more.

(ii) 8-Cl-Ado+17-AAG simultaneous combination

U266 cells were left untreated or treated with 0.5 μ M 17-AAG for 20 hours, 10 μ M 8-Cl-Ado for 20 hours, or treated simultaneously with 10 μ M 8-Cl-Ado and 0.5 μ M 17-AAG for 20 hours. Treatment with 17-AAG for 20 hours diminished levels of all client proteins by 50% compared to the endogenous levels in the untreated control (Figure 47). Treatment with 8-Cl-Ado for 20 hours resulted in 40, 20, and 5% decrease of STAT-3, Raf-1, and Akt protein levels, respectively, when compared to the endogenous levels in the untreated control. Notably, the simultaneous addition of both agents to U266 cells resulted in a further lessening of STAT-3, Raf-1, and Akt protein levels by 50, 90, and 80%, respectively, in comparison to the untreated control. Furthermore, when the client protein levels of the combination condition were compared to the client protein levels from the 17-AAG

Figure 46. Effect of other 8-Cl-Ado and 17-AAG combination sequences on STAT3, Raf-1, and Akt client protein levels in U266 cells

(i) 17-AAG → 8-Cl-Ado sequential combination

U266 cells were either left untreated or treated with 0.5 μ M 17-AAG for 20 hours, the sequential combination of 0.5 μ M 17-AAG for 8 hours followed by 10 μ M 8-Cl-Ado for 12 hours, or 10 μ M 8-Cl-Ado for 12 hours. Immunoblot assays were performed in duplicate and quantified using Odyssey infrared imaging system application software (version 1.2). Protein levels for STAT3, Raf-1, and Akt were normalized to β -actin. Data represents two independent immunoblots plotted as means plus SD. Statistical significance ($p < 0.05$) comparing the combination condition with 17-AAG alone, 8-Cl-Ado alone, or the untreated control is shown.

Figure 46

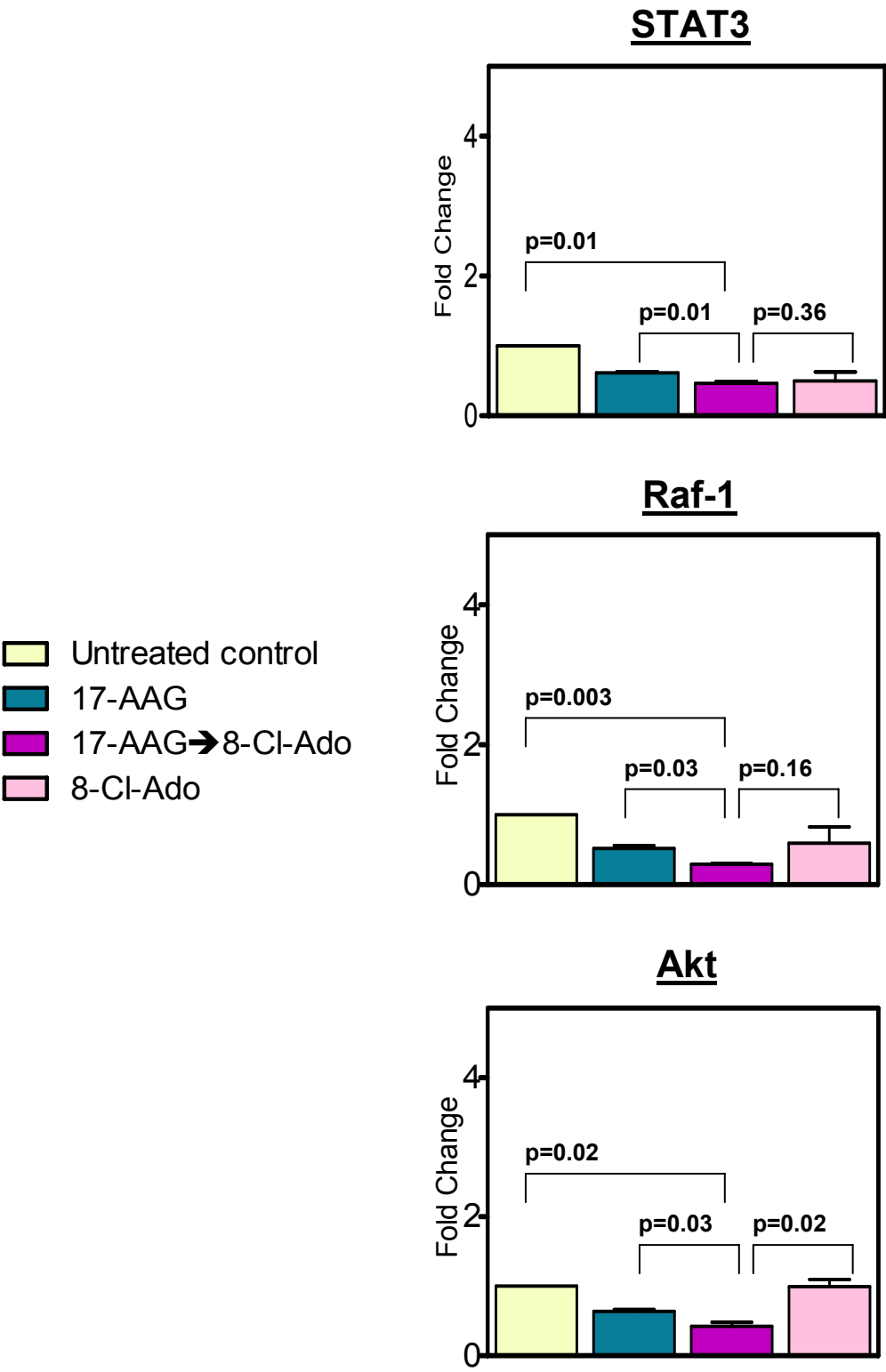
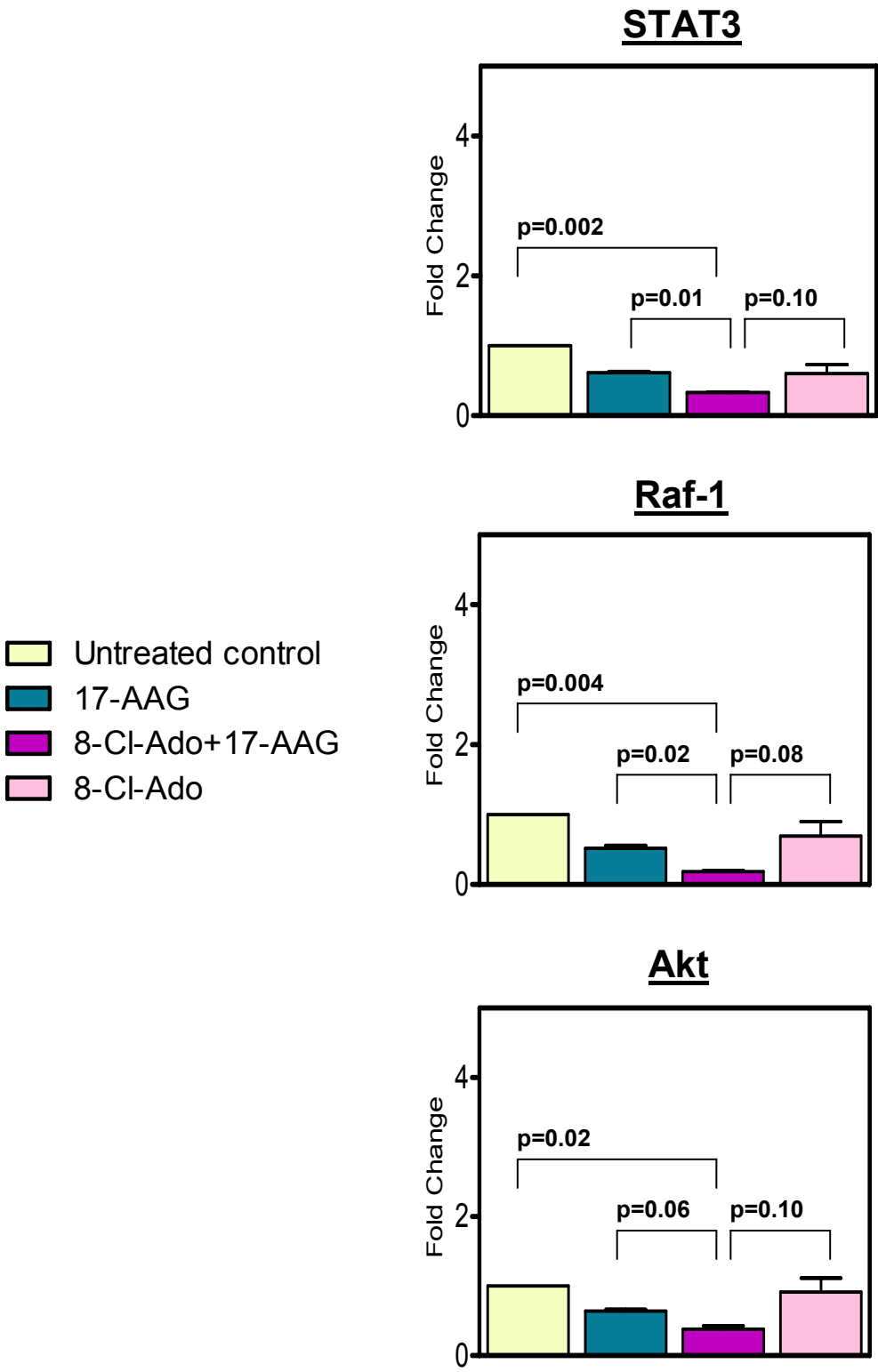


Figure 47. Effect of other 8-Cl-Ado and 17-AAG combination sequences on STAT3, Raf-1, and Akt client protein levels in U266 cells

(ii) 8-Cl-Ado+17-AAG simultaneous combination

U266 cells were either left untreated or treated with 0.5 μ M 17-AAG for 20 hours, 10 μ M 8-Cl-Ado for 20 hours, or 0.5 μ M 17-AAG and 10 μ M 8-Cl-Ado added simultaneous for 20 hours. Immunoblot assays were performed in duplicate and quantified using Odyssey infrared imaging system application software (version 1.2). Protein levels for STAT3, Raf-1, and Akt were normalized to β -actin. Data represents from two independent immunoblots plotted the mean plus SD. Statistical significance ($p < 0.05$) comparing the combination condition with 17-AAG alone, 8-Cl-Ado alone, or the untreated control is shown.

Figure 47



treatment, the difference between both treatments was statistically significant for STAT3 and Raf-1, but not Akt. However, when the client protein levels in the untreated control were compared to the protein levels in the combination treatment, a statistically significant decrease ($p < 0.05$) was calculated.

In summary, any of the three different combinations of 8-Cl-Ado and 17-AAG resulted in a statistically significant decrease of STAT3, Raf-1, and Akt client protein levels in all the evaluated MM cell lines when compared to the untreated control. The only exception was Raf-1 protein levels in RPMI-8226 cells (8-Cl-Ado→17-AAG sequential treatment) where the p value was found to be not statistically significant when compared to the untreated control (Figure 43, $p = 0.17$).

Effect of 8-Cl-Ado and 17-AAG alone and in combination on STAT-3, Raf-1, and Akt client protein mRNA levels in MM.1S and RPMI-8226 cells

To investigate if the clear reduction in STAT-3, Raf-1, and Akt expression observed in the combination treatment was due to a decrease in their mRNA levels, real time RT-PCR measuring for STAT-3, Raf-1, and Akt transcripts was performed (Figures 48, 49, and 50). Primers and probes specific for STAT-3, Raf-1, and Akt were used to detect mRNA levels of these client proteins. MM cells were either left untreated or treated with 0.5 μ M 17-AAG for 8 hours, the combination of 10 μ M 8-Cl-Ado for 12 hours followed by 0.5 μ M 17-AAG for 8 hours, or 10 μ M 8-Cl-Ado for 20 hours. Cells were harvested following drug treatment and RNA isolated for each condition as described in material and methods. Condition treatments were normalized using the housekeeping gene GAPDH and the data plotted as fold change in comparison to the untreated control. Three independent experiments with each condition treatment done in triplicate were performed.

8-Cl-Ado and 17-AAG alone or in combination did not affect STAT3 transcript levels in MM.1S and RPMI-8226 cells

In the cell line MM.1S there was a no increase in STAT3 transcript levels after 17-AAG treatment alone (Figure 48). A 2-fold increase in STAT3 transcript levels was observed following 8-Cl-Ado treatment as well as with the combination treatment. Regardless of the effect of 8-Cl-Ado in STAT3 mRNA transcripts, no significant difference was calculated for any of the condition treatments. In RPMI-8226 cells, no significant change was observed for any of the condition treatments (Figure 48).

8-Cl-Ado and 17-AAG alone or in combination did not affect Raf-1 transcript levels in MM.1S and RPMI-8226 cells

In MM.1S cells treatment with 17-AAG resulted in a decrease in Raf-1 mRNA levels by 50% when compared to the untreated control (Figure 49). A 40% reduction of Raf-1 transcripts was measured in the combination treatment. Treatment with 8-Cl-Ado alone did not affect the transcript levels of Raf-1. When comparing the combination treatment to the single agents or the untreated control, no statistical difference was calculated. In RPMI-8226 cells, 8-Cl-Ado and 17-AAG either alone or in combination did not affect the transcript levels of Raf-1 (Figure 49).

8-Cl-Ado and 17-AAG alone or in combination did not affect Akt transcript levels in MM.1S cells, only effect observed in RPMI-8226 cells for the combination treatment

In MM.1S cells, no significant change was determined for any of the treatments being evaluated (Figure 50). In RPMI-8226 cells, there was a small increase following 17-AAG treatment, which was not statistically significant. Treatment with 8-Cl-Ado alone did not have an effect on Akt transcript levels in this cell line. A small increment in Akt mRNA levels were measured in the combination treatment (less than 1.5-fold), and surprisingly,

Figure 48. 8-Cl-Ado and 17-AAG alone or in combination did not affect STAT3 transcript levels in MM.1S and RPMI-8226 cells

Cells were left untreated or treated with 0.5 μ M 17-AAG for 8 hours, 10 μ M 8-Cl-Ado for 20 hours, or the combination of 10 μ M 8-Cl-Ado for 12 h followed by 0.5 μ M 17-AAG for 8 hours. Total RNA was isolated and STAT3 mRNA levels were measured using real-time RT-PCR and represented as fold change in comparison with the untreated control. GAPDH was used as the endogenous gene for normalization and each column represents the mean and SD of triplicate experiments. Statistical significance ($p < 0.05$) comparing the combination condition with 17-AAG alone, 8-Cl-Ado alone, or the untreated control is shown.

Figure 48

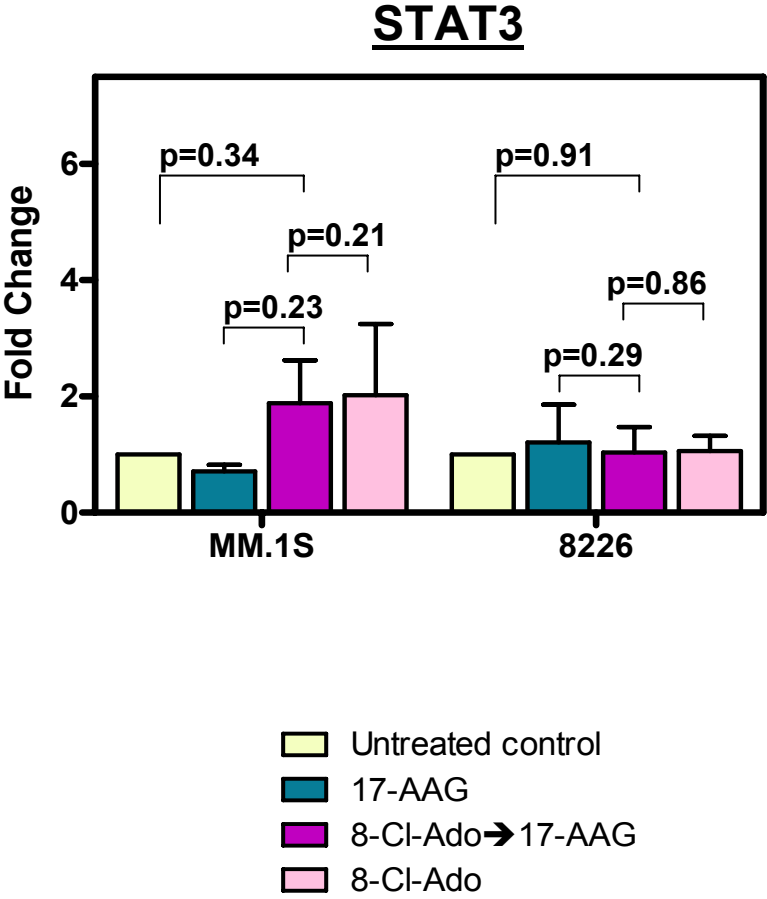


Figure 49. 8-Cl-Ado and 17-AAG alone or in combination did not affect Raf-1 transcript levels in MM.1S and RPMI-8226 cells

Cells were left untreated or treated with 0.5 μ M 17-AAG for 8 hours, 10 μ M 8-Cl-Ado for 20 hours, or the combination of 10 μ M 8-Cl-Ado for 12 h followed by 0.5 μ M 17-AAG for 8 hours. Total RNA was isolated and Raf-1 mRNA levels were measured using real-time RT-PCR and represented as fold change in comparison with the untreated control. GAPDH was used as the endogenous gene for normalization and each column represents the mean and SD of triplicate experiments. Statistical significance ($p < 0.05$) comparing the combination condition with 17-AAG alone, 8-Cl-Ado alone, or the untreated control is shown.

Figure 49

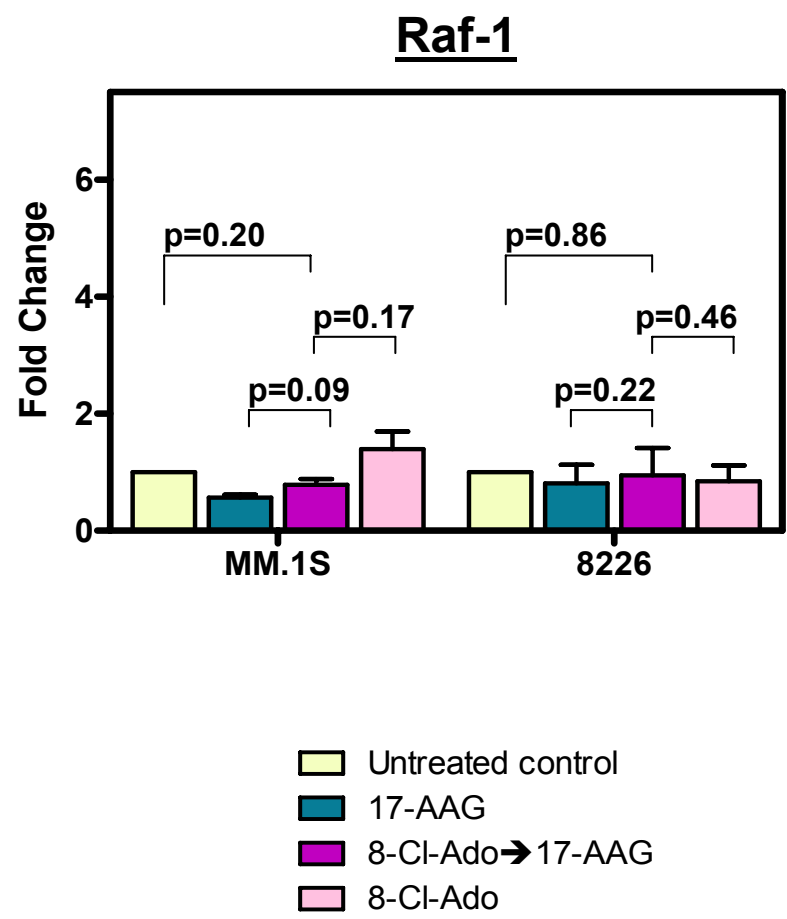
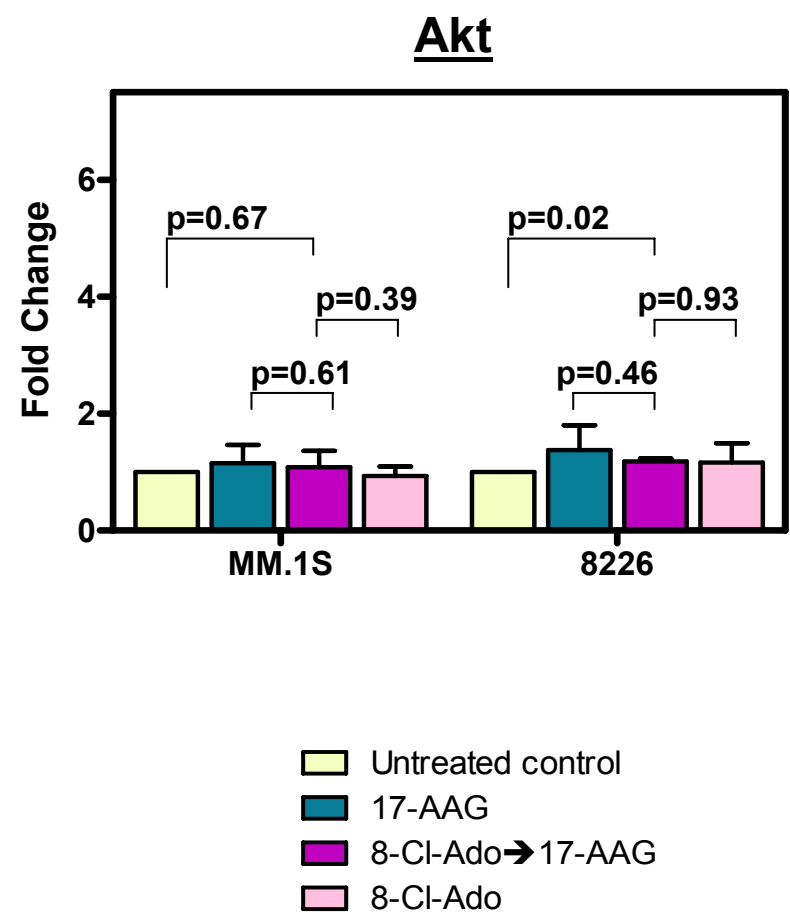


Figure 50. 8-Cl-Ado and 17-AAG alone or in combination did not affect Akt transcript levels in MM.1S cells, only effect observed in RPMI-8226 cells for the combination treatment

Cells were left untreated or treated with 0.5 μ M 17-AAG for 8 hours, 10 μ M 8-Cl-Ado for 20 hours, or the combination of 10 μ M 8-Cl-Ado for 12 h followed by 0.5 μ M 17-AAG for 8 hours. Total RNA was isolated and Akt mRNA levels were measured using real-time RT-PCR and represented as fold change in comparison with the untreated control. GAPDH was used as the endogenous gene for normalization and each column represents the mean and SD of triplicate experiments. Statistical significance ($p < 0.05$) comparing the combination condition with 17-AAG alone, 8-Cl-Ado alone, or the untreated control is shown.

Figure 50



the increase was statistically significant when compared to the untreated control ($p = 0.02$) (Figure 50).

In summary, there was not a statistically significant decrease or increase detected in STAT3, Raf-1, or Akt transcript levels with any of the treatments in neither cell line. An exception was observed for Akt mRNA levels with the combination treatment in RPMI-8226. Although there was a small induction of Akt transcript, this proved to be statistically significant. Therefore, the decrease in STAT3, Raf-1, and Akt expression levels in the combination treatment are not due to a decrease in STAT3, Raf-1, and Akt transcript levels.

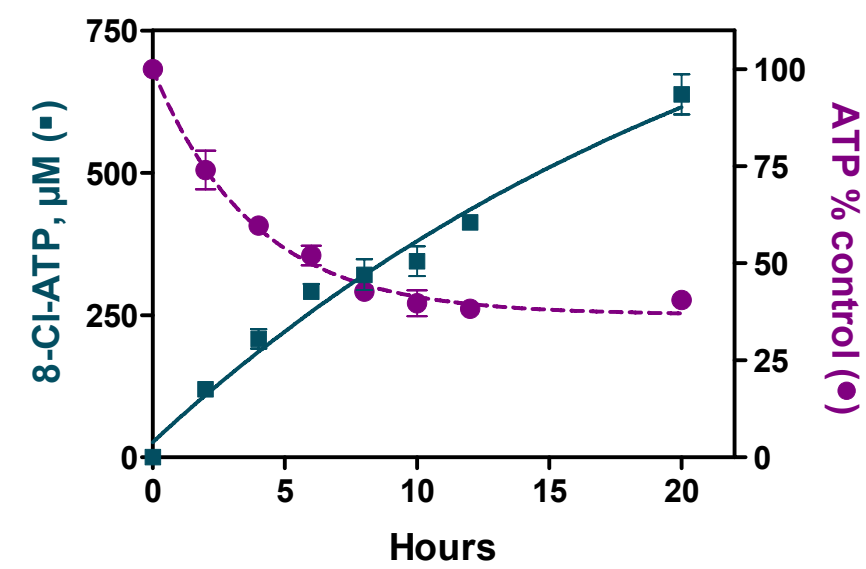
Cellular metabolism: accumulation of 8-Cl-Ado cytotoxic triphosphate and concomitant ATP concentration decrease in MM.1S cells

In the cell, treatment with 8-Cl-Ado results in its phosphorylation to the cytotoxic triphosphate form (8-Cl-ATP). The accumulation of the cytotoxic metabolite results in a parallel decrease of the ATP cellular pools (Gandhi, Ayres et al. 2001; Chen, Nowak et al. 2009). MM.1S cells were treated with 10 μM 8-Cl-Ado as a function of time in order to determine the accumulation of 8-Cl-ATP and potential depletion of cellular ATP pools (Figure 51). Cells were harvested following treatment and 8-Cl-ATP and ATP levels in each condition were analyzed and measured by HPLC methods as described in materials and methods. Each time point was performed in triplicate. Cellular ATP levels are represented as percentage of the untreated control (endogenous ATP levels 3 mM). A parallel decrease in ATP pools is observed with increasing accumulation of 8-Cl-ATP in the cell. In the first 2 hours of treatment with 8-Cl-Ado there is a decrease in ATP levels by 25% and a 100 μM accumulation of 8-Cl-ATP. By 20 hours, treatment with 8-Cl-Ado decreases ATP levels by 65%, with approximately 1 mM intracellular ATP remaining. Furthermore, an accumulation of 637 μM 8-Cl-ATP is achieved after 20 hours with 8-Cl-Ado treatment.

Figure 51. Cellular metabolism: accumulation of 8-Cl-Ado cytotoxic triphosphate and concomitant ATP concentration decrease in MM.1S cells

Cells were treated with 10 μ M 8-Cl-Ado as a function of time. Cells were harvested at the indicated times and 8-Cl-ATP (■) and ATP (●) levels in the cells were measured using HPLC as described in materials and methods. Each time point was performed in triplicate and data represented as mean \pm SD (Endogenous ATP levels in untreated cells was approximately 3 mM).

Figure 51



Sequential treatment of 8-Cl-Ado followed by 17-AAG reduces 8-Cl-Ado metabolism and ATP accumulation

In order to determine if addition of 17-AAG affected the accumulation of 8-Cl-ATP or the decrease in ATP pool, the combination condition was also evaluated. The various MM cell lines were left untreated or treated with 10 μ M 8-Cl-Ado for 20 hours or the combination of 8-Cl-Ado for 12 hours followed by 0.5 μ M 17-AAG for 8 hours. Cells were harvested at the end of treatment and cellular 8-Cl-ATP and ATP levels in the cells were measured using HPLC as described in materials and methods. The data represent mean of triplicate experiments for MM.1S and duplicate experiments for RPMI-8226, while preliminary data is showed for the U266 cell line (Table 3).

Untreated MM.1S cells contained 2988 μ M ATP endogenous concentration. Treatment with 8-Cl-Ado caused a 57% decrease in ATP levels (1268 μ M ATP concentration remaining in the cell). The combination treatment resulted in an 83% drop of the ATP pool, with only 340 μ M ATP concentration remaining in the cell after treatment. Surprisingly, the expected parallel accumulation of 8-Cl-ATP levels was not observed. Addition of 17-AAG after 8-Cl-Ado treatment resulted in only 203 μ M 8-Cl-ATP accumulation in the combination treatment compared to 607 μ M 8-Cl-ATP levels reached with treatment with 8-Cl-Ado as a single agent. A similar decrease in 8-Cl-ATP levels were observed in the other two cell lines in the combination treatment.

In RPMI-8226 cells, the endogenous ATP pool was measured to be 2699 μ M. After 8-Cl-Ado treatment, a majority of the ATP concentration remained in the cell (76%, 2064 μ M), and 8-Cl-ATP accumulation reached 1109 μ M. Addition of 17-AAG following 8-Cl-Ado treatment did not affect the levels of ATP to a great extent compared with 8-Cl-Ado alone (76% vs 64%). However, a decrease in 8-Cl-ATP levels was also observed when compared to 8-Cl-Ado treatment alone. 8-Cl-ATP accumulation was measured to be 764 μ M in the

Table 3. Sequential treatment of 8-Cl-Ado followed by 17-AAG reduces 8-Cl-Ado metabolism and ATP accumulation

Cells were either left untreated or treated with 10 μ M radiolabeled [3 H] 8-Cl-Ado for 12 hours followed by 0.5 μ M 17-AAG for 8 hours. Cells were harvested and 8-Cl-ATP and ATP levels in each condition were measured using HPLC as described in materials and methods. Triplicate experiments were performed for MM.1S, duplicate experiments for RPMI-8226, and preliminary data is showed for U266 cell line.

Table 3

Endogenous ATP μM	Treatments	8-Cl-ATP μM	ATP Decrease %	ATP in cells after treatment μM	ATP in cells after treatment %
MM.1S	<i>8-Cl-Ado</i> → <i>17-AAG</i>	203	83	340	17
2988	<i>8-Cl-Ado</i>	607	57	1268	43
RPMI-8226	<i>8-Cl-Ado</i> → <i>17-AAG</i>	764	36	1718	64
2699	<i>8-Cl-Ado</i>	1109	24	2064	76
U266	<i>8-Cl-Ado</i> → <i>17-AAG</i>	179	73	520	27
2127	<i>8-Cl-Ado</i>	267	56	936	44

combination condition compared to 1109 μM 8-Cl-ATP measured after 8-Cl-Ado treatment alone.

Preliminary data in U266 cells showed the endogenous ATP concentration in the untreated cells was 2127 μM . With 8-Cl-Ado treatment there was a decline in ATP by 56%, leaving 936 μM ATP in the cell. The concentration of 8-Cl-ATP was measured to be only 267 μM after 8-Cl-Ado treatment as a single agent. The combination treatment in U266 cells resulted in a reduction of ATP levels by 73%, meaning there was 520 μM of ATP in the cell at the end of treatment. The same decrease in 8-Cl-ATP levels were also observed when compared to the 8-Cl-ATP levels for 8-Cl-Ado treatment as a single agent. Accumulation of 8-Cl-ATP for the combination treatment was 179 μM , less than the amount measured for 8-Cl-Ado alone (267 μM).

Taken together, these results show that 8-Cl-Ado affects the ATP pools in MM.1S and U266 cells causing a decrease by more than 55%. In contrast, the ATP levels in RPMI-8226 cells do not seem to be greatly affected by 8-Cl-Ado treatment. As expected there is accumulation of the cytotoxic triphosphate 8-Cl-ATP after 8-Cl-Ado treatment in all cell lines, although the measured levels for each cell line vary among each other. Addition of 17-AAG after 8-Cl-Ado treatment results in further decrease of the ATP levels, however, an unexpected decrease in 8-Cl-ATP levels are measured in all cell lines. This suggests that 17-AAG affects the metabolism of 8-Cl-Ado to its cytotoxic triphosphate form.

Immunoprecipitation of HSP90 bound to [^3H] 17-AAG in the combination treatment with 8-Cl-Ado

The HSP90 inhibitor, 17-AAG, competes with ATP, HSP90's natural substrate, for the binding to HSP90 (Schnur, Corman et al. 1995). Binding of 17-AAG to HSP90 inhibits the stabilization of client proteins by this chaperone resulting in client protein proteasomal

degradation (Neckers and Neckers 2002). The combination treatment resulted in a further decrease in ATP levels compared to treatment with 8-Cl-Ado alone (Table 3). The combination of 8-Cl-Ado and 17-AAG resulted in marked decreased levels of the client proteins when compared to 17-AAG and 8-Cl-Ado treatments as single agents, especially in MM.1S cells (Figures 41-44). A possible explanation for this could be that 17-AAG does not have to compete against the high levels of ATP in the cell for HSP90 binding in the combination treatment since 8-Cl-Ado decreases cellular ATP pool. For this reason, immunoprecipitations and immunoblot analyses of radioactive [^3H]17-AAG bound to HSP90 were performed in MM.1S cells for the combination treatment compared to 17-AAG treatment alone (Figure 54). In order to evaluate the [^3H]17-AAG•HSP90 complex for these treatments, the following immunoprecipitations and immunoblot analyses were conducted to determine optimal conditions in untreated cells first (Figure 52 and 53).

(i) Immunoprecipitation and immuno-detection of HSP90 α/β and RNA Pol II as a function of concentration

To determine an optimal concentration of the amount of HSP90 α/β antibody to be used, a dose response was performed (Figure 52A). Untreated MM.1S cells were lysed and protein concentration quantified. 1000 μg of protein was incubated with increasing concentrations of an antibody detecting for HSP90 α/β . A protein that does not interact with 17-AAG, RNA Pol II, was also included as a negative control to rule out non-specific binding (Figure 52B). In a similar way, 1000 μg of protein were incubated with increasing concentrations of an antibody detecting for RNA Pol II, with the corresponding controls being run in parallel. Immunoprecipitations were performed as described in materials and methods. Bead-bound material was then analyzed via immunoblot using antibodies that detect HSP90 α/β and RNA Pol II protein levels. Incubation with increasing concentrations of an antibody detecting HSP90 α/β resulted in escalating immunoprecipitated amounts of

Figure 52. Immunoprecipitation and immuno-detection of HSP90 α / β and RNA Pol II as a function of concentration

Immunoprecipitation using an antibody specific for HSP90 α / β was used at increasing concentrations in MM.1S protein lysates to determine the optimal antibody concentration.

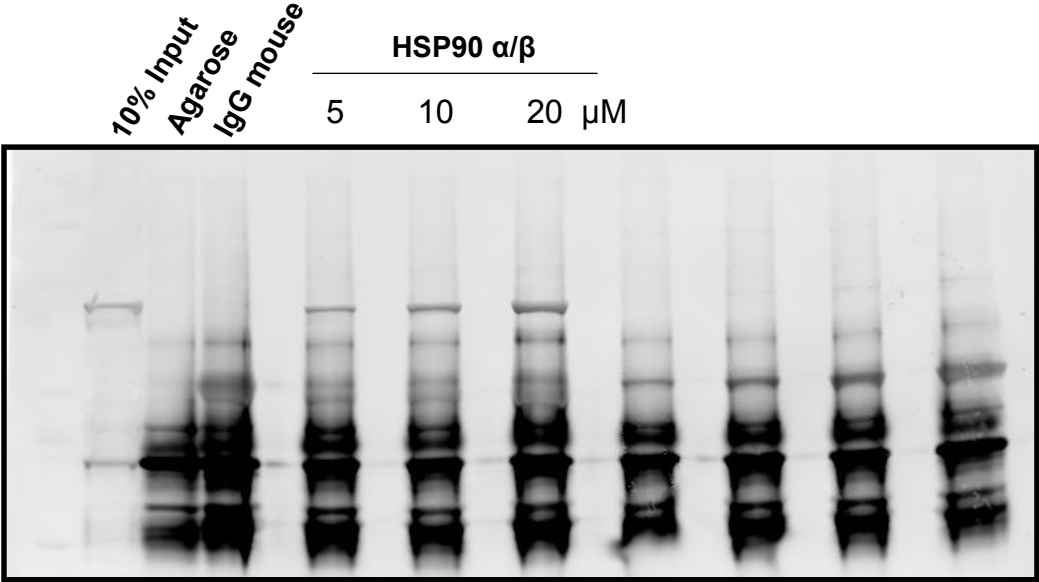
The immunoprecipitates were then analyzed by immunoblot assay detecting for HSP90 α / β

(A) protein levels. Similar immunoprecipitation and immunoblot assays were conducted

using RNA Pol II as a control protein (B).

Figure 52

A



B

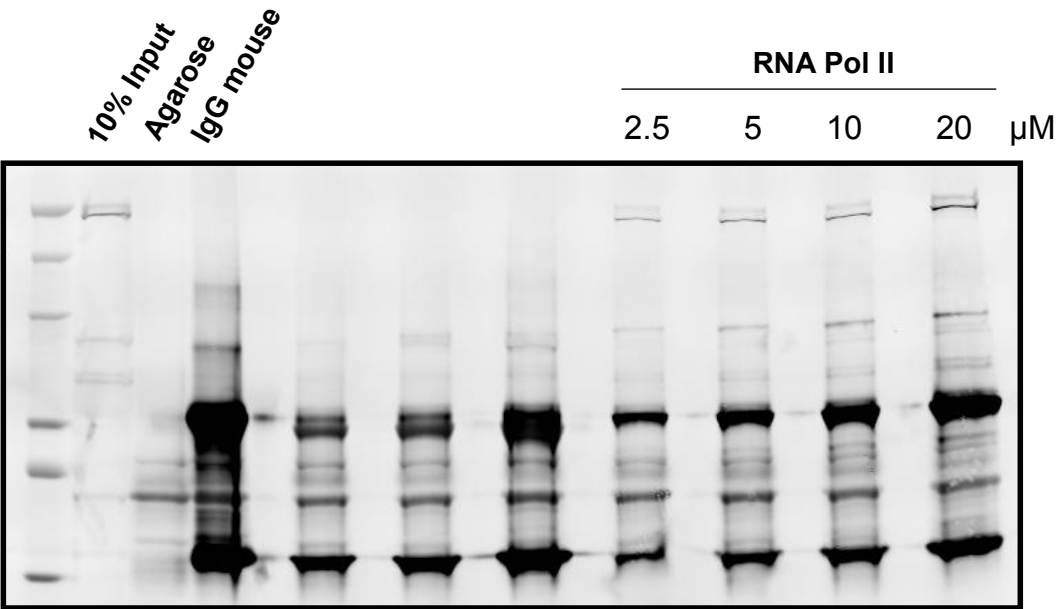
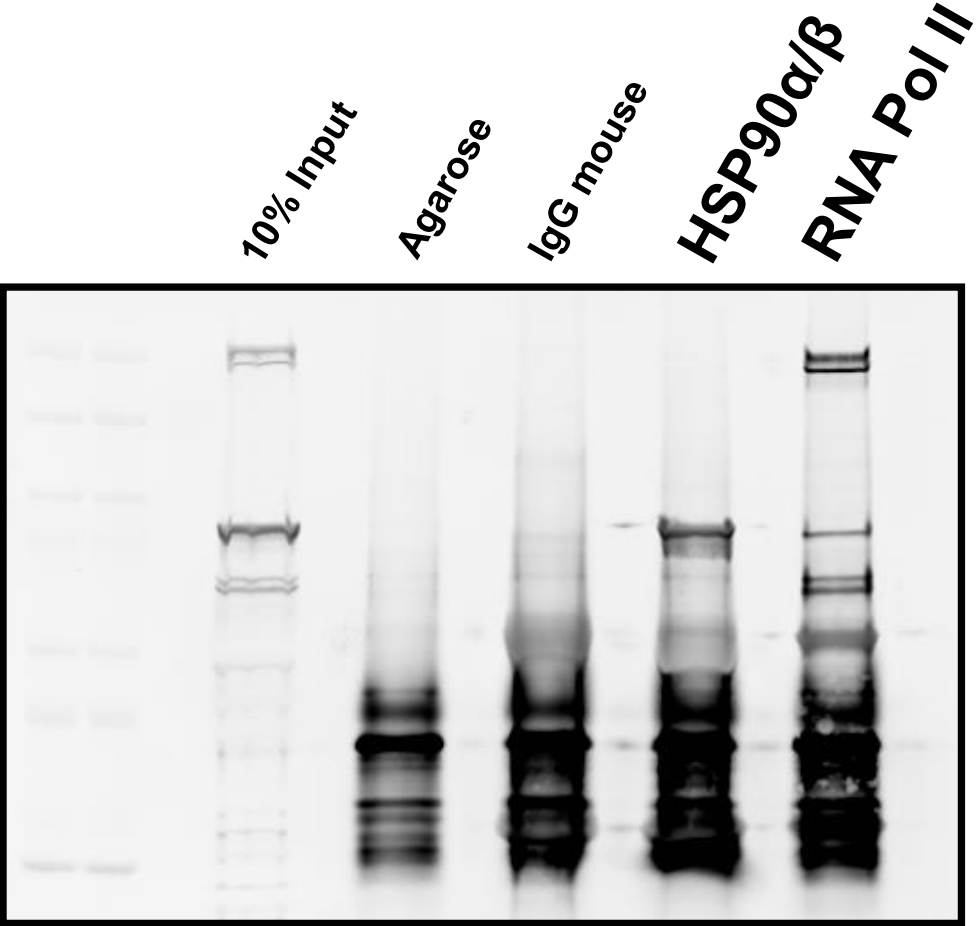


Figure 53. Immunoprecipitation and immuno-detection of HSP90 α / β and RNA Pol II

A final immunoprecipitation and immunodetection of HSP90 α / β and RNA Pol II was performed in untreated MM.1S cells once the optimal antibody concentrations were chosen. MM.1S cells were lysed and 1000 μ g/mL of protein was incubated with antibodies detecting for HSP90 α / β or RNA Pol II along with the corresponding controls for the immunoprecipitation assay. An immunoblot assay was performed for each immunoprecipitated antibody or control.

Figure 53



HSP90 α/β protein. A similar effect was also observed for RNA Pol II. The 10% input showed the presence of the evaluated proteins in MM.1S cells while the controls (agarose beads and IgG mouse) showed that non-specific protein interactions were not taking place. Based on dose response results, 10 μ M HSP90 α/β and 5 μ M RNA Pol II antibody concentrations were selected.

Once the optimal antibody concentrations were selected and proper condition controls were established, final immunoprecipitation and immunoblot analysis were performed to evaluate if non-specific pull downs occurred. Untreated MM.1S cells were lysed and protein quantified. 1000 μ g of protein was then incubated with 10 μ g agarose beads, 10 μ g IgG mouse antibody, 10 μ g HSP90 α/β , or 5 μ g RNA Pol II and immunoprecipitations were performed as described in material and methods. The immunoprecipitations were then analyzed via immunoblots detecting for HSP90 α/β and RNA Pol II (Figure 53).

(ii) Effect of 8-Cl-Ado in the binding of [3 H]17-AAG to HSP90

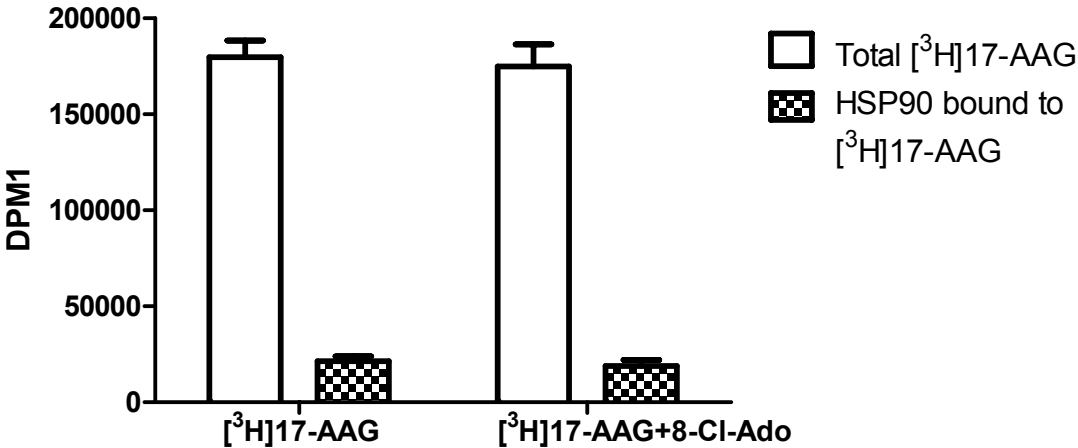
To evaluate if a decrease in cellular ATP levels allowed more 17-AAG binding to HSP90, immunoprecipitation and radioactive liquid scintillation counting for [3 H]17-AAG bound to HSP90 was performed (Figure 54). MM.1S cells were treated with 0.5 μ M [3 H]17-AAG alone for 20 hours or the combination of 10 μ M 8-Cl-Ado and [3 H]17-AAG added simultaneously for 20 hours. Cells were lysed and protein quantified for each condition. Each condition was performed twice in duplicate. Antibodies detecting for HSP90 α/β and RNA Pol II were incubated with 1000 μ g of protein. Corresponding controls were also done in parallel. Immunoprecipitations were performed as described in materials and methods and the radioactive [3 H]17-AAG bound to HSP90 α/β was counted in a liquid scintillation counter. In order to follow the balance of material, the total amount of [3 H]17-AAG was determined from the media in the cultures to the washes in the immunoprecipitation assay.

Figure 54. Immunoprecipitation of HSP90 bound to [³H] 17-AAG in the combination treatment with 8-Cl-Ado

Effect of 8-Cl-Ado in the binding of [³H] 17-AAG to HSP90

MM.1S cells were treated with 0.5 μM [³H] 17-AAG in the absence or presence of 8-Cl-Ado for 20 hours then lysed and immunoprecipitated for HSP90. The immunoprecipitated HSP90 proteins were then analyzed by liquid scintillation counting to measure the levels of [³H]-17-AAG retained in HSP90. Each column represents the mean and SD of two independent experiments done in duplicate.

Figure 54



The total amount of [^3H]17-AAG in both condition treatments was similar (175000 DPM). Immunoprecipitation of HSP90 α/β in MM.1S cells treated with [^3H]17-AAG alone determined that [^3H]17-AAG is bound to HSP90 α/β and the complex can be pulled down and radioactivity analyzed (approximately 25000 DPM). However, the combination condition did not show an increasing amount of [^3H]17-AAG binding to HSP90 α/β (approximately 25000 DPM, same as with [^3H]17-AAG treatment alone). In addition, immunoprecipitation of RNA Pol II protein indicated the absence of [^3H]17-AAG bound to RNA Pol II since the radioactive count was determined to be around 50 DPM (Data not shown).

In summary these data indicate that a 57% decrease in ATP levels due to 8-Cl-Ado treatment (Table 3) does not increase the amount of 17-AAG binding to HSP90 α/β protein (Figure 54). These results suggest that increased proteasomal degradation of client proteins due to increased levels of 17-AAG binding to HSP90 α/β protein is not the possible mechanism that results in decreased STAT-3, Raf-1, and Akt client protein levels in the combination treatment of 8-Cl-Ado and 17-AAG.

Effect of 8-Cl-Ado on 4E-BP1 protein levels in MM.1S cells

Since no change was detected for any of the client mRNA levels (Figures 48-50) or no increased levels of 17-AAG bound to HSP90 were detected (Figure 54), a repressor protein of mRNA translation was analyzed. The translation regulator protein 4E-binding protein 1 (4E-BP1) represses initiation of translation by binding to the eukaryotic initiation factor 4E (eIF4E) (Gingras, Kennedy et al. 1998). 4E-BP1 repressing activity is regulated by phosphorylation at 4 specific aminoacid residues (Gingras, Kennedy et al. 1998; Gingras, Raught et al. 2001). Once hyperphosphorylated 4E-BP1 releases eIF4E allowing translation initiation (Gingras, Raught et al. 2001). The serine/threonine kinase mTOR is one of the

upstream regulators of 4E-BP1 activity (Gingras, Kennedy et al. 1998). The mTOR pathway is sensitive to the change in cellular ATP levels (Dennis, Jaeschke et al. 2001). A decrease in ATP inhibits the kinase activity of mTOR, thus rendering it unable to phosphorylate 4E-BP1. As a result, 4E-BP1 remains bound to eIF4, inhibiting translation initiation (Gingras, Raught et al. 2001). Due to the effect of 8-Cl-Ado on the ATP levels in the cell, the phosphorylated status of 4E-BP1 was evaluated.

MM.1S cells were treated with 10 μ M 8-Cl-Ado for different time durations (Figure 55A). Starvation of MM.1S was also done for several days to be used as a positive control for hypophosphorylation of 4E-BP1 leading to translation inhibition (Figure 55B). Cells were harvested and immunoblots were performed and analyzed with antibodies detecting for 4E-BP1 and the loading control GAPDH. The multiple bands of 4E-BP1 represent its hyperphosphorylated status, and stacking of the bands represents its hypophosphorylated form (Gingras, Kennedy et al. 1998; Gingras, Raught et al. 2001). Starvation of MM.1S for 24 and 48 hours resulted in hypophosphorylation of 4E-BP1. Treatment with 8-Cl-Ado resulted in a time dependent decrease in 4E-BP1 phosphorylation levels, with a more pronounced hypophosphorylated form of 4E-BP1 appearing at 24, 48 and 72 hours.

Effect of 8-Cl-Ado and 17-AAG on 4E-BP1 protein levels in U266 cells

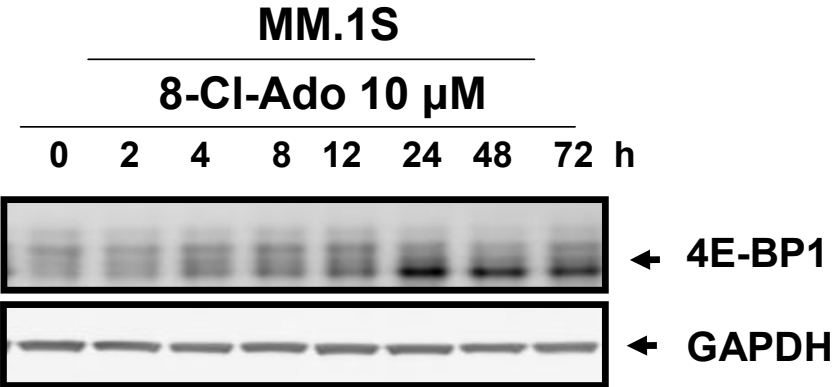
U266 cells were treated with the two different sequential or simultaneous combinations of 8-Cl-Ado and 17-AAG to determine if 17-AAG could further affect the phosphorylation status of 4E-BP1. For the first combination sequence, cells were left untreated or treated with 0.5 μ M 17-AAG for 8 hours alone, treated first with 10 μ M 8-Cl-Ado for 12 hours followed by 0.5 μ M 17-AAG for 8 hours for the combination treatment, or treated with 10 μ M 8-Cl-Ado for 20 hours alone. For the second combination sequence to be tested, cells were treated with 0.5 μ M 17-AAG for 20 hours alone, treated first with 0.5 μ M 17-AAG for 8 hours followed by 10 μ M 8-Cl-Ado for 12 hours for the combination

Figure 55. Effect of 8-Cl-Ado on 4E-BP1 protein levels in MM.1S cells

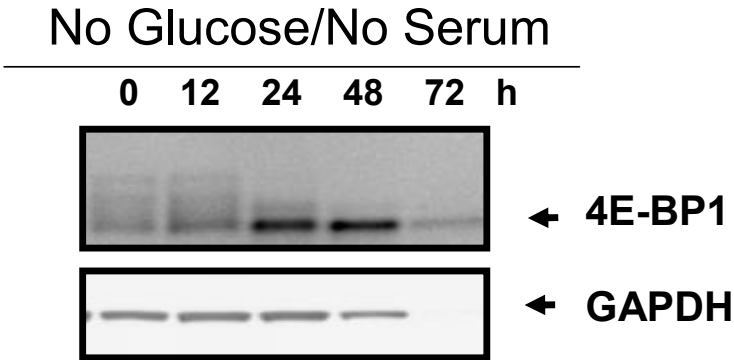
MM.1S cells were treated with 10 μ M 8-Cl-Ado for the indicated times (A). MM.1S cells were starved for the indicated times to use a positive control for dephosphorylation of 4E-BP1(B). Cells were harvested and immunoblots were performed and analyzed with antibodies detecting for 4E-BP1 and the loading control GAPDH.

Figure 55

A



B



treatment, or treated with 10 μ M 8-Cl-Ado for 12 hours alone. Finally, for the last combination condition, 10 μ M 8-Cl-Ado and 0.5 μ M 17-AAG were added simultaneously for 20 hours, and the two parallel conditions with the single agents included. Cells were harvested and immunoblots were analyzed using antibodies against 4E-BP1 and the loading control GAPDH (Figure 56).

Treatment with 17-AAG for 8 or 20 hours did not affect the hyperphosphorylation status of 4E-BP1 as shown by its multiple bands. Treatment with 8-Cl-Ado for 12 or 20 hours resulted in a decrease in phosphorylation levels in 4E-BP1. However, any of the combination treatments resulted in hypophosphorylation of 4E-BP1 as shown by the absence of multiple bands.

Taken together, 17-AAG treatment alone does not affect phosphorylation of 4E-BP1. However, 8-Cl-Ado treatment results in decrease phosphorylation of the repressing translation factor 4E-BP1, which is further hypophosphorylated by the addition of 17-AAG in any of the three combination sequences.

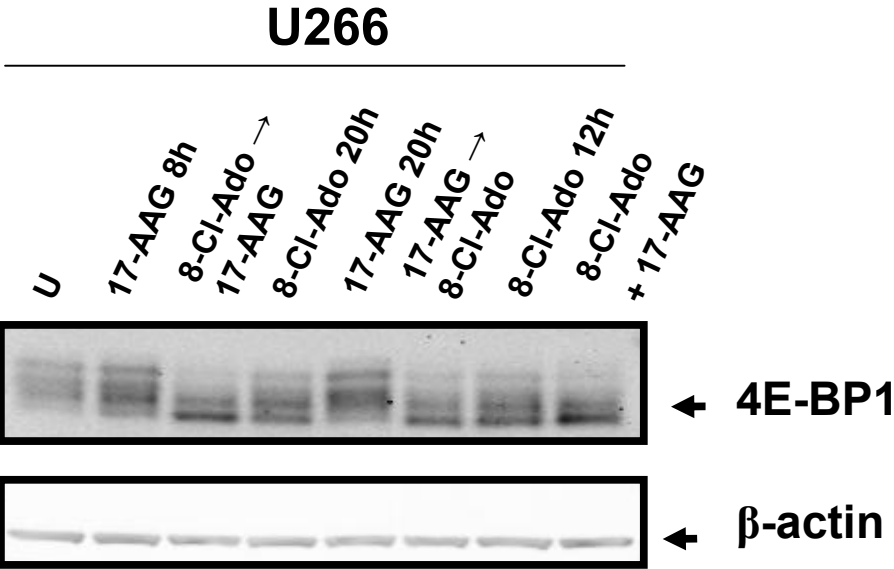
Cytotoxicity of 8-Cl-Ado followed by 17-AAG in MM cell lines

To evaluate if the decrease of client proteins in the combination treatment with 8-Cl-Ado and 17-AAG could result in increased cytotoxicity, Annexin V/7-AAD assay was performed. Plotted data represent the mean of three different experiments for each cell line (Figure 57). The endogenous cell death was subtracted from each condition. Endogenous cell death in MM.1S cells was around 10 to 15%, in RPMI-8226 cells it ranged from 15 to 20%, and in U266 cells it was less than 10%. The combination treatment contained less DMSO concentration than the established non-cytotoxic and tolerated amount by cells (<0.1%) since 17-AAG was the only drug dissolved in DMSO (0.05%). MM cells were either not treated or treated with 0.5 μ M 17-AAG alone for 8 hours, a combination treatment with

Figure 56. Effect of 8-Cl-Ado on 4E-BP1 protein levels in U266 cells

Cells were either left untreated (U) or treated with 0.5 μ M 17-AAG for 8 hours, the combination of 10 μ M 8-Cl-Ado for 12 hours followed by 17-AAG for 8 hours, 10 μ M 8-Cl-Ado for 20 hours, 0.5 μ M 17-AAG for 20 hours, the combination of 17-AAG for 12 hours followed by 8-Cl-Ado for 8 hours, 10 μ M 8-Cl-Ado for 12 hours, or the combination of 8-Cl-Ado and 17-AAG added simultaneously for 20 hours. Cells were harvested and immunoblots were performed and analyzed with antibodies detecting for 4E-BP1 and the loading control β -actin.

Figure 56



10 μ M added first for 12 hours followed by 0.5 μ M 17-AAG for 8 hours, or 10 μ M 8-Cl-Ado alone for 20 hours. Cells were harvested after treatment and cell death was measured using Annexin V/7-AAD positive staining. Eight-hour treatment with 0.5 μ M 17-AAG resulted in less than 5% cell death in all MM cells. When cells were treated with 8-Cl-Ado, there was 26, 6 and 2% cell death in MM.1S (Figure 57A), RPMI-8226 (Figure 57B), and U266 cells (Figure 57C), respectively. The combination of 8-Cl-Ado followed by 17-AAG resulted in 55, 15, and 19% cell death for MM.1S, RPMI-8226, and U266 cells, respectively.

Cytotoxicity of 8-Cl-Ado followed by 17-AAG combination sequence in MM cell lines

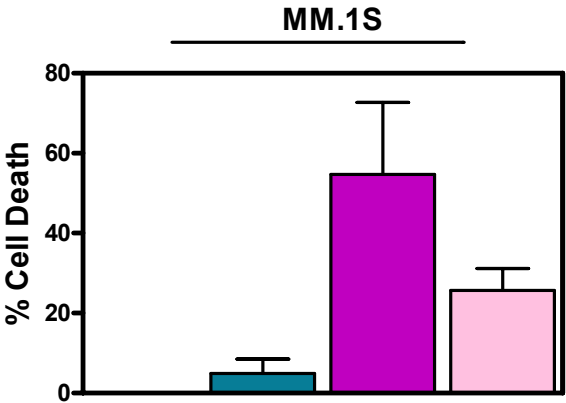
MM cells were either not treated or treated with 0.5 μ M 17-AAG alone for 8 hours, a combination treatment with 10 μ M added first for 12 hours followed by 0.5 μ M 17-AAG for 8 hours, or 10 μ M 8-Cl-Ado alone for 20 hours. The endogenous cell death was subtracted from each condition. A fractional two-drug combination analysis as described in materials and methods was performed for the combination of 8-Cl-Ado followed by 17-AAG treatment (Table 4). As previously mentioned, this analysis determines if the observed cell death obtained with annexin V/7-AAD binding assay is more than the calculated expected cell death for the combination treatment. Eight-hour treatment with 0.5 μ M 17-AAG resulted less than 5% cell death in all MM cells. When cells were treated with 8-Cl-Ado, there was 26, 6 and 2% cell death in MM.1S, RPMI-8226, and U266 cells, respectively. For the combination condition with 8-Cl-Ado followed by 17-AAG, the calculated expected cytotoxicity was 29, 9, and 6% in MM.1S, RPMI-8226, and U266 cells, respectively. When comparing the observed (measured) cell death against the expected (calculated) cell death, the measured cytotoxicity for the combination condition (55, 15, and 19% for MM.1S, RPMI-8226, and U266 cells, respectively) was more than the expected cell death for the same condition. Student's *t*-test analysis shows statistically significant difference in MM.1S and

Figure 57. Cytotoxicity of 8-Cl-Ado followed by 17-AAG in MM cell lines

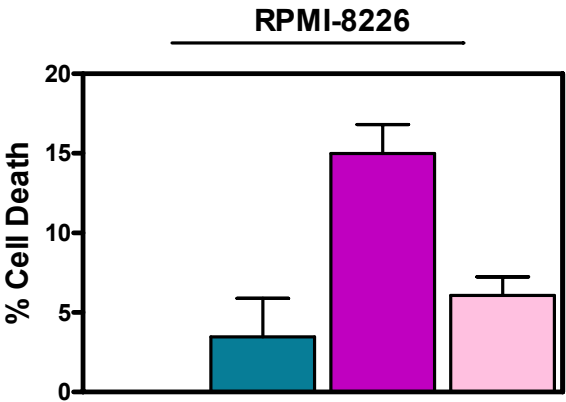
MM.1S (A), RPMI-8226 (B), and U266 (C) cells were either left untreated or treated with 0.5 μ M 17-AAG for 8 hours, 10 μ M 8-Cl-Ado for 20 hours, or the combination of 8-Cl-Ado for 12 hours followed by 17-AAG for 8 hours. Flow cytometry was performed to measure cell death, which was determined as the percentage of cells staining positive for Annexin V/7-AAD after subtracting the percentage of endogenous cell death.

Figure 57

A



B



C

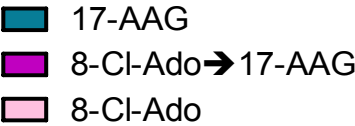
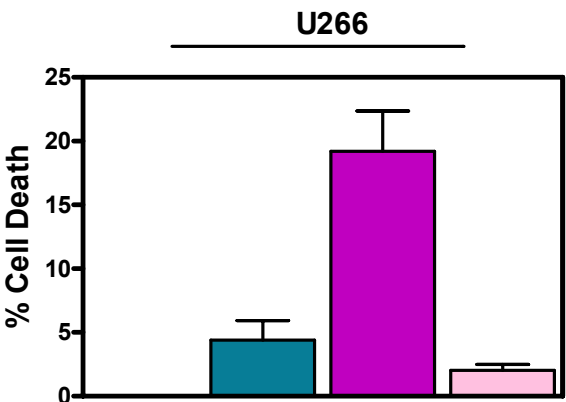


Table 4. Cytotoxicity of 8-Cl-Ado followed by 17-AAG combination sequence in MM cell lines

Cells were either left untreated or treated with 0.5 μ M 17-AAG for 8 hours, 10 μ M 8-Cl-Ado for 20 hours, or the combination of 8-Cl-Ado for 12 hours followed by 17-AAG for 8 hours.

Flow cytometry was performed to measure cell death, which was determined as the percentage of cells staining positive for Annexin V/7-AAD after subtracting the percentage of endogenous cell death. The expected percent survival for the combination condition was calculated following the fractional two-drug combination analysis. Values are the statistical significance ($p=0.05$) comparing expected cell death with observed cell death.

Table 4

8-Cl-Ado→17-AAG	17-AAG 0.5μM 8 h	8-Cl-Ado 10 μM 20 h	Combination	
			<i>Expected</i>	<i>Observed</i>
MM.1S				
<i>Cell Death</i>	5	26	29	55
<i>Cell Survival</i>	95	74	71	
				<i>p = 0.019</i>
RPMI-8226				
<i>Cell Death</i>	3	6	9	15
<i>Cell Survival</i>	97	94	91	
				<i>p = 0.011</i>
U266				
<i>Cell Death</i>	4	2	6	19
<i>Cell Survival</i>	96	98	94	
				<i>p = 0.091</i>

RPMI-8226 cell lines between the expected and observed cell death values (MM.1S, $p = 0.019$; RPMI-8226, $p = 0.011$), but not for U266 cells ($p = 0.09$).

Since these results suggested an additive effect when both drugs were combined, which may be attributed to the decrease in client protein levels and global translation attenuation, different combination sequences for 8-Cl-Ado and 17-AAG were tested for cytotoxicity in all MM cells.

Cytotoxicity of 17-AAG followed by 8-Cl-Ado combination sequence in MM cell lines

MM cell lines were either not treated or treated with 0.5 μM 17-AAG for 20 hours alone, the combination of 17-AAG for 8 hours followed by 8-Cl-Ado for 12 hours, or 10 μM 8-Cl-Ado for 12 hours alone. Cells were harvested after treatment and cell death was measured using Annexin V/7-AAD positive staining. The endogenous cell death was subtracted from each condition. A fractional two-drug combination analysis as described in materials and methods was performed for the combination of 17-AAG followed by 8-Cl-Ado treatment (Table 5). Treatment with 17-AAG for 20 hours resulted in less than 6% cell death in all MM cells. When cells were treated with 8-Cl-Ado, there was less than 5% in all MM cell lines. For the combination condition with 17-AAG followed by 8-Cl-Ado, the calculated expected cytotoxicity was 6, 6, and 7% in MM.1S, RPMI-8226, and U266 cells, respectively. When comparing the observed (measured) cell death against the expected (calculated) cell death, the measured cytotoxicity for the combination condition (7, 11, and 10% for MM.1S, RPMI-8226, and U266 cells, respectively) was not really different than the expected cell death for the same condition. Student's *t*-test analysis shows no statistically significant difference in any MM cell line ($p > 0.05$)

Table 5. Cytotoxicity of 17-AAG followed by 8-Cl-Ado combination sequence in MM cell lines

Cells were either left untreated or treated with 0.5 μ M 17-AAG for 20 hours, 10 μ M 8-Cl-Ado for 12 hours, or the combination of 17-AAG for 12 hours followed by 8-Cl-Ado for 8 hours. Flow cytometry was performed to measure cell death, which was determined as the percentage of cells staining positive for Annexin V/7-AAD after subtracting the percentage of endogenous cell death. The expected percent survival for the combination condition was calculated following the fractional two-drug combination analysis. Values are the statistical significance ($p=0.05$) comparing expected cell death with observed cell death.

Table 5

17-AAG→8-Cl-Ado	17-AAG <i>0.5μM</i> <i>20 h</i>	8-Cl-Ado <i>10 μM</i> <i>12 h</i>	Combination <i>Expected</i> <i>Observed</i>	
MM.1S				
<i>Cell Death</i>	1	5	6	7
<i>Cell Survival</i>	99	95	94	
				<i>p = 0.388</i>
RPMI-8226				
<i>Cell Death</i>	3	3	6	11
<i>Cell Survival</i>	97	97	94	
				<i>p = 0.114</i>
U266				
<i>Cell Death</i>	6	1	7	10
<i>Cell Survival</i>	94	99	93	
				<i>p = 0.061</i>

Cytotoxicity of 8-Cl-Ado and 17-AAG simultaneous combination in MM cell lines

MM cell lines were either not treated or treated with 0.5 μ M 17-AAG for 20 hours alone, 10 μ M 8-Cl-Ado for 20 hours alone, or the combination of 8-Cl-Ado and 17-AAG added simultaneously for 20 hours. Cells were harvested after treatment and cell death was measured using Annexin V/7-AAD positive staining. The endogenous cell death was subtracted from each condition. A fractional two-drug combination analysis as described in materials and methods was performed for the simultaneous combination treatment of 8-Cl-Ado and 17-AAG (Table 6). Treatment with 17-AAG for 20 hours resulted in less than 6% cell death in all MM cells. When cells were treated with 8-Cl-Ado, there was 20, 9, and 2% cell death in MM.1S, RPMI-8226, and U266 cells. For the combination condition with 17-AAG followed by 8-Cl-Ado, the calculated expected cytotoxicity was 22, 13, and 8% in MM.1S, RPMI-8226, and U266 cells, respectively. When comparing the observed (measured) cell death against the expected (calculated) cell death, the measured cytotoxicity for the combination condition (30, 14, and 26% for MM.1S, RPMI-8226, and U266 cells, respectively) was more than the expected cell death for the same condition. Student's *t*-test analysis shows statistically significant difference in MM.1S and U266 cell lines between the expected and observed cell death values (MM.1S, $p = 0.045$; U266, $p = 0.047$), but not for RPMI-8226 cells ($p = 0.29$).

Taken together, there was a statistically significant increase in cytotoxicity with the combination of 8-Cl-Ado followed by 17-AAG for MM.1S and RPMI-8226 cells, and for the simultaneous combination of both drug for MM.1S and U266 cells. However, this was not observed for the combination of 17-AAG followed by 8-Cl-Ado in any of the MM cell lines.

Table 6. Cytotoxicity of 8-Cl-Ado and 17-AAG simultaneous combination in MM cell lines

Cells were either left untreated or treated with 0.5 μ M 17-AAG for 20 hours, 10 μ M 8-Cl-Ado for 20 hours, or the combination of 8-Cl-Ado and 17-AAG added simultaneously for 20 hours. Flow cytometry was performed to measure cell death, which was determined as the percentage of cells staining positive for Annexin V/7-AAD after subtracting the percentage of endogenous cell death. The expected percent survival for the combination condition was calculated following the fractional two-drug combination analysis. Values are the statistical significance ($p=0.05$) comparing expected cell death with observed cell death.

Table 6

8-Cl-Ado+17-AAG	17-AAG	8-Cl-Ado	Combination	
	0.5μM <i>20 h</i>	10 μM <i>20 h</i>	<i>Expected</i>	<i>Observed</i>
MM.1S				
<i>Cell Death</i>	2	20	22	30
<i>Cell Survival</i>	98	80	78	
				<i>p = 0.045</i>
RPMI-8226				
<i>Cell Death</i>	4	9	13	14
<i>Cell Survival</i>	96	91	87	
				<i>p = 0.299</i>
U266				
<i>Cell Death</i>	6	2	8	26
<i>Cell Survival</i>	94	98	92	
				<i>p = 0.047</i>

CHAPTER 4: Discussion

The main purpose of this current work was to develop strategies that address the cytotoxic resistance developed using HSP90 inhibitors, such as 17-AAG. To deal with the negative effect elicited when using agents that target HSP90, two different approaches were implemented and are discussed in separate sections.

The first aim of this dissertation focuses on the ability of the transcription inhibitor Act D to inhibit transcription induction of heat shock proteins by 17-AAG.

17-AAG

The semisynthetic geldanamycin derivative, 17-AAG, entered clinical trials in 1999 making it the first heat shock protein inhibitor that was tested in humans (Biamonte, Van de Water et al. 2010). In an early phase I clinical trial, two patients with metastatic melanoma showed stable disease when treated with 17-AAG. This study reported the highest administered dose to be 450 mg/m²/week, which achieved a peak plasma concentration of 16 μ M with a half-life of 6 hours. Similar to pre-clinical studies with 17-AAG, this study reported the induction of HSP70 and downregulation of client proteins (such as c-Raf and cdk4) as the pharmacodynamic endpoints for this drug (Banerji, O'Donnell et al. 2005).

Therefore, the selected concentration of 17-AAG in this dissertation (0.5 μ M) is achievable and relevant in the clinic. MM cells treated with 17-AAG as a function of time and dose resulted in the induction of heat shock proteins, including HSP70 (Figures 9 and 10). Also, MM cells treated with 17-AAG for 8 and 12 hours resulted in downregulation of client proteins including c-Raf-1 (Figures 43 and 46).

HSP90 and stress response modulation

The targeted inhibition of HSP90 with 17-AAG results in activation of the stress response, which leads to sustained induction of heat shock proteins (Bagatell, Paine-Murrieta et al. 2000). Some of these induced heat shock proteins negatively regulate the apoptotic pathway leading to cell death resistance (Beere, Wolf et al. 2000; Pandey, Farber et al. 2000; Pandey, Saleh et al. 2000). Overexpression of cytoprotective heat shock proteins has been shown to confer resistance to several chemotherapeutic agents in hematological and solid malignancies (Garrido, Ottavi et al. 1997; Demidenko, Vivo et al. 2006; Martins, Ordonez et al. 2008). As such, the abrogation of the heat shock stress response is desired when utilizing HSP90 inhibitors. An increase in cytotoxicity has been measured in studies where cells are treated with 17-AAG following downregulation of HSP90, HSP70, or HSP27 expression levels using small interference RNA (siRNA) (Guo, Rocha et al. 2005; Rocchi, Jugpal et al. 2006; Aghdassi, Phillips et al. 2007; Chatterjee, Jain et al. 2007; Powers, Clarke et al. 2008). These series of studies have provided a proof-of-principle for the inhibition of heat shock proteins. However, the utilization of this approach in the clinic is precluded by the lack of available delivery methods for siRNA therapy.

Another approach to circumvent the activation of the heat shock stress response is to target the key members in the HSP90 cycle or the actual activator of the stress response the transcription factor HSF-1. For example, inhibitors that target cochaperone HSP70 or disrupt the interaction of HSP90 with its cochaperones or client proteins are currently being developed (Brandt and Blagg 2009; Leu, Pimkina et al. 2009). Only one HSP90 inhibitor known to date, novobiacin, does not elicit the stress response (Sharp and Workman 2006). This coumarin antibiotic binds to the second ATP pocket located in the C-terminus of HSP90. Similar to inhibitors that bind to the ATP pocket at the N-terminus such as geldanamycin and 17-AAG, novobiacin also leads to the degradation of client proteins. Degradation of HSP90 client proteins by novobiocin is moderately achieved due to its low

potency (Sharp and Workman 2006). However, the lack of induction of the heat shock response by novobiacin is an advantageous feature and is now being investigated for the development of more potent derivatives (Brandt and Blagg 2009).

Using a transcription inhibitor could be an alternative strategy to block the stress response triggered by HSP90 inhibitors, which lead to the transcription and expression of antiapoptotic heat shock proteins. The clinically used chemotherapeutic agent Act D is an established transcription inhibitor used in oncology for more than 50 years. The work presented here evaluated the feasibility of using Act D to block the induction of the heat shock stress response by 17-AAG.

Heat shock protein stress response

Heat shock factor-1 (HSF-1) is a transcription activator for of all heat shock protein genes (Voellmy 1994). HSF-1 activity is repressed when is complexed to HSP90 and other cochaperones (Zou, Guo et al. 1998; Freeman, Borrelli et al. 1999; Guo, Guettouche et al. 2001). Stress inducers trigger the release of HSF-1 from its repressing complex leading to transcription of the heat shock proteins (Ananthan, Goldberg et al. 1986; Wu 1995). Once released, the active conformation of HSF-1 is achieved through trimerization and phosphorylation (Wu 1995; Cotto, Kline et al. 1996). Activated HSF-1 translocates to the nucleus where it binds to the heat shock elements present in the promoters of the heat shock protein genes (Baler, Dahl et al. 1993). HSF-1 binds to the heat shock elements in DNA as a trimer. The heat shock elements contain three conserved repeats of the sequence nGAAn. Each subunit on the activated HSF-1 trimer binds to a specific sequence. (Wu 1995). Interaction of HSF-1 trimer with the nGAAn sequences in the heat shock elements triggers multiple rounds of heat shock protein transcription resulting in overexpression of the inducible heat shock proteins in the cell (Baler, Dahl et al. 1993).

Transcription activation through HSF-1 is needed to induce the levels of HSP90, HSP70, and HSP27.

Act D mechanism of action as a transcription inhibitor

Act D inhibits transcription by intercalating into DNA blocking binding of RNA Pol II hindering elongation (Sobell 1985; Gniazdowski, Denny et al. 2003). RNA Pol II is an enzyme required for transcription initiation and is responsible for the synthesis of mRNA from DNA. Eukaryotic RNA Pol I and RNA Pol III transcribe rRNA and tRNA genes, respectively, from DNA (Paule and White 2000). The planar phenoxazone ring of Act D intercalates in between the DNA base pairs. The two large polypeptide moieties of Act D bind to the minor groove of DNA (Sobell 1985). The phenoxazone moiety possesses no sequence selectivity for DNA, but the polypeptide side chains provide selectivity towards binding to deoxy-guanine•cytosine base pairs (Gniazdowski, Denny et al. 2003). Hence, Act D induces cytotoxicity by inhibiting global RNA synthesis leading to a decrease in protein levels (Perry and Kelley 1970).

Clinical application of Act D

Act D was introduced in clinical oncology in 1954, and currently, is generally used in the treatment of pediatric and young adult malignancies at doses that are well-tolerated (Farber, Pinkel et al. 1956; Estlin and Veal 2003; Veal, Cole et al. 2005). Act D is a curative regimen in combination with surgery for Wilms tumor in children (Estlin and Veal 2003). The most common observed toxicity with Act D administration was low platelet count and infections. Overall, a third of the patients experienced no adverse effects while less than half of the patients had grade 1 or 2 toxicity and the rest of the patients observed grade 3 or 4 toxicity (Veal, Cole et al. 2005). Close to 80% of Wilms tumor patients showing early disease are cured when treated with Act D in combination with surgery (Tattersall,

Sodergren et al. 1975). Patients with stage IV and completely necrotic Wilms tumor achieved a 100% overall 5-year survival when treated with Act D in combination with additional chemotherapeutic agents (Estlin and Veal 2003). Clinical studies with malignant melanoma have also demonstrated that Act D is a well tolerated drug in adults as well (Tattersall, Sodergren et al. 1975).

The pharmacokinetics of Act D has been evaluated in pediatric and adult patients. In children, Act D is administered as a single bolus i.v. infusion, and patients treated with 0.75-1.50 mg/m² Act D achieved peak plasma levels of 0.02-0.05 µg/mL (Veal, Cole et al. 2005). This same study determined a median peak plasma concentration of 0.025 µg/mL (range 0.003-0.1 µg/mL) with a half-life ranging from 14 to 43 hours. The studies performed in this dissertation used 0.05 µg/mL Act D for 12 hours, which is achieved in the clinic. Similarly, in adult patients treated with 10-15 µg/kg Act D obtained peak plasma levels ranging from 0.01-0.1 µg/mL (Tattersall, Sodergren et al. 1975). Act D accumulated in the bone marrow and tumor cells at higher concentrations compared to plasma. This same clinical trial in adult patients with Act D reported a median plasma concentration of less than 0.065 µg/mL with a half-life of 36 hours (Tattersall, Sodergren et al. 1975). The Act D plasma concentrations achieved in these clinical trials are sufficient to inhibit global RNA synthesis. Low doses of Act D (0.01-0.25 µg/mL) for short exposures result in preferential inhibition of ribosomal RNA synthesis (Perry and Kelley 1970). High doses of Act D (1.0-2.0 µg/mL) or low doses for long exposures result in inhibition of all RNA species (Perry and Kelley 1970; Estlin and Veal 2003).

Thus, the pharmacokinetic endpoints demonstrate that the concentrations used for the experiments presented in this dissertation are clinically achievable and biologically relevant. The selected concentration of Act D (0.05 µg/mL) inhibited global RNA synthesis by 80 and 90% in MM.1S and RPMI-8226 cells, respectively, when treated for 12 hours

(Figure 13). Concentrations of Act D ranging from 0.01 to 2.0 $\mu\text{g/mL}$ also decreased heat shock protein expression levels (Figure 11).

Heat shock protein mRNA transcription inhibition

At the transcript level, real-time RT-PCR experiments for the combination treatment demonstrated that Act D was able to diminish the constitutive (HSP90 β and HSC70; Figures 16B, 17B) and stress-inducible (HSP90 α and HSP27; Figures 16A and 18) heat shock protein transcript levels. However, the same treatment was unable to abrogate the 17-AAG-mediated induction of *HSP70* transcript levels in both cell lines (Figure 17A). Interestingly, the combination condition actually resulted in an increase in *HSP70* transcript levels when compared to 17-AAG treatment as a single agent. This discrepancy between HSP70 and the rest of the heat shock proteins may be explained by the singularities of the *HSP70* gene.

Given that the heat shock protein response is a cytoprotective reaction to cytotoxic injury, non-induced cells are primed with RNA II polymerase bound to the *HSP70* gene initiating a short *HSP70* transcript prior to pausing (Lis and Wu 1993). This pause is relieved following stress which results in HSF-1 transcription elongation. Aside from the *HSP70* gene, promoter-proximal pausing occurs in other rapidly induced genes such as c-fos and c-myc (Brown and Kingston 1997; Schneider, Albert et al. 1999; Fivaz, Bassi et al. 2000).

Similar studies by others have demonstrated that the use of transcription inhibitors were unable to block the transcription of inducible genes (Ljungman, Zhang et al. 1999; Gomes, Bjerke et al. 2006; Dey, Wong et al. 2008). Transcription inhibitors targeting RNA Pol II, such as Act D, DRB and α -amanitin, can trigger a stress response leading to the stabilization of p53 protein, which in turn lead to transcription activation and induction of p21 (Ljungman, Zhang et al. 1999). Agents that inhibit the activation of RNA Pol II also

inhibit global transcription. Activation of RNA Pol II depends on the phosphorylation of serine 5 and serine 2 residues by CDK7 and CDK9, Roscovitine inhibits cyclin-dependent kinase (CDK) 2, CDK4, CDK 7, and CDK9, and for this reason Roscovitine can also be considered an inhibitor of global transcription. (Meijer and Raymond 2003; Dey, Wong et al. 2008). It has also been reported that this inhibitor induces transcription of p21 via p53 activation (Dey, Wong et al. 2008). Another study using chromatin immunoprecipitation assays reported that the transcription inhibitor DRB resulted in induction of two p53-mediated genes, *PUMA* and *p21* (Gomes, Bjerke et al. 2006). However, in this same study, global RNA transcription was also inhibited and caused a decrease in *HPRT* and *SDHA*, which are housekeeping non-inducible genes. This is in agreement to the results presented in this dissertation. Stress-inducible *HSP70* transcript levels were not abrogated by the transcription inhibitor Act D (Figure 17A). In fact, an induction in mRNA levels of this gene occurred in the combination condition.

A potential mechanism for the lack of *HSP70* mRNA inhibition may be due to the structural aspects of Act D actions. As described earlier, intercalation of the phenoxazone ring of Act D into DNA is not specific. Only the polypeptide peptide moieties exhibit specificity towards deoxy-guanine•cytosine base pairs. The threonine carbonyl groups in the polypeptide side chains interact with the 2-amino group of guanines (Gniazdowski, Denny et al. 2003). The transcription factor NFκB mediates the transcription and expression of genes involved in proliferation and survival. The NFκB target sequence contains moderate guanine•cytosine sequences, which Act D is unable to intercalate into (Czyz and Gniazdowski 1998). Specificity protein (Sp1) is a transcription factor involved in the regulation of genes involved in early development. Sp1 binds to a deoxy-guanine•cytosine-rich DNA sequence that is blocked by Act D treatment (Czyz and Gniazdowski 1998). Since the polypeptide side chains in Act D have preferential binding to highly rich deoxy-

guanine•cytosine sequences, it has been suggested that these sequence are necessary when targeting a DNA segment (Czyz and Gniazdowski 1998).

HSP70 is a guanine•cytosine-rich gene (Kudla, Lipinski et al. 2006). Based on the real time RT-PCR data, Act D was not able to inhibit the induction of *HSP70* by 17-AAG (Figure 17A). Interestingly, one study using Act D to target the binding of the transcription factor early growth response factor 1 (EGR1) with its DNA sequence described no disruption of this interaction (Welch, Rauscher et al. 1994). EGR1 is efficiently induced in response to a variety of growth stimuli. EGR1 expression is constitutively expressed in prostate cancer contributing to tumor proliferation (Mora, Olivier et al. 2005). Although EGR1 forms a complex with a DNA segment rich in guanine•cytosine base pairs, Act D is not able to interact with this segment and inhibit their interaction (Welch, Rauscher et al. 1994). Similarly, Act D did not affect the binding of other transcription factors, such as Jun and Fos, to their DNA target sequences (Welch, Rauscher et al. 1994).

Heat shock protein expression inhibition

Unexpectedly, even when there was an increase in *HSP70* mRNA levels, this did not correlate with the protein expression levels detected via immunoblot assay (Figures 20 and 22A). Treatment with Act D followed by 17-AAG in the combination treatment did not abrogate the 17-AAG-mediated induction of *HSP70* mRNA in either cell line (Figure 17A). In RPMI-8226 cells, the induction of *HSP70* in the combination treatment was statistically different from the 17-AAG treatment as a single agent ($p = 0.03$). However at the expression level, in the combination treatment, Act D diminished the induction of HSP70 protein levels caused by 17-AAG. This result suggests that *HSP70* transcripts may either be non-functional or short-lived. The 3'-noncoding region of *HSP70* mRNA contains the AU-rich sequences, which accelerates the degradation of *HSP70* mRNA. (Hunt and Morimoto 1985). Therefore, more comprehensive studies are needed to determine the fate of HSP70

transcripts in cells when Act D and 17-AAG are added in combination. Taken together, the combination treatment resulted in a decrease of all heat shock protein levels compared to treatment with 17-AAG as a single agent. Therefore, it is expected for the combination to result in increase cytotoxicity compared to the cytotoxic effect exerted by Act D and 17-AAG as single agents (Figure 26 and Table 2).

The second strategy utilized a ribonucleoside analog 8-Cl-Ado, which is currently in a clinical trial. The approach was to inhibit transcription and translation of heat shock proteins and client proteins. Also this nucleoside analog lowers cellular bioenergy, which may facilitate additional binding of 17-AAG to HSP90.

8-Cl-Ado and inhibition of RNA synthesis

The ability of 8-Cl-Ado to inhibit 17-AAG-mediated induced transcription of heat shock proteins was evaluated based on previous studies that report that the ribonucleoside analog inhibits mRNA synthesis and post-transcriptional processing of mRNA (Stellrecht, Rodriguez et al. 2003; Chen and Sheppard 2004; Chen, Du-Cuny et al. 2010). In the cell, 8-Cl-Ado is phosphorylated by different kinases to 8-Cl-ATP (Gandhi, Ayres et al. 2001). The triphosphate metabolite affects RNA synthesis by several different mechanisms.

First, the cytotoxic metabolite of 8-Cl-Ado, 8-Cl-ATP, can be incorporated into the body of RNA leading to mRNA synthesis inhibition (Stellrecht, Rodriguez et al. 2003). In MM cells treated with 8-Cl-Ado, RNA was isolated and digested with phosphodiesterases and phosphatases to determine the composition of the RNA, and it was determined that 8-Cl-ATP was incorporated at 3'-terminal positions. These results indicated that 8-Cl-ATP

incorporated into RNA and inhibited further synthesis due to RNA synthesis chain termination. Further analysis of the specific RNA species (mRNA, rRNA, and tRNA) indicated preferential incorporation into mRNA, thus further demonstrating 8-Cl-Ado effect on transcripts.

Second, 8-Cl-Ado treatment depletes cellular ATP pools in several cell lines such as chronic lymphocytic leukemia (Balakrishnan, Stellrecht et al. 2005), breast cancer (Stellrecht, Ayres et al. 2009), mantle cell lymphoma (Dennison, Balakrishnan et al. 2009), and multiple myeloma (Gandhi, Ayres et al. 2001). ATP is a substrate for RNA synthesis and hence its decline will affect transcription (Frey and Gandhi 2010).

Third, 8-Cl-ATP can inhibit mammalian polyadenylation a required step for transcript function and stability (Chen and Sheppard 2004; Chen, Du-Cuny et al. 2010). Using primer extension assays with poly(A) polymerase, 8-Cl-ATP was identified as an inhibitor of poly(A) tail synthesis via two different mechanisms. First, in primer extension assays using poly(A) polymerase and ATP, poly (A) tail length was reduced with increasing concentrations of 8-Cl-ATP. Since 8-Cl-ATP itself was not incorporated into the poly(A) tail, as demonstrated with experiments with poly(A) polymerase and 8-Cl-ATP alone, it appears the mechanism of action is via competitive inhibition. Second, although 8-Cl-ATP was not directly incorporated into the poly(A) tail of RNA, synthetic RNA containing 3'-terminal 8-Cl-AMP residues were prepared and assayed with poly(A) polymerase and ATP. These 8-Cl-AMP modified RNA primers could not be elongated by poly(A) polymerase, and blocked poly(A)-tail addition. Thus, 8-Cl-ATP incorporation into RNA during transcription would prevent the proper processing of pre-mRNA into polyadenylated mature mRNA transcripts. The poly(A)-tail has been shown to protect mRNA from degradation, and the reduced polyadenylation would further decrease mRNA levels in addition to the observed decrease in transcription.

Collectively, these observations demonstrate that 8-Cl-Ado treatment will either inhibit or decrease mRNA synthesis. In addition, mRNA levels of short-lived transcripts will decline. In fact, a decrease in c-Met transcript levels is observed in MM cells since this transcript is short-lived (< 30 minutes) (Stellrecht, Phillip et al. 2007). Therefore, due its inhibitory actions on RNA synthesis and stability, 8-Cl-Ado was selected as the agent to combine with 17-AAG. Surprisingly, real-time RT-PCR data demonstrated that 8-Cl-Ado was not able to inhibit the transcription of any of the stress-inducible or constitutive heat shock protein mRNA levels (Figures 29, 30, and 31). Actually, similar to the combination of Act D and 17-AAG, there was an induction of *HSP70* mRNA level when 8-Cl-Ado and 17-AAG drugs were combined (Figure 30A). As previously mentioned, *HSP70* gene has some singularities that distinguish it from the rest of the heat shock protein genes. It is primed for rapid induction since *HSP70* transcription is initiated and paused until HSF-1 relieves this pause when the cell undergoes some kind of stress (Lis and Wu 1993). A second transcript induced when cells were treated with the combination treatment of 8-Cl-Ado and 17-AAG was HSP27 (Figure 31). Although this may be just specific for the sensitive cell line MM.1S since 8-Cl-Ado treatment alone induced HSP27 transcripts by 2-fold compared to the untreated control (Figure 31). In accordance to HSP27 mRNA levels, expression levels of HSP27 were induced in MM.1S when cells were treated with 8-Cl-Ado alone (Figure 35). In contrast, no induction of HSP27 mRNA for RPMI-8226 cells was measured following treatment with 8-Cl-Ado and 17-AAG in combination or 8-Cl-Ado treatment alone (Figure 31B). Also, treatment with 8-Cl-Ado did not elevate HSP27 expression levels in either RPMI-8226 or U266 cells (Figure 35).

Comparison of the extent of *HSP70* induction when MM.1S and RPMI-8226 cells are treated with 8-Cl-Ado followed by 17-AAG (Figure 30A) or with Act D followed by 17-AAG (Figure 17A) demonstrated that there is a marked increase in *HSP70* transcripts when 8-Cl-Ado is added in the combination. Studies investigating the induction of the heat shock

protein response in *Drosophila* and humans have reported that a decrease in the intracellular ATP pools stimulates the binding of HSF-1 to the *HSP70* DNA promoter, although this is not sufficient to trigger *HSP70* transcription (Jurivich, Sistonen et al. 1992; Winegarden, Wong et al. 1996). However, a second stimulus (such as 17-AAG treatment) augments the heat shock stress response resulting in elevated induction of *HSP70* mRNA (Bagatell, Paine-Murrieta et al. 2000). One of the mechanisms by which 8-Cl-Ado exerts cytotoxicity is through depletion of the ATP pools; hence these observations may explain why the combination of 8-Cl-Ado followed by 17-AAG results in an increased level of *HSP70* mRNA compared to the treatments of Act D and 17-AAG in combination.

Since 8-Cl-Ado did not block the induction of any of the heat shock protein mRNA levels, the transcript levels of several client proteins (STAT-3, Raf-1, and Akt) were measured using real-time RT-PCR. Similar to heat shock protein transcripts, MM cells treated with 8-Cl-Ado for 20 hours did not indicate a reduction on STAT3, Raf-1, or Akt mRNA levels (Figures 48-50). These results suggest that the cytotoxic metabolite of 8-Cl-Ado, 8-Cl-ATP, is not being incorporated into the mRNA body causing termination synthesis and is not inhibiting polyadenylation since similar mRNA levels of these clients are measured when compared to the endogenous mRNA levels in the untreated control.

A possible explanation for the inability of 8-Cl-Ado to decrease heat shock protein or client protein mRNA levels is that the length of the transcript could be an important feature (Figures 29-31 and 48-50). c-Met is an oncogene whose expression promotes tumorigenesis in multiple human cancers (Lai, Abella et al. 2009). A study using 8-Cl-Ado to target the depletion of c-Met transcripts reported the decrease of this transcript as a consequence, which resulted in reduced protein expression (Stellrecht, Phillip et al. 2007). However, c-Met transcript size is 8 Kb long compared to the short-length transcripts being analyzed in this work (Miller, Glover et al. 1996). For example, *HSP70*, *HSP27*, and *Raf-1* transcript length is reported to be 2.6, 2.2, and 2.8 Kb, respectively (Hunt and Morimoto

1985; Wu, Hunt et al. 1985; Hickey, Brandon et al. 1986; Shimizu, Nakatsu et al. 1987). Hence, it can be possible that the probability of 8-Cl-ATP incorporating into the RNA body is increased with long length transcript size leading to its inhibitory actions in RNA synthesis.

Finally, as described earlier for Roscovitine and other transcription inhibitors, RNA Pol II inactivation also does not always result in transcription inhibition of some genes (Ljungman, Zhang et al. 1999; Gomes, Bjerke et al. 2006; Dey, Wong et al. 2008).

However, in contrast to the lack of change in client protein mRNA levels, a decrease in client protein levels is measured by immunoblot assays after MM cells are treated with 8-Cl-Ado which is further reduced when combined with 17-AAG (Figures 41-47). These results imply that the ability of 8-Cl-Ado to produce a decrease in the endogenous ATP pool could account for the decrease in client protein levels.

Decline in ATP levels

In the cell, 8-Cl-Ado is phosphorylated by adenosine kinase to the monophosphate. 8Cl-AMP is further phosphorylated to the di- and triphosphate forms by mono- and diphosphate kinases, respectively (Gandhi, Ayres et al. 2001). However, the diphosphate form can also be phosphorylated to the cytotoxic 8-Cl-ATP by ATP synthase (Chen, Nowak et al. 2009). As previously described, treatment with 8-Cl-Ado resulted in the accumulation of the cytotoxic triphosphate 8-Cl-ATP with concomitant decrease in endogenous ATP levels (Gandhi, Ayres et al. 2001). ATP synthase is the enzyme responsible for phosphorylation of 8-Cl-ADP into 8-Cl-ATP, which was demonstrated using experiments with oligomycin, a pharmacological inhibitor of ATP synthase. This enzyme is complex V of the respiratory chain in the mitochondria, and catalyzes the conversion of ADP to ATP. Cells treated first with oligomycin followed by 8-Cl-Ado resulted in a decrease in the accumulation of 8-Cl-ATP. This indicates that 8-Cl-ADP phosphorylation to 8-Cl-ATP by ATP synthase is reduced in the presence of oligomycin. Recent studies using biochemical

methods in combination with molecular modeling suggest that 8-Cl-ATP is an inhibitor of ATP synthase, which accounts for the decrease in endogenous ATP. This study determined that the di- and tri-phosphate metabolites of 8-Cl-Ado, 8-Cl-ADP, and 8-Cl-ATP, respectively, can bind to ATP synthase and block the production of ATP from ADP. Molecular modeling performed with 8-Cl-ADP suggests that it can occupy the ADP binding site, allowing it to act as a substrate for this enzyme. Further modeling also indicated that 8-Cl-ATP can mimic ATP and bind to the ATP binding site in ATP synthase, thus inhibiting its catalytic function. (Chen, Nowak et al. 2009).

A second mechanism by which 8-Cl-Ado affects ATP levels is through its metabolism by an enzyme to succinyl-8-Cl-adenylate leading to a reduction of fumarate levels, an intermediate in the citric acid cycle, potentially affecting the production of ATP by oxidative phosphorylation (Dennison, Ayres et al. 2010). This study reported that mantle cell lymphoma cell lines treated with 8-Cl-Ado lead to the formation of two metabolites, succinyl-8-Cl-AMP and succinyl-8-Cl-Ado, through conjugation of fumarate by the enzyme adenylosuccinase. Fumarate is a metabolite and substrate in the citric acid or Krebs cycle. This cycle is part of the metabolic pathway that is involved in the chemical generation of ATP, hence a perturbation in the homeostasis of this cycle (such as the depletion of one its intermediates) may result in ATP pool depletion.

The negative effects that the metabolism of 8-Cl-Ado has on cellular ATP levels are reproducible in different tumor models. Therefore, cytotoxic mechanism of 8-Cl-Ado is not cell type dependent. Investigations of the cytotoxic effects in chronic lymphocytic leukemia (Balakrishnan, Stellrecht et al. 2005), breast cancer (Stellrecht, Ayres et al. 2009), mantle cell lymphoma (Dennison, Balakrishnan et al. 2009), and multiple myeloma (Gandhi, Ayres et al. 2001) models have reported to find a similar accumulation of 8-Cl-ATP and parallel depletion of the endogenous ATP pool after 8-Cl-Ado treatment.

In accordance with these reports, the work in this dissertation demonstrate that MM cell lines treated with 8-Cl-Ado leads to accumulation of 8-Cl-ATP and decrease in cellular ATP levels (Table 3). Unexpectedly, treatment with 8-Cl-Ado followed by 17-AAG resulted in a decrease of accumulation of 8-Cl-ATP compared with 8-Cl-Ado alone although a further decline of ATP levels was observed in all cell lines. For example, in MM cells, treatment with 8-Cl-Ado alone for 20 hours resulted in 607 μ M 8-Cl-ATP accumulation compared to 203 μ M measured in the combination treatment of 8-Cl-Ado for 12 hours followed by 17-AAG for 8 hours.

According to published literature, HSP90 is known to aid in the folding of several proteins including oncoproteins, but is also involved in the assembly of non-oncoproteins such as the apoptosome (Yamano, Mizukami et al. 2008). HSP90 is also needed for the stability and maturation of cystic fibrosis transmembrane conductance regulator (CFTR) polypeptide, which is a transporting channel that regulates passage of chloride ions (Loo, Jensen et al. 1998). As mentioned before, the diphosphate metabolite of 8-Cl-Ado, 8-Cl-ADP, can potentially bind to the ADP site in ATP synthase mimicking the natural substrate resulting in its phosphorylation to 8-Cl-ATP. Since a decline in 8-Cl-ATP levels is observed in all three MM cell lines with 17-AAG addition after 8-Cl-Ado treatment, and based on the literature demonstrating that HSP90 participates in the maturation of large protein complexes, it is tempting to speculate whether ATP synthase could be a client protein of HSP90. This hypothesis could provide a mechanistic basis for the observed decrease in 8-Cl-ATP levels measured in the combination treatment.

At least one study has reported via immunoprecipitation assays the interaction of HSP90 and the subunits of ATP synthase (Papathanassiou, MacDonald et al. 2006). However, this study did not investigate whether treatment with a known HSP90 inhibitor, such as geldanamycin or 17-AAG, could lead to the disruption of HSP90 and the subunits

of ATP synthase. Therefore, further experiments are needed to determine if ATP synthase is indeed another HSP90 client protein.

Binding of 17-AAG to HSP90 hinders the chaperoning and functional conformation of client proteins by HSP90 ultimately resulting in their proteasomal degradation (Neckers and Neckers 2002). Endogenous ATP levels in untreated MM.1S cells are approximately 3 mM, which is decreased by more than 55% (around 1.3 mM ATP remaining in the cell) after treatment with 8-Cl-Ado for 12 or 20 hours (Figure 51). Because intracellular ATP and 17-AAG compete to bind to the ATP pocket in HSP90, it is expected that more 17-AAG will bind to HSP90 since the natural substrate will no longer compete when cells are treated with 8-Cl-Ado and 17-AAG in combination. A consequence of increased 17-AAG binding to HSP90 hence could lead to an increase in degradation of client proteins (STAT3, Raf-1 and Akt), resulting in decrease levels of these protein in the treated cells. As indicated by immunoblot assays, a further decrease of the client protein levels was observed in all of the sequential or simultaneous combination treatments compared to 8-Cl-Ado and 17-AAG as single agents (Figures 42-44, 46, and 47).

Based on these results, the possibility that ATP depletion could increase binding of 17-AAG to HSP90, increasing the turn-over rate of the client proteins, was contemplated as a potential mechanism of action by which 8-Cl-Ado and 17-AAG combination resulted in increased cell death. For this reason, immunoprecipitations and immunoblot analyses of radioactive [^3H]17-AAG bound to HSP90 were performed in MM.1S cells for the combination treatment compared to 17-AAG treatment alone (Figure 54). Although [^3H]17-AAG bound to HSP90 was successfully immunoprecipitated, results indicated that when cells are treated with [^3H]17-AAG or 8-Cl-Ado in combination with [^3H]17-AAG there is no further increase in the binding of [^3H]17-AAG to HSP90. This suggests that the levels of ATP in the cell do not affect binding affinity of [^3H]17-AAG for HSP90.

Interestingly, a study investigating the effect of ATP depletion in the stabilization of the client protein ErbB2 by HSP90 concluded that a decrease in the levels of ATP results in the disruption of the HSP90•ErbB2 complex and ErbB2 degradation (Peng, Guo et al. 2005). The authors of this study lowered ATP concentration in the cell by inhibiting glycolysis and mitochondrial respiration using the pharmacological inhibitors 2-deoxy-D-glucose or antimycin A, respectively. They concluded that depletion of cellular ATP levels alters stabilization and maturation of ErbB2 by HSP90, and this depletion of the client protein ErbB2 was similar to the one obtained when cells were treated with geldanamycin. A similar decrease in protein levels was observed for the other two client proteins evaluated in this study, Raf-1 and Akt, following ATP depletion due to treatment with 2-deoxy-D-glucose or antimycin A. This indicates that a decrease in cellular ATP concentration mimics the mechanism by which HSP90 inhibitors cause cytotoxicity in the cell. Hence, the decrease of client proteins levels observed with 8-Cl-Ado treatment alone could be a result of its effect in ATP depletion. This possibility is more noticeable when comparing treatment of U266 cells with 17-AAG and 8-Cl-Ado as single agents for 20 hours (Figure 47). A similar decrease in STAT3, Raf-1 and Akt protein levels was determined for both treatments. Hence, this could provide an explanation of why the combination treatment leads to further decrease in client protein levels.

In addition to the effect that the combination of 8-Cl-Ado and 17-AAG had on heat shock proteins and client proteins, the levels of the antiapoptotic glucose-regulated protein chaperones in the endoplasmic reticulum were also evaluated. It has been reported that HSP90 inhibitors in MM cells can activate the unfolded protein response (UPR) in the endoplasmic reticulum leading to the induction of GRP78 and GRP94 chaperones in this organelle, which are HSP70 and HSP90 homologues, respectively (Davenport, Moore et al. 2007). This study used high concentrations of 17-AAG (5 μ M) for an incubation period of 24 hours, which might account for the measured induction of GRP chaperones. In contrast to

this, the work in this dissertation treated MM cells with 0.5 μ M 17-AAG for 8 hours and immunoblot assays indicate that no induction of GRP78 or GRP94 expression occurred at these specific conditions (Figure 39 and 40). In addition, metabolic perturbation (such as glucose deprivation) is a strong inducer of the stress response in the endoplasmic reticulum, although it is not known to what extent ATP depletion accounts for this effect (Schroder 2008). Based on immunoblot assays analyzing for GRP78 and GRP94 in MM.1S cells treated with 10 μ M 8-Cl-Ado for 20 hours, there is no elevation of these protein levels (Figures 39 and 40). This suggests that a decrease of ATP levels by 56% due to treatment with 8-Cl-Ado for 20 hours (Figure 51) does not trigger the endoplasmic stress response which leads to the induction of cytoprotective GRP78 and GRP94 proteins. Furthermore, GRP protein induction is not detected when both 8-Cl-Ado and 17-AAG are combined.

Protein synthesis and ATP depletion

The decrease in client protein levels in the different combination treatments with 8-Cl-Ado and 17-AAG could also be due to the effect that 8-Cl-Ado treatment has on ATP depletion, which could ultimately affect protein translation. Hence, an additional mechanism by which 8-Cl-Ado could be leading to decreased client protein levels is by negatively affecting protein synthesis. Thus, the observed decrease in STAT3, Raf-1 and Akt client protein levels may be also a result of decreased protein translation since no change was detected for any of the client protein mRNA levels when compared to the untreated controls (Figures 48-50).

Protein translation is regulated when the cell undergoes some kind of stress that perturbs homeostasis, and the mTOR (mammalian target of rapamycin) pathway is sensitive to changes in cellular ATP levels (Dennis, Jaeschke et al. 2001). 4E-BP1 regulates translation, and its activity is in turn regulated by the upstream serine/threonine

kinase mTOR (Gingras, Kennedy et al. 1998). The translation repressing activity of 4E-BP1 is regulated by phosphorylation at 4 specific amino-acid residues (Gingras, Kennedy et al. 1998; Gingras, Raught et al. 2001). In its hypophosphorylated state, 4E-BP1 represses initiation of translation by binding to the eukaryotic initiation factor 4E (eIF4E) (Gingras, Kennedy et al. 1998). In contrast, hyperphosphorylation of 4E-BP1 by upstream kinases such as mTOR results in the release of eIF4E allowing translation initiation (Gingras, Raught et al. 2001).

Negative regulation of the mTOR pathway can occur due to factors such as cellular starvation, resulting in hypophosphorylation of 4E-BP1 (Dennis, Jaeschke et al. 2001). The decrease in cellular ATP levels ultimately leads to inhibition of mTOR kinase activity, thus rendering it unable to phosphorylate 4E-BP1. As a result, 4E-BP1 remains bound to eIF4E, inhibiting translation initiation (Gingras, Raught et al. 2001).

Due to the effect of 8-Cl-Ado on the ATP levels in the cell, the phosphorylated status of 4E-BP1 was evaluated. A time-course experiment in MM.1S cells treated with 8-Cl-Ado followed by immunoblots assays analyzing for 4E-BP1 phosphorylation status indicated that treatment with 8-Cl-Ado results in hypophosphorylation of 4E-BP1 (Figure 55A) as compared to the positive control (starvation of MM.1S cells for 12, 24, 48 and 72 hours; Figure 55B). The hypophosphorylated status of 4E-BP1 could initially be attributed to the decrease in ATP concentration. This in principle could decrease kinase activity as a result of substrate availability. However, a study reported that a decline in ATP does not result in a global decrease in protein phosphorylation (Ghias, Ma et al. 2005). Additionally, in U266 cells treated with 8-Cl-Ado and 17-AAG in sequential or simultaneous combination, immunoblot analysis of 4E-BP1 expression indicated further hypophosphorylation of this protein compared to treatment with the drugs as single agents (Figure 56). Therefore, further studies addressing the effect of 8-Cl-Ado alone and in combination with 17-AAG on 4E-BP1 and global protein translation are needed.

As previously mentioned, the sequential and simultaneous combination of 8-Cl-Ado and 17-AAG results in further decrease of client protein levels compared to the agents alone. The ribosomal protein S6 (rpS6) is involved in the translation of mRNAs that encode for ribosomal proteins and translation regulators (Meyuhas 2000). Interestingly, rpS6 is a client protein of HSP90, meaning that pharmacological inhibition of HSP90 would render this chaperone unable to stabilize rpS6 leading to its proteasomal degradation (Kim, Jang et al. 2006). Based on this, it is possible that addition of 17-AAG in the combination treatment could also potentially inhibit global translation to some extent besides resulting in the proteasomal degradation of client proteins.

Although the mechanism by which 8-Cl-Ado treatment leads to hypophosphorylation of the translation repressor 4E-BP1 was not elucidated in this current study, this negative effect on the translation process could be another potential mechanism by which treatment with 8-Cl-Ado affects protein translation.

In summary, the mechanism-based combination of transcription/translation inhibitors that cause ATP depletion could be used in combination with 17-AAG as a strategy to either abrogate heat shock protein induction or decrease client protein levels resulting in increase cytotoxicity. The agents evaluated in this investigation are either approved drugs or in clinical trials. Hence, these approaches may be applied in the clinic towards the design of new drug combination strategies to target either the induction of cytoprotective heat shock proteins or further decrease client oncoprotein levels.

References

- Aghdassi, A., P. Phillips, V. Dudeja, D. Dhaulakhandi, R. Sharif, R. Dawra, M. M. Lerch and A. Saluja (2007). "Heat shock protein 70 increases tumorigenicity and inhibits apoptosis in pancreatic adenocarcinoma." Cancer Res **67**(2): 616-25.
- Ananthan, J., A. L. Goldberg and R. Voellmy (1986). "Abnormal proteins serve as eukaryotic stress signals and trigger the activation of heat shock genes." Science **232**(4749): 522-4.
- Anfinsen, C. B. (1973). "Principles that govern the folding of protein chains." Science **181**(96): 223-30.
- Bagatell, R., G. D. Paine-Murrieta, C. W. Taylor, E. J. Pulcini, S. Akinaga, I. J. Benjamin and L. Whitesell (2000). "Induction of a heat shock factor 1-dependent stress response alters the cytotoxic activity of hsp90-binding agents." Clin Cancer Res **6**(8): 3312-8.
- Bagatell, R. and L. Whitesell (2004). "Altered Hsp90 function in cancer: a unique therapeutic opportunity." Mol Cancer Ther **3**(8): 1021-30.
- Balakrishnan, K., C. M. Stellrecht, D. Genini, M. Ayres, W. G. Wierda, M. J. Keating, L. M. Leoni and V. Gandhi (2005). "Cell death of bioenergetically compromised and transcriptionally challenged CLL lymphocytes by chlorinated ATP." Blood **105**(11): 4455-62.

- Baler, R., G. Dahl and R. Voellmy (1993). "Activation of human heat shock genes is accompanied by oligomerization, modification, and rapid translocation of heat shock transcription factor HSF1." Mol Cell Biol **13**(4): 2486-96.
- Banerji, U., A. O'Donnell, M. Scurr, S. Pacey, S. Stapleton, Y. Asad, L. Simmons, A. Maloney, F. Raynaud, M. Campbell, M. Walton, S. Lakhani, S. Kaye, P. Workman and I. Judson (2005). "Phase I pharmacokinetic and pharmacodynamic study of 17-allylamino, 17-demethoxygeldanamycin in patients with advanced malignancies." J Clin Oncol **23**(18): 4152-61.
- Beere, H. M., B. B. Wolf, K. Cain, D. D. Mosser, A. Mahboubi, T. Kuwana, P. Taylor, R. I. Morimoto, G. M. Cohen and D. R. Green (2000). "Heat-shock protein 70 inhibits apoptosis by preventing recruitment of procaspase-9 to the Apaf-1 apoptosome." Nat Cell Biol **2**(8): 469-75.
- Bergsagel, D. E., C. C. Sprague, C. Austin and K. M. Griffith (1962). "Evaluation of new chemotherapeutic agents in the treatment of multiple myeloma. IV. L-Phenylalanine mustard (NSC-8806)." Cancer Chemother Rep **21**: 87-99.
- Biamonte, M. A., R. Van de Water, J. W. Arndt, R. H. Scannevin, D. Perret and W. C. Lee (2010). "Heat shock protein 90: inhibitors in clinical trials." J Med Chem **53**(1): 3-17.
- Bommert, K., R. C. Bargou and T. Stuhmer (2006). "Signalling and survival pathways in multiple myeloma." Eur J Cancer **42**(11): 1574-80.
- Brandt, G. E. and B. S. Blagg (2009). "Alternate strategies of Hsp90 modulation for the treatment of cancer and other diseases." Curr Top Med Chem **9**(15): 1447-61.

- Brown, S. A. and R. E. Kingston (1997). "Disruption of downstream chromatin directed by a transcriptional activator." Genes Dev **11**(23): 3116-21.
- Chatterjee, M., S. Jain, T. Stuhmer, M. Andrulis, U. Ungethum, R. J. Kuban, H. Lorentz, K. Bommert, M. Topp, D. Kramer, H. K. Muller-Hermelink, H. Einsele, A. Greiner and R. C. Bargou (2007). "STAT3 and MAPK signaling maintain overexpression of heat shock proteins 90alpha and beta in multiple myeloma cells, which critically contribute to tumor-cell survival." Blood **109**(2): 720-8.
- Chauhan, D., G. Li, T. Hideshima, K. Podar, C. Mitsiades, N. Mitsiades, L. Catley, Y. T. Tai, T. Hayashi, R. Shringarpure, R. Burger, N. Munshi, Y. Ohtake, S. Saxena and K. C. Anderson (2003). "Hsp27 inhibits release of mitochondrial protein Smac in multiple myeloma cells and confers dexamethasone resistance." Blood **102**(9): 3379-86.
- Chen, L. S., L. Du-Cuny, V. Vethantham, D. H. Hawke, J. L. Manley, S. Zhang and V. Gandhi (2010). "Chain termination and inhibition of mammalian poly(A) polymerase by modified ATP analogues." Biochem Pharmacol **79**(5): 669-77.
- Chen, L. S., B. J. Nowak, M. L. Ayres, N. L. Krett, S. T. Rosen, S. Zhang and V. Gandhi (2009). "Inhibition of ATP synthase by chlorinated adenosine analogue." Biochem Pharmacol **78**(6): 583-91.
- Chen, L. S. and T. L. Sheppard (2004). "Chain termination and inhibition of *Saccharomyces cerevisiae* poly(A) polymerase by C-8-modified ATP analogs." J Biol Chem **279**(39): 40405-11.

- Chng, W. J., L. G. Lau, N. Yusof and B. M. Mow (2005). "Targeted therapy in multiple myeloma." Cancer Control **12**(2): 91-104.
- Ciocca, D. R., F. E. Gago, M. A. Fanelli and S. K. Calderwood (2006). "Co-expression of steroid receptors (estrogen receptor alpha and/or progesterone receptors) and Her-2/neu: Clinical implications." J Steroid Biochem Mol Biol **102**(1-5): 32-40.
- Clemons, N. J., K. Buzzard, R. Steel and R. L. Anderson (2005). "Hsp72 inhibits Fas-mediated apoptosis upstream of the mitochondria in type II cells." J Biol Chem **280**(10): 9005-12.
- Cotto, J. J., M. Kline and R. I. Morimoto (1996). "Activation of heat shock factor 1 DNA binding precedes stress-induced serine phosphorylation. Evidence for a multistep pathway of regulation." J Biol Chem **271**(7): 3355-8.
- Czyz, M. and M. Gniazdowski (1998). "Actinomycin D specifically inhibits the interaction between transcription factor Sp1 and its binding site." Acta Biochim Pol **45**(1): 67-73.
- Dalton, W. S., P. L. Bergsagel, W. M. Kuehl, K. C. Anderson and J. L. Harousseau (2001). "Multiple myeloma." Hematology Am Soc Hematol Educ Program: 157-77.
- Davenport, E. L., H. E. Moore, A. S. Dunlop, S. Y. Sharp, P. Workman, G. J. Morgan and F. E. Davies (2007). "Heat shock protein inhibition is associated with activation of the unfolded protein response pathway in myeloma plasma cells." Blood **110**(7): 2641-9.

- DeBoer, C., P. A. Meulman, R. J. Wnuk and D. H. Peterson (1970). "Geldanamycin, a new antibiotic." J Antibiot (Tokyo) **23**(9): 442-7.
- Demidenko, Z. N., C. Vivo, H. D. Halicka, C. J. Li, K. Bhalla, E. V. Broude and M. V. Blagosklonny (2006). "Pharmacological induction of Hsp70 protects apoptosis-prone cells from doxorubicin: comparison with caspase-inhibitor- and cycle-arrest-mediated cytoprotection." Cell Death Differ **13**(9): 1434-41.
- Dennis, P. B., A. Jaeschke, M. Saitoh, B. Fowler, S. C. Kozma and G. Thomas (2001). "Mammalian TOR: a homeostatic ATP sensor." Science **294**(5544): 1102-5.
- Dennison, J. B., M. L. Ayres, K. Kaluarachchi, W. Plunkett and V. Gandhi (2010). "Intracellular succinylation of 8-chloroadenosine and its effect on fumarate levels." J Biol Chem.
- Dennison, J. B., K. Balakrishnan and V. Gandhi (2009). "Preclinical activity of 8-chloroadenosine with mantle cell lymphoma: roles of energy depletion and inhibition of DNA and RNA synthesis." Br J Haematol **147**(3): 297-307.
- Dey, A., E. T. Wong, C. F. Cheok, V. Tergaonkar and D. P. Lane (2008). "R-Roscovitine simultaneously targets both the p53 and NF-kappaB pathways and causes potentiation of apoptosis: implications in cancer therapy." Cell Death Differ **15**(2): 263-73.

- Dragovic, Z., S. A. Broadley, Y. Shomura, A. Bracher and F. U. Hartl (2006). "Molecular chaperones of the Hsp110 family act as nucleotide exchange factors of Hsp70s." Embo J **25**(11): 2519-28.
- Dutta, R. and M. Inouye (2000). "GHKL, an emergent ATPase/kinase superfamily." Trends Biochem Sci **25**(1): 24-8.
- Ehrnsperger, M., S. Graber, M. Gaestel and J. Buchner (1997). "Binding of non-native protein to Hsp25 during heat shock creates a reservoir of folding intermediates for reactivation." Embo J **16**(2): 221-9.
- Ellis, R. J. (1993). "The general concept of molecular chaperones." Philos Trans R Soc Lond B Biol Sci **339**(1289): 257-61.
- Engelhardt, M. and R. Mertelsmann (2006). "160 years of multiple myeloma: progress and challenges." Eur J Cancer **42**(11): 1507-9.
- Estlin, E. J. and G. J. Veal (2003). "Clinical and cellular pharmacology in relation to solid tumours of childhood." Cancer Treat Rev **29**(4): 253-73.
- Farber, S., D. Pinkel, E. M. Sears and R. Toch (1956). "Advances in chemotherapy of cancer in man." Adv Cancer Res **4**: 1-71.
- Felts, S. J., B. A. Owen, P. Nguyen, J. Trepel, D. B. Donner and D. O. Toft (2000). "The hsp90-related protein TRAP1 is a mitochondrial protein with distinct functional properties." J Biol Chem **275**(5): 3305-12.

- Fivaz, J., M. C. Bassi, S. Pinaud and J. Mirkovitch (2000). "RNA polymerase II promoter-proximal pausing upregulates c-fos gene expression." Gene **255**(2): 185-94.
- Freeman, M. L., M. J. Borrelli, M. J. Meredith and J. R. Lepock (1999). "On the path to the heat shock response: destabilization and formation of partially folded protein intermediates, a consequence of protein thiol modification." Free Radic Biol Med **26**(5-6): 737-45.
- Frey, J. A. and V. Gandhi (2010). "8-Amino-adenosine inhibits multiple mechanisms of transcription." Mol Cancer Ther **9**(1): 236-45.
- Gandhi, V., M. Ayres, R. G. Halgren, N. L. Krett, R. A. Newman and S. T. Rosen (2001). "8-chloro-cAMP and 8-chloro-adenosine act by the same mechanism in multiple myeloma cells." Cancer Res **61**(14): 5474-9.
- Garrido, C., P. Ottavi, A. Fromentin, A. Hammann, A. P. Arrigo, B. Chauffert and P. Mehlen (1997). "HSP27 as a mediator of confluence-dependent resistance to cell death induced by anticancer drugs." Cancer Res **57**(13): 2661-7.
- Ghias, K., C. Ma, V. Gandhi, L. C. Platanias, N. L. Krett and S. T. Rosen (2005). "8-Amino-adenosine induces loss of phosphorylation of p38 mitogen-activated protein kinase, extracellular signal-regulated kinase 1/2, and Akt kinase: role in induction of apoptosis in multiple myeloma." Mol Cancer Ther **4**(4): 569-77.

- Gingras, A. C., S. G. Kennedy, M. A. O'Leary, N. Sonenberg and N. Hay (1998). "4E-BP1, a repressor of mRNA translation, is phosphorylated and inactivated by the Akt(PKB) signaling pathway." Genes Dev **12**(4): 502-13.
- Gingras, A. C., B. Raught, S. P. Gygi, A. Niedzwiecka, M. Miron, S. K. Burley, R. D. Polakiewicz, A. Wyslouch-Cieszyńska, R. Aebersold and N. Sonenberg (2001). "Hierarchical phosphorylation of the translation inhibitor 4E-BP1." Genes Dev **15**(21): 2852-64.
- Glover, J. R. and J. M. Tkach (2001). "Crowbars and ratchets: hsp100 chaperones as tools in reversing protein aggregation." Biochem Cell Biol **79**(5): 557-68.
- Gniazdowski, M., W. A. Denny, S. M. Nelson and M. Czyz (2003). "Transcription factors as targets for DNA-interacting drugs." Curr Med Chem **10**(11): 909-24.
- Goldberg, A. L. (2003). "Protein degradation and protection against misfolded or damaged proteins." Nature **426**(6968): 895-9.
- Gomes, N. P., G. Bjerke, B. Llorente, S. A. Szostek, B. M. Emerson and J. M. Espinosa (2006). "Gene-specific requirement for P-TEFb activity and RNA polymerase II phosphorylation within the p53 transcriptional program." Genes Dev **20**(5): 601-12.
- Grivicich, I., A. Regner, C. Zanoni, L. P. Correa, G. P. Jotz, J. A. Henriques, G. Schwartzmann and A. B. da Rocha (2007). "Hsp70 response to 5-fluorouracil treatment in human colon cancer cell lines." Int J Colorectal Dis **22**(10): 1201-8.

- Gu, Y. Y., H. Y. Zhang, H. J. Zhang, S. Y. Li, J. H. Ni and H. T. Jia (2006). "8-Chloro-adenosine inhibits growth at least partly by interfering with actin polymerization in cultured human lung cancer cells." Biochem Pharmacol **72**(5): 541-50.
- Guo, F., K. Rocha, P. Bali, M. Pranpat, W. Fiskus, S. Boyapalle, S. Kumaraswamy, M. Balasis, B. Greedy, E. S. Armitage, N. Lawrence and K. Bhalla (2005). "Abrogation of heat shock protein 70 induction as a strategy to increase antileukemia activity of heat shock protein 90 inhibitor 17-allylamino-demethoxy geldanamycin." Cancer Res **65**(22): 10536-44.
- Guo, Y., T. Guettouche, M. Fenna, F. Boellmann, W. B. Pratt, D. O. Toft, D. F. Smith and R. Voellmy (2001). "Evidence for a mechanism of repression of heat shock factor 1 transcriptional activity by a multichaperone complex." J Biol Chem **276**(49): 45791-9.
- Gurbuxani, S., E. Schmitt, C. Cande, A. Parcellier, A. Hammann, E. Daugas, I. Kouranti, C. Spahr, A. Pance, G. Kroemer and C. Garrido (2003). "Heat shock protein 70 binding inhibits the nuclear import of apoptosis-inducing factor." Oncogene **22**(43): 6669-78.
- Hanahan, D. and R. A. Weinberg (2000). "The hallmarks of cancer." Cell **100**(1): 57-70.
- Hartl, F. U. (1996). "Molecular chaperones in cellular protein folding." Nature **381**(6583): 571-9.
- Hartl, F. U. and M. Hayer-Hartl (2002). "Molecular chaperones in the cytosol: from nascent chain to folded protein." Science **295**(5561): 1852-8.

- Hartl, F. U. and M. Hayer-Hartl (2009). "Converging concepts of protein folding in vitro and in vivo." Nat Struct Mol Biol **16**(6): 574-81.
- He, H., F. Soncin, N. Grammatikakis, Y. Li, A. Siganou, J. Gong, S. A. Brown, R. E. Kingston and S. K. Calderwood (2003). "Elevated expression of heat shock factor (HSF) 2A stimulates HSF1-induced transcription during stress." J Biol Chem **278**(37): 35465-75.
- Hensold, J. O., C. R. Hunt, S. K. Calderwood, D. E. Housman and R. E. Kingston (1990). "DNA binding of heat shock factor to the heat shock element is insufficient for transcriptional activation in murine erythroleukemia cells." Mol Cell Biol **10**(4): 1600-8.
- Hickey, E., S. E. Brandon, S. Sadis, G. Smale and L. A. Weber (1986). "Molecular cloning of sequences encoding the human heat-shock proteins and their expression during hyperthermia." Gene **43**(1-2): 147-54.
- Hideshima, T., C. Mitsiades, G. Tonon, P. G. Richardson and K. C. Anderson (2007). "Understanding multiple myeloma pathogenesis in the bone marrow to identify new therapeutic targets." Nat Rev Cancer **7**(8): 585-98.
- Hideshima, T., K. Podar, D. Chauhan and K. C. Anderson (2005). "Cytokines and signal transduction." Best Pract Res Clin Haematol **18**(4): 509-24.

- Hunt, C. and R. I. Morimoto (1985). "Conserved features of eukaryotic hsp70 genes revealed by comparison with the nucleotide sequence of human hsp70." Proc Natl Acad Sci U S A **82**(19): 6455-9.
- Jagannath, S., R. A. Kyle, A. Palumbo, D. S. Siegel, S. Cunningham and J. Berenson (2010). "The current status and future of multiple myeloma in the clinic." Clin Lymphoma Myeloma **10**(1): E1-16.
- Jemal, A., R. Siegel, E. Ward, Y. Hao, J. Xu and M. J. Thun (2009). "Cancer statistics, 2009." CA Cancer J Clin **59**(4): 225-49.
- Jurivich, D. A., L. Sistonen, R. A. Kroes and R. I. Morimoto (1992). "Effect of sodium salicylate on the human heat shock response." Science **255**(5049): 1243-5.
- Kalinowska, M., W. Garncarz, M. Pietrowska, W. T. Garrard and P. Widlak (2005). "Regulation of the human apoptotic DNase/RNase endonuclease G: involvement of Hsp70 and ATP." Apoptosis **10**(4): 821-30.
- Kamal, A., L. Thao, J. Sensintaffar, L. Zhang, M. F. Boehm, L. C. Fritz and F. J. Burrows (2003). "A high-affinity conformation of Hsp90 confers tumour selectivity on Hsp90 inhibitors." Nature **425**(6956): 407-10.
- Kampinga, H. H., J. Hageman, M. J. Vos, H. Kubota, R. M. Tanguay, E. A. Bruford, M. E. Cheetham, B. Chen and L. E. Hightower (2009). "Guidelines for the nomenclature of the human heat shock proteins." Cell Stress Chaperones **14**(1): 105-11.

- Kang, B. H., J. Plescia, T. Dohi, J. Rosa, S. J. Doxsey and D. C. Altieri (2007). "Regulation of tumor cell mitochondrial homeostasis by an organelle-specific Hsp90 chaperone network." Cell **131**(2): 257-70.
- Kang, B. H., J. Plescia, H. Y. Song, M. Meli, G. Colombo, K. Beebe, B. Scroggins, L. Neckers and D. C. Altieri (2009). "Combinatorial drug design targeting multiple cancer signaling networks controlled by mitochondrial Hsp90." J Clin Invest **119**(3): 454-64.
- Khaleque, M. A., A. Bharti, D. Sawyer, J. Gong, I. J. Benjamin, M. A. Stevenson and S. K. Calderwood (2005). "Induction of heat shock proteins by heregulin beta1 leads to protection from apoptosis and anchorage-independent growth." Oncogene **24**(43): 6564-73.
- Kim, R., M. Emi, K. Tanabe and S. Murakami (2006). "Role of the unfolded protein response in cell death." Apoptosis **11**(1): 5-13.
- Kim, S. A., J. H. Yoon, S. H. Lee and S. G. Ahn (2005). "Polo-like kinase 1 phosphorylates heat shock transcription factor 1 and mediates its nuclear translocation during heat stress." J Biol Chem **280**(13): 12653-7.
- Kim, T. S., C. Y. Jang, H. D. Kim, J. Y. Lee, B. Y. Ahn and J. Kim (2006). "Interaction of Hsp90 with ribosomal proteins protects from ubiquitination and proteasome-dependent degradation." Mol Biol Cell **17**(2): 824-33.

- Kim, Y. S., S. V. Alarcon, S. Lee, M. J. Lee, G. Giaccone, L. Neckers and J. B. Trepel (2009). "Update on Hsp90 inhibitors in clinical trial." Curr Top Med Chem **9**(15): 1479-92.
- Kingston, R. E., T. J. Schuetz and Z. Larin (1987). "Heat-inducible human factor that binds to a human hsp70 promoter." Mol Cell Biol **7**(4): 1530-4.
- Komarova, E. Y., E. A. Afanasyeva, M. M. Bulatova, M. E. Cheetham, B. A. Margulis and I. V. Guzhova (2004). "Downstream caspases are novel targets for the antiapoptotic activity of the molecular chaperone hsp70." Cell Stress Chaperones **9**(3): 265-75.
- Kudla, G., L. Lipinski, F. Caffin, A. Helwak and M. Zylicz (2006). "High guanine and cytosine content increases mRNA levels in mammalian cells." PLoS Biol **4**(6): e180.
- Kuehl, W. M. and P. L. Bergsagel (2002). "Multiple myeloma: evolving genetic events and host interactions." Nat Rev Cancer **2**(3): 175-87.
- Lai, A. Z., J. V. Abella and M. Park (2009). "Crosstalk in Met receptor oncogenesis." Trends Cell Biol **19**(10): 542-51.
- Landry, J. and J. Huot (1995). "Modulation of actin dynamics during stress and physiological stimulation by a signaling pathway involving p38 MAP kinase and heat-shock protein 27." Biochem Cell Biol **73**(9-10): 703-7.

- Laskey, R. A., B. M. Honda, A. D. Mills and J. T. Finch (1978). "Nucleosomes are assembled by an acidic protein which binds histones and transfers them to DNA." Nature **275**(5679): 416-20.
- Lee, Y. J., D. H. Lee, C. K. Cho, H. Y. Chung, S. Bae, G. J. Jhon, J. W. Soh, D. I. Jeoung, S. J. Lee and Y. S. Lee (2005). "HSP25 inhibits radiation-induced apoptosis through reduction of PKCdelta-mediated ROS production." Oncogene **24**(23): 3715-25.
- Lei, K., A. Nimnual, W. X. Zong, N. J. Kennedy, R. A. Flavell, C. B. Thompson, D. Bar-Sagi and R. J. Davis (2002). "The Bax subfamily of Bcl2-related proteins is essential for apoptotic signal transduction by c-Jun NH(2)-terminal kinase." Mol Cell Biol **22**(13): 4929-42.
- Leu, J. I., J. Pimkina, A. Frank, M. E. Murphy and D. L. George (2009). "A small molecule inhibitor of inducible heat shock protein 70." Mol Cell **36**(1): 15-27.
- Liang, P. and T. H. MacRae (1997). "Molecular chaperones and the cytoskeleton." J Cell Sci **110** (Pt 13): 1431-40.
- Lis, J. and C. Wu (1993). "Protein traffic on the heat shock promoter: parking, stalling, and trucking along." Cell **74**(1): 1-4.
- Ljungman, M., F. Zhang, F. Chen, A. J. Rainbow and B. C. McKay (1999). "Inhibition of RNA polymerase II as a trigger for the p53 response." Oncogene **18**(3): 583-92.

- Loo, M. A., T. J. Jensen, L. Cui, Y. Hou, X. B. Chang and J. R. Riordan (1998). "Perturbation of Hsp90 interaction with nascent CFTR prevents its maturation and accelerates its degradation by the proteasome." Embo J **17**(23): 6879-87.
- Luo, J., N. L. Solimini and S. J. Elledge (2009). "Principles of cancer therapy: oncogene and non-oncogene addiction." Cell **136**(5): 823-37.
- Martins, A. S., J. L. Ordonez, A. Garcia-Sanchez, D. Herrero, V. Sevillano, D. Osuna, C. Mackintosh, G. Caballero, A. P. Otero, C. Poremba, J. Madoz-Gurpide and E. de Alava (2008). "A pivotal role for heat shock protein 90 in Ewing sarcoma resistance to anti-insulin-like growth factor 1 receptor treatment: in vitro and in vivo study." Cancer Res **68**(15): 6260-70.
- Maurizi, M. R. and D. Xia (2004). "Protein binding and disruption by Clp/Hsp100 chaperones." Structure **12**(2): 175-83.
- Mehlen, P., K. Schulze-Osthoff and A. P. Arrigo (1996). "Small stress proteins as novel regulators of apoptosis. Heat shock protein 27 blocks Fas/APO-1- and staurosporine-induced cell death." J Biol Chem **271**(28): 16510-4.
- Meijer, L. and E. Raymond (2003). "Roscovitine and other purines as kinase inhibitors. From starfish oocytes to clinical trials." Acc Chem Res **36**(6): 417-25.
- Meyuhas, O. (2000). "Synthesis of the translational apparatus is regulated at the translational level." Eur J Biochem **267**(21): 6321-30.

- Miller, P., C. DiOrio, M. Moyer, R. C. Schnur, A. Bruskin, W. Cullen and J. D. Moyer (1994). "Depletion of the erbB-2 gene product p185 by benzoquinoid ansamycins." Cancer Res **54**(10): 2724-30.
- Miller, R. T., S. E. Glover, W. S. Stewart, J. C. Corton, J. A. Popp and R. C. Cattley (1996). "Effect on the expression of c-met, c-myc and PPAR-alpha in liver and liver tumors from rats chronically exposed to the hepatocarcinogenic peroxisome proliferator WY-14,643." Carcinogenesis **17**(6): 1337-41.
- Mitsiades, C. S., N. S. Mitsiades, N. C. Munshi, P. G. Richardson and K. C. Anderson (2006). "The role of the bone microenvironment in the pathophysiology and therapeutic management of multiple myeloma: interplay of growth factors, their receptors and stromal interactions." Eur J Cancer **42**(11): 1564-73.
- Montesano Gesualdi, N., G. Chirico, G. Pirozzi, E. Costantino, M. Landriscina and F. Esposito (2007). "Tumor necrosis factor-associated protein 1 (TRAP-1) protects cells from oxidative stress and apoptosis." Stress **10**(4): 342-50.
- Mora, G. R., K. R. Olivier, R. F. Mitchell, Jr., R. B. Jenkins and D. J. Tindall (2005). "Regulation of expression of the early growth response gene-1 (EGR-1) in malignant and benign cells of the prostate." Prostate **63**(2): 198-207.
- Mounier, N. and A. P. Arrigo (2002). "Actin cytoskeleton and small heat shock proteins: how do they interact?" Cell Stress Chaperones **7**(2): 167-76.

- Nathan, D. F., M. H. Vos and S. Lindquist (1997). "In vivo functions of the *Saccharomyces cerevisiae* Hsp90 chaperone." Proc Natl Acad Sci U S A **94**(24): 12949-56.
- Neckers, L. (2007). "Heat shock protein 90: the cancer chaperone." J Biosci **32**(3): 517-30.
- Neckers, L. and K. Neckers (2002). "Heat-shock protein 90 inhibitors as novel cancer chemotherapeutic agents." Expert Opin Emerg Drugs **7**(2): 277-88.
- Nieto-Miguel, T., C. Gajate, F. Gonzalez-Camacho and F. Mollinedo (2008). "Proapoptotic role of Hsp90 by its interaction with c-Jun N-terminal kinase in lipid rafts in edelfosine-mediated antileukemic therapy." Oncogene **27**(12): 1779-87.
- Obermann, W. M., H. Sondermann, A. A. Russo, N. P. Pavletich and F. U. Hartl (1998). "In vivo function of Hsp90 is dependent on ATP binding and ATP hydrolysis." J Cell Biol **143**(4): 901-10.
- Omura, S., Y. Iwai, Y. Takahashi, N. Sadakane, A. Nakagawa, H. Oiwa, Y. Hasegawa and T. Ikai (1979). "Herbimycin, a new antibiotic produced by a strain of *Streptomyces*." J Antibiot (Tokyo) **32**(4): 255-61.
- Onuoha, S. C., E. T. Coulstock, J. G. Grossmann and S. E. Jackson (2008). "Structural studies on the co-chaperone Hop and its complexes with Hsp90." J Mol Biol **379**(4): 732-44.
- Ostrovsky, O., N. T. Ahmed and Y. Argon (2009). "The chaperone activity of GRP94 toward insulin-like growth factor II is necessary for the stress response to serum deprivation." Mol Biol Cell **20**(6): 1855-64.

- Ostrovsky, O., C. A. Makarewich, E. L. Snapp and Y. Argon (2009). "An essential role for ATP binding and hydrolysis in the chaperone activity of GRP94 in cells." Proc Natl Acad Sci U S A **106**(28): 11600-5.
- Pandey, P., R. Farber, A. Nakazawa, S. Kumar, A. Bharti, C. Nalin, R. Weichselbaum, D. Kufe and S. Kharbanda (2000). "Hsp27 functions as a negative regulator of cytochrome c-dependent activation of procaspase-3." Oncogene **19**(16): 1975-81.
- Pandey, P., A. Saleh, A. Nakazawa, S. Kumar, S. M. Srinivasula, V. Kumar, R. Weichselbaum, C. Nalin, E. S. Alnemri, D. Kufe and S. Kharbanda (2000). "Negative regulation of cytochrome c-mediated oligomerization of Apaf-1 and activation of procaspase-9 by heat shock protein 90." Embo J **19**(16): 4310-22.
- Papathanassiou, A. E., N. J. MacDonald, A. Bencsura and H. A. Vu (2006). "F1F0-ATP synthase functions as a co-chaperone of Hsp90-substrate protein complexes." Biochem Biophys Res Commun **345**(1): 419-29.
- Parcellier, A., M. Brunet, E. Schmitt, E. Col, C. Didelot, A. Hammann, K. Nakayama, K. I. Nakayama, S. Khochbin, E. Solary and C. Garrido (2006). "HSP27 favors ubiquitination and proteasomal degradation of p27Kip1 and helps S-phase re-entry in stressed cells." Faseb J **20**(8): 1179-81.
- Parcellier, A., E. Schmitt, S. Gurbuxani, D. Seigneurin-Berny, A. Pance, A. Chantome, S. Plenchette, S. Khochbin, E. Solary and C. Garrido (2003). "HSP27 is a ubiquitin-binding protein involved in I-kappaBalpha proteasomal degradation." Mol Cell Biol **23**(16): 5790-802.

- Park, H. S., J. S. Lee, S. H. Huh, J. S. Seo and E. J. Choi (2001). "Hsp72 functions as a natural inhibitory protein of c-Jun N-terminal kinase." Embo J **20**(3): 446-56.
- Paul, C., F. Manero, S. Gonin, C. Kretz-Remy, S. Viroit and A. P. Arrigo (2002). "Hsp27 as a negative regulator of cytochrome C release." Mol Cell Biol **22**(3): 816-34.
- Paule, M. R. and R. J. White (2000). "Survey and summary: transcription by RNA polymerases I and III." Nucleic Acids Res **28**(6): 1283-98.
- Pelham, H. R. (1986). "Speculations on the functions of the major heat shock and glucose-regulated proteins." Cell **46**(7): 959-61.
- Peng, X., X. Guo, S. C. Borkan, A. Bharti, Y. Kuramochi, S. Calderwood and D. B. Sawyer (2005). "Heat shock protein 90 stabilization of ErbB2 expression is disrupted by ATP depletion in myocytes." J Biol Chem **280**(13): 13148-52.
- Perry, R. P. and D. E. Kelley (1970). "Inhibition of RNA synthesis by actinomycin D: characteristic dose-response of different RNA species." J Cell Physiol **76**(2): 127-39.
- Polier, S., Z. Dragovic, F. U. Hartl and A. Bracher (2008). "Structural basis for the cooperation of Hsp70 and Hsp110 chaperones in protein folding." Cell **133**(6): 1068-79.

- Powers, M. V., P. A. Clarke and P. Workman (2008). "Dual targeting of HSC70 and HSP72 inhibits HSP90 function and induces tumor-specific apoptosis." Cancer Cell **14**(3): 250-62.
- Pratt, W. B., Y. Morishima and Y. Osawa (2008). "The Hsp90 chaperone machinery regulates signaling by modulating ligand binding clefts." J Biol Chem **283**(34): 22885-9.
- Pratt, W. B., Y. Morishima, H. M. Peng and Y. Osawa (2010). "Proposal for a role of the Hsp90/Hsp70-based chaperone machinery in making triage decisions when proteins undergo oxidative and toxic damage." Exp Biol Med (Maywood) **235**(3): 278-89.
- Pratt, W. B. and D. O. Toft (2003). "Regulation of signaling protein function and trafficking by the hsp90/hsp70-based chaperone machinery." Exp Biol Med (Maywood) **228**(2): 111-33.
- Prodromou, C., S. M. Roe, R. O'Brien, J. E. Ladbury, P. W. Piper and L. H. Pearl (1997). "Identification and structural characterization of the ATP/ADP-binding site in the Hsp90 molecular chaperone." Cell **90**(1): 65-75.
- Qiu, X. B., Y. M. Shao, S. Miao and L. Wang (2006). "The diversity of the DnaJ/Hsp40 family, the crucial partners for Hsp70 chaperones." Cell Mol Life Sci **63**(22): 2560-70.
- Rajkumar, S. V., P. G. Richardson, T. Hideshima and K. C. Anderson (2005). "Proteasome inhibition as a novel therapeutic target in human cancer." J Clin Oncol **23**(3): 630-9.

- Rane, M. J., Y. Pan, S. Singh, D. W. Powell, R. Wu, T. Cummins, Q. Chen, K. R. McLeish and J. B. Klein (2003). "Heat shock protein 27 controls apoptosis by regulating Akt activation." J Biol Chem **278**(30): 27828-35.
- Ravagnan, L., S. Gurbuxani, S. A. Susin, C. Maise, E. Daugas, N. Zamzami, T. Mak, M. Jaattela, J. M. Penninger, C. Garrido and G. Kroemer (2001). "Heat-shock protein 70 antagonizes apoptosis-inducing factor." Nat Cell Biol **3**(9): 839-43.
- Reddy, R. K., J. Lu and A. S. Lee (1999). "The endoplasmic reticulum chaperone glycoprotein GRP94 with Ca(2+)-binding and antiapoptotic properties is a novel proteolytic target of calpain during etoposide-induced apoptosis." J Biol Chem **274**(40): 28476-83.
- Reddy, R. K., C. Mao, P. Baumeister, R. C. Austin, R. J. Kaufman and A. S. Lee (2003). "Endoplasmic reticulum chaperone protein GRP78 protects cells from apoptosis induced by topoisomerase inhibitors: role of ATP binding site in suppression of caspase-7 activation." J Biol Chem **278**(23): 20915-24.
- Ritossa, F. (1996). "Discovery of the heat shock response." Cell Stress Chaperones **1**(2): 97-8.
- Rocchi, P., P. Jugpal, A. So, S. Sinneman, S. Ettinger, L. Fazli, C. Nelson and M. Gleave (2006). "Small interference RNA targeting heat-shock protein 27 inhibits the growth of prostatic cell lines and induces apoptosis via caspase-3 activation in vitro." BJU Int **98**(5): 1082-9.

- Roe, S. M., M. M. Ali, P. Meyer, C. K. Vaughan, B. Panaretou, P. W. Piper, C. Prodromou and L. H. Pearl (2004). "The Mechanism of Hsp90 regulation by the protein kinase-specific cochaperone p50(cdc37)." Cell **116**(1): 87-98.
- Rouse, J., P. Cohen, S. Trigon, M. Morange, A. Alonso-Llamazares, D. Zamanillo, T. Hunt and A. R. Nebreda (1994). "A novel kinase cascade triggered by stress and heat shock that stimulates MAPKAP kinase-2 and phosphorylation of the small heat shock proteins." Cell **78**(6): 1027-37.
- Saleh, A., S. M. Srinivasula, L. Balkir, P. D. Robbins and E. S. Alnemri (2000). "Negative regulation of the Apaf-1 apoptosome by Hsp70." Nat Cell Biol **2**(8): 476-83.
- Samali, A., J. Cai, B. Zhivotovsky, D. P. Jones and S. Orrenius (1999). "Presence of a pre-apoptotic complex of pro-caspase-3, Hsp60 and Hsp10 in the mitochondrial fraction of jurkat cells." Embo J **18**(8): 2040-8.
- Schmitt, E., A. Parcellier, S. Gurbuxani, C. Cande, A. Hammann, M. C. Morales, C. R. Hunt, D. J. Dix, R. T. Kroemer, F. Giordanetto, M. Jaattela, J. M. Penninger, A. Pance, G. Kroemer and C. Garrido (2003). "Chemosensitization by a non-apoptogenic heat shock protein 70-binding apoptosis-inducing factor mutant." Cancer Res **63**(23): 8233-40.
- Schneider, E. E., T. Albert, D. A. Wolf and D. Eick (1999). "Regulation of c-myc and immunoglobulin kappa gene transcription by promoter-proximal pausing of RNA polymerase II." Curr Top Microbiol Immunol **246**: 225-31.

- Schnur, R. C., M. L. Corman, R. J. Gallaschun, B. A. Cooper, M. F. Dee, J. L. Doty, M. L. Muzzi, C. I. DiOrio, E. G. Barbacci, P. E. Miller and et al. (1995). "erbB-2 oncogene inhibition by geldanamycin derivatives: synthesis, mechanism of action, and structure-activity relationships." J Med Chem **38**(19): 3813-20.
- Schroder, M. (2008). "Endoplasmic reticulum stress responses." Cell Mol Life Sci **65**(6): 862-94.
- Schulte, T. W. and L. M. Neckers (1998). "The benzoquinone ansamycin 17-allylamino-17-demethoxygeldanamycin binds to HSP90 and shares important biologic activities with geldanamycin." Cancer Chemother Pharmacol **42**(4): 273-9.
- Sharp, S. and P. Workman (2006). "Inhibitors of the HSP90 molecular chaperone: current status." Adv Cancer Res **95**: 323-48.
- Shashidharamurthy, R., H. A. Koteiche, J. Dong and H. S. McHaourab (2005). "Mechanism of chaperone function in small heat shock proteins: dissociation of the HSP27 oligomer is required for recognition and binding of destabilized T4 lysozyme." J Biol Chem **280**(7): 5281-9.
- Shchepinov, M. S. (2007). "Reactive oxygen species, isotope effect, essential nutrients, and enhanced longevity." Rejuvenation Res **10**(1): 47-59.
- Shimizu, K., Y. Nakatsu, M. Oh-uchida, S. Nomoto and M. Sekiguchi (1987). "[Activated c-raf-1 gene from human stomach cancer]." Gan To Kagaku Ryoho **14**(6 Pt 2): 2140-6.

- Sitia, R. and I. Braakman (2003). "Quality control in the endoplasmic reticulum protein factory." Nature **426**(6968): 891-4.
- Smith, D. F., W. P. Sullivan, T. N. Marion, K. Zaitsev, B. Madden, D. J. McCormick and D. O. Toft (1993). "Identification of a 60-kilodalton stress-related protein, p60, which interacts with hsp90 and hsp70." Mol Cell Biol **13**(2): 869-76.
- Sobell, H. M. (1985). "Actinomycin and DNA transcription." Proc Natl Acad Sci U S A **82**(16): 5328-31.
- Solit, D. B., F. F. Zheng, M. Drobnjak, P. N. Munster, B. Higgins, D. Verbel, G. Heller, W. Tong, C. Cordon-Cardo, D. B. Agus, H. I. Scher and N. Rosen (2002). "17-Allylamino-17-demethoxygeldanamycin induces the degradation of androgen receptor and HER-2/neu and inhibits the growth of prostate cancer xenografts." Clin Cancer Res **8**(5): 986-93.
- Soncin, F., X. Zhang, B. Chu, X. Wang, A. Asea, M. Ann Stevenson, D. B. Sacks and S. K. Calderwood (2003). "Transcriptional activity and DNA binding of heat shock factor-1 involve phosphorylation on threonine 142 by CK2." Biochem Biophys Res Commun **303**(2): 700-6.
- Stankiewicz, A. R., G. Lachapelle, C. P. Foo, S. M. Radicioni and D. D. Mosser (2005). "Hsp70 inhibits heat-induced apoptosis upstream of mitochondria by preventing Bax translocation." J Biol Chem **280**(46): 38729-39.

- Stellrecht, C. M., M. Ayres, R. Arya and V. Gandhi (2009). "A unique RNA-directed nucleoside analog is cytotoxic to breast cancer cells and depletes cyclin E levels." Breast Cancer Res Treat.
- Stellrecht, C. M., C. J. Phillip, F. Cervantes-Gomez and V. Gandhi (2007). "Multiple myeloma cell killing by depletion of the MET receptor tyrosine kinase." Cancer Res **67**(20): 9913-20.
- Stellrecht, C. M., C. O. Rodriguez, Jr., M. Ayres and V. Gandhi (2003). "RNA-directed actions of 8-chloro-adenosine in multiple myeloma cells." Cancer Res **63**(22): 7968-74.
- Strobeck, M. (2007). "Multiple myeloma therapies." Nat Rev Drug Discov **6**(3): 181-2.
- Supko, J. G., R. L. Hickman, M. R. Grever and L. Malspeis (1995). "Preclinical pharmacologic evaluation of geldanamycin as an antitumor agent." Cancer Chemother Pharmacol **36**(4): 305-15.
- Susin, S. A., H. K. Lorenzo, N. Zamzami, I. Marzo, B. E. Snow, G. M. Brothers, J. Mangion, E. Jacotot, P. Costantini, M. Loeffler, N. Larochette, D. R. Goodlett, R. Aebersold, D. P. Siderovski, J. M. Penninger and G. Kroemer (1999). "Molecular characterization of mitochondrial apoptosis-inducing factor." Nature **397**(6718): 441-6.
- Takahashi, K., K. Suzuki, Y. Uehara and T. Ono (1992). "Growth inhibition by anchorage-deficiency is associated with increased level but reduced phosphorylation of mutant p53." Jpn J Cancer Res **83**(4): 358-65.

- Tassone, P., P. Tagliaferri, M. Rossi, M. Gaspari, R. Terracciano and S. Venuta (2006). "Genetics and molecular profiling of multiple myeloma: novel tools for clinical management?" Eur J Cancer **42**(11): 1530-8.
- Tatsuta, T. (2009). "Protein quality control in mitochondria." J Biochem **146**(4): 455-61.
- Tattersall, M. H., J. E. Sodergren, S. K. Dengupta, D. H. Trites, E. J. Modest and E. Frei, 3rd (1975). "Pharmacokinetics of actinomycin D in patients with malignant melanoma." Clin Pharmacol Ther **17**(6): 701-8.
- Terpos, E., A. Rahemtulla and M. A. Dimopoulos (2005). "Current treatment options for myeloma." Expert Opin Pharmacother **6**(7): 1127-42.
- Tissieres, A., H. K. Mitchell and U. M. Tracy (1974). "Protein synthesis in salivary glands of *Drosophila melanogaster*: relation to chromosome puffs." J Mol Biol **84**(3): 389-98.
- Trinklein, N. D., W. C. Chen, R. E. Kingston and R. M. Myers (2004). "Transcriptional regulation and binding of heat shock factor 1 and heat shock factor 2 to 32 human heat shock genes during thermal stress and differentiation." Cell Stress Chaperones **9**(1): 21-8.
- Uehara, Y., M. Hori, T. Takeuchi and H. Umezawa (1985). "Screening of agents which convert 'transformed morphology' of Rous sarcoma virus-infected rat kidney cells to 'normal morphology': identification of an active agent as herbimycin and its inhibition of intracellular src kinase." Jpn J Cancer Res **76**(8): 672-5.

- Uehara, Y., M. Hori, T. Takeuchi and H. Umezawa (1986). "Phenotypic change from transformed to normal induced by benzoquinonoid ansamycins accompanies inactivation of p60src in rat kidney cells infected with Rous sarcoma virus." Mol Cell Biol **6**(6): 2198-206.
- Veal, G. J., M. Cole, J. Errington, A. Parry, J. Hale, A. D. Pearson, K. Howe, J. C. Chisholm, C. Beane, B. Brennan, F. Waters, A. Glaser, S. Hemsworth, H. McDowell, Y. Wright, K. Pritchard-Jones, R. Pinkerton, G. Jenner, J. Nicholson, A. M. Elsworth and A. V. Boddy (2005). "Pharmacokinetics of dactinomycin in a pediatric patient population: a United Kingdom Children's Cancer Study Group Study." Clin Cancer Res **11**(16): 5893-9.
- Vertii, A., C. Hakim, A. Kotlyarov and M. Gaestel (2006). "Analysis of properties of small heat shock protein Hsp25 in MAPK-activated protein kinase 2 (MK2)-deficient cells: MK2-dependent insolubilization of Hsp25 oligomers correlates with susceptibility to stress." J Biol Chem **281**(37): 26966-75.
- Voellmy, R. (1994). "Transduction of the stress signal and mechanisms of transcriptional regulation of heat shock/stress protein gene expression in higher eukaryotes." Crit Rev Eukaryot Gene Expr **4**(4): 357-401.
- Wandinger, S. K., K. Richter and J. Buchner (2008). "The Hsp90 chaperone machinery." J Biol Chem **283**(27): 18473-7.

- Wang, M., Y. Liu, S. Liu and D. Zheng (2004). "8-Chloro-adenosine sensitizes a human hepatoma cell line to TRAIL-induced apoptosis by caspase-dependent and - independent pathways." Oncol Rep **12**(1): 193-9.
- Weinstein, I. B. and A. Joe (2008). "Oncogene addiction." Cancer Res **68**(9): 3077-80; discussion 3080.
- Welch, J. J., F. J. Rauscher, 3rd and T. A. Beerman (1994). "Targeting DNA-binding drugs to sequence-specific transcription factor.DNA complexes. Differential effects of intercalating and minor groove binding drugs." J Biol Chem **269**(49): 31051-8.
- Whitesell, L. and S. L. Lindquist (2005). "HSP90 and the chaperoning of cancer." Nat Rev Cancer **5**(10): 761-72.
- Whitesell, L., E. G. Mimnaugh, B. De Costa, C. E. Myers and L. M. Neckers (1994). "Inhibition of heat shock protein HSP90-pp60v-src heteroprotein complex formation by benzoquinone ansamycins: essential role for stress proteins in oncogenic transformation." Proc Natl Acad Sci U S A **91**(18): 8324-8.
- Whitesell, L., S. D. Shifrin, G. Schwab and L. M. Neckers (1992). "Benzoquinonoid ansamycins possess selective tumoricidal activity unrelated to src kinase inhibition." Cancer Res **52**(7): 1721-8.

- Winegarden, N. A., K. S. Wong, M. Sopta and J. T. Westwood (1996). "Sodium salicylate decreases intracellular ATP, induces both heat shock factor binding and chromosomal puffing, but does not induce hsp 70 gene transcription in *Drosophila*." J Biol Chem **271**(43): 26971-80.
- Woodruff, H. B. and S. A. Waksman (1960). "The actinomycins and their importance in the treatment of tumors in animals and man. Historical background." Ann N Y Acad Sci **89**: 287-98.
- Wu, B., C. Hunt and R. Morimoto (1985). "Structure and expression of the human gene encoding major heat shock protein HSP70." Mol Cell Biol **5**(2): 330-41.
- Wu, C. (1995). "Heat shock transcription factors: structure and regulation." Annu Rev Cell Dev Biol **11**: 441-69.
- Wytenbach, A., O. Sauvageot, J. Carmichael, C. Diaz-Latoud, A. P. Arrigo and D. C. Rubinsztein (2002). "Heat shock protein 27 prevents cellular polyglutamine toxicity and suppresses the increase of reactive oxygen species caused by huntingtin." Hum Mol Genet **11**(9): 1137-51.
- Xanthoudakis, S., S. Roy, D. Rasper, T. Hennessey, Y. Aubin, R. Cassady, P. Tawa, R. Ruel, A. Rosen and D. W. Nicholson (1999). "Hsp60 accelerates the maturation of pro-caspase-3 by upstream activator proteases during apoptosis." Embo J **18**(8): 2049-56.

- Yamano, T., S. Mizukami, S. Murata, T. Chiba, K. Tanaka and H. Uono (2008). "Hsp90-mediated assembly of the 26 S proteasome is involved in major histocompatibility complex class I antigen processing." J Biol Chem **283**(42): 28060-5.
- Yang, S. Y., X. Z. Jia, L. Y. Feng, S. Y. Li, G. S. An, J. H. Ni and H. T. Jia (2009). "Inhibition of topoisomerase II by 8-chloro-adenosine triphosphate induces DNA double-stranded breaks in 8-chloro-adenosine-exposed human myelocytic leukemia K562 cells." Biochem Pharmacol **77**(3): 433-43.
- Zaarur, N., V. L. Gabai, J. A. Porco, Jr., S. Calderwood and M. Y. Sherman (2006). "Targeting heat shock response to sensitize cancer cells to proteasome and Hsp90 inhibitors." Cancer Res **66**(3): 1783-91.
- Zhang, S., D. Zheng and S. Liu (1998). "[8-chloro-adenosine induced apoptosis in various human tumor cell lines]." Zhonghua Zhong Liu Za Zhi **20**(2): 88-9.
- Zou, J., Y. Guo, T. Guettouche, D. F. Smith and R. Voellmy (1998). "Repression of heat shock transcription factor HSF1 activation by HSP90 (HSP90 complex) that forms a stress-sensitive complex with HSF1." Cell **94**(4): 471-80.

Vita

Fabiola Cervantes Gomez was born in Ciudad Juarez, Mexico on July 28, 1981 to parents Ana Gloria Cervantes and Felizardo Gomez. She grew up in Ciudad Juarez where she attended El Chamizal High School from 1996 to 1999. She enrolled at Universidad Autonoma de Ciudad Juarez in September 1999 but later transferred to the University of Texas at El Paso in El Paso, TX. She worked under the mentorship of Dr. Keith Pannel in the Department of Chemistry doing organometallic synthesis. She completed her Bachelor of Science degree in Chemistry in May 2005. She matriculated into the Graduate School of Biomedical Sciences at the University of Texas Health Science Center at Houston in August 2005. She later joined the laboratory of Dr. Varsha Gandhi in the Department of Experimental Therapeutics in June 2006. She conducted her doctoral work under Dr. Gandhi's supervision and will complete her Doctor of Philosophy degree in May 2010.

Copyright © 2010 Fabiola Cervantes Gomez

All rights reserved